Acartia spp. (Copepoda: Calanoida) as model organisms to evaluate the toxicity of emerging contaminants: an ecotoxicogenomic approach

Flavio Rotolo (K890197X)

Thesis submitted for the degree of Doctor of Philosophy – XXI cycle

Life and Biomolecular Sciences

October 2022

The Open University

School of Life, Health and Chemical Sciences – Milton Keynes (UK)

Stazione Zoologica Anton Dohrn

Department of Integrative Marine Ecology – Naples (Italy)

Supervision Panel

Director of Studies: **Dr. Ylenia Carotenuto** (Stazione Zoologica Anton Dohrn, Italy)

Internal Supervisor: **Dr. Isabella Buttino** (Istituto Superiore per la Protezione e Ricerca Ambientale, Italy; Stazione Zoologica Anton Dohrn, Italy)

External Supervisor: **Prof. Sami Souissi** (Université de Lille, France)

Examination Panel

External Examiner: **Prof. Ceri Lewis** (Exeter University, UK)

Internal Examiner: **Dr. Antonietta Spagnuolo** (Stazione Zoologica Anton Dohrn, Italy)

Chair: **Dr. Pasquale De Luca** (Stazione Zoologica Anton Dohrn, Italy)

Abstract

Copepods are small crustaceans of great ecological and ecotoxicogenomic importance. Among them, *Acartia tonsa*, invasive species in the Mediterranean Sea, is a model species in ecotoxicology. *Acartia clausi*, native of the Mediterranean, is a candidate alternative model species in this field.

In this PhD project, we compared physiological (naupliar immobilisation, egg hatching success, egg production, faecal pellet production, adult survival) and molecular (quantitative gene expression) responses of both copepod species exposed to nickel chloride ($NiCl_2$) and nickel nanoparticles (NiNPs), through ecotoxicological bioassays and RT-qPCR. A *de novo* transcriptome of *A. clausi* females exposed to elutriates of polluted sediments was also generated.

We were able to keep multi-generational cultures of *A. clausi*, fed the optimal diet of *Rhinomonas reticulata*, for up to four months, with 26 days from eggs to F2 generation.

Bioassays confirmed that nauplii of *A. clausi* were more sensitive than those of *A. tonsa*, approximately 6 (NiNPs) and 95 times ($NiCl_2$). Adults of both species were less affected by these toxicants, with mild effects mostly on egg production. Effects of both toxicants on egg hatching success was mainly due to Ni ions, which are continuously released from NiNPs.

The first *de novo* assembled transcriptome for *A. clausi* exposed to elutriates of polluted sediments revealed 1,000 differentially expressed genes (743 up-, 257 down-regulated). The response was mostly in up-regulation of proteolysis and detoxification, and down-regulation of ribosomal proteins.

Comparative gene expression in copepod females showed greater responses in *A. clausi*, especially with $NiCl_2$, mostly with a down-regulation of genes involved in detoxification, indicating an inhibition of molecular defences. For *A. clausi*, down-regulation of vitellogenin seems correlated with low egg production.

Overall, we provided novel information on the physiology and molecular biology of *A. clausi* and on NiNPs behaviour, which could threaten marine environment in the near future.

Acknowledgements

This thesis could not have been written without the help of many persons.

First, I wish to thank the Open University and the Stazione Zoologica Anton Dohrn for this important opportunity I was given.

Thanks to Dr. Ylenia Carotenuto, the only person with whom I could have embarked on this journey. Throughout these years she has known perfectly when it was the right time to teach me and lead me in the right direction, so that I would not feel lost, and when to give me freedom, so that I could explore new ideas on my own.

Thanks to Dr. Isabella Buttino, Dr. Valentina Vitiello and all the colleagues at ISPRA Livorno for the hospitality, the tutoring and the great experience I had. Dr. Buttino was of great help for the thesis as internal supervisor, constantly providing support and advice.

Thanks to Prof. Sami Souissi for his help as external supervisor: he gave me many precious suggestions which were of great help for the thesis. We wish also to thank his colleagues of the Université de Lille, Prof. Philippe Zinck and PhD student Mr. Wajid Ali, for the kind help with DLS analyses.

We wish to thank Dr. Roncalli at Stazione Zoologica Anton Dohrn and Dr. Lenz from the University of Hawai'i at Manoa for the help and support with RNA-seq data.

We thank Dr. Teresa Verde and Dr. Gennaro Matrullo of ARPA Campania for the kind help with the ICP-MS analysis.

Thanks to all the technicians who kindly helped me with my experiments and cheered me up: Mariano Amoroso, Massimo Perna, Carmen Minucci, Ferdinando Tramontano.

Thanks also to Gabriella Grossi for the constant and kind support with the bureaucratic aspects of this PhD.

Thanks to my lab mates and colleagues, the *gruppo mensa*, with whom I shared many meals and drinks, laughs and rants: Jessica, Luis, Daniele, Elena, Marco, Lorenzo, Leandro, Viviana, Anna Chiara, Isabella, Anna, Luigi, Martina, and many others.

Thanks to Veria and her beautiful and joyous family, who always made me feel at home in this magical, frantic city of "a thousand colours".

Thanks to Giuseppe, Gerlando and Luigi, my best friends, for the good times, the long conversations and the happy memories.

Thanks to my parents Caterina and Silvio, my sister Corinna and my grandparents Enzo and Virginia, for always believing in me and sustaining me up to this point.

And thanks to Laura, my soulmate, my rock, for always being by my side… or behind my back, cheering for me.

Il mondo esisteva prima dell'uomo ed esisterà dopo, e l'uomo è solo un'occasione che il mondo ha per organizzare alcune informazioni su se stesso.

Italo Calvino

Table of contents

List of figures

List of tables

List of abbreviations

µg/L: micrograms per litre

AChE: acetylcholinesterase

AChR: acetylcholine receptor

AgNPs: silver nanoparticles

A_L: amplification length

ARA: arachidonic acid

B[a]P: benzo[a]pyrene

BCV: Biological Coefficient of Variation

BDW: bidistilled water

BLAST: Basic Local Alignment Search Tool

bp: base pairs

BP: biological process

BphA: bisphenol A

CAT: catalase

CC: cellular component

CDA: chitin deacetylase

cDNA: complementary DNA

CHT: chitinase

COI: cytochrome oxidase I

CPM: counts per million

C_t: threshold cycle

CYP: cytochrome P450

DDT: dichlorodiphenyltrichloroethane

DEGs: differentially expressed genes

DEPC: diethylpyrocarbonate

DHA: docosahexaenoic acid

DLS: Dynamic Light Scattering

dNTPs: deoxyribose nucleotides triphosphate

DOM: dissolved organic matter

E: amplification efficiency

E56: elutriate of sediments sampled in station 56

EC_{10}: effective concentration for 10% of the population

EC_{50}: effective concentration for 50% of the population

ENMs: engineered nanomaterials

EP: egg production

EPA: eicosapentaenoic acid

EPS: extracellular polymeric substances

EQS: environmental quality standards

FDR: false discovery rate

FP: faecal pellets

FSW: 0.22 µm-filtered seawater

GO: gene ontology

GOI: genes of interest

GPx: glutathione peroxidase

GSH: reduced glutathione

GSS: glutathione synthase

GSSG: oxidised glutathione

GST: glutathione S-transferase

h: hour

HC_5: hazardous concentration for 5% of the population

HCD: historical control data

HS: hatching success

HSP: heat-shock protein

HUFAs: highly-unsaturated fatty acids

ICP-MS: Inductively Coupled Plasma-Mass Spectrometry

ind./L: individuals per litre

LC_{50}: lethal concentration for 50% of the population

LCL: lower control limits

LOD: limit of detection

log_2FC: log_2 fold change

LOQ: limit of quantification

LTER-MC: long-term ecological research Marechiara

MF: molecular function

mg/L: milligrams per litre

MHC: myosin heavy chain

M-LP: Mpv17-like protein

mRNA: messenger RNA

NCBI: National Centre for Biotechnology Information

ng/µL: nanograms per microlitre

NGS: next generation sequencing

NI: naupliar immobilisation

$NiCl_2$: nickel chloride

NiNPs: nickel nanoparticles

NMs: nanomaterials

NPs: nanoparticles

nr: non-redundant protein sequence database

n-TiO_2: nanoscale titanium dioxide

PAF-AH: platelet-activating factor acetylhydrolase

PAHs: polycyclic aromatic hydrocarbons

PHGPx: phospholipid-hydroperoxide glutathione peroxidase

POC: particulate organic carbon

POPs: persistent organic pollutants

PSU: practical salinity unit

QDs: quantum dots

RGs: reference genes

RHINO: *Rhinomonas reticulata*

RHODO: *Rhodomonas baltica*

RIN: RNA Integrity Number

RNA-seq: RNA sequencing

ROS: reactive oxygen species

RPM: revolutions per minute

RT-qPCR: real time quantitative polymerase chain reaction

SD: standard deviation

SEST: sestrin

SOD: superoxide dismutase

SSH: suppression subtractive hybridization

SWIB: DNA topoisomerase III

TEM: transmission electron microscopy

UCL: upper control limit

VTG: vitellogenin

Chapter 1 State of the art and thesis aims

1.1 Ecological role of copepods

Copepods (phylum Arthropoda, subphylum Crustacea, superclass Multicrustacea, class Copepoda; World Register of Marine Species, 2022) are small aquatic crustaceans, extremely abundant worldwide; with over 21,000 described species and more than 14,700 currently accepted species (Walter and Boxshall, 2022), copepods are considered the most numerous metazoans on Earth (Turner, 2004) and are estimated to represent 70% of the ocean's biomass (Wells, 1984).

The name "Copepoda" has its roots in the Greek words *kope* (oar) and *podos* (foot), referring to the pair of swimming legs on the same somite, moved together in an oars-like fashion. Copepods have a wide variety of sizes and feeding strategies (Turner, 2004); most species are typically small (≤ 10 mm), planktonic, free-living and filter feeder (grazers of phytoplankton), with a single, centrally-located eye; others are parasitic and can be up to 25 cm long (LeBlanc, 2007) (**Figure 1.1**). They can be found virtually everywhere there is water, from freshwater to estuarine to hypersaline conditions, and they can inhabit the water column and the benthos, from the intertidal area to deep ocean basins (LeBlanc, 2007; Walter and Boxshall, 2022).

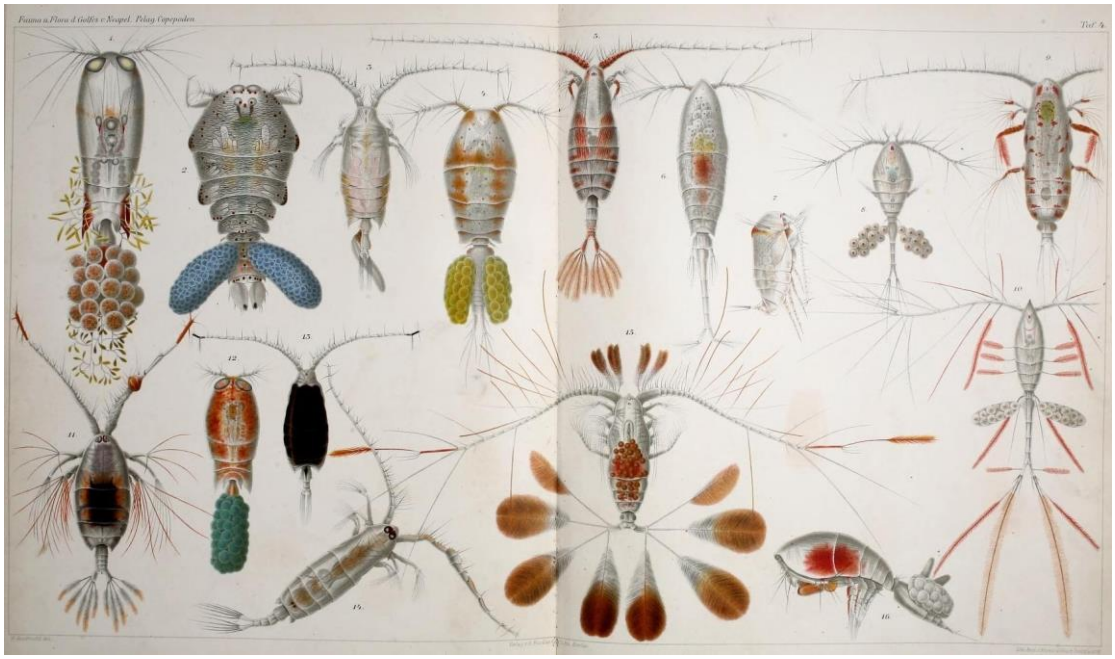

Figure 1.1 A depiction of diversity in forms and sizes of copepods of the Gulf of Naples. Source: Giesbrecht, 1892.

Among the most important genera of small, planktonic copepods there are: *Paracalanus*, *Pseudocalanus*, *Acartia*, *Clausocalanus* (Order Calanoida); *Oithona*, *Oncaea*, *Corycaeus* (Order Cyclopoida); and *Microsetella* (Order Harpacticoida) (Turner, 2004).

As one of the most important components of total zooplankton (on average 80%), copepods play a critical ecological role in food webs, linking the phytoplankton that they feed on to their predators in higher trophic levels (such as fish larvae, larger copepods, and other carnivorous zooplankton like chaetognaths, ctenophores and jellyfish) (Turner, 2004). In this way, they channel energy from primary producers and microbial loop to secondary producers, representing one of the main mechanisms of transfer and cycling of dissolved organic matter (DOM) in the sea (reviewed by Steinberg and Landry, 2017; Walter and Boxshall, 2022).

In addition to this, copepods release particulate organic carbon (POC) in the marine environment mostly through sloppy feeding and excretion of faecal pellets, but also through moults and carcasses; this causes the POC to sink, allowing its availability to higher depths, below the photic zone (Steinberg and Landry, 2017). This transport of POC, called biological pump, is strengthened by the diel vertical migrations of zooplankton along the water column: during the night they reside in surface waters, where they feed, and then they move to the mesopelagic zone, where they reside during the day, thus allowing the transfer of organic carbon (reviewed by Steinberg and Landry, 2017).

Copepod reproduction occurs via mating, when male copepods attach the spermatophore containing the sperms to the genital pores of the female; as soon as the female lays the eggs, these are being fertilised as they exit the genital pores (Ianora *et al.*, 2007). Eggs laid by the female are, thus, already fertilised, *i.e.* they are zygotes, or embryos. For the sake of simplicity, and to allow comparisons between our data and those present in scientific literature regarding copepod reproductive physiology and ecotoxicology (Gorbi *et al.*, 2012), throughout the thesis copepod embryos will be referred to as “eggs”. Another important characteristic of copepods is, in fact, their ability to produce different types of eggs: other than regular, subitaneous eggs, there are diapause and oligopause eggs, which can tolerate adverse environmental conditions and hatch with more favourable parameters (Buttino *et al.*, 2019 and references therein; Drillet *et al.*, 2011b; Invidia *et al.*, 2004). Although dormancy is more common for freshwater zooplankton rather than marine zooplankton, due to the typically larger fluctuations in limnic habitats (Drillet *et al.*, 2011b), there are several reported cases of dormancy eggs produced by marine or euryhaline copepods. For example, eggs of three species of calanoid copepods (*Acartia tonsa*, *Centropages hamatus* and *Labidocera aestiva*) resisted to anoxic or sulfidic conditions for up to two weeks, and it was

suggested that eggs switch to anaerobic metabolism when exposed to such conditions (Marcus *et al.*, 1997).

Partly because of this capacity to produce eggs which can be stored, copepods can be maintained in laboratory conditions (Vitiello *et al.*, 2016). In particular, in recent years they have been proposed as food source in aquaculture for planktivorous fishes and fish larvae (Drillet *et al.*, 2011a; Olivotto *et al.*, 2009). Copepods, in fact, particularly those belonging to Order Calanoida, are being preferred over the traditional *Artemia salina* plus rotifers diet because of their typical springing movement, because of their small naupliar stages and because of their greater content in highly-unsaturated fatty acids (HUFAs) (Drillet *et al.*, 2011a; Olivotto *et al.*, 2008a, 2008b and references therein).

The paramount importance of copepods in ecology makes them one of the most important metazoan groups on the planet. Because of this, they have found large utilisation also in ecotoxicology.

1.2 Ecotoxicology: definition and background

One of the many definitions of ecotoxicology describes it as a "research area which studies the toxic effects of environmental agents on biological populations, communities, and ecosystems" (Tolleson, 2018). It is considered an integrative science since it requires knowledge from toxicology, ecology, chemistry, parasitology, microbiology, engineering, modelling, mathematics, climatology, public policy, and environmental legislation (Férard and Blaise, 2013). Studies and predictions on the presence of pollutants in the environment are not simple, considering that their distribution, mobilisation and chemical conversion are influenced by combinations of anthropogenic and non-anthropogenic processes (Tolleson, 2018).

The term "ecotoxicology" derives from the Greek words *oikos* (house), *toxicon* (poison) and *logos* (study). The origin of this word is attributed to the French scientists Jean-Marie Pelt and Jean-Michel Jouany, who coined the word in the late 1960s referring to environmental toxicology; subsequently, in 1969, the term was introduced for the first time in public by René Truhaut, at an international meeting in Stockholm (Committee of the International Council of Scientific Unions) (Férard, 2013). Studies of effects of environmental pollution on biological communities, however, began much earlier: one of the first examples is in 1863, when fishes were introduced for toxicity testing for the first time to investigate the pollution of rivers in Scotland (Penny and Adams, 1863). Toxicity tests, or bioassays, in fact, are carried out as a means of determining the no-adverse biological effects

concentration of a chemical in the environment, predicting its harm or no harm concentrations after exposure of organisms for certain periods of time (Cairns and Pratt, 1989).

One of the most important steps for the establishment of ecotoxicology as a distinct research area, separated from human toxicology, can be traced back to 1962, year of publication of Rachel Carson's *Silent spring*. In the book, the American biologist documented the detrimental effects of indiscriminate use of pesticides (most notably DDT, dichlorodiphenyltrichloroethane) in her country, during the 1940s and 1950s. The title describes the changes to local animal communities and especially to top predators like birds: due to pesticide exposure, very high and unusual mortality rates were recorded in the avifauna, and thus spring was eerily deprived of its sounds (Carson, 1962).

That period, from the end of World War II to the 1960s, was to be called "the age of darkness" in terms of environmental action (Blaise and Férard, 2006): there was a lack of knowledge and tools on how to assess human impact on the environment and, moreover, the primary bases for regulatory decisions were only chemical and physical determinations, not biological assays (Cairns and Pratt, 1989). In that context, several pollution events occurred with catastrophic consequences: for example, the DDT contamination cited above, and only mentioning the metal poisoning epidemics in Japan, of mercury (Minamata disease) and cadmium (Itai-Itai disease), which affected humans too with dramatic repercussions (Newman, 2008).

Silent spring is now considered one of the most influential books of all time, given the enormous impact it had on environmental protection, food production and human and environmental health (Pimentel, 2012). Now it is known that pesticides belong to a category of chemicals called persistent organic pollutants (POPs) that accumulate in the body of organisms and cannot be excreted; thus, through a process called biomagnification, they can be found in top predators at extremely higher concentrations with respect to those found in target animals (Goerke *et al.*, 2004; Govaerts *et al.*, 2018). After its publication, different nations implemented programs for the reduction of pesticides and several US and Canada investigators became concerned with the use of pesticides (Pimentel, 2012). More generally, since the 1960s biological evidence with invertebrates, algae and mostly fishes became more common, together with chemical analyses, in environmental risk assessment required by regulations (Blaise and Férard, 2006; Férard, 2013). However, it was only with the Stockholm Convention (2004) that POPs' production and use were globally prohibited; and nonetheless many issues related to the environmental effect of these chemicals still needs to be solved (Werner and Hitzfeld, 2012).

Nowadays, environmental regulations are generally stricter and environmental agencies operate worldwide, using both chemical and biological data for risk assessment (Graham *et al.*, 2013). For example, the latest disposition in terms of ecotoxicology and risk assessment of marine sediments in the Italian legislation indicates a battery of model organisms, from bacteria and algae to several phyla of invertebrates, to be used in standardised bioassays (DM 173, 2016). By integrating chemical and ecotoxicological analyses, marine dredged materials are classified and accordingly managed, with options spanning from reuse as beach nourishments to confinement in landfills (Benedetti *et al.*, 2012).

1.3 Nanomaterials and nickel nanoparticles

Nowadays, among many toxic substances considered dangerous for the environment, some are known as emerging contaminants (or contaminants of emerging concern); their effects are still to be fully clarified as they are far less investigated, with respect to other anthropogenic pollutants, despite the hazard they pose to humans and to the environment (Corsi *et al.*, 2021). The study of nanomaterials, a class of emerging contaminants, is considered one of the major ongoing challenges for the scientific community (Blasco *et al.*, 2015).

Although the American engineer Eric Drexler is generally considered to have coined the term "nanotechnology" (Drexler, 1981), the first one to predict the importance of this field was Richard Feynman 20 years earlier (Klaine *et al.*, 2013). In 1959, in fact, at the annual meeting of the American Physical Society, the American physicist delivered a thought-provoking talk entitled *There's Plenty of Room at the Bottom*, in which he discussed for the first time about «the problem of manipulating and controlling things on a small scale» and asked: «Why cannot we write the entire 24 volumes of the *Encyclopaedia Britannica* on the head of a pin?» (Feynman, 1959). Years later, as a matter of fact, Feynman's intuition proved right, and we now widely produce and use nanomaterials.

Nanomaterials (NMs) are compounds with at least one dimension comprised between 1 and 100 nm (nanoscale); nanoparticles (NPs) are NMs that have all three dimensions in nanoscale (Corsi *et al.*, 2021; Garner *et al.*, 2017; Klaine *et al.*, 2013). When produced by anthropic activities, NMs are called engineered nanomaterials (ENMs). Because of their incredibly small scale, and consequently high surface-to-volume ratio, NMs have high surface reactivity and peculiar physical properties such as great strength and elasticity (He *et al.*, 2018; Klaine *et al.*, 2013; Sharma *et al.*, 2018). For example, multiwalled carbon nanotubes,

elongated structures composed entirely of carbon, are up to 300 times stronger than the high-carbon steel used to create cutting tools for manufacturing (Klaine *et al.*, 2013).

NMs are used for several purposes in many industries and technologies: metallurgy, aviation, bioengineering, medicine, personal care products, food and agriculture industry, ceramics, environmental remediation, and are contained in commercially available products such as sunscreens, paints and semiconductors (Baker *et al.*, 2014; He *et al.*, 2018 and references therein; Wu and Kong, 2020 and references therein). Among them, silver nanoparticles (AgNPs) and nanoscale titanium dioxide (TiO_2) are the most utilised ENMs and are considered to reach high exposure concentrations for marine organisms (Corsi *et al.*, 2021).

Being similar in size to biomolecules, NMs can pass through cellular membranes; this property allows complex smart drugs therapies but may also imply disturbances of subcellular biochemical pathways (Klaine *et al.*, 2013). Given their widespread production and unregulated disposal, NMs are eventually released in the marine environment at high rates, sinking into the sediments, and this represents a major challenge for the scientific community (Blasco *et al.*, 2015; Corsi *et al.*, 2021), also because their transport and behaviour in seawater remain poorly understood (Corsi *et al.*, 2014).

As for effects on the biota, we know that invertebrates can take up NPs mainly through the gut (upon inhalation or ingestion), potentially moving them within the body (Klaine *et al.*, 2013), but also through contact with lungs, skin or gills (Behra and Krug, 2008). Baker *et al.* (2014) summarised the effects of NPs taken up by marine organisms (including bacteria, algae, arthropods, annelids, bivalves, gastropods, echinoderms and fishes), with effects such as increased oxidative stress, growth reduction, limited mobility, accumulation in gut and sub-lethal toxicity or mortality, especially due to release of ions. For example, it was recently tested that two species of bivalves (the blue mussel *Mytilus edulis* and the eastern oyster *Crassostrea virginica*) ingested TiO_2 NPs after a short-term exposure and managed to excrete 90% of them after a subsequent depuration period (Doyle *et al.*, 2015). Another recent research showed that plants too can absorb NMs: an experiment with the angiosperm *Coriandrum sativum* exposed to nanosized nickel oxide (nNiO) showed that this NM was absorbed by the plant; as a result, it decreased growth rate, antioxidant activity, fresh and dry weight of *C. sativum* in a concentration-dependent manner (Miri *et al.*, 2017).

In the study of Jarvis *et al.* (2013), the copepod *Acartia tonsa* was fed for 7 days the diatom *Thalassiosira weissflogii* cultured with ZnO NPs (zinc oxide nanoparticles, a metal oxide commonly found in sunscreens because of its UV light absorption properties). The feeding on ZnO-exposed diatoms caused in *A. tonsa* a decrease in reproduction and survival, giving an example of trophic transfer of metal caused by metal oxide NPs exposure (Jarvis

et al., 2013). Moreover, *A. tonsa* larvae were exposed to nickel nanoparticles (Zhou *et al.*, 2016a) and to CdSe/ZnS quantum dots (QDs, semiconductor nanocrystals used for example in solar panels) (Zhou *et al.*, 2016b), and both induced an increase in mortality.

It was recently discovered that proteins and other biomolecules tend to form aggregates onto the surface of NPs, constituting what is called biomolecular corona or eco-corona, with unpredictable effects for their pharmacological and toxicological profile (Hadjidemetriou and Kostarelos, 2017). In general, the eco-corona is more likely to form around negatively charged NMs, increasing their diameter, whereas positively charged NMs tend to prevent such aggregation, remaining more easily taken up by organisms (Bergami *et al.*, 2017; Corsi *et al.*, 2021 and references therein). For example, extracellular polymeric substances (EPS, composed mostly by polysaccharidic material) produced by the marine diatom *Phaeodactylum tricornutum* formed an eco-corona around negatively charged polystyrene NPs, reducing their aggregation rate and also reducing reactive oxygen species (ROS) production, suggesting an antioxidant scavenging activity of EPS (Grassi *et al.*, 2020). However, another study with neonates of the freshwater crustacean *Daphnia magna* Straus, 1820 showed that proteins released by this species created an eco-corona around both negatively and positively charged polystyrene NPs, increasing the uptake of negatively charged NPs too, which were also less efficiently excreted (Nasser and Lynch, 2016).

The nanomaterial chosen for my PhD project are nickel nanoparticles (NiNPs) (**Figure 1.2**). They are used in several industries as catalysts, sensors, lubricants, coatings, and in fields such as electronics, magnetics, fuel industry, energy technology, ceramics and biomedicine (Gomes *et al.*, 2019; Wu and Kong, 2020 and references therein). One of the most recent applications of NiNPs, for example, is as catalyst in the reversible hydration of CO_2 to carbonic acid, which is of high importance for CO_2 capture technologies and mineralization processes (Kanold *et al.*, 2016). They also possess an extremely high compressive strength of up to 32 GPa, unprecedented for metallic materials (Sharma *et al.*, 2018).

The use of NiNPs has progressed with the common industrial use of nickel (Kanold *et al.*, 2016). Nickel is a ubiquitous element in the biosphere, naturally found in the Earth's crust (Muñoz and Costa, 2012); its alloys are used for the manufacturing of stainless steel, medical implants and jewellery (Muñoz and Costa, 2012), but it is also used for several industrial and commercial applications such as food processing, electroplating, catalysis, battery manufacturing, forging (Buttino *et al.*, 2011; Kanold *et al.*, 2016). Nickel is a transition metal which exists in five different oxidation states and can be found in different chemical species (metallic nickel, soluble compounds, oxides, sulphides, silicates), each with a different toxicity and capacity to penetrate cells (Muñoz and Costa, 2012).

Essential metals are fundamental for the correct functioning of living organisms, as they take place in various metabolic and signalling pathways (Valko *et al.*, 2005). However, maintaining chemiosmotic equilibrium of metals is crucial (especially for non-essential metals such as nickel) as they can induce well-known oxidative effects in cells and tissues, mostly because of their ability to lose electrons, catalysing oxidative reactions (Regoli and Giuliani, 2014; Teschke, 2022). These processes are known as Haber Weiss and Fenton reactions, chemical reactions occurring in the cytosol and nucleus, in which metal ions react with hydrogen peroxide to produce hydroxyl radicals (Muñoz and Costa, 2012; Regoli and Giuliani, 2014; Stohs and Bagchi, 1995). Such molecules are classified as ROS (reactive oxygen species); they are normally formed in these metabolic reactions, but their production is increased in stressful conditions or under exposure to toxic substances (Tarrant *et al.*, 2019; Wang and Wang, 2010).

ROS are highly reactive and harmful compounds, as they can affect living organisms in several ways: they can alter the equilibrium of ions, especially calcium homeostasis; cause peroxidation of lipids and thus damage to cellular membranes; damage DNA; deplete protein sulfhydryls (Stohs and Bagchi, 1995; Valko *et al.*, 2005). In addition to this, metal ions induce carcinogenic effect in mammals, allegedly because of their role in targeting transcription factors, cellular regulatory proteins or signalling proteins which play a role in cell growth, apoptosis, or regulation of the cellular cycle (Teschke, 2022; Valko *et al.*, 2005). In particular, Ni(II) ions are not among metal ions with highest reactivity and their involvement in Fenton chemistry requires the presence of a strong oxidiser, such as hydrogen peroxide or ascorbate, or thiol-containing agents, in addition with a ligand to reduce its oxidative potential (Muñoz and Costa, 2012; Regoli and Giuliani, 2014).

Several studies have reported toxic and carcinogenic effects of nickel on humans and other organisms (Teschke, 2022; Valko *et al.*, 2005). In the most recent World Cancer Report, nickel compounds are considered carcinogenic to humans for lungs, nasal cavity and paranasal sinus, especially through exposure in metal alloy industry (International Agency for Research on Cancer, 2020).

Nickel toxicity for marine organisms is known as well. A study of 2013 summarised the effects of chronic nickel salts toxicity for 17 marine species, including microalgae, macroalgae, bivalves, echinoderms, polychaetes and fishes (DeForest and Schlekat, 2013). The species which proved to be most sensitive to nickel salts, in terms of EC_{10} (effective concentration which induces effects on 10% of the tested population of organisms), was the tropical sea urchin *Diadema antillarum* (about 48 times more sensitive to nickel than the European sea urchin *Paracentrotus lividus*), while the least sensitive were the green alga

Dunaliella tertiolecta and the fishes *Cyprinodon variegatus* and *Atherinops affinis*. In conclusion, based on values of HC_5 (hazardous concentration for 5% of the species) the authors suggested for dissolved nickel in temperate European marine waters a conservative threshold of 0.0039 mg/L and a broadly applicable threshold of 0.0209 mg/L (calculated excluding *D. antillarum*, which is not found in European waters) (DeForest and Schlekat, 2013). As for environmental concentrations of dissolved nickel in seawater, generally it ranges from 0.0001 to 0.0005 mg/L (Cempel and Nikel, 2006). The highest value reported for European marine waters was 0.00375 mg/L (Heijerick and Van Sprang, 2008), but values up to 2 mg/L were found in water near industrial sites (Eisler, 1998). Although risk assessment of nickel has been performed since decades in Europe, the same is not true for NiNPs, hence there is need of information on their concentration and effect on environment and biological communities (Gomes *et al.*, 2019).

Figure 1.2 A – Nickel nanoparticles (NiNPs), or nickel nanopowder. **B** – NiNPs seen through electron microscopy (scale bar = 60 µm). Source: **A** – www.nanoshel.com; **B** – www.ssnano.com.

As for effects of NiNPs on marine invertebrates, Kanold *et al.* (2016) tested NiNPs on the larval development of the sea urchin *P. lividus* and observed a reduction in size of the larval stage with respect to the control. Moreover, NiNPs are spermiotoxic for the ascidian *Ciona intestinalis*, altering their fertilising ability and causing development anomalies (Gallo *et al.*, 2016). In the study of Oleszczuk *et al.* (2015), *D. magna* was exposed to NiNPs in addition with ionic and non-ionic surfactants (anthropic substances which reduce surface tension); the addition of surfactants increased NPs size causing their aggregation and reduced mortality of *D. magna* neonates, indicating that the availability of NPs was reduced. NiNPs toxicity was also evaluated on the soil oligochaete *Enchytraeus crypticus*, resulting in an increased inflammatory response and interferences with the nervous system (Gomes *et al.*, 2019).

The effects of NiNPs on copepods are not well-known and most studies focus on the calanoid copepod *A. tonsa*. In a recent study, Zhou *et al.* (2016a) exposed *A. tonsa* specimens to NiNPs at 8.5 and 17 mg/L for 4 days and observed that hatching success of eggs produced by exposed females was reduced with respect to the control, at both concentrations. They also showed, through electron microscopy, that adult females can ingest and excrete NiNPs through faecal pellets after exposure at the highest concentration (Zhou *et al.*, 2016a) (**Figure 1.3**).

Nickel as a salt has, of course, different toxicity, properties and behaviour with respect to nickel in the form of nanoparticles. Being in nanoscale, NiNPs can directly damage cellular membranes and physically harm or impede organisms through contact (Ghobashy *et al.*, 2021; Oleszczuk *et al.*, 2015); moreover, as it was reported in the paragraph above, they can be ingested, altering the feeding and digestion processes of organisms (Zhou *et al.*, 2016a). Like other metal nanoparticles, NiNPs can release ions (which favour the production of ROS), at a rate which depends mostly on the surface area of the exposed particles (Hang *et al.*, 2018). In this regard, as any nanomaterial NiNPs are subject to sedimentation and resuspension, and they can form aggregates with natural organic matter or other molecules present in the suspension, which in general reduces their toxicity (Corsi *et al.*, 2021; Hadjidemetriou and Kostarelos, 2017).

Nickel chloride and nickel nanoparticles are thus very diverse substances: the first, a salt, is completely soluble in water and immediately bioavailable, while the second is a nanosized metal powder which can release ions in solution over time. These differences have to be taken into account when comparing them. However, it seems that detrimental effects of both substances on marine organisms are mainly due to the release of Ni ions. For instance, in a recent study it was reported that a NiNPs solution at 10 mg/L (in which dissolved nickel was measured to a value of about 0.14 mg Ni/L) induced in *A. tonsa* a naupliar immobilisation which was similar to the immobilisation caused by $NiCl_2$ at 0.10 mg Ni/L, *i.e.* at a similar value of dissolved nickel (Zhou *et al.*, 2016a). This matter will be addressed in more detail in chapter 4 and 6, in which we will present original data from this thesis on effects of $NiCl_2$ and NiNPs.

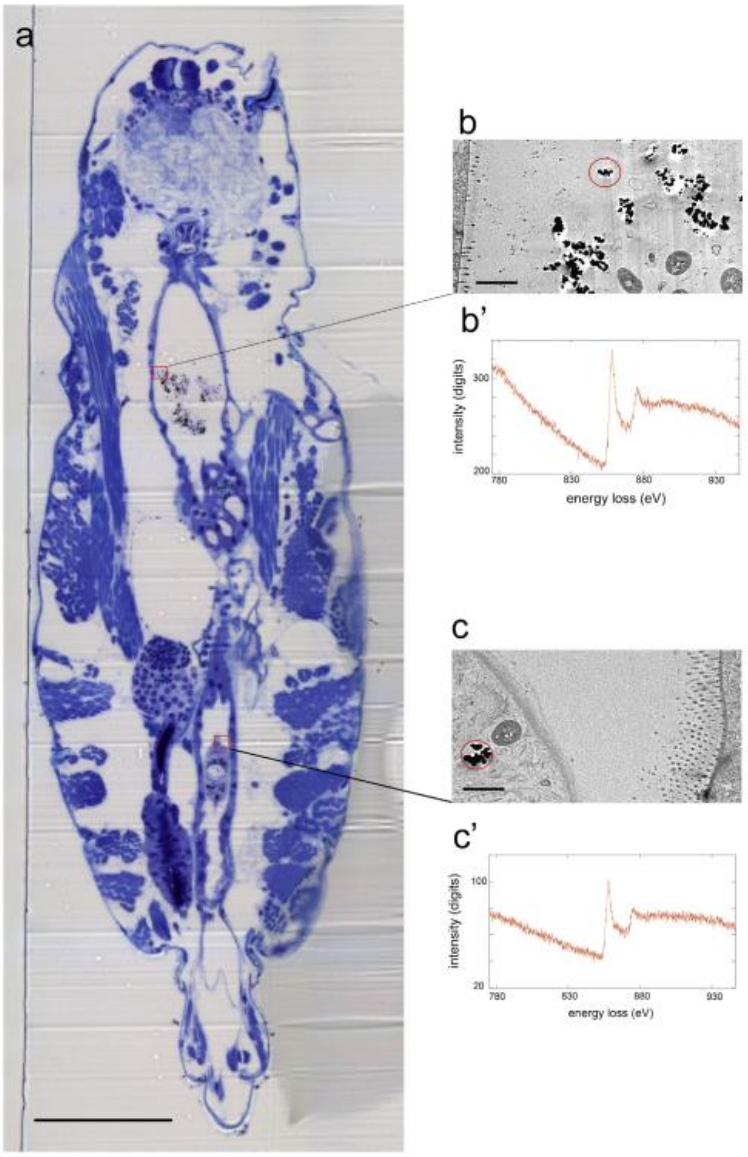

Figure 1.3 a – Ultrathin longitudinal section, analysed with transmission electron microscopy (TEM), of a female of the copepod *Acartia tonsa* exposed to nickel nanoparticles (NiNPs) at 17 mg/L for 4 days. Red squares show NiNPs in the gut (upper square) and in faecal pellets in the intestine (lower square) (scale bar = 100 µm). **b**, **c** – TEM images of the corresponding squares showing NiNPs ingested and about to be excreted (scale bar = 1 µm). **b'**, **c'** – Energy loss spectra confirms that the particles are made of nickel. Source: Zhou *et al.*, 2016a.

To summarise, NMs are commonly used in several fields but their risks are not yet fully understood, so new regulations will require information on their ecotoxicological effects (Werner and Hitzfeld, 2012). As a future perspective, there is the need for better methods of nanomaterials detection in biological and environmental media, also during bioassays, as well as a characterisation of the effects of weathered NMs, more representative of their environmental condition (Klaine *et al.*, 2013). There is still little information on environmental concentrations of nanomaterials, which in most cases can only be predicted (Gottschalk *et al.*, 2013), but the constant and unmonitored release of ENMs in the marine

environment can make their predicted concentrations approach acute toxicity thresholds (Corsi *et al.*, 2021; Garner *et al.*, 2017). So, while it is true that part of the scientific literature looks at high concentrations of NPs, and realistic concentrations should be tested as more is known about the real quantities of NPs in the environment (Behra and Krug, 2008), it is important to assess the sensitivity of organisms to these materials regardless of environmental values. The development of adequate test methods for NMs is currently one of the big challenges for ecotoxicologists (Werner and Hitzfeld, 2012).

1.4 Ecotoxicogenomics: overview and approaches

In recent years, with the increasing development of genomics, a new branch of ecotoxicology gradually emerged as a separate field of study: ecotoxicogenomics. Ecotoxicogenomics is a hybrid discipline that combines ecology, toxicology and genomics; it assesses the molecular mechanism of action and toxicity of substances within cells, tissues or organisms and links these results to deleterious effects at the cellular, tissue, organism, and population levels (Osachoff and van Aggelen, 2013). The term "toxicogenomics" is usually synonymous, but can imply applications closer to human toxicology with respect to environmental toxicology. According to Waters and Fostel (2004), among the main goals of ecotoxicogenomics there is identifying useful biomarkers (physiological or molecular parameters used to predict a toxic effect) of exposure to toxic substances and elucidating the molecular mechanisms of toxicity.

Historically, genomics has seen a significant rise during the last decades, most notably because of the breakthrough of new techniques and thanks to pharmaceutical industry in the 1990s: recombinant DNA technologies, improved DNA and RNA isolation methodologies, DNA sequencing, and more powerful computers (Osachoff and van Aggelen, 2013). More broadly, genomics includes the three "omics" disciplines: transcriptomics, the study of mRNA levels (transcriptome); proteomics, the study of collections of proteins (proteome); and metabolomics, which studies the products of biological processes (metabolome) (Committee on Applications of Toxicogenomic Technologies to Predictive Toxicology, 2007). Consequently, the management and analysis of all these molecular data, *i.e.* bioinformatics, is very strictly related to genomics (Osachoff and van Aggelen, 2013).

Briefly, proteomics identifies alterations in protein levels, activity and modification states, and relies for example on antibodies assays such as ELISA (Enzyme-linked immunosorbent assay) or protein separation through PAGE (polyacrylamide gel electrophoresis) followed by identification via mass spectrometry (Osachoff and van Aggelen, 2013; Waters and

Fostel, 2004). Metabolomics requires the application of nuclear magnetic resonance (NMR) spectroscopy to characterize patterns of chemical metabolites (Tennant, 2002).

Transcriptomics, or gene expression profiling, is considered a new powerful endpoint for ecotoxicology (Snell *et al.*, 2003). It relies mainly on two techniques to investigate alterations in gene expression levels: real-time quantitative polymerase chain reaction (RT-qPCR) and next generation sequencing of the whole transcriptome (RNA-seq). RT-qPCR evaluates gene expression in a quantitative manner based on the polymerase chain reaction technology, but the instrument reads the results simultaneously, as the reaction occurs. This technique is considered a gold standard for comparison across different disciplines thanks to its high throughput, reproducibility, specificity and sensitivity (Burns *et al.*, 2005). RNA-seq is a recently developed approach which, unlike hybridisation-based approaches, is not limited to detecting transcripts that correspond to existing genomic sequences, and thus is particularly important for organisms whose genomic sequences are yet to be determined (Wang *et al.*, 2009). RNA-seq allows to catalogue all RNA transcripts (including mRNAs, non-coding RNAs and small RNAs) in a cell type and to determine the transcriptional structure of genes in terms of their start sites, 5'- and 3'-ends, novel transcribed regions, splicing patterns and other post-transcriptional modifications (Wang *et al.*, 2009). In general terms, RNA-seq is most useful in species whose genome or transcriptome is still unknown, while RT-qPCR is used to precisely quantify the expression of known target genes.

One of the first ecotoxicogenomics studies investigated molecular and morphological effects on the American bullfrog, *Rana catesbeiana*, exposed to environmentally relevant concentrations of triclosan, a bactericidal agent (Veldhoen *et al.*, 2006). The authors combined RT-qPCR analyses with observations of body weight, length and developmental stage of *R. catesbeiana* and witnessed changes in the postembryonic development, a thyroid hormone-mediated process, and alterations in the expression profile of thyroid hormone receptor. This set of physiological and molecular effects is called phenotypic anchoring, and is useful to link the patterns of altered gene expression to specific parameters of well-defined, conventional indices of toxicity, so that it will be possible to search for evidence of toxicity or injury prior to its complete manifestation (Tennant, 2002). Moreover, anchoring the molecular expression profile in phenotype (for a precise time of exposure to a specific concentration) helps defining the sequence of key molecular events in the mode-of-action of a toxicant (Waters and Fostel, 2004).

As other examples of phenotypic anchoring, embryos of the sea urchin *P. lividus* were exposed to increasing concentrations of copper and fixed specific stages of development (early blastula, late gastrula and pluteus) to investigate the regulation of genes involved in

different biological processes (stress, skeletogenesis, development/differentiation, detoxification) (Morroni *et al.*, 2019). The results showed a clear correlation between the increase in morphological anomalies and the up-regulation of those genes due to copper exposure. Boran and Şaffak (2018) exposed larvae of the zebrafish *Danio rerio* to NiNPs and $NiCl_2$, and found that acute toxicity was higher for the latter; this was confirmed by DNA damage (through comet assay) and gene expression of target genes, related to stress, which were both greater after $NiCl_2$ exposure. Lastly, in another study with caged mussels (*Mytilus galloprovicialis*) to assess impacts of an offshore gas platform, effects of trace metals were analysed on several biological processes: lysosomal destabilisation, activity of acetylcholinesterase (which indicates neurotoxicity), induction of oxidative stress genes and DNA integrity (strand breaks and micronuclei) (Gorbi *et al.*, 2008).

Considering the importance of ecotoxicogenomics not only for research purposes but also for monitoring, it is clear why papers and guidelines often recommended that regulatory agencies worldwide integrate ecotoxicogenomic data and molecular biomarkers in risk assessment, among the other parameters to be considered (Benedetti *et al.*, 2012; Committee on Applications of Toxicogenomic Technologies to Predictive Toxicology, 2007; Regoli *et al.*, 2014).

1.5 Ecotoxicogenomics of copepods

Finding model species is crucial in marine ecotoxicological and ecotoxicogenomics studies. Such species should be abundant, widely distributed, ecologically relevant and experimentally manageable in the laboratory, and they should help elucidate acute, chronic and development toxicity of pollutants. Copepods meet all these conditions, and their potential in ecotoxicology has long been recognised (Raisuddin *et al.*, 2007) (please refer to chapter 1.1 for more information). Increased understanding of copepod physiology (monitored with endpoints such as survival, development, growth, fecundity, respiration and swimming behaviour) is important also because it can help both to predict how natural copepod populations will respond to environmental change and to optimize live-feed production for aquaculture, two emerging issues (Tarrant *et al.*, 2019).

Aquatic toxicology is generally more focused on freshwater rather than marine water (Leung *et al.*, 2001). In fact, one of the first and most common crustacean species used for ecotoxicology studies is the freshwater branchiopod *D. magna* (Kulkarni *et al.*, 2013), employed since the 1930s (Naumann, 1934). For marine ecosystems, one of the most relevant order of copepods for ecotoxicology is Harpacticoida, most notably the genus *Tigriopus*

Norman, 1868. The most important species within the genus include *Tigriopus japonicus* (western Pacific), *T. brevicornis* (northern Europe), *T. californicus* (western America) and *T. fulvus* (southern Europe); other marine Harpacticoida include *Amphiascus tenuiremis*, *Nitocra spinipes* and *Tisbe battagliai* (reviewed by Raisuddin *et al.*, 2007).

Tigriopus japonicus has been adopted since the 1970s in ecotoxicity tests in studies of effects of cadmium and copper on its development (D'Agostino and Finney, 1974). More recently, Wang and Wang (2010) exposed adults of *T. japonicus* to $NiCl_2$ (up to 3 mg/L) for a period of up to 12 days, and demonstrated that nickel affected the biochemical detoxification pathway (such as metallothioneins and superoxide dismutase) and induced neurotoxicity in the copepod due to increased acetylcholinesterase activity. *Tigriopus japonicus* adults were also exposed to environmentally realistic concentrations of endocrine disruptor bisphenol A (BphA), and it resulted in reproductive depression and delayed egg hatching (Dahms *et al.*, 2017). The authors concluded that such response might depend on the ecology of this specific taxon; *T. japonicus* is in fact a sediment-ingesting species, and BphA is easily bound to sediments (Dahms *et al.*, 2017).

Tigriopus fulvus, on the other hand, is indicated as a test organism in an Italian ecotoxicological method for risk assessment (UNICHIM, 2014). This method was tested in an inter-laboratory comparison (Faraponova *et al.*, 2016) to apply and validate the bioassay protocol, consisting in the exposure of larval stage of *T. fulvus* to increasing concentrations of copper for 96 h and the evaluation of its mortality rate as endpoint. *Tigriopus fulvus* is now one of the available species which can be chosen to test marine sediments in studies of ecological risk assessment, according to Italian legislation (DM 173, 2016).

A similar inter-laboratory study was performed with the calanoid copepod *A. tonsa* exposed to $NiCl_2$ (Gorbi *et al.*, 2012). *A. tonsa* is one of the most common model species used in ecotoxicology, mentioned in different ISO (International Organization for Standardization) protocols (see chapter 1.6.1). Besides *A. tonsa*, two other copepod species are mentioned in ISO standardised protocols: the harpacticoids *Tisbe battagliai and Nitocra spinipes* (ISO, 1999).

Within calanoids, another species used in ecotoxicology is the estuarine *Eurytemora affinis*, employed since the 1970s with a broad range of contaminants (Raisuddin *et al.*, 2007). For example, this species was exposed to naphthalene and three of its methylated forms in acute and chronic exposure: acute exposure resulted in toxicity levels proportional to the number of methyl groups, whereas chronic exposure caused significant reductions in life length, egg production and mean brood size (Ott *et al.*, 1978). Sullivan *et al.* (1983) exposed *E. affinis* to copper and cadmium, and reported that both heavy metals reduced

swimming velocities and development rates of nauplii. A protocol was proposed for a bioassay with nauplii of *E. affinis*, to test the chronic toxicity of elutriates of sediments, with mortality and growth rates as endpoints (Lesueur *et al.*, 2013). More recently, Das *et al.* (2020) used a multigenerational, lifecycle trait approach to study the effects of heavy metals and resuspended polluted sediments through different generations of *E. affinis*.

As pointed out by Tarrant *et al.* (2019), studies regarding physiological status of model organisms must be supported by a molecular approach to gain a comprehensive mechanistic understanding of copepod physiology following toxic exposure (the so called "ecotoxicogenomic approach"). Most of the copepod species studied in ecotoxicogenomics are members of Order Calanoida (*A. tonsa*, *E. affinis*, *Calanus spp*.); other represented species belong to Orders Harpacticoida (*Tigriopus spp.* and *Tisbe holoturiae*), Cyclopoida (*Apocyclops royi* and *Paracyclopina nana*) and Siphonostomatoida (the parasitic species *Lepeophtheirus salmonis* and *Caligus rogercresseyi*) (reviewed by Tarrant *et al.*, 2019). There is a growing diversity of species, whose ecological importance drives molecular physiology studies (Tarrant *et al.*, 2019).

In general, commonly used biomarker genes for RT-qPCR analyses in copepods exposed to stressors include, among others: catalase (CAT), cytochrome P450 (CYP), glutathione synthase and S-transferases (GSS, GSTs), heat-shock proteins (HSPs), superoxide dismutase (SOD) and vitellogenin (VTG) (Tarrant *et al.*, 2019). The expression of these genes is triggered by several environmental agents, including heavy metals, endocrine disruptors and organic pollutants. In particular, antioxidant enzymes like catalases and superoxide dismutases are involved in quenching reactive oxygen species (ROS). ROS are compounds harmful for the organism, normally formed in metabolic reactions (as reported in chapter 1.3) but they occur more often under exposure to environmental contaminants or generic stress conditions (Tarrant *et al.*, 2019; Wang and Wang, 2010). Heat-shock proteins are molecular chaperons involved in the folding and transport of proteins, and in repairing damaged proteins; they are usually up-regulated in response to increased temperature, exposure to xenobiotics and generic stress (Aufricht, 2005; Kadiene *et al.*, 2020; Rhee *et al.*, 2009). Cytochromes are enzymes which belong to phase I metabolic processes, involved in converting xenobiotics to a form which is less toxic for the organism or to a form that can be excreted in phase II (Kadiene *et al.*, 2020). The family of glutathione-related enzymes are involved in phase II detoxification reactions, *i.e.*, the conjugation of reduced glutathione (GSH) to the xenobiotic, facilitating its excretion (Lauritano *et al.*, 2021; Lee *et al.*, 2008a). As an example, the expression of ten glutathione S-transferase (GST) genes was studied in adults of *T. japonicus* exposed to different trace metals such as arsenic, cadmium, copper, silver (Lee *et*

al., 2008a); the study showed that the expression of GSTσ was highly up-regulated in trace metal-exposed copepods and that this gene might be an important biomarker of exposure to trace metals in *T. japonicus*. Finally, vitellogenin is a precursor to several egg yolk proteins and it has been proposed as a marker of the reproductive condition in copepods (Lee *et al.*, 2008b; Tarrant *et al.*, 2019).

Compared to the "gene of interest" approach, "omic" studies enable identification of wider set of genes and pathways affected by contaminants. So far, seven copepod genomes have been sequenced and assembled: *E. carolleeae* (Eyun *et al.*, 2017), *E. affinis* (Choi *et al.*, 2021), *Oithona nana* (Madoui *et al.*, 2017), *T. californicus* (Barreto *et al.*, 2018), *T. kingsejongensis* (Lee *et al.*, 2020), *T. japonicus* (Jeong *et al.*, 2020), *A. tonsa* (Jørgensen *et al.*, 2019). However, functional genomic studies involving transcriptome sequencing and *de novo* assembly are particularly important in ecotoxicogenomics, as they provide information on differential gene expression, *i.e.*, transcripts and unigenes that are most or least expressed, with respect to control, after a specific treatment. For example, a toxicogenomic study conducted on the calanoid *Pseudodiaptomus annandalei* exposed to $NiCl_2$ (Jiang *et al.*, 2013), showed up-regulation of transcripts involved in cellular cytoskeleton, metabolism, antioxidant defence and stress responses.

Recently, two transcriptomes of *A. tonsa* have been published: one following exposure to NiNPs (Zhou *et al.*, 2018) and the other to handling stress and salinity shock (Nilsson *et al.*, 2018). In particular, the *de novo* assembled transcriptome by Zhou *et al.* (2018), generated with *A. tonsa* adults exposed to NiNPs for 4 days, identified about 17,000 unigenes, of which 373 were differentially expressed (mostly down-regulated, ribosome-related genes). The transcriptome of *A. tonsa* adults subject to handling stress and salinity shock for 10 min, on the other hand, revealed 276 and 573 differentially expressed genes respectively, indicating that these factors too influence transcriptional patterns (Nilsson *et al.*, 2018); hence, attention has to be paid also to copepod maintenance.

1.6 Species of interest

1.6.1 Acartia tonsa

One of the species of interest for the aims of my PhD project is the calanoid copepod *Acartia* (*Acanthacartia*) *tonsa* Dana, 1849 (World Register of Marine Species, 2022) a species distributed worldwide in temperate and subtropical regions. Despite being euryhaline and tolerating salinities from 5 to 35 PSU (practical salinity unit) (Miller and Marcus, 1994),

and also tolerating sudden changes in salinities (Calliari *et al.*, 2008), it is typically confined to brackish waters (about 30 PSU salinity) (Belmonte and Potenza, 2001). This species is also documented to be eurytherm, being able to adapt to temperatures ranging from − 1 to 32°C (Gonzalez, 1974). It is a filter feeder species with a strong mechanosensory capability, to sense hydrodynamic disturbances, avoid predators and capture prey (Paffenhöfer, 1991).

As for other calanoid copepods, the development of *A. tonsa* is indirect, and it comprehends 11 phases before the adult (**Figure 1.4**). After the hatching of the egg, which has a diameter of about 80 µm, there are six naupliar phases (NI-NVI; larval stage), then five copepodite phases (CI-CV; juvenile stage), which then moult into adults. At temperatures between 15 and 20°C, eggs hatch to nauplii within 48 h, and after 5-6 days they metamorphose into copepodids; the adult stage is reached usually after 12-20 days post hatching (**Figure 1.5**). Males are usually 800 µm long, and their first pair of antennae are curved in the first segments; females are 1000 to 1500 µm long (Buttino *et al.*, 2019).

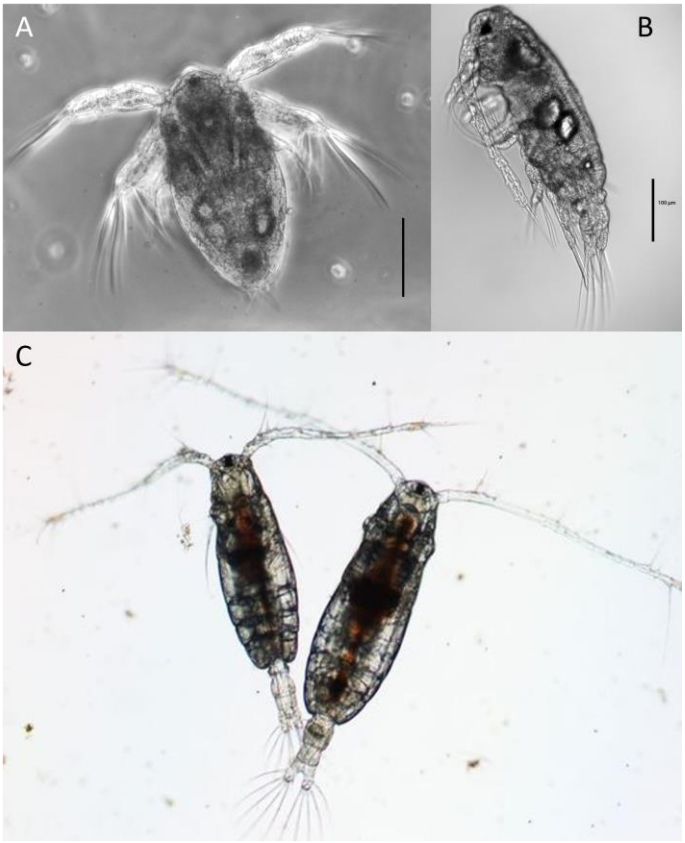

Figure 1.4 Life stages of *Acartia tonsa*. **A** – Nauplius (larva) (scale bar = 50 µm); **B** – copepodid (juvenile) (scale bar = 100 µm); **C** – male (left) and female (right) adults. The male is slightly smaller and its first antennae are curved in the first segments. Source: modified from Buttino *et al.*, 2019.

Acartia tonsa was first proposed for marine pollution studies in 1977 (Lee, 1977). Since then, this species has been reared in laboratories for environmental research studies

and for monitoring effects of different substances and conditions: for instance, various pH and dissolved oxygen values (Invidia *et al.*, 2004; Marcus *et al.*, 1997), algal toxins (Vargas *et al.*, 2006), marine polluted sediments (Carotenuto *et al.*, 2020), crude oil with chemical dispersant (Almeda *et al.*, 2014), microplastics (Syberg *et al.*, 2017), nanomaterials (Zhou *et al.*, 2016a). Studies with this species have also regarded the optimisation of rearing and feeding protocols (Zhang *et al.*, 2013) and the possibility of preserving eggs at low temperatures (Vitiello *et al.*, 2016). Depending on the geographical area, several strains of *A. tonsa* can be defined: Atlantic, Baltic and Mediterranean strains, each one having slight physiological differences in egg production or egg type (Hansen *et al.*, 2016).

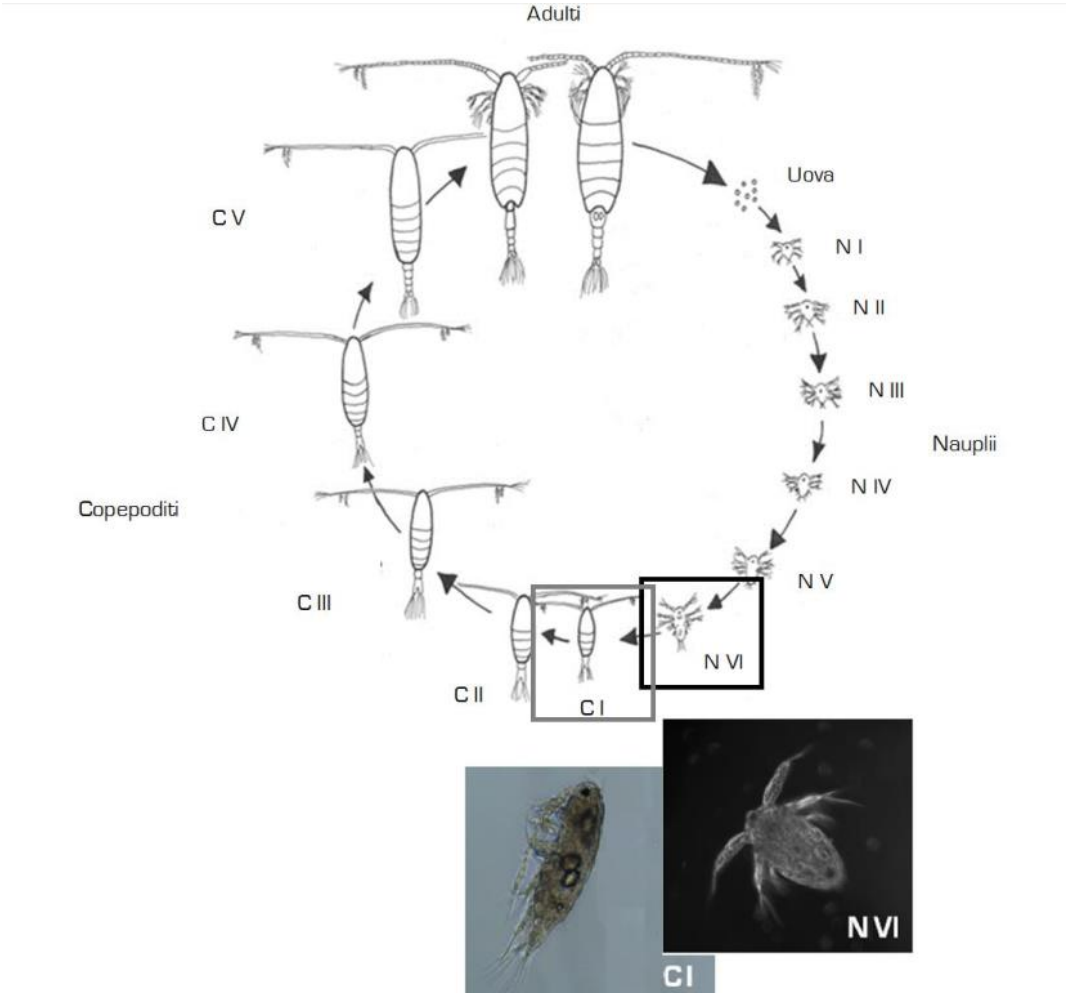

Figure 1.5 Schematic of the complete lifecycle of *A. tonsa*. Uova: egg; copepoditi: copepodids; adulti: adults; N: naupliar stage; C: copepodid stage. See text for details. Source: Buttino *et al.*, 2019.

Nowadays *A. tonsa* is widely used for environmental risk assessment to evaluate the quality of marine matrices with standardised bioassays (or toxicity tests). There are different standardised test protocols based on the analysis of different endpoints (such as egg hatching success, larval and adult mortality, larval development ratio), whose alterations affect

productivity and offspring recruitment of the species. These are the test protocols commonly used for *A. tonsa*:

- Acute test (UNICHIM, 2012a). The required stage is the egg and the endpoint is the percentage of immobilisation or mortality of the hatched nauplii after 48 h of exposure. The ISO standard is similar but the required stage is copepodid V or adult (ISO, 1999).
- Semichronic test (UNICHIM, 2012b). The required stage is the egg and the endpoint is the percentage of immobilisation or mortality of the hatched nauplii after 7 days of exposure.
- Larval development ratio (LDR) test (Buttino *et al.*, 2018; ISO, 2015). The required stage is the egg and the endpoint is the ratio between juveniles (copepodids) and larvae (nauplii) after a certain number of days of exposure, depending on the time needed to obtain more than 50% adult stages in the control.

Moreover, *A. tonsa* has been recently included in the aforementioned decree of the Italian legislation as one model organism that can be used to test the quality of marine sediments, in order to define their final use (DM 173, 2016).

The main concern with the employment of *A. tonsa* in ecotoxicology is that in the Mediterranean Sea it is considered an invasive species, introduced in the 1980s in the northern Adriatic Sea (first documented by Gaudy and Viñas, 1985) probably due to human activities such as extensive aquaculture (Belmonte and Potenza, 2001). Within a few years, it had become the dominant planktonic copepod species in a lagoon of the Po river (Sacca di Goro lagoon, northern Adriatic Sea), resulting in a reduction of diversity or even in the disappearance of formerly abundant species, most notably *Acartia margalefi* and *Paracartia latisetosa* (Sei *et al.*, 1996).

A recent study analysed datasets of mesozooplankton from 1975 to 2017 in the Lagoon of Venice (northern Adriatic Sea) (Camatti *et al.*, 2019). The authors found no significant increases of *A. tonsa* abundance in the period 1997-2002; however, they suggested that this species might take advantage of eutrophic ecosystems, because its abundance was positively associated with increases in temperature, phytoplankton, particulate organic carbon (POC), chlorophyll a, and counter gradient of salinity, and also because it increased locally in one eutrophic station. Lastly, in the years 2014-2017, *A. tonsa* was found to be the dominant *Acartia* species in the Lagoon of Venice (Camatti *et al.*, 2019).

The current distribution of *A. tonsa* in the Mediterranean describes it as an alien species in Adriatic, Aegean, Baltic, Black, Ionian (Greek part), North and Marmara Sea (World Register of Marine Species, 2022).

Considering this, and given the high adaptability of *A. tonsa* to different environmental conditions, the use of this species as a model organism for ecotoxicological bioassays in areas where its distribution is not recorded could represent a risk, which is why it is suggested to investigate the possibility of using native species (Carotenuto *et al.*, 2020).

1.6.2 Acartia clausi

The second species of interest for my PhD project is the calanoid copepod *Acartia* (*Acartiura*) *clausi* Giesbrecht, 1889 (World Register of Marine Species, 2022). *Acartia clausi* is a worldwide-distributed species in temperate regions and native of the Mediterranean Sea; it is mainly coastal and neritic, not entirely adapted to brackish waters (Belmonte and Potenza, 2001; Sei *et al.*, 2006). *Acartia clausi* is considered euryhaline and eurytherm, tolerating ranges of salinities from 0 to 36 PSU (Gaudy *et al.*, 1989) and being found at temperatures ranging from − 1 to 30°C (Lee and McAlice, 1979). *Acartia clausi*'s lifecycle and morphology are very similar to those of *A tonsa*; morphological differences of the two species lie in the fifth leg and are shown in **Figure 1.6** (ICRAM, 2006).

The main difference between the two species of interest, however, is their distribution and ecology. In the Mediterranean Sea *A. clausi* is considered one of the most important species of its genus and is described as the most common species in the family *Acartiidae* in the entire Ponto-Mediterranean Province (Belmonte and Potenza, 2001). In the Gulf of Naples (Tyrrhenian Sea) *A. clausi* is the dominant copepod species from spring to summer, and the second most important species in terms of annual averages (Mazzocchi *et al.*, 2012). In particular, highest abundances of this species are recorded from April to July, with a peak in June, whereas in late autumn and winter *A. clausi* is very rarely encountered (Mazzocchi *et al.*, 2012). **Figure 1.7** depicts the distribution of *A. clausi* in the Mediterranean Sea as of July 2022.

In the Northern Adriatic Sea, *A. clausi* and *A. tonsa* show a clear spatial separation, with the first typically inhabiting coastal areas with higher seawater influence and the latter being restricted to brackish waters (Belmonte and Potenza, 2001). However, there are cases, in Atlantic temperate regions, in which the two species coexist (Lee and McAlice, 1979).

Acartia clausi's physiology and ecology have been studied over the years. For instance, studies focused on temperature and salinity effects on metabolism (Gaudy *et al.*, 2000), effects of algal toxins (Guisande *et al.*, 2002), egg tolerance to anoxic and sulfidic conditions (Sei *et al.*, 2006), algal diet and carotenoid content (Nobakht *et al.*, 2016), effect of temperature on fatty acids transfer (Werbrouck *et al.*, 2016). This species was also found

suitable as live food for rearing larvae of Asian seabass, for aquaculture purposes (Rajkumar and Kumaraguru vasagam, 2006).

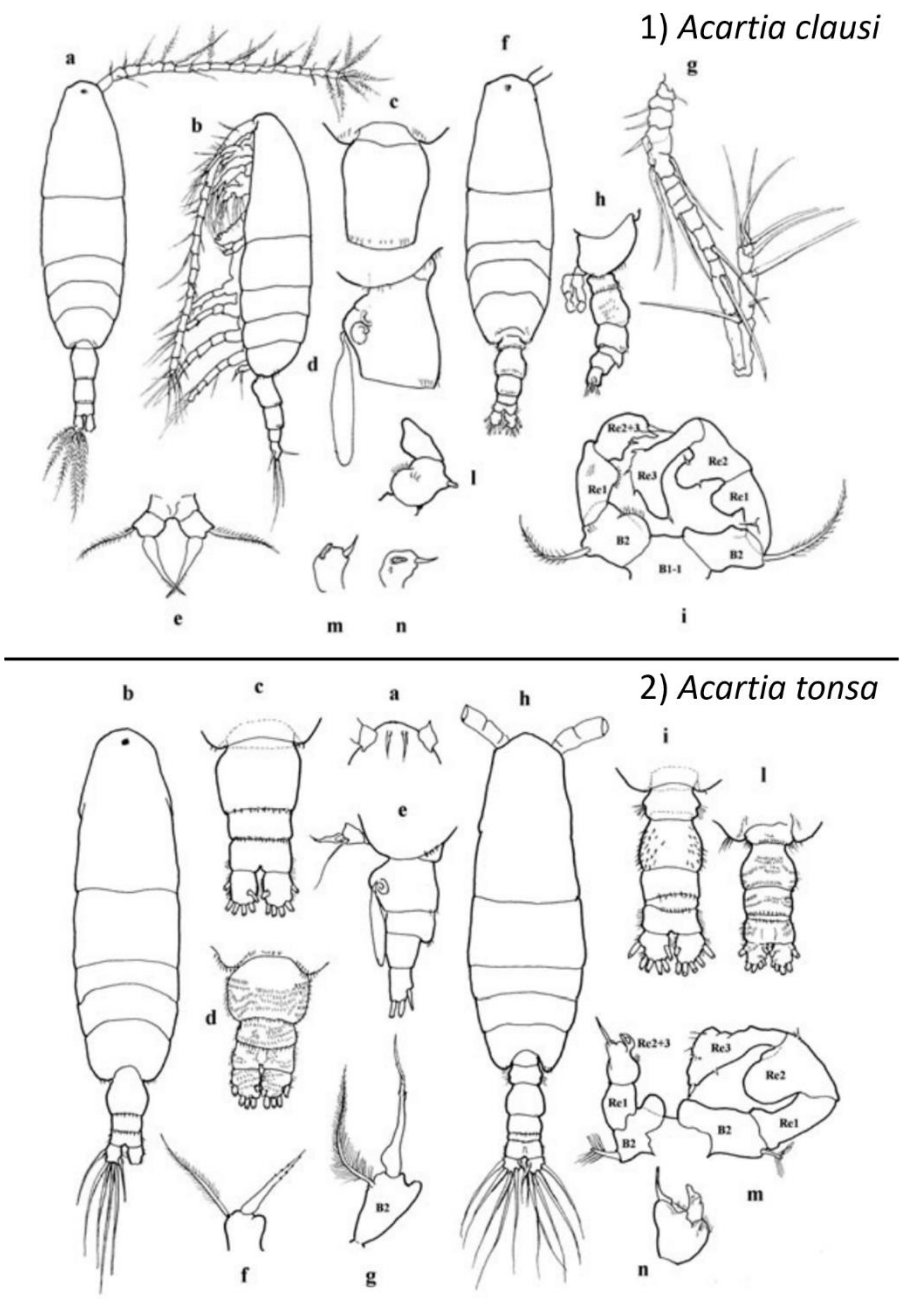

Figure 1.6 Morphology of *Acartia clausi* and *Acartia tonsa* adults.
1) *A. clausi*. Female: **a**-**e**. **d** – Side view of first segment of the urosome (genital segment) with spermatheca; **e** – fifth leg. Male: **f**-**n**. **h** – Side view of urosome; **i** – fifth leg (modified for mating).
2) *A. tonsa*. Female: **b**-**g**. **e** – Side view of urosome with spermatheca; **f**-**g** – fifth leg (left ramus). Male: **h**-**n**. **i**-**l** – Dorsal view of urosome; **m** – fifth leg (modified for mating). Source: modified from ICRAM, 2006.

Despite *A. clausi* has rarely been used in ecotoxicological bioassays (Carotenuto *et al.*, 2020), in recent years there has been an increasing interest for ecotoxicology application with this species. The pilot work by Buttino (1994) was one of the first studies to analyse

effects of phenol and ammonia on *A. clausi*'s egg production and viability, as well as on faecal pellet production; while recently, for example, Beiras *et al.* (2019) developed a method to test microplastics toxicity with *A. clausi* larvae. *Acartia clausi* is also mentioned in the APAT-ICRAM Italian guidelines as a species that can be used to test toxicity of marine sediments (APAT-ICRAM, 2007).

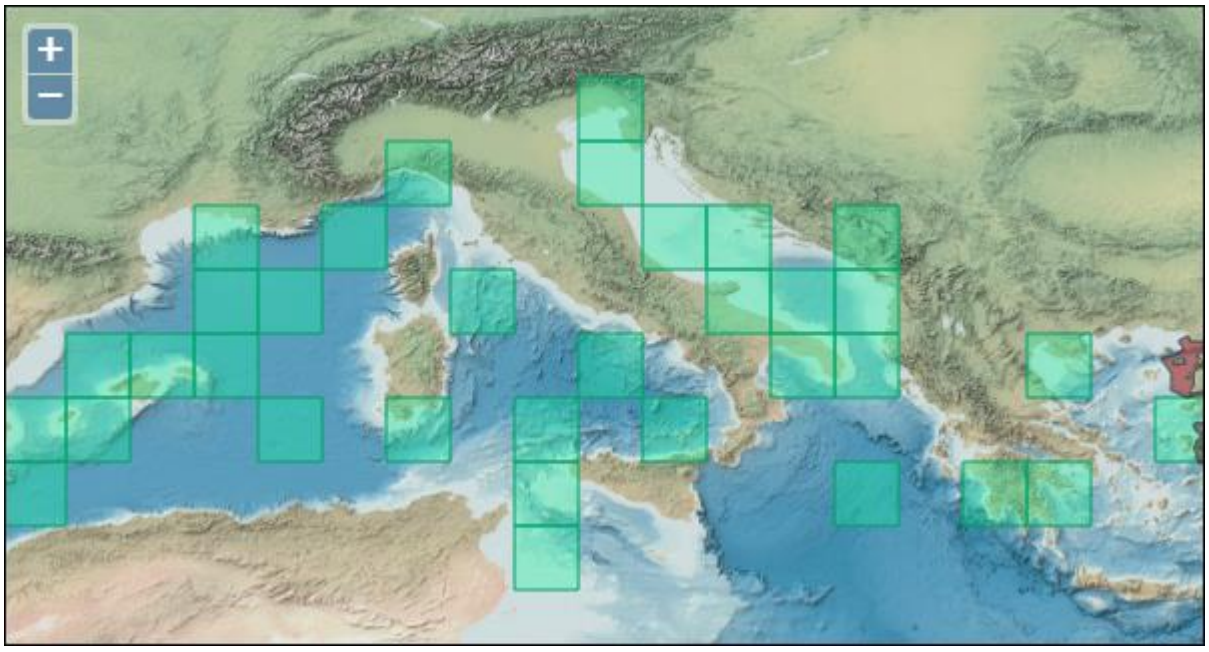

Figure 1.7 Distribution of *Acartia clausi* in the Mediterranean Sea as of July 2022. Green boxes indicate indigenous occurrence. Source: World Register of Marine Species, 2022.

Concerning molecular biology studies applied to *A. clausi*, this species is not among the most studied copepods in this research area (Tarrant *et al.*, 2019), but studies are emerging. For example, Lindeque *et al.* (2013) developed a method to distinguish resting eggs of the Acartiidae family (among which *A. clausi*) at the species level through PCR analysis of the mitochondrial cytochrome oxidase I (COI) gene. The same biomarker gene has also been used in a recent integrative taxonomy study in the Gulf of Naples, which assessed copepod species diversity at morphological and molecular level (Di Capua *et al.*, 2022). Recently, Semmouri *et al.* (2020) identified *A. clausi* specimens in a zooplankton community through metatranscriptomics analysis based on ribosomal 18S transcripts. However, these molecular taxonomy studies are relatively useful for ecotoxicology and more functional genomics studies are needed in the future.

Considering this, *A. clausi* has the ecological relevance and the potential to be used in ecotoxicology and ecotoxicogenomics studies. As mentioned in the previous chapter, in fact, *A. tonsa* is widely used as model organism in ecotoxicology, but it can pose a threat to the biodiversity of local communities of the Mediterranean Sea, being an alien species. *Acartia*

clausi could be used as an alternative species, more representative of the Mediterranean Sea. It is then important to gain more information about *A. clausi*'s sensitivity to environmental pollutants, both from an ecological and a molecular point of view, considering that gene expression analyses are regarded as powerful tools for ecotoxicology and are encouraged for an ecotoxicogenomic approach (Snell *et al.*, 2003), and that it is recommended to go beyond the use of standard model organisms, especially when studying ENMs, in order to increase the knowledge on the impacts on biota (Corsi *et al.*, 2021).

1.7 Aims and research questions

The aim of my PhD project is to evaluate the suitability of the copepod *A. clausi* as model organism in ecotoxicological studies. This evaluation was done using both a toxicological and a molecular approach, comparing the results obtained for *A. clausi* with those obtained for *A. tonsa* exposed to the same toxicants, *i.e.*, the reference toxicant nickel chloride ($NiCl_2$) and the emerging contaminant nickel nanoparticles (NiNPs).

The first aim was to analyse, for the first time, the long-term physiological responses and sensitivity of a multigenerational *A. tonsa* culture reared in laboratory. Briefly, I examined the results of ecotoxicological tests performed over 8 years with a culture of *A. tonsa*; these results constituted a set of historical control data (HCD) which I displayed by the means of control charts, a graph that allows to assess the statistical stability of a specific dataset over time. I also compared our HCD with the reference values suggested by previous studies on *A. tonsa,* with the final aim of confirming the constant sensitivity and robustness of this species as a model in ecotoxicology when reared for the long term.

The second aim was to evaluate the suitability of *A. clausi* to be maintained in laboratory conditions over multiple generation, in order to test its feasibility as a model species. In this way it can be available throughout the year, regardless of the seasonal cycle, also for laboratories not equipped for zooplankton sampling; moreover, bioassays conducted using organisms reared in controlled laboratory conditions are less influenced by unpredictable natural conditions occurring in wild populations (Raisuddin *et al.*, 2007). Throughout the PhD I have been rearing *A. clausi*, sampled in the Gulf of Naples, under laboratory-controlled conditions through multiple generations. As explained above, egg production and larval viability are some of the key endpoints for bioassays, and they both depend on food quality and quantity (Zhang *et al.*, 2013). So, I tested the most efficient algal diet for *A. clausi* and monitored the population growth with a weekly census over the rearing period.

The third aim of this PhD was to perform ecotoxicological tests on both copepod species, and compare their responses to the same toxicants ($NiCl_2$ and NiNPs). First, I performed the standard test methodologies on *A. tonsa* exposed to the toxicants at the appropriate concentrations, based on the available scientific literature. The purpose was to confirm previous results (Zhou *et al.*, 2016a), and most importantly, to have comparable data on the concentrations tested on *A. clausi*, using the same stock solutions of toxicants. I used the following bioassays, each one with a specific target phase of the copepod lifecycle, duration and endpoint:

- Acute test, in which egg hatching success and immobilisation of early life stages are recorded after 48 h of egg exposure.
- Chronic test, which evaluates daily female productivity, in terms of egg production rate, egg hatching success, faecal pellet production and adult survival, during 4 days of adult exposure.

Finally, I performed the toxicity tests mentioned above, with both $NiCl_2$ and NiNPs, on *A. clausi.* NiNPs had already been tested on *A. tonsa* (Zhou *et al.*, 2016a), but to our knowledge there are no information on their effects on *A. clausi*.

In order to characterise the two toxicants at the two tested salinities (one for each species), so to rule out possible differences or alteration in the behaviour of the substances due to salinity, I also performed two types of chemical analyses: inductively coupled plasma-mass spectrometry (ICP-MS), to quantify the amount of dissolved nickel ions in the stock solution and in the test vessels, and dynamic light scattering (DLS), to measure size of nanoparticles and possible formation of aggregates.

The fourth aim of my PhD was to compare the molecular response of the two copepod species. I exposed adult females of *A. tonsa* and *A. clausi* to both toxicants, at the same concentrations used for the corresponding chronic test and for the same duration (4 days), and then collected them for subsequent total RNA extraction, cDNA retrotranscription and quantitative gene expression analysis by RT-qPCR. The genes of interest (GOI) approach was chosen to compare gene expression responses in the two copepod species exposed to the same toxicant. For *A. tonsa*, the reference transcriptome used for gene mining, choosing GOI and designing specific primers was that of Zhou *et al.* (2018). However, as we did not know *a priori* whether *A. tonsa* specific primers would have also amplified the same genes in *A. clausi*, and since there are no other available transcriptomes for this species, we generated and functionally annotated a *de novo* assembled transcriptome of *A. clausi* exposed to polluted sediments. This transcriptome was used to design primers specific for *A. clausi*, amplifying the same functional genes selected for *A. tonsa*.

GOI for both copepod species were selected preferably among the differentially expressed genes (DEGs) of both transcriptomes, with a focus on genes involved in detoxification (catalase, superoxide dismutase, glutathione-related enzymes), reproduction (vitellogenin), neurological functions (acetylcholinesterase), generic metabolism (chitinase), muscular functions (myosin heavy chain), and others. Lastly, RT-qPCR analysis was used to assess the relative expression of GOI in both copepod species exposed to the toxic treatment vs. control copepods.

The final, overarching aim was to propose *A. clausi* as an alternative model organism for ecotoxicogenomic studies, and to give a further tool of investigation for marine ecological risk assessment in coastal areas.

The specific research questions are:

- Are *A. tonsa*'s physiological parameters in toxicity tests stable, when reared for the long term in a multigenerational culture?
- Can a multigenerational culture of *Acartia clausi* be reared in laboratory conditions all over the year?
- How does *Acartia clausi* respond to toxicants, both in terms of physiology (egg production, egg hatching success, larval and adult mortality) and gene expression (RT-qPCR of genes involved in reproduction, detoxification, neurotoxicity, and others)?
- Do *Acartia tonsa* and *A. clausi* have different sensitivity to the same toxicants, in terms of physiological endpoints and gene expression?
- Is *Acartia clausi* a valid candidate model organism in ecotoxicogenomics? Can this species be alternative to *A. tonsa* in risk assessment studies in coastal areas?

Chapter 2 Analysis of historical control data of ecotoxicological bioassays with *Acartia tonsa*

The material in chapter 2 forms the basis of the paper "Rotolo F., Vitiello V., Pellegrini D., Carotenuto Y., Buttino I. (2021). Historical control data in ecotoxicology: eight years of tests with the copepod *Acartia tonsa*" published in the journal Environmental Pollution, in which I played a major role.

2.1 Introduction

Ecotoxicological studies play a paramount role in environmental risk assessment and biomonitoring of the oceans; through exposure of test organisms we can forecast possible consequences of environmental pollution on marine organisms (Brooks *et al.*, 2019; Gorbi *et al.*, 2012; Smeti *et al.*, 2007). The calanoid copepod *A. tonsa* is considered a model species in this area of research and is broadly reared in laboratory conditions and used in ecotoxicological studies to elucidate short-term (acute) and long term (chronic) effects of chemicals (please refer to chapters 1.5 and 1.6.1 for more information on this species).

The Mediterranean strain of *A. tonsa*, typically confined to brackish waters of coastal lagoons and river estuaries of the Northern Adriatic Sea (Belmonte and Potenza, 2001), has never been observed to produce diapause or oligopause eggs until now; on the other hand, its subitaneous eggs can be maintained viable at low temperatures (4°C) for up to one year, with slight reductions of egg hatching success over time (Vitiello *et al.*, 2016). The possibility to successfully cold-store eggs is extremely useful because it allows to obtain biological materials for ecotoxicological bioassays in due time, regardless of the seasonal cycle of the model organism.

Bioassays, or toxicity tests, are used to monitor specific biological parameters, called endpoints, whose alterations may affect productivity and offspring recruitment of the species (Buttino *et al.*, 2018).They often include a reference toxicant as a reliable and certain method

to evaluate the status and sensitivity of the test species (Lee, 1980), which for *A. tonsa* is nickel chloride ($NiCl_2$), proposed as reference toxicant in various interlaboratory comparisons (Gorbi *et al.*, 2012) and in guideline protocols (UNICHIM, 2012a).

The most frequent bioassays with *A. tonsa*, include a short-term acute toxicity test, which evaluates naupliar immobilisation or mortality (Environment and Climate Change Canada, 2019; Gorbi *et al.*, 2012; UNICHIM, 2012a) and adult mortality (ISO, 1999; US EPA, 1976) after 48 h of exposure. The acute test is probably the most reproducible and versatile method to assess potential toxicity of environmental matrices with *A. tonsa*. For example, it has been performed to assess the quality of elutriated derived by marine sediments (Buttino *et al.*, 2018; Carotenuto *et al.*, 2020), toxicity of microplastics and antibacterial agents (Syberg *et al.*, 2017) and nanomaterials (Zhou *et al.*, 2016a). During the last decade, the Italian Institute for Environmental Protection and Research (ISPRA) has routinely performed acute tests with *A. tonsa* exposed to marine matrices. Such dataset represents a unique opportunity to analyse historical control data (HCD) of this species.

HCD are values compiled from previous studies performed under similar conditions (same methods and species), which can be useful to identify the normal response for a specific experimental setup, and therefore determine when a value might be outside the norm (Brooks *et al.*, 2019). The main tools for grouping and analysing HCD are control charts, which are useful to recognise and adjust anomalies in a variety of processes (Smeti *et al.*, 2007). These charts, originally developed to easily manage the quality of manufactured products (Shewhart, 1931), were later proposed for use in clinical laboratories to verify the reliability of tests (Levey and Jennings, 1950). Control charts display a central line (mean of the dataset) and statistically determined upper and lower control limits (UCL and LCL, respectively), usually set at mean ± 3 SD (standard deviation) and mean ± 2 SD, to determine whether a state of statistical control exists among observations in the dataset, *i.e.,* if the process did not change over time (ISO, 1991, 2007).

Nowadays control charts are still used in clinical laboratories (Coskun, 2006), and they found use also, for example, for prenatal molecular diagnosis (Weng *et al.*, 2020), for microbiological (Eissa, 2016) or chemical (Arciszewski *et al.*, 2018) analyses of waters. Historical control data are commonly used in the interpretation of mammalian toxicology studies for human safety assessment, but are less used in environmental toxicity studies, probably because of the lack of guidelines, despite representing a valuable tool for interpretation (Brooks *et al.*, 2019). However, in some cases, control charts have been used to compare small datasets of environmental toxicology. For example, control charts were used to assess changes in cell sensitivity of the benthic diatom *Cylindrotheca closterium* after exposure to

copper sulphate (the reference toxicant), at different concentrations and conditions; the resulting EC_{50} (effective concentration which induces effects on 50% of the tested population of organisms) were plotted in a standard sensitivity control chart (Araújo *et al.*, 2008). In another study, control charts were made to compare physiological parameters (like body weight and fork length) of fishes captured in a polluted river over several years, and to compare historical data of population censuses (Arciszewski *et al.*, 2017). Chronic toxicity bioassay for soil with the earthworm *Eisenia foetida* was tested with different reference toxicants (in order to find the most suitable), and the results were plotted in control charts (Yeardley *et al.*, 1995). To our knowledge, however, no historical control data are published for *A. tonsa*.

In this chapter, we analysed a dataset composed of 59 acute tests conducted with *A. tonsa* over eight years, from December 2012 to December 2020, at ISPRA Livorno, and generated Shewhart-like control charts (ISO, 1991). The dataset included mean values of egg hatching success (HS) and naupliar immobilisation (NI) in seawater (negative control), and EC_{50} of reference toxicant $NiCl_2$ (positive control), after 48 h of egg exposure. The aim was to analyse, for the first time, a historical dataset of physiological responses of *A. tonsa*, to confirm the stability of these parameters and the robustness of this species in ecotoxicology, when reared in a multigenerational culture for the long term. We also compared our HCD with the reference values reported in previous studies (Gorbi *et al.*, 2012), in order to compare the sensitivity of *A. tonsa* to the same toxicants over time and assess the stability of the copepod culture. In the methods section below, the experimental details of *A. tonsa* culture and acute tests carried out at ISPRA (Livorno, Italy) are described. Although these experiments were not specifically conducted during the present PhD study, we are reporting the methodological procedure for completeness and clarity of data analysis.

2.2 Materials and methods

2.2.1 Acartia tonsa *culture*

The Mediterranean strain of *Acartia tonsa*, originally obtained from cultures coming from the Northern Adriatic Sea, is presently reared, over multiple generations, at the Plankton Laboratory (ISPRA) since 2008. The original gene pool was never renewed by addition of new wild specimens collected at sea. Copepods were kept in 20 L propylene tanks, containing filtered seawater (FSW) at salinity 30 PSU. Seawater was collected in an unpolluted site along the Tyrrhenian coast (South of Livorno), filtered onto 0.22 µm mesh and brought

to the required salinity with the addition of distilled water. Culture was maintained in a thermostatic chamber at 20 ± 1°C and 14:10 L:D photoperiod, with low intensity artificial light, and the water content was partially renewed monthly. A light bubbling was granted in each container through a glass pipette. The density of the population in the tanks did not exceed 100 ind/L to favour high egg production (Zhang *et al.*, 2015).

Acartia tonsa culture was fed twice a week on a mixed algal diet of *Isochrysis galbana*, *Rhinomonas reticulata* and *Rhodomonas baltica*, collected during their exponential growth phase, at the final concentration of 1500 µg C/L. This concentration represents the optimal carbon concentration to support high egg production rate and larval survival of *A. tonsa* (Zhang *et al.*, 2013). Algal strains were cultured using f/2 growth medium without silicates (Zhang *et al.*, 2013).

2.2.2 Acute test

Acute tests of naupliar immobilisation (NI) with *A. tonsa* were performed according to the reference methods, with few modifications (Gorbi *et al.*, 2012; UNICHIM, 2012a). Briefly, groups of about 50 eggs were transferred in crystallising dishes filled with 10 mL of FSW at 30 PSU (negative control) or $NiCl_2$ at different concentrations (positive control). Eggs were either collected the day of the test or used after cold-storage at 4°C for a maximum of one month, since this time did not reduce the percentage of egg hatching success (HS) (Vitiello *et al.*, 2016). Under a stereomicroscope (M80, Leica Microsystems, Milan, Italy), two eggs were gently collected from the vessel with a Pasteur pipette and transferred into a 2.5 mL well of a 24-well plate, filled with 2.5 mL of the relative treatment; plates were incubated in a thermostatic chamber at 20 ± 1°C, 14:10 L:D photoperiod. The tests were performed in three replicates of five wells each, for a total of 10 eggs for each replicate and 30 for each treatment.

A stock solution of nickel chloride hexahydrate ($NiCl_2 \times 6\ H_2O$, Carlo Erba Reagents, Milan, Italy) at concentration of 1000 mg/L was diluted with distilled water to a nominal concentration of 10 mg/L, corresponding to a dissolved Ni concentration of 10.0 ± 0.09 mg Ni/L, measured with ICP OES 720 (Agilent Technologies, Santa Clara, California) (Vitiello *et al.*, 2016). From this stock, final concentrations of 0.4, 0.2, 0.1 and 0.05 mg Ni/L were obtained through serial dilutions in FSW.

Egg HS and NI were evaluated after 48 h of exposure by inspecting wells under an inverted microscope (Nikon TMS). Nauplii were considered immobilised or dead if after

15 s of observation and after physical stimulation they did not actively swim. The percentage of egg HS was calculated as follows:

$$\text{HS}\ (\%) = \frac{\text{HE}}{\text{HE} + NHE} \times 100$$

Where HE represented the number of hatched eggs and NHE the number of non-hatched eggs. The percentage of NI was calculated as follows:

$$\text{NI}\ (\%) = \frac{\text{IN}}{\text{HE}} \times 100$$

Where IN represented the number of immobilised or dead nauplii.

The test was considered acceptable if the negative control had egg HS ≥ 80% and NI ≤ 20%, and if EC_{50} of $NiCl_2$ in positive control was 0.24 ± 0.12 mg Ni/L after 48 h exposure (Gorbi *et al.*, 2012; UNICHIM, 2012a). EC_{50} was calculated using PROBIT Analysis version 1.5 (UNICHIM, 2012a).

2.2.3 Historical control data analysis

The historical control data analysed here included acute tests with *A. tonsa* conducted over eight years, from December 2012 to December 2020, for a total of 59 bioassays. Within this group, 35 tests included data of positive control, exposed to $NiCl_2$, for which the corresponding EC_{50} were calculated. For each bioassay, the following values were considered: mean and standard deviation (SD) of percentage of egg HS and percentage of NI, for negative and positive control and EC_{50}.

Data were arranged in a Shewhart-like control charts, displaying the mean (central line) ± SD (control limits) of the whole dataset; to show variability of the data with respect to the mean value, mean ± 1 SD, mean ± 2 SD and mean ± 3 SD were also indicated (ISO, 1991, 2007).

For negative control, four separate control charts were made: 1) means of egg HS, 2) SD of means of egg HS, 3) means of NI, 4) SD of means of NI. Measures of location and dispersion within the sample (*i.e.* average and SD of the individual test runs) were arranged in separate control charts as suggested by the protocols (Baudo *et al.*, 2015; ISO, 1991, 2007). Analyses and graphical representations were made using GraphPad Prism version 6.01.

2.3 Results

Historical control data of acute tests with *A. tonsa* are shown in **Figures 2.1** and **2.2**. **Figure 2.1A** shows mean percentage of egg HS of *A. tonsa* in negative control; every single value fell within the control limits of mean ± 3 SD and only two values were lower than mean − 2 SD, being 70% (18th run) and 69.55% (46th run). Only 6 out of 59 single test runs (10.2%) were below the reference value (≥ 80%) (UNICHIM, 2012a). The highest value being 96.67% (5th run) and the lowest 69.55% (46th run). Overall, the average of egg HS was 85.60% ± 5.90 SD.

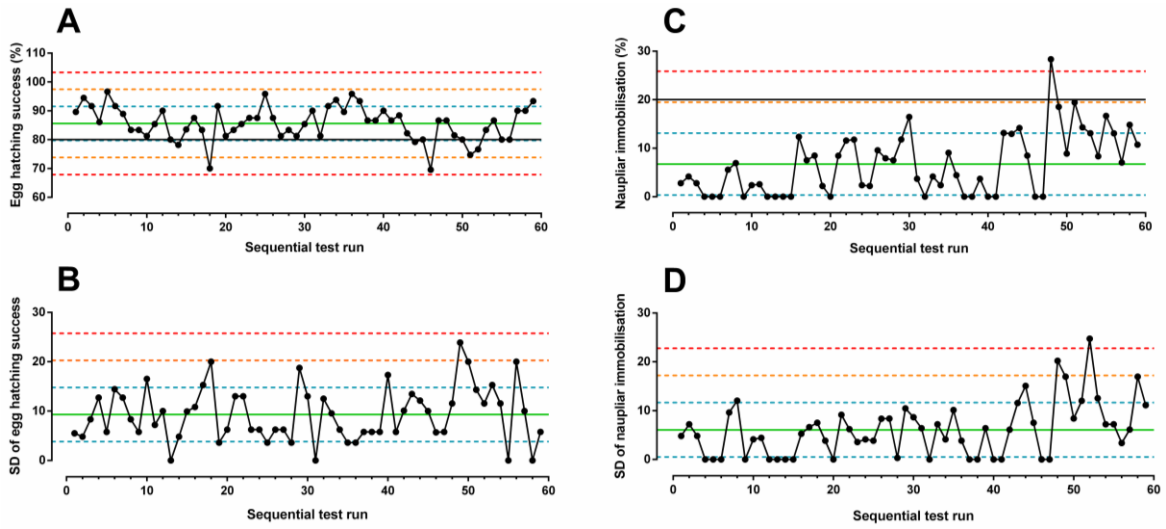

Figure 2.1 Shewhart-like control charts of historical data of negative controls in acute tests with *Acartia tonsa*, from December 2012 to December 2020. **A** – Percentage of egg hatching success (HS). **B** – Standard deviation (SD) of percentage of egg HS. **C** – Percentage of naupliar immobilisation (NI). **D** – SD of percentage of NI. The X axis shows sequential test runs, corresponding to independent bioassays during the investigated period. For each run, the value is the average of three replicates. The green line represents the mean of the dataset; cyan dashed lines indicate mean ± 1 SD, orange dashed lines indicate mean ± 2 SD and red dashed lines show mean ± 3 SD. Black lines indicate the reference values: 80% for egg HS (**A**), 20% for NI (**C**) (Gorbi *et al.*, 2012; UNICHIM, 2012a).

Control chart for SD of mean percentage of egg HS showed an average SD of 9.32% (**Figure 2.1B**); the lowest value (0%) occurred 4 times (13th, 31st, 55th 58th run), and in only one case a value exceeded mean + 2 SD (upper orange line), which was also the highest value in the dataset (23.88%, 49th run).

Mean percentage of NI, recorded in acute tests performed with *A. tonsa* during the analysed period, is shown in **Figure 2.1C**. On average, the dataset showed a mean value of 6.73% ± 6.38 SD, with 16 tests having NI of 0%. Every value in the dataset fell within the

range of mean + 2 SD except one, which was the highest value, exceeding mean + 3 SD (28.33%, 48th run). This value was the only one to exceed the reference values suggested by Gorbi et al. (2012) as ≤ 20%.

The distribution of standard deviation for the percentage of NI in negative controls, is shown in **Figure 2.1D**. A mean of 6.08% ± 5.56 SD was generated for the overall dataset, which showed only one value higher than the mean + 2 SD (20.21%, 48th run) and one which exceeded the mean + 3 SD (24.75%, 52nd run).

As for the control chart of EC_{50} of $NiCl_2$ (mg Ni/L), a mean of 0.135 ± 0.047 mg Ni/L was generated for the whole dataset analysed **(Figure 2.2)**. The lowest value was 0.002 mg Ni/L (3rd run) and the highest 0.191 mg Ni/L, which recurred twice (18th and 34th test). All values but three fell within the range of mean ± 2 SD, having EC_{50} of 0.002, 0.011 and 0.036 mg Ni/L, respectively, on runs 3, 4 and 5; these three values, however, did not exceed the mean − 3 SD.

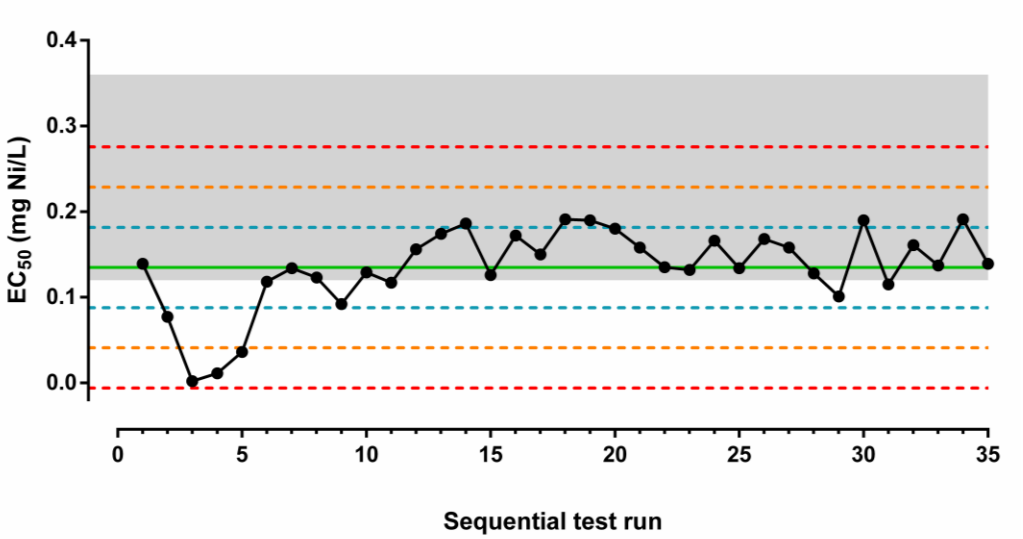

Figure 2.2 Shewhart-like control chart of historical data for EC_{50} of $NiCl_2$ (mg Ni/L) (positive control) in acute tests with *Acartia tonsa*, from December 2012 to December 2020. The X axis shows sequential test runs, corresponding to independent bioassays during the investigated period. The green line represents the mean of the dataset; cyan dashed lines indicate mean ± 1 SD, orange dashed lines indicate mean ± 2 SD and red dashed lines show mean ± 3SD. The grey area corresponds to the interval of mean ± SD of the reference values (0.24 ± 0.12 mg Ni/L) (Gorbi *et al.*, 2012; UNICHIM, 2012a).

2.4 Discussion

The copepod *Acartia tonsa* is reared in laboratory with the advantage of reducing the variability of environmental factors in controlled conditions (Buttino *et al.*, 2018; Lee, 1977); moreover, laboratory culture enables to synchronise *A. tonsa* life stages, which are

the target endpoint in standardized bioassays (Environment and Climate Change Canada, 2019; ISO, 1999, 2015; UNICHIM, 2012b). On the other hand, it is known that inbreeding might negatively affect growth, survival rate and immune response in reared crustaceans (Moss *et al.*, 2007; Wang *et al.*, 2020). This does not seem to have occurred in our culture, despite being reared in laboratory conditions since 2008 without replenishments of organisms from wild populations. Similar findings, concerning behaviour and reproduction, were recorded for *A. tonsa* culture maintained in laboratory conditions for 12 years (Tiselius *et al.*, 1995). The authors compared cultured and wild populations of *A. tonsa* and evaluated egg production and feeding behaviour. Cultured specimens, despite being roughly the 120th generation of the same population, had half the feeding activity with respect to wild organisms, yet they produced twice as many eggs, and they remained more time in patches of food-rich water (Tiselius *et al.*, 1995).

Our data on egg HS, naupliar viability and sensitivity to a reference toxicant, arranged in Shewhart-like control charts, in fact showed that these physiological parameters for *A. tonsa* were homogeneous, with respect to the mean value of the whole dataset, over long-term periods, confirming they are stable and reliable endpoints for this species reared in laboratory. The culture maintained good and stable percentages of egg HS and naupliar viability, and a constant sensitivity, in terms of EC_{50} for acute test exposure, to the reference toxicant.

Regarding the percentage of egg HS, the low level of variability over time is confirmed by the fact that 96.6% of test runs fell within the mean ± 2 SD and 71.2% fell within the mean ± 1 SD limit (ISO, 1991). Our control chart referred to SD of egg HS, revealed that no test runs had values of SD higher than the upper control limit (+ 3 SD) defined in international guidelines, confirming that each value in the means control chart was statistically stable (ISO, 1991). The standardised methods suggest a value ≥ 80% for egg HS, as validation parameter (Gorbi *et al.*, 2012; UNICHIM, 2012a). Six of our tests had sub-optimal percentages of egg HS and, according to the protocols mentioned above, should have not been considered as good controls in bioassays. However, following naupliar viability of those hatched eggs, two of these tests showed NI equal to 0% (14th and 46th runs), and the others were all below the reference value of 20%. Hence, we suggest not to exclude *a priori* bioassays in which egg HS percentage was below 80%, when NI remains below 20%. In fact, in our long-term observations, a low percentage of egg HS was sometimes uncorrelated with a low naupliar viability, which is the final endpoint in acute tests.

Overall, the mean percentage of NI recorded in our long-term analyses (6.7%) is well below the reference limit of 20% proposed in literature (Gorbi *et al.*, 2012) as a validation

parameter for ecotoxicological tests. We noticed that, only in the last runs of the dataset, both mean and SD of NI were above the mean value, with one value falling above both the + 3 SD control limit and the reference value. However, the overall mean + 2 SD (19.5%) remained lower than the reference limit, suggesting the robustness of our data. Here we confirm the suitability of such a long-term *A. tonsa* culture for bioassays and of the well-adopted rearing protocols. Both egg HS and naupliar viability can be considered as good and stable physiological parameters for such species reared in laboratory.

As for the control chart including data of EC_{50} for the reference toxicant $NiCl_2$, our dataset appeared homogenous as well, with most of the values (74.3%) comprised within the mean ± 1 SD limit. Only 3 out of 35 observations (8.6%) had values outside the mean ± 2 SD. For these three test runs, however, both egg HS and NI in the controls were in line with the respective mean values; this made us consider that the quality of egg batches used for these test runs was comparable to the quality of batches used for other tests. It is possible, hence, that such lower EC_{50} values were related to an intrinsic variability in the biological response of the naupliar stage to the reference toxicant. Mean and SD values of egg HS (%), NI (%) and EC_{50} of $NiCl_2$ (mg Ni/L) generated from the whole dataset over the investigated period, are summarised in **Table 2.1** and compared with the reference values (Gorbi *et al.*, 2012; UNICHIM, 2012a). Overall, the mean value of EC_{50} calculated here was lower than that proposed in the interlaboratory study (Gorbi *et al.*, 2012) (0.135 ± 0.047 mg Ni/L; n = 35 vs 0.24 ± 0.12 mg Ni/L, respectively). However, looking at the specific results obtained by the participating members (eight laboratories and one reference laboratory), our values appear closer to those obtained by the reference laboratory (0.198 ± 0.048 mg Ni/L; n = 6) and by one participant (0.139 ± 0.036 mg Ni/L) (Gorbi *et al.*, 2012). Similar EC_{50} for $NiCl_2$ were obtained in other acute tests with *A. tonsa* (0.13 mg Ni/L) (Carotenuto *et al.*, 2020). Considering also that our long-term dataset, spanning over eight years of tests, was continuously lower than the suggested reference value (Gorbi *et al.*, 2012), we propose for acute tests an EC_{50} of 0.14 ± 0.09 mg Ni/L for the Mediterranean strain of *A. tonsa* exposed to $NiCl_2$, calculated considering the mean ± 2 SD of our HCD. The approach of doubling the SD when proposing new reference limits is adopted by literature and guidelines (Gorbi *et al.*, 2012; UNICHIM, 2012a).

Despite HCD represent a valuable tool for data interpretation, they are not commonly used in environmental toxicity studies (Brooks *et al.*, 2019). To the best of our knowledge, in fact, this is the first report of historical control data and control charts regarding physiological parameters of a copepod species reared over multiple generations. Studies in which *A. tonsa* populations have been reared over several years or decades, did not provide values

of HS and/or naupliar viability over time (deMayo *et al.*, 2021; Drillet *et al.*, 2008, 2011b; Krause *et al.*, 2017; Tiselius *et al.*, 1995). As a future perspective, it is advisable that other laboratories, which perform routine bioassays and in possession of long-term datasets, made their own control charts, in order to allow data comparison, establishment of new reference intervals and improvement of test protocols (Brooks *et al.*, 2019).

Table 2.1 Overall mean and SD values of egg HS (%), NI (%) and EC_{50} of $NiCl_2$ (mg Ni/L) for acute test, from historical control data (HCD) with *A. tonsa*, from December 2012 to December 2020. † n = 59; †† n = 35; * corresponding reference values (Gorbi *et al.*, 2012; UNICHIM, 2012a).

Parameter	**Historical control data**	**Reference values ***
Egg hatching success (%)	85.60 ± 5.90 †	≥ 80
Naupliar immobilisation (%)	6.73 ± 6.38 †	≤ 20
EC_{50} of $NiCl_2$ (mg Ni/L)	0.135 ± 0.047 ††	0.24 ± 0.12

In conclusion, our study demonstrated that the Mediterranean strain of *A. tonsa,* reared in laboratory conditions since 2008 without replenishments of organisms from wild populations, maintained overall good and stable physiological parameters in terms of production of healthy eggs and offspring. This reinforces the suitability of such species for ecotoxicological studies when reared in multigenerational culture for at least 12 years.

Chapter 3 Multigenerational rearing of *Acartia clausi*

3.1 Introduction

The development of methodologies for rearing copepod cultures in laboratory conditions, available throughout the year, is important for *in vivo* laboratory studies regarding copepod physiology and aquaculture. There is a need for reliable multigenerational cultures as copepods are required in research fields such as phylogeny, biology and ecology, including the availability of copepods for toxicity testing in bioassays (Drillet *et al.*, 2011a). Improved understanding of copepod physiology can also help to predict the response of natural copepod populations to environmental change (Tarrant *et al.*, 2019).

There are several advantages for multigenerational culturing of copepods for toxicity testing, as opposed to collect specimens *in situ*, such as not depending on seasonal cycle of the species, reducing the variability of unknown environmental factors and synchronising life stages (Anahi *et al.*, 2014; Mazzocchi *et al.*, 2012). The group of Hansen and collaborators at the Roskilde University (Denmark) started a continuous laboratory culture of *Acartia tonsa* in 1981 with these purposes; this decadal culture is still used nowadays for toxicological studies (Drillet *et al.*, 2011b). A multigenerational culture of *A. tonsa* has also been reared at ISPRA Livorno laboratories since 2008 for testing acute and chronic toxicity of marine environmental matrices, and a recent study showed that physiological parameters of cultured copepods and their response to the reference toxicant both remained stable and optimal throughout the years, confirming the suitability of this species for ecotoxicological studies also after years of culturing (Rotolo *et al.*, 2021; please refer to chapter 2). In recent years, different research works have been published regarding the laboratory rearing of *A. tonsa*. In particular, a focus was addressed on optimisation of monoalgal diets to maximise egg production rates, egg hatching success, naupliar viability and adult survival (Zhang *et al.*, 2013), and another on effects of population density and food concentrations on fecundity and feeding rate of adult copepods (Zhang *et al.*, 2015); algal diet and crowding are two parameters which could improve protocols for the multigenerational culturing of *A. tonsa* for ecotoxicological purposes.

Other examples of optimisation of multigenerational rearing of copepods regard the Mediterranean species *Temora stylifera* and *Centropages typicus* (Buttino *et al.*, 2012). The authors proposed a pilot re-circulating system for culturing of these species, which maximised offspring production by concentrating naupliar and copepodid stages, in view of studying larval physiology or responses to ecotoxicological tests (Buttino *et al.*, 2012). Similarly,

a large volume re-circulating system was proposed for rearing the copepod *Calanus helgolandicus*, in view of obtaining healthy individuals of any stage which could be used for eco-physiological or molecular studies throughout the year (Carotenuto *et al.*, 2012).

Another relevant application of culturing copepods through multiple generations is in the aquaculture field. The use of copepods as live feed for planktivorous fishes and fish larvae is in fact preferred over the traditional diet of *Artemia salina* nauplii and rotifers, and is one of the recent open challenges for aquaculture (Drillet *et al.*, 2011a; Olivotto *et al.*, 2008a, 2009). Copepods have higher contents of highly-unsaturated fatty acids (HUFAs), biomolecules essential for growth and development of the fish, as compared to traditional diets of *Artemia salina* nauplii and rotifers (*Brachionus spp*.) (Rasdi and Qin, 2016). Particularly, they are very rich in the omega-3 family such as docosahexaenoic acid (DHA; C22:6n−3), eicosapentaenoic acid (EPA; 20:5n−3) and arachidonic acid (ARA; 20:4n−6) (Payne and Rippingale, 2001); this fraction of fatty acids can be further increased by feeding them microalgae that are pre-enriched on nutrients like N, P and C (Rasdi and Qin, 2016). In addition, their typical springing movements stimulate a feeding response in larvae (Bengston, 2007), and their naupliar stages are small and more suitable as live feed of fish larvae (Payne and Rippingale, 2001).

Rearing copepods in laboratory-controlled cultures at high density is, however, not easy (Payne and Rippingale, 2001). The most represented Orders are Calanoida, Harpacticoida and Cyclopoida (Ajiboye *et al.*, 2011). Calanoid copepods are reported to not tolerate high densities and therefore require large volumes, making it more difficult to optimise ideal rearing protocols (Støttrup, 2006). On the other hand, harpacticoid copepods are relatively easy to rear at high density but they are benthic species and this limits their access to foraging fish larvae, unlike the calanoids, which are pelagic species (Ajiboye *et al.*, 2011; Støttrup, 2006). The use of cyclopoid copepods is more common for freshwater aquaculture but is not widespread as some species are not entirely digested by fish larvae or even predate directly on the fish larvae (Ajiboye *et al.*, 2011). The main copepod species reared for marine aquaculture are *Acartia tonsa*, *A. tsuensis*, *Eurytemora affinis*, *Schizopera elatensis*, *Tisbe holoturiae* and *Tigropus japonicus* (reviewed by Ajiboye *et al.*, 2011).

The calanoid copepod *Acartia clausi* has rarely been reported as live feed for fish larvae. Biochemical analyses showed that this species is a rich source of omega-3 fatty acids and it has higher protein and lipid content with respect to *A. salina* nauplii and rotifers (Rajkumar and Kumaraguru vasagam, 2006). The same study also demonstrated that larvae of Asian seabass fed with reared *A. clausi* adults had greater weight gain and survival ratio compared to non-copepod diets (Rajkumar and Kumaraguru vasagam, 2006). The nutritional

profile of this copepod species can also be improved through algal diets: it was proven that copepods fed a mixed diet of the haptophyte *Isochrysis galbana* and the diatom *Chaetoceros calcitrans* had higher total carotenoid contents (antioxidant pigments, essential for protecting cells from light and other stressors) with respect to the same species as a monoalgal diet (Nobakht *et al.*, 2016). To our knowledge, however, in scientific literature there is no data on multigenerational cultures with this copepod species reared for ecotoxicological purposes.

In view of the growing interest in using *A. clausi* for ecotoxicology, optimisation of rearing protocols is needed. In this chapter, we will present data from the culture of *A. clausi*, which was continuously reared under laboratory-controlled conditions through multiple generations, throughout several months of two years. Population dynamics and diet optimisation will be discussed, in view of proposing *A. clausi* as a species feasible to rear in plankton laboratories.

3.2 Materials and methods

3.2.1 Zooplankton collection, culture maintenance and population census

Zooplankton samples for multigenerational cultures were collected throughout two years, during late spring and summer (from May to September 2020, and from June to August 2021) in the Gulf of Naples, at the long-term ecological research station MareChiara (LTER-MC; Zingone *et al.*, 2019), using a 200 µm Nansen net. Within 1 h from the sampling, collected zooplankton was transferred to the laboratory, and *Acartia clausi* adult copepods were sorted under a stereomicroscope (MZ12, Leica, Milan, Italy; 4× magnification) to start laboratory cultures.

Cultures started with a variable number of adults (from tens to hundreds of copepods, depending on specimen density in the sampling). *A. clausi* adults were incubated into glass beakers of 3 or 5 L, depending on the density of specimens, which did not exceed 100 ind/L to favour high egg production (Zhang *et al.*, 2015). Beakers were filled with 0.22 µm filtered seawater (FSW) at a salinity of 37 PSU, collected from the same site of the zooplankton sampling, and kept in a thermostatic chamber at 20 ± 2°C, at 12:12 h light:dark photoperiod, with slight aeration provided through a glass pipette. Every week cultures were cleaned by partially renewing water and checking salinity. Any operation with copepods required filtering a volume of culture with specific mesh sizes, depending on the developmental phase which was to be isolated. Specifically:

- 300 μm mesh for the isolation of adults;
- 150 μm mesh for the isolation of copepodids;
- 50 μm mesh for the isolation of nauplii and eggs.

After filtration, filters were gently backwashed into Petri dishes and copepods were transferred back to glass beakers with renewed FSW and algal food.

On few occasions, adults were added to the culture after a sampling, or were removed from the culture when they were needed for a specific ecotoxicological test. Besides the main culture, in fact, occasionally we maintained smaller cultures of adults to obtain eggs for bioassays, or cultures with only eggs and nauplii produced by cultured adults.

According to the study of Zhang *et al.* (2013), the following algal species are considered the optimal diet for multigeneration cultivation of *A. tonsa*, and are used for *A. clausi* as well:

- *Rhodomonas baltica* (Cryptophyta – Cryptophyceae) (CCAP 979/9, SZN_FE202), "RHODO", cellular volume ≈ 942 μm^3;
- *Rhinomonas reticulata* (Cryptophyta – Cryptophyceae) (CCAP 995/2, SZN_FE208), "RHINO", cellular volume ≈ 321 μm^3.

Algae were cultured in 500 mL vented flasks, using f/2 growth medium without silicates (Guillard, 1975). Copepod cultures were fed twice a week a mixture of the two algae, collected in the exponential growth phase, provided at a concentration of 750 μg C/L each, for a total carbon concentration of 1500 μg C/L. It corresponded to a cellular concentration of 0.6×10^4 cells/mL and 1.35×10^4 cells/mL, respectively for RHODO and RHINO, calculated using their cellular volume. This amount was identified by Zhang *et al.* (2013) as the optimal carbon concentration to support maximum egg production rates and larval survival of *A. tonsa*. To assess algal density, a small aliquot of each culture was taken, fixed with Lugol solution (Sigma-Aldrich Life Science, Milan, Italy), left to settle in a Sedgewick Rafter counting chamber and then counted at an inverted microscope (Axioskop 2 MOT, Zeiss, Oberkochen, Germany; 10× magnification).

Throughout the cultivation period, separately for 2020 and 2021, we performed weekly censuses of the culture, to assess the density of the main developmental phases and their population dynamics. Population census started after 10 weeks from the establishment of the cultures in 2020 (due to closure caused by COVID-19 pandemic) and after 2 weeks in 2021. A sample of 50 mL was taken from the culture beaker with a wide mouth 25 mL pipette, in two replicates, after gentle agitation. Samples were placed in a Petri dish, and nauplii, copepodids, females and males were counted under the stereomicroscope. Values of abundances

in the 50 mL sample were then converted in abundances per litre of culture (ind./L, *i.e.*, individual per litre), and the average of the two samples was calculated.

3.2.2 Feeding experiment

To standardise the best protocol to obtain *A. clausi* in good physiological conditions for subsequent ecotoxicological bioassays, we analysed the effects of each unialgal diet on egg production, egg hatching success, faecal pellet production and adult survival, in order to identify the most suitable for this species.

As suggested in standardised protocols (ISO, 2015) and in the literature (Zhang *et al.*, 2013), each diet was provided at a cell density corresponding to a carbon concentration of 1500 µg C/L, specifically:

- RHODO: 1.2×10^4 cells/mL;
- RHINO: 2.7×10^4 cells/mL.

Couples of male and female adult copepods, collected from the laboratory culture, were transferred in crystallising dishes containing 50 mL of FSW and one of the two algal diets. Dishes were incubated in a thermostatic chamber at 20 ± 2°C, 12:12 h light:dark photoperiod, kept on a shaking plate (Labortechnik KS 125 Basic, IKA, Staufen, Germany) with slight agitation (70 RPM), to prevent algal sedimentation. After 24 h, each couple was transferred in a new crystallising dish with fresh medium, every day for 15 days. Soon after transfer, crystallising dishes were inspected under an inverted microscope (Axiovert 25, Zeiss, Oberkochen, Germany; 2.5× magnification) to count laid eggs, faecal pellets and adult mortality. Samples were incubated again at the same conditions, and after 48 h were fixed with absolute ethanol (Sigma-Aldrich Life Science, Milan, Italy; 10% of total volume). Hatched eggs were then counted at the inverted microscope and the percentage of egg hatching success was calculated using the formula described in chapter 2.2.2. The test with each alga was performed with 6 replicates.

Differences in egg production rate and faecal pellet production between the two algal diets and among days were analysed using a two-way ANOVA, followed by a Bonferroni's multiple comparison test. Percentages of male and female survival were calculated using a survival curve and results were tested with a Log-rank (Mantel-Cox) test.
Statistical analyses were performed using GraphPad Prism version 6.01 (GraphPad Software Inc., San Diego, California, USA).

3.3 Results

3.3.1 Population census

Results of census surveys performed weekly for two cultures of *A. clausi*, in terms of relative abundances of nauplii, copepodids, adult males and females, are shown in **Figure 3.1** (red stars in the graphs indicate times in which specimens were added to the culture after a sampling or removed from the culture when needed for a specific test).

Acartia clausi population reared in 2020 from May to September showed a fluctuating pattern in naupliar density throughout the months, with recurring peaks of about 300 ind./L at about every 30 days (on day 1, 35, 63 and 84) (**Figure 3.1A)**. A similar fluctuating pattern was observed for copepodids, whose peaks in abundances followed those of nauplii after one week of rearing (day 7 and 42), with values of 40-60 ind./L. However, after the high density measured on day 49, copepodid abundances constantly decreased till the end of the census (119 days). Adults, on the other hand, had a more stable trend, with abundances slightly lower with respect to copepodids. Males had higher abundances, except for the first two observations, where females were more abundant (day 1 and 7, with 50 and 30 ind./L, respectively).

The almost three-weeks gap from day 85 to 103 corresponded to the vacation period and the closure of the SZN during August. Despite this break, during which *A. clausi* was fed with algae supplemented through a peristaltic pump, the culture was still viable, with a maximum of 30 males and 30 females per litre on day 112 and 119, respectively. Those adults were then employed in the ecotoxicology bioassays (see chapter 4) and the census was stopped.

In 2021, the culture of *A. clausi* reared from June to August showed a different trend compared to 2020, with relatively high naupliar abundances during the first 14 days and a gradual but constant increase of nauplii until a maximum density of 500 ind./L reached on day 42 (**Figure 3.1B**); this peak was followed by an abrupt reduction the subsequent week. Abundance values and trends were similar among adults and copepodids, ranging from 10 to 20 ind./L in most surveys. It is to be noted that the highest value of relative abundance of females (30 ind./L, day 14) was followed by the increase in nauplii mentioned above.

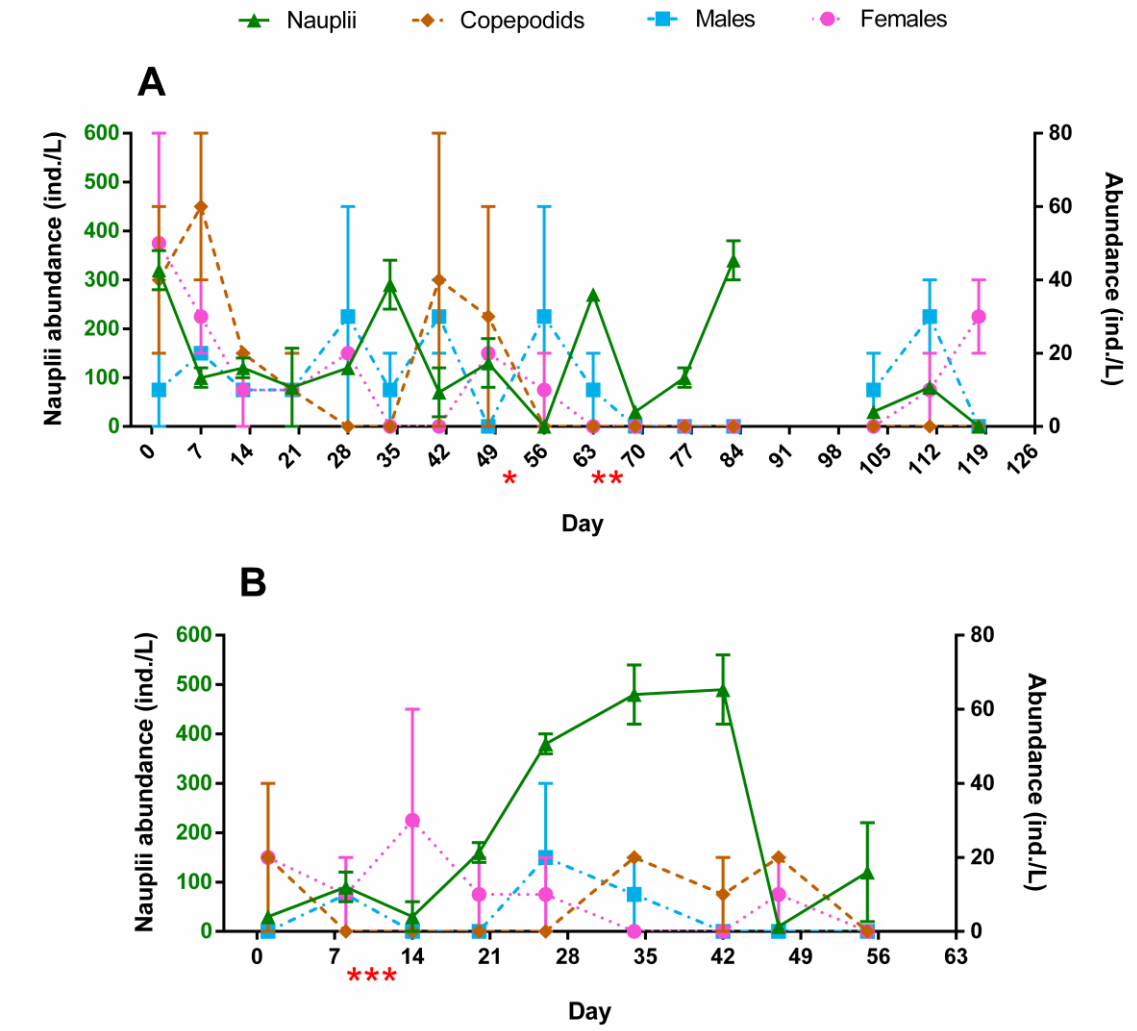

Figure 3.1 Weekly censuses of *Acartia clausi* cultures, showing temporal dynamics and relative abundances of nauplii (left Y axis) and of copepodids, adult males and adult females (right Y axis), in terms of ind./L. **A** – Culture reared in 2020, from May to September. * Between the two dates, 20 males and 20 females were added; ** between the two dates, 7 males and 16 females were added. **B** – Culture reared in 2021, from June to August. *** Between the two dates, 18 males and 18 females were removed. Values are mean ± SD; n = 2.

3.3.2 Feeding experiment

Figure 3.2 shows the results of the 15 days feeding experiment with adults of *A. clausi* fed a monoalgal diet of RHODO and RHINO.

Values of egg production (EP) (eggs/f) (**Figure 3.2A**) were highest with RHODO for the first two days (14.4 ± 6.0 and 11.8 ± 1.3 eggs/f, respectively) (average ± standard deviation); however, from the third day this value decreased until the end of the experiment reaching 1.5 ± 0.7 eggs/f. Egg production of *A. clausi* fed RHINO showed a fluctuating pattern, with increasing values until day 4 (10.6 ± 4.7 eggs/f), followed by a subsequent reduction until day 7, and a second peak in EP on day 10 (8.5 ± 3.4 eggs/f). On average over the 15

days experiment, *A. clausi* produced 3.5 ± 4.2 eggs/f and 5.2 ± 3.2 eggs/f with RHODO and RHINO, respectively. A two-way ANOVA followed by a Bonferroni's multiple comparison test indicated that there was a statistically significant difference in EP between the two diets during the 15 days experiments, and specifically on days 1, 4 and 10 ($F_{(1, 94)} = 8.651$; $p = 0.004$). The same test also showed that differences were significant between first and last day for RHODO diet only ($F_{(14, 94)} = 8.104$; $p < 0.0001$). However, the interaction term (which indicates the combined effect of both time and diet) for this test was significant ($F_{(14, 94)} = 3.291$; $p = 0.0003$), thus indicating that the effect of each variable on EP also depended on the value of the other variable.

Figure 3.2B depicts percentages of egg hatching success. The RHINO diet supported a very high egg hatching throughout the 15 days experiment, with values ranging from 68.8 ± 19.2% to 100.0 ± 0.0% in the first eight days; for the remaining period values were still above 60%, except for day 10, 14 and 15 (30.7 ± 15.12%, 16.7 ± 28.9% and 0.0 ± 0.0%, respectively). On the other hand, RHODO diet induced very low hatching success in *A. clausi* from the first day of the experiment (31.3 ± 6.7%), which then continued decreasing reaching 0.0 ± 0.0% from day 7 until the end of the incubation. Average values of egg HS over the whole tested period were 7.16 ± 10.60% for RHODO and 67.87 ± 30.03% for RHINO. Differences between algal diets were statistically significant ($F_{(1, 94)} = 222.5$; $p < 0.0001$) on most of the tested days; whereas differences between day 1 and day 15 were statistically significant only for RHINO diet ($F_{(14, 94)} = 5.001$; $p < 0.0001$). In this case, too, the interaction term was statistically significant ($F_{(14, 94)} = 3.169$; $p = 0.0004$).

Faecal pellet (FP) production (faecal pellet/f; **Figure 3.2C**), similarly to EP, was highest for RHODO on the first day (33.9 ± 20.6 faecal pellet/f) but kept decreasing for the remaining period, with less than 10 faecal pellet/f from day 4. Faecal pellet production with RHINO diet, on the other hand, remained overall stable and lower than RHODO for the whole period. The average values over the 15 days were 14.4 ± 4.5 faecal pellet/f for RHINO and 9.1 ± 8.6 faecal pellet/f with RHODO. Values between diets were statistically different only on the first day ($F_{(1, 94)} = 13.81$; $p = 0.0003$); differences among first and last day of experiment were significant for RHODO ($F_{(14, 94)} = 4.833$; $p < 0.0001$). The interaction was negligible for this test ($F_{(14, 94)} = 1.563$; $p = 0.1044$).

Finally, male and female survival curves (**Figure 3.2D** and **E**, respectively) had similar patterns with the two diets. At the end of the experiment, in fact, the percentage of survival for both males and females were 40% with RHODO and 60% with RHINO; however, male survival started to decrease from day 3, while female survival remained stable until day 8. A log-rank (Mantel-Cox) test confirmed that differences were not statistically significant for

male (chi square = 0.317; df = 1; p = 0.574) or female survival (chi square = 0.384; df = 1; p = 0.536).

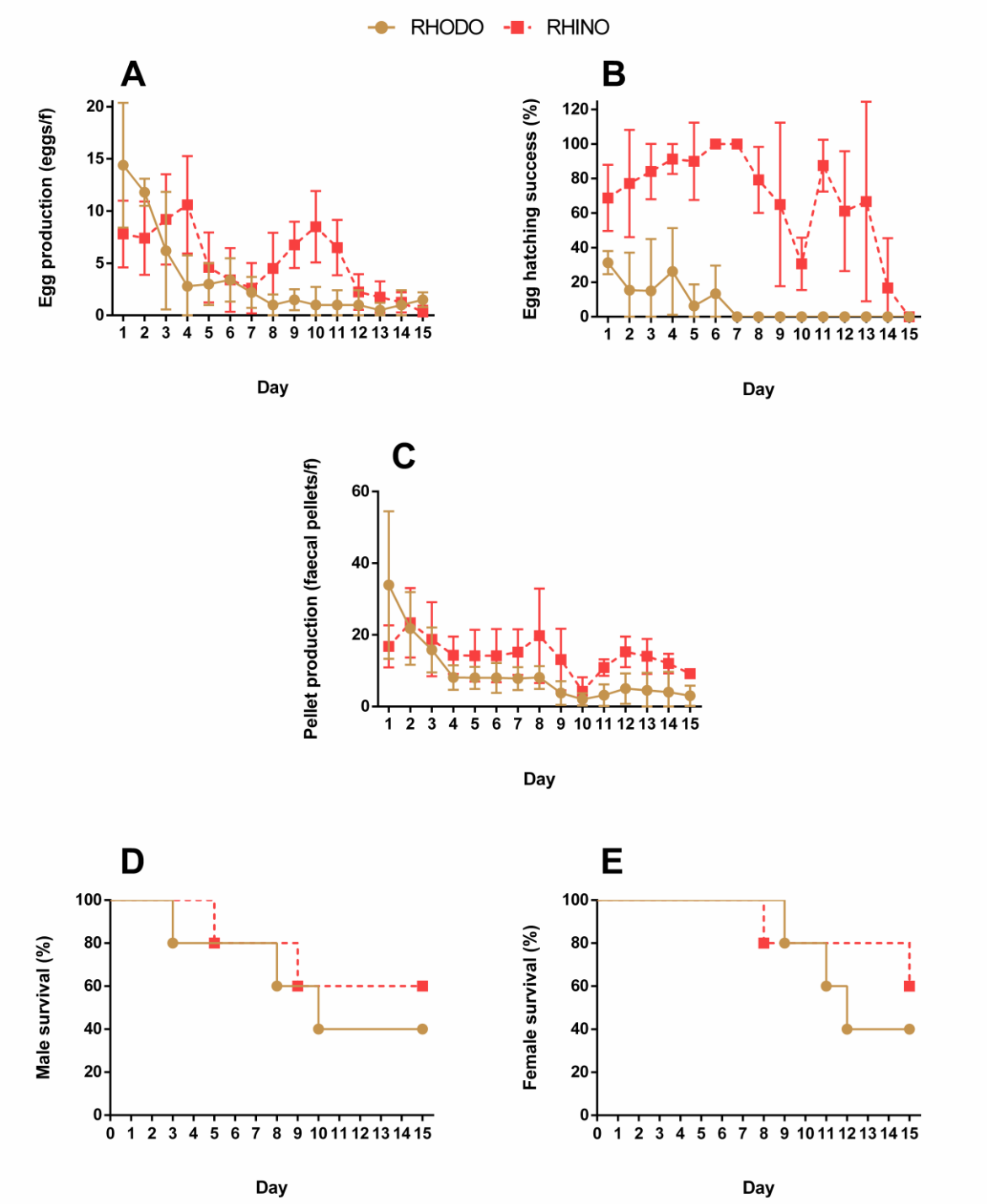

Figure 3.2 Feeding experiment with *Acartia clausi* fed monoalgal diets: *Rhodomonas baltica*, 1.2×10^4 cells/mL (RHODO) and *Rhinomonas reticulata*, 2.7×10^4 cells/mL (RHINO). **A** – Egg production (eggs/f); **B** – egg hatching success (%); **C** – faecal pellet production (faecal pellets/f); **D** – male survival curve (%); **E** – female survival curve (%). For **A-C**, values are mean ± SD; n = 6.

3.4 Discussion

Rearing copepods in laboratory conditions, as opposed to collecting them *in situ*, brings several advantages, such as reducing the variability of unknown environmental factors and synchronising life stages (Anahi *et al.*, 2014; Mazzocchi *et al.*, 2012). For example, the Baltic strain of *A. tonsa* reared at high densities had low values of adult mortality and good egg hatching success (82 to 94%) (Drillet *et al.*, 2014). Holste *et al.* (2004) found that egg hatching success of the Baltic strain of *A. tonsa* increased with salinity, with a maximum of 85% at 25 g/L. On the other hand, wild populations of *A. tonsa* were studied in different densities and temperatures to assess egg hatching success, and lowest values ranged from 5 to 45% (Anahi *et al.*, 2014); and a study on seasonal variability of the eggs of natural populations of the calanoid *Temora longicornis* showed that spring-summer eggs had a lower hatching success of 12-80%, which were then found to be resting egg stages (Castellani and Lucas, 2003). For this reason, it is important to develop methods and diets for rearing wild specimens collected *in situ*.

In this study, we reared the copepod *A. clausi* sampled in the Gulf of Naples in laboratory conditions and tested two algal diets, previously used for the cultivation of *Acartia tonsa* (Zhang *et al.*, 2013), to find the most suitable for this species. Our results show that rearing this species in a laboratory culture is feasible for at least two months, and up to four months with the addition of freshly collected specimens. The highest relative abundance values, recorded with weekly censuses, were 490, 60, 30, and 50 ind./L, respectively for nauplii, copepodids, males and females. Population dynamics showed that, especially for the culture of 2020, there was a clear succession of developmental stages, represented by subsequent peaks in nauplii, copepodids and adults. Peaks of the same stage approximately recurred every 30 days, indicating that this is the time required for the complete development of this species at 20°C from eggs to actively reproducing adults and next generation of offspring.

During the cultivation period we also reared cultures with only eggs and nauplii produced by cultured adults. In one of these nauplii cultures, 6 days after its start we observed the first copepodids, 23 days after its start we observed the first adults, and 26 days after its start we observed the first eggs and nauplii produced by the adults. This means that nauplii obtained in a laboratory culture took 26 days to moult into mature adults which could lay viable eggs (F2 generation), in good agreement with results of the weekly census.

To our knowledge there are no other data of development or physiological parameters with this species reared in laboratory conditions through one or multiple generations.

However, the congeneric species *A. tonsa* has a similar development period: 5-6 days from nauplius to copepodid stage and 12-20 days from nauplius to adult stage, depending on density and temperature (Buttino *et al.*, 2019). Similar results were reported for other Mediterranean copepods: *Calanus helgolandicus* (7 days from nauplius to copepodid, 21 days for nauplius to adult; Carotenuto *et al.*, 2012), *Temora stylifera* and *Centropages typicus* (19 days for both; Buttino *et al.*, 2012).

Adults observed after day 100, in the 2020 culture, are probably derived from the last nauplii recorded before the summer break (day 84). The fact that the culture was still viable indicates that it is amenable to be reared for long periods (30 days) of automatic supply of algal food without recurrent cleaning and water exchange. It is not to be excluded that, on the other hand, the partial renewal of water, which was performed every week and required filtering and manipulation of culture organisms, could have stressed specimens, decreasing their survival rate. It is known, in fact, that handling stress has repercussions on reared adults of *A. tonsa* in terms of survival and transcription of stress genes (Nilsson *et al.*, 2018). Protocols need to be optimised in the future also considering this aspect.

During the cultivation period of one of the minor cultures, however, in one case we registered a high mortality of fresh adult cultures after two weeks of culturing, and in other cases we had to add more fresh specimens to the culture to ensure it had enough viable organisms (results not shown). This means that more effort is still required to standardize and optimize the culture on the long-term.

As for the feeding experiment, the RHINO diet proved to be more efficient for every parameter over the whole 15 days, and especially for HS from the first day, with differences that were statistically significant for EP and HS. However, for these last two parameters, the interaction term in the two-way ANOVA was significant, making it more difficult to predict effects of time and diet on copepod fecundity. Mixed diets of RHINO and other microalgae (*Tetraselmis suecica* and *Isochrysis galbana*) were tested on *A. clausi* by Sei *et al.* (2006). Authors found that the diet which supported a higher development success was the one with RHINO and *I. galbana*, adding that RHINO was appropriate for the copepod also because when this alga was lacking, it caused the arrest of development at early stages.

The fact that during the first days, EP and FP were significantly higher with the RHODO diet, but abruptly decreased soon after, probably indicates that the mixed diet copepods were fed before the test was a better compromise for these physiological parameters. Hence, while a mixed diet can probably compensate for a low-quality diet and ensure average parameters in a multigeneration culture, RHINO is better for *A. clausi* when used as a monoalgal diet in shorter feeding experiments (two weeks). For this reason, *R.*

reticulata was selected as diet for *A. clausi* in ecotoxicological tests (which will be discussed in the next chapter).

In the future, more efforts are required for the multigenerational cultivation of this species, in order to have available organisms in laboratory conditions throughout the year, not depending on the reproductive season. First, a broader range of algal diets should be tested, including more species, also provided as a mixed diet, and at different concentrations. It should also be considered that, in a multigenerational culture of copepods, different stages of the same species coexist, each with different sizes. Because of this, algal diets should also include species with smaller dimensions such as *I. galbana*, more easily eaten by nauplii and copepodids (Zhang *et al.*, 2013). It should also be considered that an addition of other algal species for short periods of time could improve parameters of the culture, similar to what was reported for *C. helgolandicus* fed a diet with *R. baltica* and *I. galbana*, to which the diatom *Thalassiosira weissflogii* was added at low concentrations for less than 2 months (Carotenuto *et al.*, 2012).

In view of proposing *A. clausi* as alternative species in ecological risk assessment, moreover, it should be important to assess viability of eggs after a period of cold-storage. Such possibility was successfully tested with *A. tonsa*: eggs cold-stored for one month had an egg hatching success which was not different with respect to the control; eggs were even cold-stored for up to one year with slight reductions of egg hatching success (Vitiello *et al.*, 2016). In this way, acute tests could be started more easily, without sorting adults first, and eggs could be transferred for ecotoxicological analyses to other laboratories which are not in conditions to collect wild organisms. Our preliminary results with cold-storing of eggs of *A. clausi* were not ideal (data not shown), but improving and optimising algal diets and culture protocols can lead to better results.

Overall, our results showed that *A. clausi*, an important copepod species in the Gulf of Naples, can be successfully reared in laboratory conditions over multiple generations from two to four months, and that one generation takes approximatively 26 days, from egg to actively reproducing adults. We also identified a suitable monoalgal diet for this species for shorter experimental periods of up to 15 days. Notwithstanding the difficulties we encountered, this work could be the starting point for studying and optimising a complete rearing protocol for multigenerational culturing of *A. clausi*.

Chapter 4 Physiological responses of *A. tonsa* and *A. clausi* exposed to $NiCl_2$ and NiNPs: physical-chemical characterisation of toxicants and ecotoxicological tests

4.1 Introduction

Copepods are organisms of paramount importance for their worldwide distribution, abundance, diversity and their ecological role in food webs as link between primary and secondary producers (Steinberg and Landry, 2017; Turner, 2004; Walter and Boxshall, 2022). Because of these characteristics, they are considered model organisms in ecotoxicology, as they can be employed to test alterations in physiological parameters, called endpoints (such as survival, development, growth, fecundity, respiration and swimming behaviour), induced by a variety of contaminants and environmental matrices: raw sediments, heavy metals, microplastics, endocrine disruptors and nanomaterials (Buttino *et al.*, 2018; Raisuddin *et al.*, 2007).

Among copepods, the calanoid *Acartia tonsa* is a species distributed worldwide, largely employed and reared for standardised toxicity tests since the 70s (Gorbi *et al.*, 2012; Lee, 1977). These bioassays are also used under Italian law to assess the toxicity of sediments and pore waters, in order to define their final use (DM 173, 2016). However, in the Mediterranean Sea *A. tonsa* is an invasive species, introduced in the 1980s, and since then it displaced other native copepod species (Camatti *et al.*, 2019; Gaudy and Viñas, 1985). Hence, there is an increasing interest in proposing local species for ecotoxicological bioassays (such as the congeneric species *A. clausi*, native of the Mediterranean Sea), in areas where the diffusion of *A. tonsa* could pose a threat to local communities (Carotenuto *et al.*, 2020).

Recently, nauplii and adults of *A. clausi* and *A. tonsa* were exposed to elutriates of polluted sediments and to the reference toxicant $NiCl_2$, and physiological responses were compared (Carotenuto *et al.*, 2020). As result, *A. clausi* specimens (particularly nauplii) showed a greater sensitivity with respect to those of *A. tonsa*. It is important, therefore, to assess and compare the sensitivity of this native species as it may lead to a different safety threshold for pollutants in the Mediterranean Sea. In this PhD project, in addition to the reference toxicant, we also exposed *A. clausi* to NiNPs, an engineered nanomaterial (ENM) which induces several detrimental effects in biota, such as size reduction in larvae of sea urchins (Kanold *et al.*, 2016), spermiotoxicity for ascidians (Gallo *et al.*, 2016),

neurotoxicity in copepods (Wang and Wang, 2010) and reduction of egg hatching success and naupliar viability in *A. tonsa* (Zhou *et al.*, 2016a).

ENMs are emerging contaminants with at least one dimension in nanoscale (1-100 nm), diffused and employed worldwide in several fields, whose effects on environmental components are still to be fully determined (Corsi *et al.*, 2021; Klaine *et al.*, 2013). Ghobashy *et al.* (2021) reviewed the main proposed mechanisms for toxicity of AgNPs (silver nanoparticles), one of the most employed and studied ENMs: they can physically damage cell membranes due to the nano-size; they can release Ag ions, which can generate reactive oxygen species (ROS); it is also suggested that AgNPs could serve as a "Trojan horse", avoiding cellular barriers and causing damage to the cell, such as release of Ag^+ ions and lipid peroxidation. Such mechanisms were also hypothesised for other ENMs, such as NiNPs (Corsi *et al.*, 2021; Wu and Kong, 2020).

The behaviour of engineered nanomaterials (ENMs) in seawater is complex: it involves being subject to mixing, sedimentation and resuspension, as well as interactions with proteins, polysaccharides, natural organic matter and extracellular polymeric substances with the formation of an eco-corona; aggregation of particles, moreover, is usually proportional to salinity, which in general indicates that a higher salinity causes particles to be less bioavailable and reactive, and, thus, less toxic (Corsi *et al.*, 2021; Hadjidemetriou and Kostarelos, 2017).

For example, in a recent study nauplii of *Artemia salina* were exposed to AgNPs at three different water salinities, and the authors found that, although the release of Ag ions increased with increasing salinity, AgNPs were more toxic at the lower salinities (Asadi Dokht Lish *et al.*, 2019). Silver ions, as well as metal ions in general, are in fact easily bound by chlorine species (abundant in seawater), with the result that ion bioavailability and uptake by organisms is reduced, as a higher salinity indicates a higher competition for free metals (Barus *et al.*, 2021; Corsi *et al.*, 2021; Holmes *et al.*, 2014). Similarly, microplastic particles were found to adsorb more efficiently heavy metal ions at lower salinities, and, in addition to this, metal ions adsorbed from microplastics were released more efficiently at lower salinities (Barus *et al.*, 2021). Such influences of salinity on toxicity of metal ions also occur with nickel, as it was proven that at lower salinities Ni ions have a higher acute toxicity on marine crustaceans (Damasceno *et al.*, 2017; Leonard *et al.*, 2011).

Oleszczuk *et al.* (2015) exposed *Daphnia magna* neonates to different types of ENMs (NiNPs, ZnO and TiO_2) together with ionic and non-ionic surfactants; the authors concluded that the observed reduction in NPs toxicity in the presence of surfactants was due to the formation of aggregates which decreased the availability of NPs for the cladoceran. Size of

copper particles of two different sizes (copper NPs, average size 10 nm; copper microparticles, average size 45 μm) was correlated with the release mechanisms of metal ions, as ion release rate from nanoparticles was much higher with respect to microparticles (Palza *et al.*, 2015). This is in agreement with Hang *et al.* (2018), who reported that for ENMs of different sizes, shapes, structures and surface energies, the rate of ion release was dependent only on the total surface area exposed. A study measured size of NiNPs at different concentrations, and found that size of particles at 50 mg/L after 48 h increased from roughly 150 to 850 nm, in seawater at 30 PSU (Zhou *et al.*, 2016a).

These examples show a negative correlation between salinity and bioavailability of metal ions, and a positive correlation between salinity and diameter of nanoparticles (both of which ultimately cause a reduction in toxicity). This is why it is important to characterise the behaviour of nanoparticles at the different salinities at which our two copepod species are maintained, and see if they affect the diameter of the particles or concentration of the released ions. The two copepod species are in fact reared each at a specific salinity *optimum* (30 PSU for *A. tonsa* and 37 PSU for *A. clausi*) to grant ideally for each the best conditions and the less possible stress (Carotenuto *et al.*, 2020).

In this chapter, we will provide data on the characterisation of NiNPs (emerging contaminant) and $NiCl_2$ (the nickel salt used as a reference toxicant in ecotoxicology with *A. tonsa*), at 30 and 37 PSU, to rule out the possibility that this difference in salinity could also imply a difference in diameter of particles or concentration of Ni ions, in which case it would be difficult to compare results between the two copepod species. We also analysed NiNPs stock solution in BDW, to see if a possible release of ions over time occurs regardless of salinity. Furthermore, we will present data on ecotoxicological tests performed with nauplii and adults of both *A. clausi* and *A. tonsa*, with both toxicants, after a short term (acute) or long term (chronic) exposure. Our aim was to compare their physiological responses (naupliar immobilisation, egg hatching success, egg production, faecal pellet production and adult mortality) to NiNPs and $NiCl_2$, to obtain novel scientific insights regarding the less studied *A. clausi*. More specifically, the hypothesis we wanted to test was if adults of *A. clausi* are more sensitive to $NiCl_2$ when compared to adults of *A. tonsa*, as reported by scientific literature for nauplii of these species (Carotenuto *et al.*, 2020). Furthermore, we wanted to investigate the responses of *A. clausi* to NiNPs, which has never been addressed in scientific literature, and observe if in this case too there is a greater sensitivity of both adults and nauplii of *A. clausi*.

4.2 Materials and methods

4.2.1 ICP-MS analysis

To determine whether the different salinities at which the two copepods are reared influenced the behaviour of the two toxicants, and in particular the amount of Ni ions in solution, $NiCl_2$ and NiNPs solutions were analysed using Inductively Coupled Plasma-Mass Spectrometry (ICP-MS). The analyses were performed at the Agenzia Regionale Protezione Ambientale (ARPA) Campania for courtesy of Dr. Teresa Verde and Dr. Gennaro Matrullo.

$NiCl_2$ was prepared as described in chapter 2.2.2. NiNPs (nickel nanopowder, Sigma-Aldrich Life Science, Milan, Italy) were weighed with an analytical scale (KERN KB, Sigma-Aldrich Life Science, Milan, Italy) and added to bi-distilled water (BDW) to obtain a stock solution of 850 mg/L. Before taking any volume, the solution was kept on a magnetic stirrer (ARGOlab M2-D Pro, Giorgio Bormac, Carpi, Italy) at about 700 RPM for about 10 min, to guarantee proper separation of particles. Any volume was taken from the stock solution with the stirring still in function, to avoid sedimentation of particles.

From both stock solutions, final dilutions of 0.2 mg Ni/L ($NiCl_2$) and 17 mg/L (NiNPs) were done in seawater at 30 and 37 PSU, at t_0 and after 48 h, in two replicates of 50 mL incubated in a thermostatic chamber at 20 ± 2°C, on a shaking plate (Labortechnik KS 125 Basic, IKA, Staufen, Germany) with slight agitation (70 RPM). These concentrations, timepoints and incubation parameters were chosen according to those of the chronic test (see chapter 4.2.5). The stock solution of NiNPs was analysed too, at t_0 and after 72 h, in two replicates of 50 mL, in order to verify whether Ni ions were released from the NPs in the stock solution over time. For the duration of this experiment, the stock solution was kept at 4°C, covered in aluminium foil.

At the respective time point, each sample was centrifuged in an Allegra 64R refrigerated centrifuge (Beckman Coulter Life Sciences, Indianapolis, Indiana, USA) at 10,000 RPM (10,286 g), 15°C, for 30 min, twice, to separate nanoparticles from dissolved ions (the supernatant) (Zhou *et al.*, 2016a). After each centrifugation, the supernatant was carefully collected with a plastic pipette; after the second centrifugation, no pellet was seen in the supernatant observed under the stereomicroscope (as recommended by Padoan *et al.*, 2017). The remaining supernatant of each sample (around 15 mL) was then analysed with an Agilent 7500ce (Agilent, Santa Clara, California, USA). Samples in seawater were diluted 1:10 in BDW, as the instrument could not read samples in SW. Before the analysis, 4-5 drops

of 65% diluted nitric acid were added to each sample. BDW and FSW at each salinity were used as blanks by the instrument in the calibration line.

Data were analysed using GraphPad Prism version 6.01 (GraphPad Software Inc., San Diego, California, USA), with an unpaired t-test (for analyses on the stock solution) and a multiple, unpaired t-test corrected for multiple comparisons using the Holm-Sidak method (for analyses on dilutions in seawater).

4.2.2 DLS analysis

To determine whether the different salinities at which the two copepods are maintained influenced the behaviour of NiNPs, specifically diameter and aggregation of nanoparticles in seawater, NiNPs solutions were analysed using Dynamic Light Scattering (DLS). The analyses were performed at the Université de Lille, courtesy of Mr. Wajid Ali, Prof. Philippe Zinck and Prof. Sami Souissi.

NiNPs stock solution was prepared as described in chapter 4.2.1. From the stock, final dilutions of 8.5 and 17 mg/L were made in seawater at 30 and 37 PSU, each in three replicates of 50 mL. NiNPs dilutions were incubated as reported in the paragraph above and analysed soon after the preparation (t_0) and after 48 h.

At the respective time point, 3 mL of each sample was centrifuged in an Allegra 64R refrigerated centrifuge (Beckman Coulter Life Sciences, Indianapolis, Indiana, USA) at 4,985 RPM (4,000 g) for 30 min, twice (Zhou *et al.*, 2016a). After centrifugation, they were analysed with a Zetasizer Nano ZS (Malvern Instruments Limited, Malvern, UK) (detection range: 0.3 nm – 10 µm; standard laser: 4 mW, 633 nm; measurement angles: 13° + 173°).

Data were analysed using GraphPad Prism version 6.01 (GraphPad Software Inc., San Diego, California, USA), with a multiple, unpaired t-test corrected for multiple comparisons using the Holm-Sidak method.

4.2.3 Culture maintenance

Acartia tonsa and *A. clausi* cultures were reared in laboratory conditions and handled according to the methodologies described in detail in chapter 3.2.1. Briefly, cultures were kept in a thermostatic chamber at 20 ± 2°C, 12:12 h light:dark, with slight aeration provided through a glass pipette. Salinity was 30 and 37 PSU, respectively, for the two species. Small glass beakers (1 or 2 L) were used to acclimate organisms before specific experiments or

before a test which required a batch of fresh eggs. In general, the number of replicates was chosen in function of the availability of fresh organisms in culture.

4.2.4 Acute test

Methodologies for the acute test are described in chapter 2.2.2. Briefly, groups of about 50 eggs (less than 24 h old, collected early in the morning from batches of adults isolated from the main culture the day before the test) of *Acartia tonsa* or *A. clausi* were transferred in crystallising dishes filled with 10 mL of FSW at 30 or 37 PSU, respectively. Under a stereomicroscope (M80, Leica Microsystems, Milan, Italy), two eggs were gently collected from the vessel with a thin-mouth Pasteur pipette and transferred into a 2.5 mL well of a 24-well plate (Corning), filled with 2.5 mL of the relative treatment (FSW, $NiCl_2$ or NiNPs); plates were incubated in a thermostatic chamber at 20 ± 1°C, 14:10 L:D photoperiod. The tests were performed in three replicates of five wells each, for a total of 10 eggs for each replicate and 30 eggs in total for each condition.

A stock solution of nickel chloride hexahydrate ($NiCl_2 \times 6\ H_2O$, Carlo Erba Reagents, Milan, Italy) at concentration of 1000 mg/L was diluted with distilled water to a nominal concentration of 10 mg/L, corresponding to a dissolved Ni concentration of 10.0 ± 0.09 mg Ni/L, measured with ICP OES 720 (Agilent Technologies, Santa Clara, California) (Vitiello *et al.*, 2016). For. *A. tonsa*, final concentrations of 0.05, 0.1, 0.2 and 0.4 mg Ni/L (concentrations commonly used to calculate the EC_{50} for this species (Rotolo *et al.*, 2021)) were obtained from the 10 mg Ni/L stock solution through serial dilutions in FSW. On the other hand, as *A. clausi* nauplii are more sensitive with respect to those of *A. tonsa* (Carotenuto *et al.*, 2020), we employed lower concentrations for the former species. Specifically, from the intermediate stock solution of $NiCl_2$ at 10 mg Ni/L, we obtained the following serial dilutions in FSW: 0.00125, 0.0025, 0.005, 0.01 and 0.02 mg Ni/L. These concentrations were chosen starting from the two lowest concentrations employed in literature (Carotenuto *et al.*, 2020) (0.01 and 0.02 mg Ni/L), which still provoked a remarkable value of naupliar immobilisation, and then progressively halving the value to obtain other lower concentrations.

NiNPs solution was prepared as described in chapter 4.2.1. From the stock solution, serial dilutions in seawater were made, up to final concentrations of 6.25, 12.5, 25, 50 mg/L for *A. tonsa* (chosen similarly to Zhou *et al.* (2016a)), whereas a broader range of concentrations was prepared for *A. clausi*, as NiNPs were never tested on this species: 0.016, 0.08, 0.4, 2, 10 mg/L. In this case, we chose as the highest concentration the one inducing

moderate responses in naupliar immobilisation in *A. tonsa* (Zhou *et al.*, 2016a) (10 mg/L), and progressively dividing this value by 5 to obtain other four lower concentrations. Any operation with NiNPs and $NiCl_2$ was performed under a chemical hood (Dynamika, Arredi Tecnici Villa, Catania, Italy).

Glassware used for the toxicity tests was decontaminated for 24 h with 2% diluted nitric acid (HNO_3) and then rinsed, as reported in different protocols, also for ENMs (Handy *et al.*, 2012; US EPA, 2002).

Egg hatching success (HS) and naupliar immobilisation (NI) were calculated as reported in chapter 2.2.2. Data were analysed using GraphPad Prism version 6.01 (GraphPad Software Inc., San Diego, California, USA), with an ordinary one-way ANOVA followed by a Tukey's multiple comparison test. EC_{50} was calculated using PROBIT Analysis version 1.5 (UNICHIM, 2012a).

4.2.5 Chronic and detoxification test

Chronic test was performed in accordance with methods of Carotenuto *et al.* (2020) and Zhou *et al.* (2016a). The purpose was to confirm previous results for *A. tonsa* (Zhou *et al.*, 2016a) and to have comparable data on the concentrations tested on *A. clausi*, using the same batches of toxicants.

Briefly, couples of male and female adults of *A. tonsa* and *A. clausi*, collected from the laboratory culture, were transferred in crystallising dishes containing 50 mL of FSW, algae and toxicant solution. Dishes were incubated in a thermostatic chamber at 20 ± 2°C, 12:12 h light:dark photoperiod, kept on a shaking plate (Labortechnik KS 125 Basic, IKA, Staufen, Germany) with slight agitation (70 RPM), to prevent algal sedimentation. After 24 h, each couple was transferred in a new crystallising dish with fresh medium, every day for 4 days. Soon after transfer, crystallising dishes were inspected under an inverted microscope (Axiovert 25, Zeiss, Oberkochen, Germany; 2.5× magnification) to count laid eggs, faecal pellets and adult mortality. Vessels were incubated again at the same conditions, and after 48 h were fixed with absolute ethanol (Sigma-Aldrich Life Science, Milan, Italy; 10% of total volume). Hatched eggs were then counted at the inverted microscope and the percentage of egg hatching success was calculated using the formula described in chapter 2.2.2. $NiCl_2$ and NiNPs solutions were prepared as described in chapters 4.2.4 and 4.2.1, respectively. Specific salinity of FSW, algal diets, toxicant concentrations are reported below for the two copepod species.

- *Acartia tonsa*: salinity 30 PSU; algal diet *Rhodomonas baltica* at 1.2×10^4 cells/mL (corresponding to 1500 µg C/L; Zhang *et al.*, 2013) (RHODO). The tested concentrations were chosen based on the scientific literature, as there are already published data on the effects of $NiCl_2$ and NiNPs on *A. tonsa* egg production and egg hatching success over consecutive days (Zhou *et al.*, 2016a): 17 mg/L for NiNPs and 0.2 mg Ni/L for $NiCl_2$. In this latter case, however, we decided to use a higher value than that reported by Zhou *et al.* (2016a) as their highest concentration of 0.1 mg Ni/L did not provoke remarkable effects. For each control and toxicant condition, seven couples of *A. tonsa* adults were employed (n = 7).
- *Acartia clausi*: salinity 37 PSU; algal diet *Rhinomonas reticulata* at 2.7×10^4 cells/mL (corresponding to 1500 µg C/L; Zhang *et al.*, 2013) (RHINO). Concentrations were 0.05, 0.1, 0.2 mg Ni/L for $NiCl_2$ and 4.25, 8.5, 17 mg/L for NiNPs. In this case, the rationale behind the choice of concentrations was to grant, for each toxicant, the highest concentration in common with *A. tonsa* and progressively halving the value to obtain two other concentrations, expecting adults of this copepod species to be more sensitive, as was observed with their nauplii (Carotenuto *et al.*, 2020). For $NiCl_2$, nine couples of *A. clausi* adults were employed (n = 9); for NiNPs, ten couples of *A. clausi* adults were employed (n = 10).

In preliminary tests with *A. tonsa*, we observed a very low egg hatching success with $NiCl_2$ from the first day of incubation. This result could have been due to a direct toxic effect of $NiCl_2$ on the eggs left to hatch into the crystallising dish for 48 h, or to an indirect harmful and fast effect of $NiCl_2$ on the females which had laid the eggs (maternal effect). Therefore, we decided to set up a further experiment (detoxification test). After 4 days of incubation in FSW, $NiCl_2$ or NiNPs, males and females were transferred into FSW and algal medium for one additional day (24 h). Tests included 5 replicates for *A. tonsa* exposed to both $NiCl_2$ and NiNPs, 9 replicates for *A. clausi* in $NiCl_2$, and 7 replicates for *A. clausi* in NiNPs.

In chronic tests performed on *A. tonsa* exposed to NiNPs, aliquots of the toxicants used every day were obtained from a stock solution prepared at the beginning of the test (Zhou *et al.*, 2016a); this procedure reduces uncertainty related to preparation of multiple solutions every day. However, to evaluate the possibility that Ni ions were released from NPs of the stock solution during the 4-days experiments, we set up an additional chronic test with *A. clausi* in which the stock of NiNPs was prepared every day (chronic test with daily-renewed

NiNPs stock solution). This test was performed with 9 couples of *A. clausi* adults only using the concentration of 17 mg/L.

Data were analysed using GraphPad Prism version 6.01 (GraphPad Software Inc., San Diego, California, USA). Statistical tests were an ordinary two-way ANOVA followed by a Tukey's multiple comparison test, to compare averages among treatments on each of the 4 days (chronic test); an ordinary one-way ANOVA followed by a Tukey's multiple comparison test to compare averages of each treatment in the 5th day (detoxification test); a multiple, unpaired t-test corrected for multiple comparisons using the Holm-Sidak method to compare averages of each condition between day 4 and 5 (chronic vs. detoxification test). Percentages of male and female survival were calculated through a survival curve and results were compared using a Log-rank (Mantel-Cox) test.

4.3 Results

4.3.1 ICP-MS analysis

Figure 4.1 shows ICP-MS quantitative analysis of nickel dissolved from NiNPs stock solution in BDW at the concentration of 850 mg/L. Soon after preparation (t_0), the stock solution had a measured dissolved Ni concentration of 4.61 ± 0.63 mg Ni/L (mean ± SD), that significantly increased to 8.58 ± 0.04 mg Ni/L after 72 h (unpaired t-test, t = 8.907; df = 2; p = 0.012).

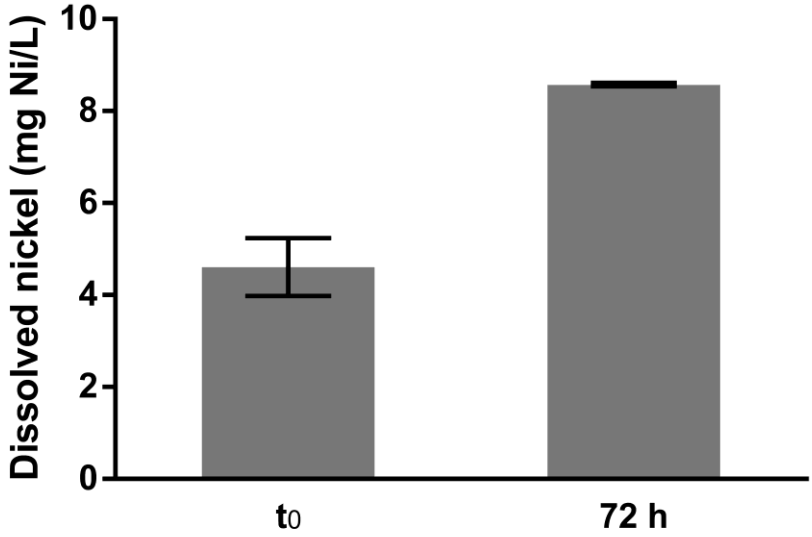

Figure 4.1 ICP-MS quantitative analysis of dissolved nickel in NiNPs stock solution in BDW (850 mg/L), at t_0 and after 72 h. Values are mean ± SD; n = 2.

Dissolved nickel measured in $NiCl_2$ and NiNPs, at t_0 and after 48 h, at 30 and 37 PSU, are shown in **Figure 4.2**. Values in $NiCl_2$ solution at 0.2 mg Ni/L (nominal concentration) were similar among timepoints and salinities, ranging from 0.14 to 0.17 mg Ni/L (**Figure 4.2A**). Differences between salinities were not statistically significant at t_0 ($t = 0.672$; $df = 2$; $p = 0.570$) nor at 48 h ($t = 0.306$; $df = 2$; $p = 0.788$); differences between timepoints were not significant for 30 ($t = 0.151$; $df = 2$; $p = 0.894$) nor for 37 PSU ($t = 1.353$; $df = 2$; $p = 0.309$).

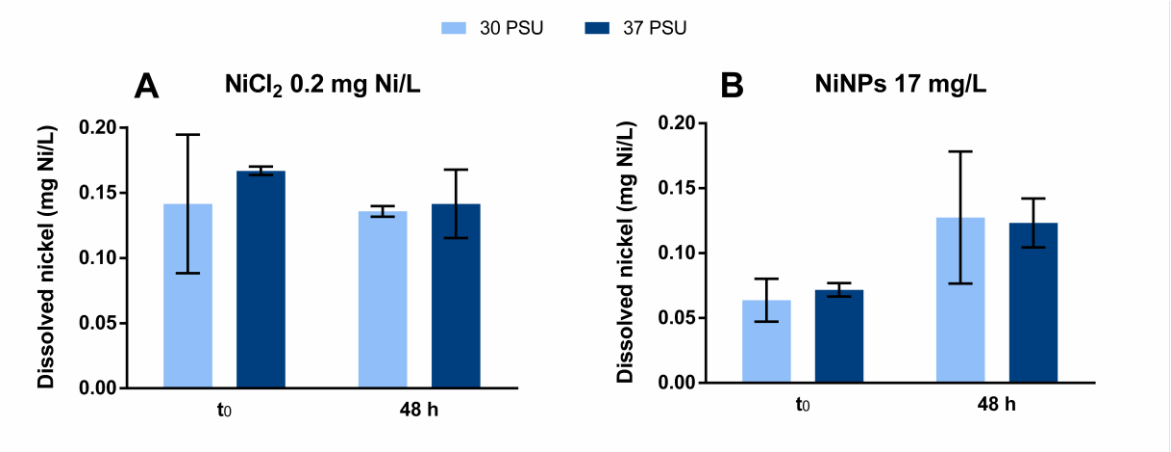

Figure 4.2 ICP-MS quantitative analysis of dissolved nickel in FSW, at 30 and 37 PSU, for NiCl2 at 0.2 mg Ni/L (**A**) and for NiNPs at 17 mg/L (**B**). Samples for the analysis were collected at t_0 and after 48 h. Values are mean ± SD; n = 2.

Values of Ni dissolved from NiNPs at 17 mg/L were similar among salinities at t_0 for 30 and 37 PSU (0.06 ± 0.02 and 0.07 ± 0.01, respectively); after 48 h, they increased to 0.13 ± 0.05 and 0.12 ± 0.02 (for 30 and 37 PSU, respectively) (**Figure 4.2B**). Differences between the two salinities, however, were not statistically significant at t_0 ($t = 0.644$; $df = 2$; $p = 0.586$) nor after 48 h ($t = 0.109$; $df = 2$; $p = 0.923$); differences between timepoints were as well not statistically significant for 30 ($t = 1.680$; $df = 2$; $p = 0.235$) or 37 PSU ($t = 3.730$; $df = 2$; $p = 0.065$).

4.3.2 DLS analysis

Size range of NiNPs in FSW at salinities 30 and 37 PSU, measured through DLS, is shown in **Figure 4.3**. NiNPs solution at the concentration of 8.5 mg/L showed a size ranging from 243.5 nm (30 PSU, t_0) to 107.8 nm (30 PSU,48 h) (**Figure 4.3A**). For 37 PSU, size variation measured at t_0 (128.6 nm) was lower with respect to the size after 48 h (191.6 nm). However, this size variability between the two different salinities was not statistically

significant for t_0 ($t = 1.073$; $df = 4$; $p = 0.362$) nor for 48 h ($t = 1.173$; $df = 4$; $p = 0.306$). Similarly, differences between t_0 and 48 h were not statistically significant for 30 ($t = 0.992$; $df = 4$; $p = 0.394$) or 37 PSU ($t = 2.272$; $df = 4$; $p = 0.086$).

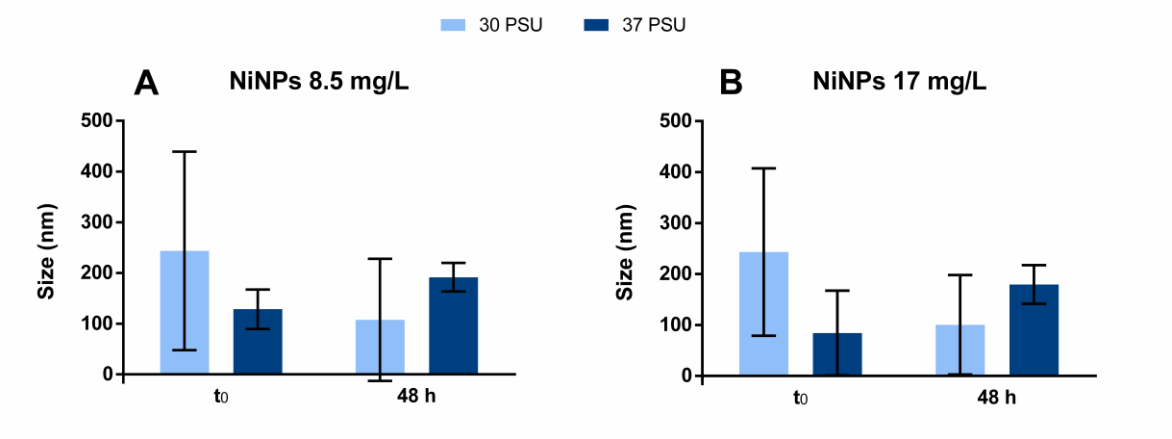

Figure 4.3 DLS analysis of size of nanoparticles in FSW, at 30 and 37 PSU, for NiNPs at 8.5 mg/L (**A**) and at 17 mg/L (**B**). Samples for the analysis were collected at t_0 and after 48 h. Values are mean ± SD; n = 3.

Figure 4.3B shows size range of NiNPs solution at the concentration of 17 mg/L in FSW at 30 and 37 PSU. In this case too, differences of NiNPs size between salinities were not statistically significant at t_0 ($t = 1.495$; $df = 4$; $p = 0.209$) or after 48 h ($t = 1.310$; $df = 4$; $p = 0.260$); differences between timepoints were also not significant, for both 30 ($t = 1.296$; $df = 4$; $p = 0.265$) and 37 PSU ($t = 1.803$; $df = 4$; $p = 0.146$).

4.3.3 Acute test

Results of acute test with *A. tonsa* exposed to $NiCl_2$ (**Figure 4.4A**, **B**) and NiNPs (**Figure 4.4C**, **D**) showed that in control condition egg hatching success (HS) was 87.9 ± 11.1% (mean ± SD) and naupliar immobilisation (NI) was 11.7 ± 9.8%. For the tested concentrations of $NiCl_2$ (from 0.05 to 0.4 mg Ni/L), HS was similar to that of the control, ranging from 76.7 ± 11.6% to 87.3 ± 6.3%, with no significant differences ($F_{(4, 13)} = 0.561$; $p = 0.695$) (**Figure 4.4A**). NI, on the contrary, showed a concentration-dependent response when compared to the control. For $NiCl_2$, differences among treatments were statistically significant for 0.1 (50.0 ± 16.7%) and 0.4 mg Ni/L (69.6 ± 19.5%) ($F_{(4, 13)} = 7.570$; $p = 0.002$) (**Figure 4.4B**). The EC_{50} for naupliar immobilisation was 0.221 mg Ni/L (0.091 – 2.191; lower 95% confidence limit – upper 95% confidence limit).

HS in the concentrations of NiNPs ranged from 70.6 ± 10.9% to 80.0 ± 20.0% (**Figure 4.4C**). Differences were not statistically significant between concentrations and the control,

which was the same as in the $NiCl_2$ test (87.9 ± 11.1%) ($F_{(4, 13)}$ = 0.956; p = 0.464). NiNPs caused higher percentages of NI (from 27.2 ± 11.8% to 80.0 ± 18.9%), with respect to the control (11.7 ± 9.8%) (**Figure 4.4D**). In particular, values measured at 25 and 50 mg/L were statistically different with respect to those measured in control, 6.25 and 12.5 mg/L ($F_{(4, 13)}$ = 17.69; p < 0.0001). The EC_{50} for this treatment was 18.445 mg/L (10.250 – 29.647).

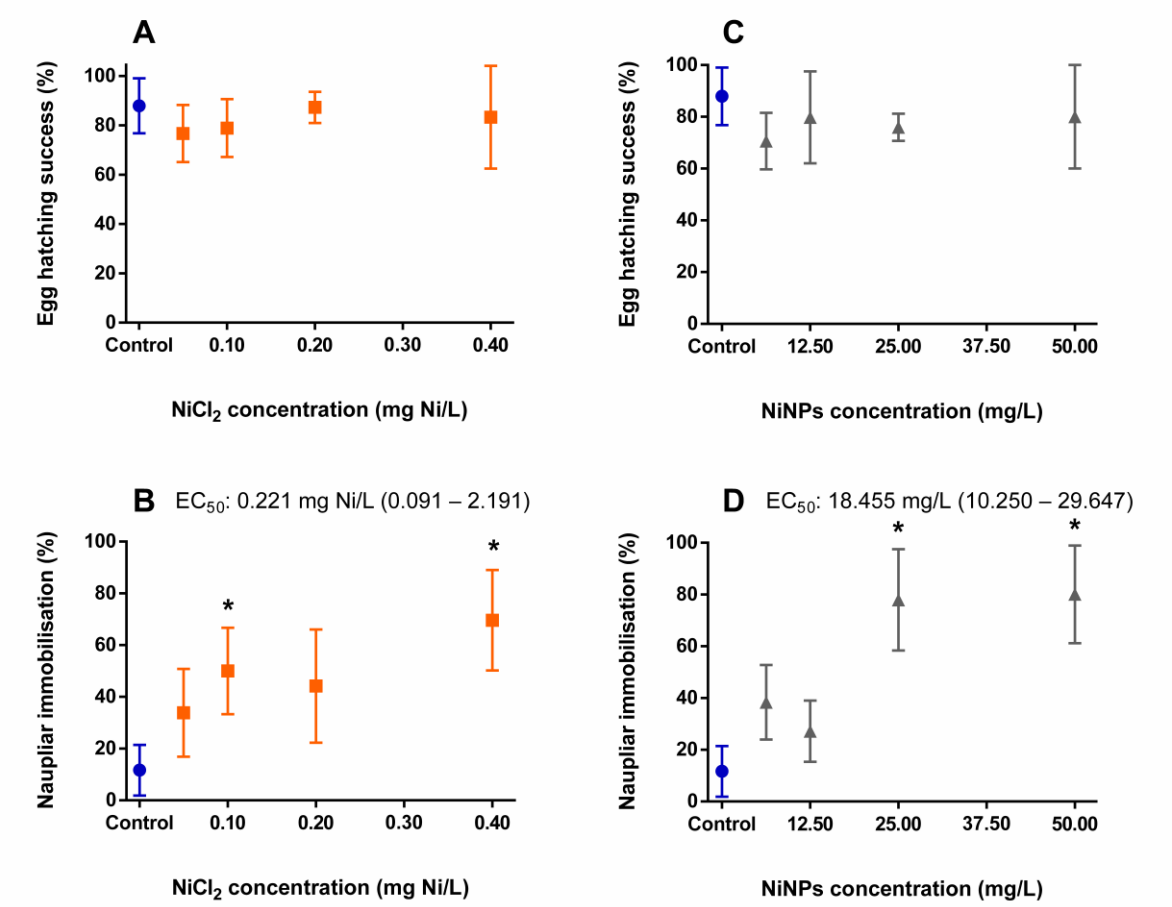

Figure 4.4 *Acartia tonsa* acute test with $NiCl_2$ and NiNPs. **A** – Egg hatching success (%) and **B** – naupliar immobilisation (%) at different concentrations of $NiCl_2$. **C** – Egg hatching success (%) and **D** – naupliar immobilisation (%) at different concentrations of NiNPs. Values of EC_{50} for both toxicants are reported, with lower and upper 95% confidence limits in brackets. Values are mean ± SD; n = 3. * indicates statistically significant differences among treatments (one-way ANOVA followed by a Tukey's multiple comparison test; p < 0.05).

Results of the acute test with *A. clausi* are shown in **Figure 4.5A**, **B** and **Figure 4.5C**, **D**, respectively, for $NiCl_2$ and NiNPs. In the test with $NiCl_2$, HS in the control was 85.9 ± 12.2%, similar to that recorded for the different concentrations of $NiCl_2$, with values ranging from 84 to 93% (**Figure 4.5A**). These differences between treatment and control were not statistically significant ($F_{(5, 12)}$ = 0.610; p = 0.694). NI, on the other hand, which in

the control was 29.2 ± 26.0%, had a concentration-dependent response, with values from 51.5 ± 7.9% (0.00125 mg Ni/L) to 85.6 ± 6.8% (0.02 mg Ni/L) (**Figure 4.5B**). In this case, differences were statistically significant between treatments ($F_{(5, 12)}$ = 7.928; p = 0.002), except for control versus 0.00125 mg Ni/L. EC_{50} for $NiCl_2$ was 0.002319 mg Ni/L (0.00013 – 0.005547).

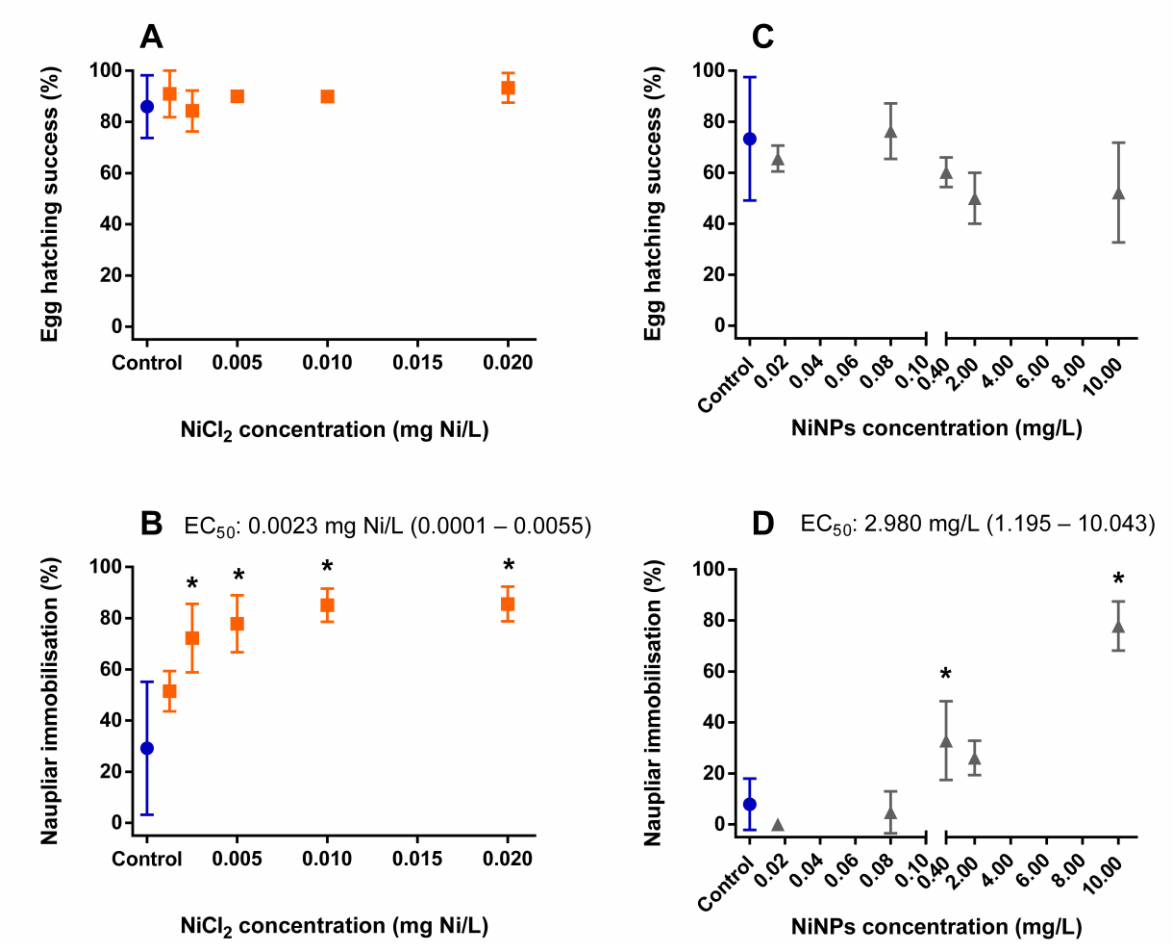

Figure 4.5 *Acartia clausi* acute test with $NiCl_2$ and NiNPs. **A** – Egg hatching success (%) and **B** – naupliar immobilisation (%) at different concentrations of $NiCl_2$. **C** – Egg hatching success (%) and **D** – naupliar immobilisation (%) at different concentrations of of NiNPs. Values of EC_{50} for both toxicants are reported, with lower and upper 95% confidence limits in brackets. Values are mean ± SD; n = 3. * indicates statistically significant differences between control and treatment (one-way ANOVA followed by a Tukey's multiple comparison test; $p < 0.05$).

In the test with NiNPs, the control had a HS of 73.3 ± 24.2%; NiNPs caused a lower HS with respect to $NiCl_2$, with the lowest value being 50.0 ± 10.0% (2 mg/L) (**Figure 4.5C**). Differences with respect to the control, however, were not statistically significant ($F_{(5, 15)}$ = 1.430; p = 0.270). NI in the control was 7.9 ± 10.1%, while for NiNPs it ranged from 0% (0.016 mg/L) to 77.8 ± 9.6% (10 mg/L) (**Figure 4.5D**). Differences with respect to the control were statistically significant for 0.4 and 10 mg/L, whereas 10 mg/L was different

also with respect to all other NiNPs concentrations ($F_{(5, 15)} = 28.54$; $p < 0.0001$). EC_{50} value for NiNPS was 2.980 mg/L (1.195 – 10.043).

4.3.4 Chronic and detoxification test

Results of the chronic test with *A. tonsa* exposed to $NiCl_2$ at 0.2 mg Ni/L and NiNPs at 17 mg/L are shown in **Figure 4.6**. Means ± SD of EP, HS and FP of the 4 days are summarised in **Table 4.1**.

Egg production (EP) of females of *A. tonsa* exposed to $NiCl_2$ during the 4-days period was slightly higher in the control with respect to the other treatments (**Figure 4.6A**). Control females produced from 21.4 (day 1) to 24.8 eggs/f (day 4) as compared to the two treatments, which had a similar temporal trend: from 9.7 to 6.7 eggs/f for $NiCl_2$ and from 9.8 to 7.6 eggs/f for NiNPs. A two-way ANOVA followed by a Tukey's multiple comparison test was used to find statistically significant differences among conditions for each of the 4 days of test. Control was different with respect to $NiCl_2$ and NiNPs on day 1, 3 and 4 ($F_{(2, 57)} = 25.56$; $p < 0.0001$). There were no significant differences, instead, among the different days for each condition ($F_{(3, 57)} = 0.266$; $p = 0.850$). The interaction term, which indicates the combined effect of both time and treatment, for this parameter was negligible ($F_{(6, 57)} = 0.469$; $p = 0.828$). On the detoxification day (day 5), EP was similar among conditions, with 23.7 eggs/f in the control, 23.2 eggs/f for $NiCl_2$ and 18.0 eggs/female for NiNPs (one-way ANOVA followed by a Tukey's multiple comparison test; $F_{(2, 10)} = 0.356$; $p = 0.710$). However, comparing day 4 with day 5 (*i.e.*, the last day of chronic test with the detoxification test) with a multiple unpaired t-test corrected for multiple comparisons using the Holm-Sidak method, differences were significant only in the $NiCl_2$ treatment ($t = 2.673$; $df = 10$; $p = 0.023$), not for NiNPs or control ($p = 0.135$ and $p = 0.847$, respectively).

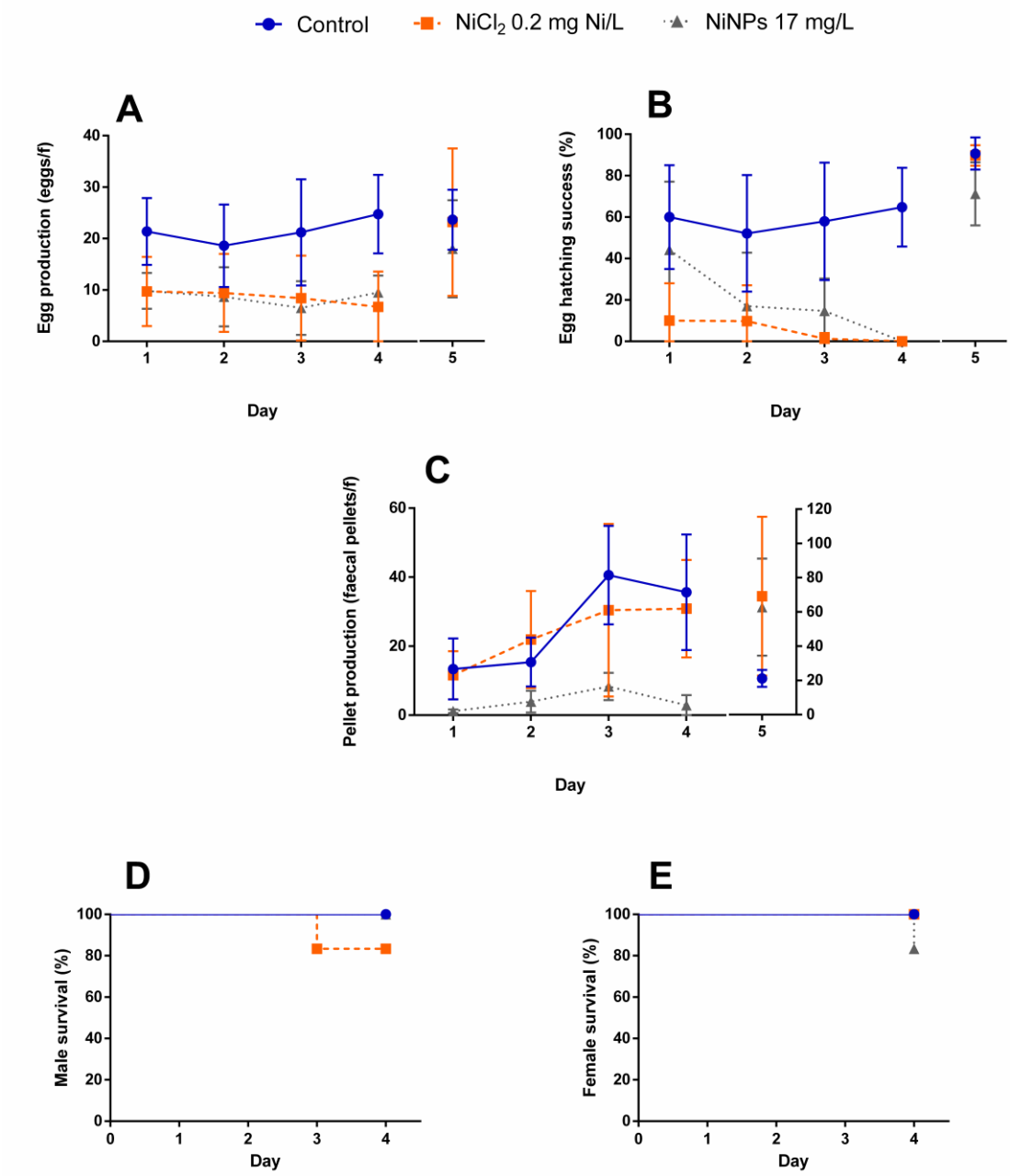

Figure 4.6 *Acartia tonsa* chronic test (days 1-4) plus detoxification test (day 5) with $NiCl_2$ and NiNPs, fed *Rhodomonas baltica*, 1.2×10^4 cells/mL. **A** – Egg production per female (eggs/f); **B** – egg hatching success (%); **C** – faecal pellet production per female (faecal pellets/f) (please note the different scale for day 5); **D** – male survival curve (%); **E** – female survival curve (%). For **A**-**C** values are mean ± SD; for chronic test, n = 7; for detoxification test, n = 5.

Table 4.1 Chronic test with *A. tonsa* exposed to $NiCl_2$ and NiNPs. Values are mean ± SD of 4 days; n = 7.

	EP (eggs/f)	**HS (%)**	**FP (f. pellets/f)**
Control	21.49 ± 8.12	58.73 ± 25.13	26.26 ± 11.73
$NiCl_2$ 0.2 mg Ni/L	8.57 ± 7.36	5.28 ± 9.52	23.70 ± 15.03
NiNPs 17 mg/L	8.63 ± 4.44	19.00 ± 18.60	4.07 ± 2.64

Egg HS in the control was on average 58.73 ± 25.13% during the four days of the test (**Figure 4.6B**; **Table 4.1**). A marked decrease of egg hatching success was observed for both toxicant treatments over time: from 44.2% to 0.0% for NiNPs at 17 mg/L, and from 10.1% to 0.0% for $NiCl_2$ at 0.2 mg Ni/L. Differences were statistically significant between control and the two treatments on day 2, 3 and 4; on day 1, control was statistically different only with respect to $NiCl_2$ ($F_{(2, 57)} = 40.91$; $p < 0.0001$). There were no statistically significant differences among days for each condition ($F_{(3, 57)} = 2.082$; $p = 0.113$). The interaction term was not significant either ($F_{(6, 57)} = 1.591$; $p = 0.166$). In the detoxification test, HS was high for control and $NiCl_2$ (about 90%), with NiNPs showing a slightly lower percentage (71.7%). Differences among day 4 and 5 were statistically significant for HS in $NiCl_2$ ($t = 48.563$; $df = 10$; $p < 0.0001$) and NiNPs ($t = 9.217$; $df = 7$; $p < 0.0001$), not in control ($p = 0.076$). On day 5, there were statistical differences between NiNPs and the other conditions ($F_{(2, 10)} = 4.778$; $p = 0.035$).

Faecal pellet (FP) production in the control increased during the 4 days, with a minimum of 13.4 (day 1) to a peak of 40.6 faecal pellets/f (day 3) (**Figure 4.6C**). In the $NiCl_2$ treatment, for the first two days, values were comparable to the control, with a smaller 4-days average of 23.7 ± 15.0 faecal pellets/f. FP production was overall very low for NiNPs (4.1 ± 2.7 faecal pellets/f). Differences were statistically significant on day 2, 3 and 4 between $NiCl_2$ and NiNPs, and on day 3 and 4 between control and NiNPs ($F_{(2, 57)} = 21.22$; $p < 0.0001$). Among days, there were significant differences in FP production for control (day 1 and 2 versus day 3) and $NiCl_2$ (day 1 versus day 3 and 4) ($F_{(3, 57)} = 7.277$; $p = 0.0003$). The interaction term for this parameter was negligible ($F_{(6, 57)} = 1.474$; $p = 0.203$). FP production in the detoxification test for $NiCl_2$ (69.2 ± 46.4 faecal pellets/f) and NiNPs (62.8 ± 28.4 faecal pellets/f) was higher with respect to that measured during the chronic test. Differences between day 4 and 5 were statistically significant for NiNPs ($t = 4.148$; $df = 7$; $p = 0.004$), not for control ($p = 0.215$) or $NiCl_2$ ($p = 0.063$). Differences among conditions within day 5 were not statistically significant ($F_{(2, 10)} = 1.996$; $p = 0.186$).

Survivorship of *A. tonsa* males (**Figure 4.6D**) and females (**Figure 4.6E**) throughout the 4 days was very high, with minimum values of survival percentage of 83.33% for males exposed to $NiCl_2$ at 0.2 mg Ni/L (day 3) and the same minimum value for females exposed to NiNPs at 17 mg/L (day 4) (when different colours and symbols are not clearly visible, they are overlapped). Log-rank Mantel-Cox tests of survival curves indicated no significant differences among conditions for both males (chi square = 1.833; df = 2; p = 0.400) and females (chi square = 2.000; df = 2; p = 0.368).

Results of the chronic test with *A. clausi* and $NiCl_2$ (at concentrations 0.05, 0.1 and 0.2 mg Ni/L) are shown in **Figure 4.7**. Means of EP, HS and FP over the tested period are summarised in **Table 4.2**.

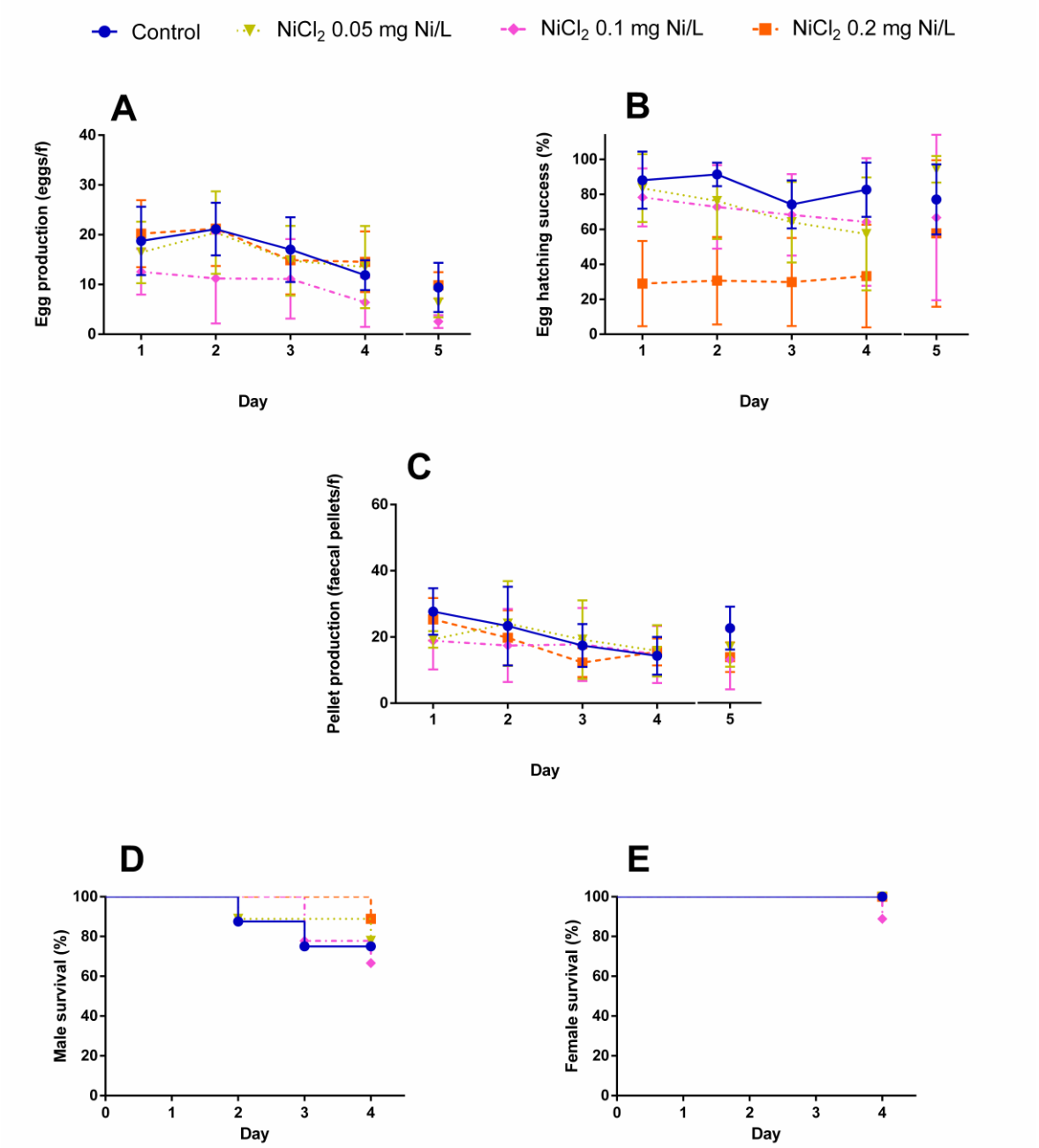

Figure 4.7 *Acartia clausi* chronic test (days 1-4) plus detoxification test (day 5) with $NiCl_2$, fed *Rhinomonas reticulata*, 2.7×10^4 cells/mL. **A** – Egg production per female (eggs/f); **B** – egg hatching success (%); **C** – faecal pellet production per female (faecal pellets/f); **D** – male survival curve (%); **E** – female survival curve (%). For **A-C** values are mean ± SD; for chronic test, n = 9; for detoxification test, n = 9.

EP of females of *A. clausi* exposed to $NiCl_2$ was comparable between all conditions, with a slight decrease over the 4 days (around 18 eggs/f on day 1 and about 14 eggs/f on day 4) (**Figure 4.7A**). The lowest values were registered for 0.1 mg Ni/L, with a 4-days

average of 10.33 ± 6.64; differences for this concentration were statistically significant on day 2 versus every other condition ($F_{(3, 120)} = 8.596$; $p < 0.0001$). Differences among the tested period were statistically significant for control between day 2 and 4 ($F_{(3,120)} = 6.760$; $p = 0.0003$). The interaction term was not statistically significant in this case ($F_{(9, 120)} = 0.437$; $p = 0.913$). In the detoxification test (day 5), EP for each condition was slightly lower with respect to the previous test, with a minimum of 2.5 ± 1.3 eggs/f for 0.1 mg Ni/L concentration. Differences between day 4 and 5 were significant only for 0.05 mg Ni/L ($t = 2.186$; $df = 13$; $p = 0.048$); they were not significant for control, 0.1 nor 0.2 mg Ni/L ($p = 0.313$, $p = 0.162$ and $p = 0.164$, respectively). Differences among conditions on day 5 were statistically significant for control versus 0.1 mg Ni/L and for 0.2 versus 0.1 mg Ni/L ($F_{(3, 14)} = 4.809$; $p = 0.017$).

Table 4.2 Chronic test with *A. clausi* and $NiCl_2$. Values are mean ± SD of 4 days; n = 9.

	EP (eggs/f)	**HS (%)**	**FP (f. pellets/f)**
Control	17.19 ± 5.42	84.09 ± 13.08	20.69 ± 7.76
$NiCl_2$ 0.05 mg Ni/L	16.29 ± 7.43	70.31 ± 24.11	19.59 ± 8.73
$NiCl_2$ 0.1 mg Ni/L	10.33 ± 6.64	70.89 ± 25.04	17.20 ± 9.84
$NiCl_2$ 0.2 mg Ni/L	17.72 ± 6.81	30.70 ± 25.98	18.22 ± 5.79

Highest egg HS during the test with $NiCl_2$ was recorded in the control (average 84.09 ± 13.08%), with slightly lower values registered in the two smallest concentration of $NiCl_2$ (0.05 and 0.1; around 70% on average for both) (**Figure 4.7B**). The highest concentration, instead, induced a low and stable egg HS throughout the test (30.70 ± 25.98%). Differences were statistically significant for control versus 0.2 on each day; 0.1 and 0.05 were also statistically different from 0.2 from day 1 to 3 ($F_{(3, 120)} = 33.94$; $p < 0.0001$). Differences between days, instead, were not significant ($F_{(3, 120)} = 1.958$; $p = 0.124$). The interaction term was not relevant for this parameter ($F_{(9, 120)} = 0.593$; $p = 0.801$). HS in the detoxification test remained similar for control and 0.1, whereas it increased for 0.05 from 57.4 ± 32.3 to 94.2 ± 7.6%, and also for 0.2 from 33.3 ± 29.3 to 57.6 ± 41.8%. These differences were statistically significant, between day 4 and 5, only for 0.05 ($t = 2.934$; $df = 13$; $p = 0.012$), not for control, 0.1 or 0.2 mg Ni/L ($p = 0.627$, $p = 0.926$, $p = 0.248$, respectively). There were no differences among conditions on day 5 ($F_{(3, 14)} = 1.429$; $p = 0.276$).

Production of FP, like EP, was similar among all conditions, which had averages around 20 faecal pellets/f (**Figure 4.7C**; **Table 4.2**). In particular, in the control FP gradually decreased from 27.7 ± 7.0 (day 1) to 14.3 ± 5.7 faecal pellets/f (day 4); all treatments had a

similar trend too and were not statistically different ($F_{(3, 120)}$ = 1.081; p = 0.360). Differences between days, on the other hand, in the same conditions were statistically significant for control (day 1 versus day 4) and 0.2 mg Ni/L (day 1 versus day 3) ($F_{(3, 120)}$ = 6.116; p = 0.0007). The interaction term was not statistically significant ($F_{(9, 120)}$ = 1.123; p = 0.352). In the detoxification test, FP production did not shift much from previous values. Control had the highest value (22.7 ± 6.5 faecal pellets/f), with other treatments having smaller, comparable to that of the fourth day of chronic test. Differences were not statistically significant between day 4 and 5 for each condition (p = 0.065, p = 0.748, p = 0.780, p = 0.534 respectively for control, 0.05, 0.1 and 0.2 mg Ni/L) nor among conditions on day 5 ($F_{(3, 14)}$ = 1.456; p = 0.269).

Survival for *A. clausi* exposed to $NiCl_2$ was very high, with little, if any, casualties, especially for females (**Figure 4.7E**). Male survival at the end of the test was lowest in 0.1 treatment (66.7%) and highest in 0.2 (88.9%) (**Figure 4.7D**). These differences were not statistically significant for both male (chi square = 1.273; df = 3; p = 0.736) and female survival (chi square = 2.889; df = 3; p = 0.409).

Results of the chronic test with *A. clausi* and NiNPs (at concentrations 4.25, 8.5 and 17 mg/L) are shown in **Figure 4.8**. Means of EP, HS and FP over the tested period are summarised in **Table 4.3**.

Control had higher EP values with respect to NiNPs solutions, with an average ± SD over the four days of 20.73 ± 6.81 eggs/f. NiNPs at 8.5 and 17 mg/L had similar values, with 17 having the lowest average (8.64 ± 7.01 eggs/f) (**Figure 4.8A**). Differences were statistically significant on day 1 and 2 for control versus 8.5 and 17 ($F_{(3, 103)}$ = 13.47; p < 0.0001). These differences were not statistically significant among days ($F_{(3, 103)}$ = 1.649; p = 0.183). The interaction term showed no remarkable significant effects of time and treatment ($F_{(9, 103)}$ = 0.709; p = 0.700). In the detoxification test (day 5) values remained similar to those of day 4, with no significant differences between day 4 and 5 (p = 0.234, p = 0.279, p = 0.912, p = 0.968 respectively for control, 4.25, 8.5 and 17 mg/L) nor between conditions on day 5 ($F_{(3,14)}$ = 1.069; p = 0.394).

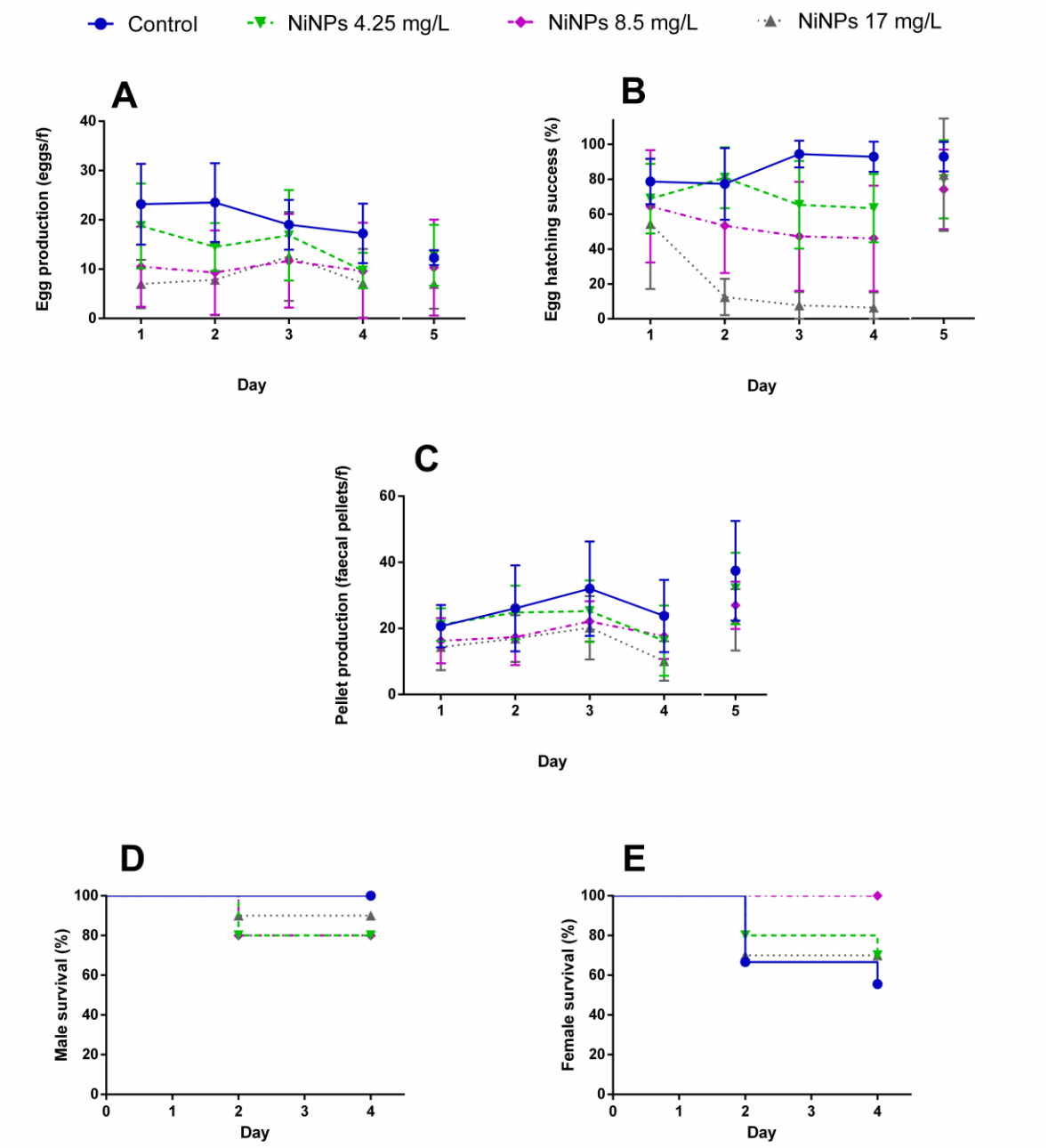

Figure 4.8 *Acartia clausi* chronic test (days 1-4) plus detoxification test (day 5) with NiNPs, fed *Rhinomonas reticulata*, 2.7×10^4 cells/mL. **A** – Egg production per female (eggs/f); **B** – egg hatching success (%); **C** – faecal pellet production per female (faecal pellets/f); **D** – male survival curve (%); **E** – female survival curve (%). For **A**-**C** values are mean ± SD; for chronic test, n = 10; for detoxification test, n = 7.

Table 4.3 Chronic test with *A. clausi* and NiNPs. Values are mean ± SD of 4 days; n = 10.

	EP (eggs/f)	**HS (%)**	**FP (f. pellets/f)**
Control	20.73 ± 6.81	85.82 ± 12.46	25.63 ± 11.16
NiNPs 4.25 mg/L	14.96 ± 6.56	69.61 ± 20.52	21.86 ± 8.23
NiNPs 8.5 mg/L	10.28 ± 8.99	52.79 ± 30.18	18.38 ± 7.06
NiNPs 17 mg/L	8.64 ± 7.01	20.27 ± 15.97	15.41 ± 7.39

Figure 4.8B shows egg HS of *A. clausi*, with a clear concentration-dependent response. Control and 4.25 mg/L had a stable trend over the 4 days (averages of 85.82 ± 12.46 and 69.61 ± 20.52%, respectively); the other concentrations, and especially 17, had instead a decreasing trend, going from 64.5 ± 32.2 to 46.1 ± 30.2% in 8.5 mg/L and from 54.3 ± 37.2 to 6.5 ± 8.6% in 17 mg/L. Except day 1, when treatments had no statistical differences, concentration 17 mg/L was different with respect to every other condition on day 2, 3 and 4; on day 3 and 4, control was also statistically different with respect to 8.5 mg/L ($F_{(3, 103)} = 39.60$; $p < 0.0001$). These differences were also statistically significant between days: for concentration 17 mg/L, egg HS on day 1 was different with respect to every other day ($F_{(3, 103)} = 2.384$; $p = 0.017$). The interaction term was not relevant for egg hatching success ($F_{(9, 103)} = 2.133$; $p = 0.101$). In the detoxification test, control had a nearly identical percentage of HS, while for every treatment an increase was registered with respect do day 4; this increase was highest for 17 mg/L, which changed from 6.5 ± 8.6% to 81.8 ± 32.0%. Differences between these two days were statistically significant for 17 mg/L ($t = 6.018$; $df = 11$; $p < 0.0001$), but not for control, 4.25 or 8.5 mg/L ($p = 0.906$, $p = 0.202$ and $p = 0.180$, respectively). Differences within conditions on day 5 were not significant ($F_{(3, 14)} = 0.300$; $p = 0.825$).

As for FP production (**Figure 4.8C**), differences between conditions were not marked. For every condition there was a mild growing trend, with a decrease on day 4. Control had highest values (4-days average of 25.63 ± 11.16 faecal pellets/f), with 17 mg/L having the lowest (4-days average of 15.41 ± 7.39 faecal pellets/f). Differences were statistically significant between conditions ($F_{(3, 103)} = 7.752$; $p < 0.0001$) and between days ($F_{(3, 103)} = 5.050$; $p = 0.003$). The interaction term was not significant from a statistical point of view ($F_{(9, 103)} = 0.470$; $p = 0.892$). The detoxification test induced a slight increase in FP production for every condition (with control being still highest and 17 mg/L lowest); differences between day 4 and 5 were significant for 4.25 mg/L ($t = 2.673$; $df = 11$; $p = 0.022$) and 17 mg/L ($t = 2.95$; $df = 11$; $p = 0.013$) and were not significant for control ($p = 0.213$) and 8.5 ($p = 0.061$). Differences within day 5 were not significant ($F_{(3, 14)} = 1.567$; $p = 0.242$).

Survivorship of *A. clausi* males (**Figure 4.8D**) was very high throughout the test, with no dead males in the control and the lowest value on day 4 of 80.0% for 4.25 and 8.5 mg/L. Survival curve of females (**Figure 4.8E**), instead, showed a lower survival for concentrations 4.25 and 17 mg/L, with the lowest value on the last day of 55.6% for the control. Differences were not statistically significant for male (chi square = 2.258; df = 3; p = 0.521) or female survival (chi square = 5.050; df = 3; p = 0.167).

Results of the chronic test with *A. clausi* and NiNPs at 17 mg/L, with the stock solution renewed every day, are shown in **Figure 4.9**. Means of EP, HS and FP over the tested period are summarised in **Table 4.4**.

EP in control and NiNPs 17 mg/L was stable during the test, with 4-days averages of 13.34 ± 5.20 and 5.08 ± 4.75 eggs/f, respectively (**Figure 4.9A**). Differences between the two conditions were statistically significant for day 2, 3 and 4 ($F_{(1, 44)} = 32.73$; $p < 0.0001$); differences between days, instead, were not ($F_{(3, 44)} = 0.650$; $p = 0.587$). The interaction term was not statistically significant ($F_{(3, 44)} = 0.214$; $p = 0.886$).

As opposite to what we observed in the previous test, egg HS with daily-renewed stock solution of NiNPs at 17 mg/L had values comparable to that of the control for the first two days (about 75%), reached a minimum of 32.7 ± 38.4% on the third day, and rose again on the fourth day to 55.6 ± 37.5% (**Figure 4.9B**). In this chronic test with daily-renewed stock solution of NiNPs, at a final concentration of 17 mg/L, the 4-days average of HS was much higher (60.34 ± 34.98%) with respect to the 4-days average of HS in the chronic test with NiNPs at the same final concentration but with the stock solution not daily-renewed (20.27 ± 15.97%). A t-test performed between these two averages indicated that there was a statistical difference ($t = 3.271$; $df = 17$; $p = 0.005$). Differences between control and daily-renewed NiNPs were not statistically significant ($F_{(1, 44)} = 4.858$; $p = 0.089$), nor were differences between days ($F_{(3, 44)} = 1.983$; $p = 0.130$). The interaction term was not relevant as well ($F_{(3, 44)} = 2.222$; $p = 0.099$)

FP production in the test with daily renewed NiNPs was stable among days for each condition, with 4-days averages of 17.52 ± 5.46 (control) and 8.11 ± 4.61 faecal pellets/f (NiNPs 17) (**Figure 4.9C**). These differences between conditions were statistically significant on day 1, 3 and 4 ($F_{(1, 44)} = 37.87$; $p < 0.0001$); there were no significant differences among days, although the p-value was close to the confidence threshold ($F_{(3, 44)} = 2.713$, $p = 0.056$). The interaction term was, however, not statistically significant ($F_{(3, 44)} = 1.117$; $p = 0.353$).

Survivorship of males (**Figure 4.9D**) and females (**Figure 4.9E**) were both very high throughout the test; the lowest value on the last day was in females exposed to NiNPs (62.5%). Differences were not statistically significant both for male (chi square = 0.002; df = 1; p = 0.967) and female survival (chi square = 1.496; df = 1; p = 0.221).

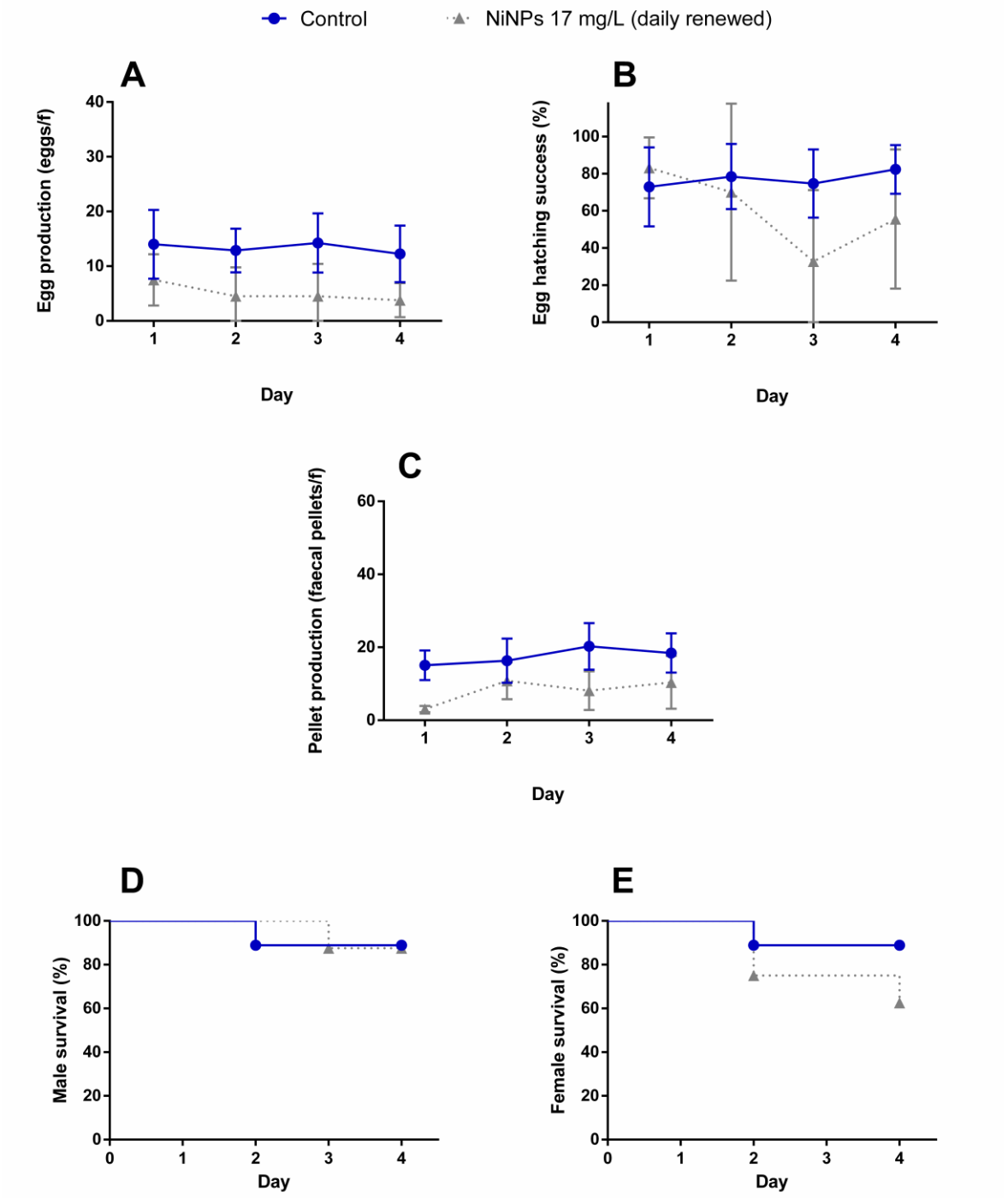

Figure 4.9 *Acartia clausi* chronic test with NiNPs (renewing the stock solution each day), fed *Rhinomonas reticulata*, 2.7×10^4 cells/mL. **A** – Egg production per female (eggs/f); **B** – egg hatching success (%); **C** – faecal pellet production per female (faecal pellets/f); **D** – male survival curve (%); **E** – female survival curve (%). For **A**-**C** values are mean ± SD; n = 9.

4.4 Discussion

Chemical characterisation of toxic substances is crucial in view of studying emerging contaminants and their effects on biota (Blasco *et al.*, 2015). Among them, engineered nanomaterials (ENMs) are an important class, diffused and employed worldwide in several

fields, whose effects on environmental components are still to be determined (Corsi *et al.*, 2021). ENMs have peculiar physical-chemical properties, which make them toxic for marine organisms in a variety of ways. Marine organisms can inhale or ingest ENMs mainly through the gut, potentially moving them within the body (Klaine *et al.*, 2013), or through contact with lungs, skin or gills (Behra and Krug, 2008); this causes effects such as increased oxidative stress, growth reduction, limited mobility, accumulation in gut, sub-lethal toxicity and mortality (Baker *et al.*, 2014). The main described mechanisms of toxicity are the following: release of metal ions, which generate reactive oxygen species (ROS) and cause oxidative damage to cells or lipids; physical damage to cellular membranes; or direct assimilation in cells (the "Trojan horse" effect), which leads to cellular damage (Corsi *et al.*, 2021; Ghobashy *et al.*, 2021).

Table 4.4 Chronic test with *A. clausi* and NiNPs (daily renewed stock solution). Values are mean ± SD of 4 days; n = 9.

	EP (eggs/f)	**HS (%)**	**FP (f. pellets/f)**
Control	13.34 ± 5.20	77.06 ± 17.54	17.52 ± 5.46
NiNPs 17 mg/L (daily renewed)	5.08 ± 4.75	60.34 ± 34.98	8.11 ± 4.61

The interactions of ENMs are complex, as they tend to aggregate with each other and with ions and biomolecules, thus reducing their toxicity (Corsi *et al.*, 2021; Hadjidemetriou and Kostarelos, 2017). In addition to this, salinity of seawater alters the ion release rate from nanoparticles and ion bioavailability, with a higher salinity usually corresponding to a lower toxicity of metals (Barus *et al.*, 2021; Damasceno *et al.*, 2017; Holmes *et al.*, 2014).

Copepods – organisms of paramount importance for their abundance, diversity and their ecological role in food webs –, are also model organisms in ecotoxicology, as they can be employed to test the effects of a variety of contaminants, from raw sediments to microplastics and endocrine disruptors (Raisuddin *et al.*, 2007). While the copepod *A. tonsa* is broadly employed and reared worldwide for this purpose, it is an invasive species in the Mediterranean Sea (Camatti *et al.*, 2019). Here, we investigated the response of this species in parallel with that of *A. clausi*, a less studied copepod species native of the Mediterranean, with the aim of comparing their responses to NiNPs, an emerging contaminant, and $NiCl_2$, a nickel salt used as a reference toxicant in ecotoxicology. We also wanted to characterise the chemical behaviour of $NiCl_2$ and NiNPs (in terms of concentration of dissolved nickel and diameter of particles) at the two different salinities that the copepod species are reared at, to exclude the possibility that salinity causes an alteration of these toxicants.

Our results of ICP-MS analysis on $NiCl_2$ samples in seawater confirmed the value of the nominal concentration of the salt (0.2 mg/L). Our measures, moreover, fell within the range of variability identified by Vitiello *et al.* (2016) when measuring through ICP-MS a stock solution prepared with the same batch of $NiCl_2$ that we used: to the nominal concentration of 10 mg/L corresponded a measured dissolved Ni concentration of 10.0 ± 0.09 mg Ni/L.

ICP-MS and DLS results proved that different salinities at which the two copepod species are reared (30 PSU for *A. tonsa* and 37 PSU for *A. clausi*) do not influence the chemical behaviour of the two toxicants in solution, *i.e.* dissolved nickel concentration for $NiCl_2$, dissolved nickel concentration of NiNPs, and size of NiNPs. Values of NiNPs size ranged from 100 to 250 nm, a result comparable to that of Zhou *et al.* (2016a), who reported sizes of around 150 nm for NiNPs at similar concentrations, at the same salinity and timepoints. Neither did the two tested timepoints (t_0 and 48 h) influence dissolved nickel in $NiCl_2$ or size of NiNPs.

Time, instead, was relevant for the nickel ions dissolved from NiNPs: in the 850 mg/L stock solution, concentration of dissolved nickel almost doubled in 72 h. This confirmed our hypothesis that NiNPs keep releasing Ni ions over time also in the stock solution kept at 4°C. According to pioneer studies which tested NiNPs or other metallic particles on marine organisms, the toxicity of this class of contaminants is mostly due to the release of nickel ions, which may induce sub-lethal effects and, consequently, chronic health impacts (Baker *et al.*, 2014; Gong *et al.*, 2011; Zhou *et al.*, 2016a). These are caused by the well-known capacity of Ni ions (and metal ions in general) to catalyse oxidative reactions which produce hydroxyl radicals (Regoli and Giuliani, 2014; Teschke, 2022). These compound, which belong to the ROS category, ultimately may cause different toxic effects, such as: alteration of ion equilibrium; peroxidation of lipids and thus damage to cellular membranes; damage to DNA; depletion of protein sulfhydryls; or carcinogenesis in mammals (Stohs and Bagchi, 1995; Teschke, 2022; Valko *et al.*, 2005).

Zhou *et al.* (2016a) noticed that a NiNPs solution at 10 mg/L (in which the measured value of dissolved nickel was about 0.14 mg Ni/L) induced in *A. tonsa* a similar naupliar immobilisation as compared to $NiCl_2$ at 0.10 mg Ni/L, *i.e.* at a similar value of dissolved nickel. We found similar results with egg HS in the chronic test with adults: after 48 h, the concentration of dissolved Ni in NiNPs at 17 mg/L was around 0.13 mg Ni/L, which is close to the concentration measured in $NiCl_2$ (nominal concentration: 0.2 mg/L).

In this view, it is explained why egg HS in chronic tests with NiNPs gradually diminished every day, reaching in 2-3 days values registered with $NiCl_2$, to quickly rise in the

detoxification test with FSW: the aliquot of NiNPs stock solution used to make test dilutions, on day 1 (corresponding to ICP-MS analysis at t_0) had a significantly lower concentration of dissolved nickel with respect to the same solution used on day 4 (corresponding to ICP-MS analysis at 72 h). This non-renewed solution, besides removing the uncertainties of multiple preparations of the toxicant, is more representative of the fate of NPs when released in the marine environment. On the other hand, this also explains why in the chronic test with daily-renewed stock solutions, HS remained higher: ion concentration was similar to that of t_0 for each day of the test.

This gradual release of ions over time also occurred in the dilutions in seawater (17 mg/L) after 48 h, but of smaller magnitude, not statistically significant. Zhou *et al.* (2016a) reported that in NiNPs solutions at three concentrations (1, 5, 10 mg/L), after 48 h dissolved nickel had a concentration which was approximately 100 times lower (0.015, 0.055, 0.139 mg Ni/L, respectively). This relationship occurred also for our values: 0.127 mg Ni/L after 48 h from a solution of 17 mg/L in seawater and 8.575 mg Ni/L after 72 h from a solution of 850 mg/L in BDW.

This finding implies that NiNPs constantly release Ni ions for an undetermined period of time, in laboratory solutions with seawater or distilled water, also stored in the dark and at 4°C. We did not find in scientific literature other studies which measured the release of ions from NPs over time in a solution and correlated it to effects on biota. Considering that metal NPs in general end up in the marine environment and in sediments, where mixing and currents which naturally occur in marine biomes can increase ion dissolution, this should be regarded as an environmental problem of great concern, especially for larvae and benthic organisms (Baker *et al.*, 2014; Blasco *et al.*, 2015; Corsi *et al.*, 2021). While for some NPs acute exposure might have a very localised impact, manufacture and release in environment of these compounds is set to dramatically increase in the near future (Baker *et al.*, 2014). More studies are needed in the future to deepen environmental concentrations and long-term dissolution of ions.

We noticed, however, a great disparity of methods in scientific literature for ICP-MS analyses of nanoparticles: no uniform protocol was found in several papers dealing with ICP-MS of metallic NPs of comparable size, as everyone differed for centrifugation speed, centrifugation time, number of centrifugations or other parameters (Casals *et al.*, 2014; Chao *et al.*, 2011; Deville *et al.*, 2016; Fabricius *et al.*, 2014; Kanold *et al.*, 2016; Navratilova *et al.*, 2015; Padoan *et al.*, 2017; Teo and Pumera, 2014; Yin *et al.*, 2015; Zhou *et al.*, 2016a). This lack of a uniform protocol is probably because NPs have only recently been studied, and

more studies will be needed to develop a comparable protocol, which would make it easier to study these substances.

Concerning the acute tests with nauplii of the two species, neither of the two toxicants decreased significantly egg HS, as shown in other studies (Buttino *et al.*, 2018; Carotenuto *et al.*, 2020; Zhou *et al.*, 2016b). This can be regarded as a discrepancy between acute and chronic test, as in the latter HS was instead very low for both species exposed to toxicants at the highest concentrations. However, it may be due to the different circumstances in which eggs are deposited in the toxicant solution: in the acute test, eggs are laid by cultured females and then deposited in the test vessel, whereas for the chronic test eggs are laid by females directly incubated in the toxicant solution, hence eggs are exposed since the very first stages of development, which are the most sensitive in marine invertebrates (Baker *et al.*, 2014). Moreover, in chronic experiments egg viability also depends on the mother's conditions (Miralto *et al.*, 1999). It is possible, hence, that the mechanism of toxicity of Ni ions on copepod eggs targets specific cellular and/or molecular processes occurring in the early-developing embryos, and that indirect exposure of the female to the same toxicants may exacerbate the outcome. Similar trans-generational effect has been reported in copepods exposed to cytotoxic lipid-peroxidation products (oxylipins) synthesized by marine diatoms, that affect embryo viability through direct incubation and indirect maternally-mediated exposure (Ianora *et al.*, 2004).

Naupliar immobilisation, on the other hand, was influenced by both toxicants. For *A. tonsa* values of HS, NI and EC_{50} of $NiCl_2$ were well within the standards of scientific literature and standard protocols (Gorbi *et al.*, 2012; UNICHIM, 2012a). EC_{50} for NiNPs was also very similar to values found in literature (20.19 mg/L) (Zhou *et al.*, 2016a). Concentrations of $NiCl_2$ for *A. clausi*, instead, were chosen considering that nauplii of this species were shown to have a greater sensitivity with respect to those of *A. tonsa* (Carotenuto *et al.*, 2020). These results were confirmed by our data of NI: in the aforementioned study, EC_{50} for $NiCl_2$ was extrapolated to 0.005 mg Ni/L (0.004 – 0.006 mg Ni/L), while our value, calculated employing lower concentrations, was almost twice as small, in the order of micrograms per litre (0.0023 mg Ni/L, 0.00013 – 0.005547 mg Ni/L). This value, indicating the concentration at which half of a population of *A. clausi* nauplii are immobilised or dead, is dangerously close to the average values for nickel concentration in marine waters reported in scientific literature. Studies report average concentrations in the order of tenths of micrograms per litre (0.0001 to 0.0005 mg/L, Cempel and Nikel, 2006 and references therein; 0.00034 to 0.00039 mg/L offshore, Paraskevopoulou *et al.*, 2010), but values of one order of magnitude higher have been reported in polluted sites (0.0027 and 0.00134 mg/L in coastal and offshore

stations respectively, Paraskevopoulou *et al.*, 2010; 0.00375 mg/L, Heijerick and Van Sprang, 2008), *i.e.* values within the range of *A. clausi* EC_{50}. Values of Ni concentration were even higher near industrial sites (2 mg/L; Eisler, 1998). An analysis of the chemical composition of elutriates of sediments (*i.e.*, the water-dissolved fraction of sediments) from a polluted area in the Mediterranean Sea, showed values of dissolved Ni below the quantification limits of 0.01 mg/L, but we cannot exclude that Ni was below the detection limit of 0.002 mg/L (Carotenuto *et al.*, 2020; values were also reported in **Table 5.1**, in the following chapter). Ni concentrations were found greater in raw sediments too, with respect to control areas (65-241 mg/kg and 427-1612 mg/kg in sediments, respectively, in a control and polluted area in the Aegean Sea; Paraskevopoulou *et al.*, 2010).

This, in addition to the constant release of Ni from nanoparticles which was discussed above, can pose a serious threat for the marine environment and recruitment of copepod species in particular. DeForest and Schlekat (2013) compared HC_5 of nickel for several marine species and proposed a conservative threshold (0.0039 mg/L) and a broadly applicable threshold (0.0209 mg/L) for dissolved nickel in temperate European marine waters. These values, especially the latter, would be higher than EC_{50} of *A. clausi* nauplii.

To our knowledge, there are no data in scientific literature on EC_{50} of NiNPs, besides that of Zhou *et al.* (2016a). To make a comparison with marine invertebrates, NiNPs were tested at 0.03, 0.3 and 3 mg/L for 48 h on the larval development of the sea urchin *P. lividus*; there were no observed lethal effects, but 0.3 mg/L treatment caused a slight size reduction of the larval stage with respect to the control, while 3 mg/L treatment gave a greater size reduction (Kanold *et al.*, 2016).

Comparing our EC_{50} values of the two species, we calculated that nauplii of the native *A. clausi*, with respect to nauplii of *A. tonsa*, were 95.3 times more sensitive to $NiCl_2$ and 6.2 times more sensitive to NiNPs. This is in agreement with results in literature and with our results of ICP-MS, which indicated that concentration of Ni dissolved from NiNPs is roughly 100 times lower than the nominal concentration of NiNPs.

To our knowledge, few chronic tests as the ones described in this thesis have been performed in ecotoxicology (Carotenuto *et al.*, 2020; Zhou *et al.*, 2016a); similar experiments, aimed at a long-term and continuous assessment of egg production, egg hatching success and feeding rate, are common for copepod species when used to study the quality of an algal diet (Barreiro *et al.*, 2006; Dutz, 1998; Zhang *et al.*, 2013, 2015).

Our results show that adults of both copepod species had a similar response to the toxicants at the same concentrations, as opposed to what we saw with nauplii. For both species, the most relevant adverse effect was the reduction of egg HS, which was most likely

due to nickel ions. The two-way ANOVA confirmed (for both species, at any concentration) that there were no statistically relevant differences between control and NiNPs on day 1, but there were from day 2 until the end of the test. This was also true confronting the same treatment over different days (for *A. clausi*), as a further proof of the gradual release of Ni from NiNPs. On the other hand, differences between control and $NiCl_2$ at the highest concentration were, for both species, statistically significant since day 1. Again, this is particularly clear when looking at the ICP-MS data: after 48 h, the concentration of dissolved Ni in NiNPs at 17 mg/L was nearly identical to the one measured in $NiCl_2$; hence, values of egg HS with NiNPs from day 2-3 become very similar to those with $NiCl_2$. It is interesting to note that, although in no case the interaction term was statistically significant, this factor, when relative to egg HS, had a p-value close to the significance threshold of 0.05, in the tests with NiNPs, for both species. This indicates that the effect of NiNPs on copepod egg hatching is more complex than expected and could be modified by the time of exposure and the release of ions.

For both toxicants, values of HS greatly rose after one day of depuration in seawater (detoxification test) and become similar to the control value, in both species. This probably indicates that the effect is indeed direct on the eggs, and not maternally mediated. We exclude the hypothesis that the observed reduction is a fast and transient maternal effect because in further experiments we reduced the depuration time to 12 h and noticed similar increases in HS, indicating that the depuration time is not involved either (data not shown). Similarly, we exclude that nickel ions caused a delay (instead of an inhibition) in egg HS, because we tried assessing HS after 96 h, instead of 48 h, and observed similar and low values (data not shown).

In a similar test with *A. tonsa,* the same concentration of NiNPs had a comparable descending trend of HS, though with higher values (from 70% to 10%, roughly, during the 4 days) (Zhou *et al.*, 2016a). HS in the control was, for both species, in line with averages from similar experiments with the same toxicants and the same species (around 80% for *A. tonsa,* Zhou *et al.*, 2016a; 82% for *A. clausi*, Carotenuto *et al.*, 2020). To our knowledge, there are no other studies in scientific literature with *A. clausi* and $NiCl_2$ or NiNPs. We can compare, however, our control group with others (although with different diets or conditions) which all have values of HS comprised between 80 and 100%, for *A. tonsa* (Castro-Longoria, 2003; Zhang *et al.*, 2013) and for *A. clausi* (Buttino, 1994; Castro-Longoria, 2003).

Other detrimental effects were, for *A. tonsa*, a reduction of EP with both toxicants and of FP productions with NiNPs. In *A. clausi*, FP production was slightly reduced by NiNPs

17 mg/L; EP, instead, decreased with $NiCl_2$ (at 0.1 mg Ni/L concentration) and with the two highest concentrations of NiNPs.

FP production in copepods is considered a proxy of feeding rates (Nejstgaard *et al.*, 2001). FP production is not commonly measured in ecotoxicological studies, and most of the data we found in the literature are from study of algal diets. Our values of FP production of *A. tonsa* in control appear slightly lower: a similar experiment with the same algal species (*Rhodomonas baltica*) at one third of the carbon content used in our test (500 µg C/L) resulted on average in production of 54 faecal pellets/f and 22 eggs/f (Zhang *et al.*, 2013), and another study with a similar microalgae (*Rhinomonas reticulata*) at the same carbon content with respect to our test gave roughly 75-100 faecal pellets/f and 20-40 eggs/f each day (Zhang *et al.*, 2015). FP production reported for *A. clausi* appeared similar to our values (roughly 30-50 faecal pellets/f, Buttino, 1994; 20-40 faecal pellets/f, Calliari and Tiselius, 2005).

As for EP, studies with *A. tonsa* reported comparable results for control: 16.8 eggs/f (Carotenuto *et al.*, 2020) and roughly 20 eggs/f (Zhou *et al.*, 2016a). However, as opposite to what we found, Zhou *et al.* (2016a) did not observe significant reductions in egg production of *A. tonsa* exposed for 4 days to NiNPs 17 mg/L. Other studies reported roughly similar values of eggs per female in control conditions for *A. tonsa* (5-25 eggs/f, Castro-Longoria, 2003) and for *A. clausi* (on average 7.2 eggs/f, Carotenuto *et al.*, 2020; around 20 eggs/f, Dutz, 1998; 2-15 eggs/f, Castro-Longoria, 2003; 20-30 eggs/f, Buttino, 1994; 10-20 eggs/f, Calliari and Tiselius, 2005).

Interestingly, the daily-renewed solution of NiNPs too caused a similar decrease in EP and in FP production of *A. clausi*, indicating that these effects were not caused by the release of Ni ions (like egg HS), but by the particles, perhaps by a mechanical effect of occlusion in the gut; it was demonstrated, in fact, that *A. tonsa* females can ingest and excrete NiNPs (Zhou *et al.*, 2016a). NiNPs, hence, may cause a reduction of EP as the result of a shift in the molecular balance: exposure to this toxicant might induce copepod females to remove molecular resources (*i.e.*, to reduce gene expression) from reproduction to allocate energy, instead, on processes such as maintenance of physiological homeostasis, integrity of cellular processes or detoxification. Another explanation (which could also account for the lower production of FP) could be a general intoxication, leading to poor appetite and low feeding rate, which was reported for the copepods *Calanus pacificus* and *Paracalanus parvus* fed different species of toxic dinoflagellates (Huntley *et al.*, 1986).

Physiological parameters of treated organisms in detoxification tests, in most cases returned to values similar to those of the control, indicating that one day in seawater was

enough for adults of both species to depurate and restore their parameters to normal values. Survival rate of males or females was not influenced by a toxicant for either species, as occurred in similar studies (Carotenuto *et al.*, 2020). However, research works with a life-trait approach showed that female lifespan of the calanoid copepod *Pseudodiaptomus annandalei*, when exposed to two different concentrations of cadmium, were 9 or 8 days shorter than in the control (Kadiene *et al.*, 2019). Perhaps with similar life-traits studies it would be possible to assess if detoxification has long-term repercussions on adult mortality.

Overall, adults of *A. clausi* and *A. tonsa* seemed to have comparable responses, despite the great difference in sensitivity among nauplii. This stage-specific sensitivity was reported also between nauplii and copepodids of *P. annandalei* after a 96 h exposure to cadmium, with nauplii being roughly three times more sensitive in terms of LC_{50} (lethal concentration) (Kadiene *et al.*, 2019). Larval stages are, in fact, in general, orders of magnitude more sensitive to toxicants with respect to adults (Medina *et al.*, 2002); likely, this greater sensitivity of larval stages is due to their small size, *i.e.* their higher surface contact area in relation to volume (Baker *et al.*, 2014; Rand, 1995), or to different detoxification abilities of nauplii and adults (Green *et al.*, 1996). Most marine organisms have a microscopic and planktonic larval stage, many of which settle in shallow coastal waters; it is this fragile stage that might be subject to deleterious effects of NPs and other contaminants, especially when close to discharge inputs (Baker *et al.*, 2014).

More studies and regulations are needed to deepen these effects and safeguard the recruitment of marine organisms. In this view, the use of *A. clausi* in ecological risk assessment in the Mediterranean Sea can be useful to identify and apply safety thresholds which respect the physiological parameters of local species; for this purpose, the optimisation of culture protocols to have a stable, multigenerational laboratory culture of *A. clausi* is of great importance.

Chapter 5 *De novo* transcriptome assembly of *A. clausi* exposed to pollutants

5.1 Introduction

Among the main goals of ecotoxicogenomics (a hybrid discipline that combines ecology, toxicology and genomics) (Tarrant *et al.*, 2019; Tennant, 2002), there is identifying useful biomarkers of exposure to toxic substances, which might be used to predict a toxic effect, and elucidating the molecular mechanisms of toxicity (Waters and Fostel, 2004). In this view, RNA sequencing, or RNA-seq, is a next generation sequencing (NGS) approach for high throughput sequencing of transcriptomes, a powerful tool for identifying the complete gene expression profile of organisms (Wang *et al.*, 2009).

A transcriptome is the complete set of messenger RNA (mRNA), non-coding RNA and small RNA transcripts produced by a particular cell, cell type or organism (Morozova *et al.*, 2009). RNA-seq, hence, allows to catalogue all RNA transcripts and to determine the transcriptional structure of genes in terms of their start sites, 5'- and 3'-ends, novel transcribed regions, splicing patterns and other post-transcriptional modifications (Wang *et al.*, 2009). For this reason, RNA-seq is in general most useful in species whose genome or transcriptome is still not available, generating a so called *de novo* assembly (Wang *et al.*, 2009).

Currently, there is not an ideal pipeline for RNA-seq; rather, there are several possible procedures for RNA-seq studies, depending on the specific application (Conesa *et al.*, 2016). In general, RNA-seq workflow begins with the fragmentation and conversion of the total or fractionated RNA population (poly A+) into a library of cDNA fragments, which are then ligated to primer adaptors at both ends. Each molecule is sequenced in single or paired-end options (paired-end option being preferable for *de novo* transcript discovery or isoform expression analysis) in a high-throughput NGS machine, typically Illumina, to generate millions of short reads representing the transcriptome; depending on the technology used, the reads are typically 30-400 bp long (Conesa *et al.*, 2016).

After this, to infer expression of specific transcripts, two possibilities are open: in the case of organisms with available reference genomes or transcriptomes, reads are mapped (*i.e.*, aligned) onto the reference sequences; if there is no genome or transcriptome available for the studied organism, reads are *de novo* (*i.e.*, anew, for the first time) assembled into longer contigs, which are then treated as the expressed transcriptome to which reads are mapped back again (Conesa *et al.*, 2016). Among the different programs and software which

perform this alignment of sequences, there are Bowtie2 (Langmead *et al.*, 2009) and kallisto (Bray *et al.*, 2016). Kallisto allows to quantify the abundances of transcripts reducing potential errors associated with multiple mapping, also granting a higher speed with respect to other programs; it is thus considered more appropriate for gene expression analysis (Bray *et al.*, 2016). After this operation, differential expression analysis and functional annotation are carried out to infer, respectively, the level of expression of the transcribed sequences and the biological function of each transcript (by comparing it to similar sequences in online databases).

Currently, despite their ecological relevance, relatively little is known about copepod genomic sequences, as their genomic resources and RNA-seq studies are limited to few species (Amato and Carotenuto, 2018). To date, in fact, seven copepod genomes have been sequenced and published: the calanoid *Eurytemora carolleeae* (Eyun *et al.*, 2017) (formerly known as *E. affinis*; Alekseev and Souissi, 2011; Sukhikh *et al.*, 2020) and *E. affinis* (Choi *et al.*, 2021); the cyclopoid *Oithona nana* (Madoui *et al.*, 2017); the harpacticoids *Tigriopus californicus* (Barreto *et al.*, 2018), *T. kingsejongensis* (Lee *et al.*, 2020) and *T. japonicus* (Jeong *et al.*, 2020). The genome of the calanoid *Acartia tonsa* was sequenced in 2019, which with 2.5 Gb of total genome size proved to be the largest among the other available copepod genomes (Jørgensen *et al.*, 2019). Transcriptomic studies on copepods, on the other hand, are less scarce. Among the available transcriptomes, there are, for instance, those of *A. tonsa* exposed to nickel nanoparticles, (Zhou *et al.*, 2018), *Temora longicornis* under heat stress (Semmouri *et al.*, 2019), *Neocalanus flemingeri* in diapause conditions (Roncalli, 2018) and *E. affinis* exposed to benzo[a]pyrene (B[a]P) (Lee *et al.*, 2018).

Within the work of this PhD thesis, we generated, through high-throughput RNA sequencing, a *de novo* transcriptome assembly followed by differential gene expression analysis of *A. clausi* females exposed for 4 days to elutriates of sediments collected from the Bagnoli-Coroglio area, a heavily polluted industrial area in the Campania region (Southern Italy) (Carotenuto *et al.*, 2020). Elutriates, obtained after stirring raw sediment with water in a 1:4 proportion, contain the water-soluble fraction of contaminants released from the sediment, and thus simulate the effects of dredging of sediments (APAT-ICRAM, 2007; US EPA, 1991). Marine sediments, in fact, are regarded as sinks for several pollutants, organic and inorganic, which are constantly released in the marine environment mainly from boats or industrial activity (Bebianno *et al.*, 2015).

Thanks to the ABBaCo project, sediments in the Bagnoli-Coroglio area were sampled and elutriates were subject to both chemical and ecotoxicological analyses. In particular, the toxicity of three sediment-derived elutriates from the sampling areas (E25, E56 and E84)

were recently tested on females of *A. clausi* (Carotenuto *et al.*, 2020). Moreover, to further investigate the molecular responses of this species after chronic exposure to the elutriates, a subset of females was also harvested for later gene expression analysis. Specifically, *A. clausi* females exposed to the elutriate E56 were used in this PhD study to generate a *de novo* assembled transcriptome and a differential expression analysis between females exposed to elutriates and females in control. This elutriate was chosen to generate the reference transcriptome as it contained a very high concentration of heavy metals, especially mercury, and polycyclic aromatic hydrocarbons (PAHs), including naphthalene, anthracene and B[a]P, notorious for being extremely toxic also on marine organisms (Hylland, 2006; Wang *et al.*, 2017). Polycyclic aromatic hydrocarbons (PAHs) are a vast class of contaminants including molecules with at least two benzene rings, and which are most frequently associated with toxicity; they are considered among the most widespread organic pollutants in aquatic environments (Armstrong *et al.*, 2022; Yu *et al.*, 2018). Though the concentrations of PAHs are low in different environments, marine organisms are inevitably exposed to PAHs during their lifecycle (Yu *et al.*, 2018). The transcriptome generated from females exposed to this elutriate could provide interesting information on the responses of copepods to such a complex environmental mixture of different chemicals found in a polluted site.

The transcriptome we generated was useful as a molecular response, in the form of a complete gene expression profile, to be linked to the physiological responses to the same sediments reported for *A. clausi* females by Carotenuto *et al.* (2020); more importantly, it represented the opportunity to have a reference transcriptome for *A. clausi*, that despite its great ecological relevance still lacked publicly available genomic resources. This reference transcriptome, as well as the differential expression analysis, will be useful for the aim of this PhD, as it could allow us to select potential genes of interest (GOI) and design species-specific primers for *A. clausi* exposed to $NiCl_2$ and NiNPs.

5.2 Materials and methods

5.2.1 Total RNA extraction, quantity and quality assessment

Adult females of *A. clausi* fed *Rhinomonas reticulata* were exposed for 4 days to FSW (control) and elutriate derived from sediments sampled in station 56 (E56), that contained in total 12 heavy metals (total concentration 5,059.44 μg/L), and 7 PAHs (total concentration 8.62 μg/L) (Carotenuto *et al.*, 2020); for ease of reference, we reported in **Table 5.1** the concentrations of all chemical species measured in E56. After the fourth day, females were

transferred into 1.5 mL plastic tubes (Eppendorf), in three replicates for each treatment, with 9 or 10 females in each replicate. Water was removed via a thin-mouth Pasteur pipette, tubes were flash-frozen in liquid nitrogen and stored at – 80°C until RNA extraction.

Table 5. 1 Chemical analysis of elutriate 56 (E56) prepared from sediments of the Bagnoli-Coroglio area (Naples, Italy). For several chemical species (heavy metals and polycyclic aromatic hydrocarbons (PAHs)) are reported the following parameters: concentration measured in E56; threshold values (annual average) of Environmental Quality Standards (EQS) defined by the European Commission (EC, 2008); limit of detection (LOD) and limit of quantification (LOQ) of metals. In bold, concentrations of chemicals with values exceeding EQS. * indicates chemical species defined by the European Commission as priority hazardous substances. Heavy metals values are given as mean ± SD. Source: Carotenuto *et al.* (2020).

Chemical species	E56 (µg/L)	EQS (µg/L)	LOD (µg/L)	LOQ (µg/L)
Heavy metals				
Al	< 10		3.2	10
Sb	4.9 ± 1.0		0.1	2
As	19.1 ± 4.0		0.1	1
Ba	123 ± 24.7		3.3	30
Be	< 5		1.3	5
B	3,492 ± 768		19.1	100
Cd*	< 5	0.2	0.1	5
Co	< 2		0.2	2
Cr	10.4 ± 2.4		0.4	1
Fe	94.1 ± 19.8		1.7	50
Mn	1,073 ± 2.15		0.2	1
Hg*	**0.63 ± 0.2**	0.05	0.1	0.5
Mo	37.5 ± 8.6		0.8	3
Ni	< 10		2.1	10
Pb	1.53 ± 0.4		0.05	1
Cu	< 10		2.2	10
Se	31.3 ± 6.9		2.4	10
V	172 ± 36		0.9	5
Zn	< 10		0.9	10
Total	*5,059.44*			
PAHs				
Naphthalene	**4.00**	1.2		
Acenaphthylene	2.06			
Acenaphthene	1.08			
Fluorene	0.02			
Anthracene*	**0.20**	0.1		
Phenanthrene	0.29			
Fluoranthene	0.05			
Pyrene	0.16			
Benz[a]anthracene	0.12			
Dibenz(a,h)anthracene	< 0.01			
Chrysene	0.13			
Benzo(b)fluorantene*	**0.13**	0.03		

Benzo(k)fluoranthene*	**0.10**	
Benzo(a)pyrene*	**0.10**	0.05
Indeno(1,2,3-cd)pyrene*	**0.09**	0.002
Benzo(g,h,i)perylene*	**0.07**	
Total	*8.62*	

Total RNA of *A. clausi* was extracted using the TRIzol® reagent method (Invitrogen, San Diego, California, USA), following the method described in Asai *et al.* (2015). Briefly, soon after removing samples from – 80°C storage, 0.5 mL of TRIzol® were added to each one; then, they were homogenised with TissueLyser II (Qiagen, Germantown, Maryland, USA) using 3 mm sterile aluminium beads. Samples were homogenized at 20.1 Hz for 3 min and 2 min in succession. Each homogenised samples were transferred into a new 1.5 mL tube and resuspended 3-4 times by means of a 1 mL sterile syringe needle to ensure complete disruption of ribonucleoproteic complexes. After the addition of 0.1 mL of chloroform (Sigma-Aldrich Life Science, Milan, Italy) for phase separation, tubes were vigorously shaken by hand for about 15 seconds, incubated at room temperature for 5 min, then centrifuged at 12,000 RPM for 15 min at 4°C with a refrigerated centrifuge (5417C, Eppendorf, Hamburg, Germany). RNA remained in the upper aqueous phase, which was carefully collected in a new tube; an equal volume of chloroform was added. Tubes were centrifugated again with the same parameters and the supernatant was transferred into a new tube. For RNA precipitation, 0.25 mL of isopropanol (Sigma-Aldrich Life Science, Milan, Italy) and 1 µL of glycogen (Invitrogen, Carlsbad, California, USA) were added, then the volume was gently resuspended. After shaking by hand for 15 seconds, 15 min of incubation at room temperature, samples were centrifuged again with the same parameters. After this, the supernatant was carefully removed, and the pellet (RNA) was washed with 0.5 mL of 80% absolute ethanol, resuspended and centrifuged at 8,000 RPM for 5 min at 4°C; this procedure was performed twice. After removing the supernatant again, the pellet was air-dried for 1 h. Total RNA was resuspended in 10 µL of 0.1% v/v diethylpyrocarbonate (DEPC) treated water and stored at – 80°C.

Quantity and quality (purity and integrity) of extracted *A. clausi* RNA were assessed by NanoDrop (ND-1000 UV-Vis spectrophotometer; NanoDrop Technologies Inc., Wilmington, Delaware, USA) and Agilent 2100 Bioanalyzer (Agilent Technologies, Santa Clara, California, USA). 2 µL of total RNA (diluted 1:2 with DEPC water) were read at the NanoDrop to measure the absorbance maximum at 260 nm and to assess the RNA concentration (ng/µL). Purity was evaluated as A260/230 and A260/280 ratios, which indicate possible contamination of phenol or proteins and usually range between 1.8 and 2.2 for pure RNA samples. Integrity was assessed through an Agilent Bioanalyzer 2100 system by

running 100-200 ng of RNA sample in each lane of a 6000 Nano LabChip, in parallel with a DNA Ladder of the same Nano LabChip as a reference. The Bioanalyzer allows a precise RNA integrity analysis using the RNA Integrity Number (RIN), which is computed by comparison of the areas of 18S and 28S rRNA, the height of the 28S rRNA peak and the fast area ratio (Schroeder *et al.*, 2006). RIN values range from 1 to 10, with 1 being the most degraded profile and 10 the most intact. Two samples which were not successfully analysed were diluted and ran again using a Pico LabChip.

RNA aliquots were not run in an agarose gel electrophoresis because in preliminary RNA extractions we noticed that *A. clausi* females had a low RNA yield (in the order of tens of ng/µL from about 10 females) and, when run on an agarose gel electrophoresis, no RNA bands were visible (data not shown).

5.2.2 De novo *transcriptome sequencing and assembly*

After assessing quantity and quality of extracted total RNA samples, 6-8 µL for each of six samples (total RNA ranging from 260 to 950 ng) were sent to Genomics Core Facility of the European Molecular Biology Laboratory (EMBL) (Heidelberg, Germany) for high-throughput sequencing.

Six cDNA libraries of *A. clausi*'s transcriptome (E56-exposed females and control females) were prepared using Truseq™ RNA Sample Prep Kit (Illumina, San Diego, USA) according to the manufacturer's recommendations. Samples were barcoded, pooled and sequenced using a single lane of Illumina NextSeq 500 (Illumina, San Diego, California, USA) in a High Flow 75PE (75 paired-end) format.

Quality assessment, filtering and *de novo* assembly of the transcriptome was performed by Matthew C. Cieslak from University of Hawai'i at Mānoa; general support with RNA-seq was offered by Dr. Victoria Roncalli of Stazione Zoologica Anton Dohrn and Dr. Lenz of University of Hawai'i at Mānoa. After quality assessment using the software FastQC (version 1.0.0; http://www.bioinformatics.babraham.ac.uk/projects/fastqc/), from each RNA-seq library, Illumina adapters (TruSeq3-PE), reads < 50 bp long, reads with an average Phred score < 30 and the first 9 bp from each read, were removed using Trimmomatic (v. 0.36) (Bolger *et al.*, 2014).

A reference *de novo* transcriptome was generated for *A. clausi* individuals by pooling high-quality reads from two libraries (first replicate of the control, first replicate of treatment) using Trinity (v. 2.0.6) on the Mason Linux cluster of the National Centre for Genome Analysis Support (NCGAS; Indiana University, Bloomington, Indiana, USA) (Grabherr *et*

al., 2011). Trinity parameters were set to: --seqType fq --CPU 32 --max_memory 300G --min_contig_length 300 -- normalize_max_read_cov 50. A summary of the statistics was obtained using the script TrinityStats.pl (v. 2.0.6).

The completeness of the assembly was assessed by self-mapping the quality-filtered reads to the reference transcriptome using kallisto (default settings; v.0.43.1) (Bray *et al.*, 2016) and searching for the presence and completeness of "core genes" using the Arthropod data set as reference (n = 2,675) with BUSCO (v. 1.22) (Simão *et al.*, 2015).

5.2.3 Differential expression analysis

Gene expression was quantified by mapping each quality-filtered library (n = 6) against the *A. clausi* reference transcriptome using kallisto (default settings; v.0.43.1) (Bray *et al.*, 2016). Raw counts generated by kallisto mapping were used as input to perform differential expression analysis between females exposed to E56 and those in control condition, using R/Bioconductor and the edgeR package to identify Differentially Expressed Genes (DEGs) (Robinson *et al.*, 2010).

To remove transcripts expressed at a low level, they were filtered for CPM (counts per million of mapped reads) > 1 in at least three replicates. Expression levels of filtered transcripts were then normalised using the default TMM (trimmed mean of M values) method (Robinson and Oshlack, 2010). Values of statistical significance were obtained by performing a hypergeometric test and corrected p-value using the False Discovery Rate (FDR) method (Benjamini and Hochberg, 1995), and transcripts having an FDR < 0.05 and $|\log_2 FC|$ (fold change) ≥ 2 were considered DEGs. Biological coefficient of variation (BCV) and dispersion, estimates of the difference between replicates, were also calculated.

5.2.4 Functional annotation and functional enrichment analysis of the de novo *transcriptome*

Assembled transcripts were functionally annotated using OmicsBox – Bioinformatics made easy 2.0.36 (BioBam Bioinformatics, 2019; https://www.biobam.com/omicsbox), which uses the Blast2GO methodology for functional annotation (Götz *et al.*, 2008). This software uses the Basic Local Alignment Search Tool (BLAST; https://blast.ncbi.nlm.nih.gov/Blast.cgi) to search for similarities between query reads and sequences deposited in the National Centre for Biotechnology Information (NCBI) non-redundant protein sequence database (nr) (Altschul *et al.*, 1990).

The BLAST program used was BLASTx-fast (E-value cut-off set to 10^{-3}) (Altschul *et al.*, 1990), which compares a nucleotide query sequence translated in all reading frames against the non-redundant (nr) protein sequence database. To narrow the field of this analysis, a taxonomy filter for Arthropods was set (6656 Arthropoda). The number of BLAST hits was set to 20, and the remaining options were left as default.

In addition to the BLASTx search, the query sequences were searched onto the InterPro database (InterProScan annotation). Significantly matched transcripts with the best alignments were then mapped and annotated (E-value cut-off set to 10^{-6}) according to gene onthology (GO) functional categories: GO annotation, in fact, assigns to each transcript which has obtained a BLAST hit a specific biological process (BP), molecular function (MF) and cellular component (CC).

After the complete GO attribution, the validate annotation function was used to assign the most fitting function for each sequence. Validate gene ontology annotation removes all redundant terms for a given sequence, so that if two or more GO terms lying on the same GO branch are assigned to the same sequence, only the most specific GO terms are assigned (any term is considered redundant and is removed if a child term coexists for the same sequence).

After this, for all the transcripts, all GO terms retrieved via InterProScan were merged to the already existing GO annotation through the function merge (add and validate) InterPro to GO. Lastly, GO-Enzyme Code Mapping was selected to map existing Gene Ontology terms to Enzyme Codes.

A second BLAST was run on the sequences with no BLAST hits, without a taxonomy filter; other options were chosen as reported above for the first BLAST.

Finally, functional enrichment analysis (for up- and down-regulated genes, separately, with respect to the whole transcriptome), in *A. clausi* females exposed to E56 versus females in control conditions, was carried out through OmicsBox using the Fisher's exact test with multiple testing correction of false discovery rate (FDR < 0.05).

5.3 Results

5.3.1 Total RNA extraction, quantity and quality assessment

Six total RNA samples, extracted from *A. clausi* females exposed for 4 days to filtered seawater (control condition) or to E56 elutriate and fed on *Rhinomonas reticulata*, had a mean ± SD concentration of 67.03 ± 34.35 ng/µL, with average A260/A230 and A260/280

ratios of 1.76 and 1.97, respectively. RINs ranged from 7.30 to 9.50 (average 9.08). The reports showed no genomic DNA contamination and clear rRNA peaks in all cases. The results generated by the Bioanalyzer for each of the six samples are shown in **Figure 5.1**.

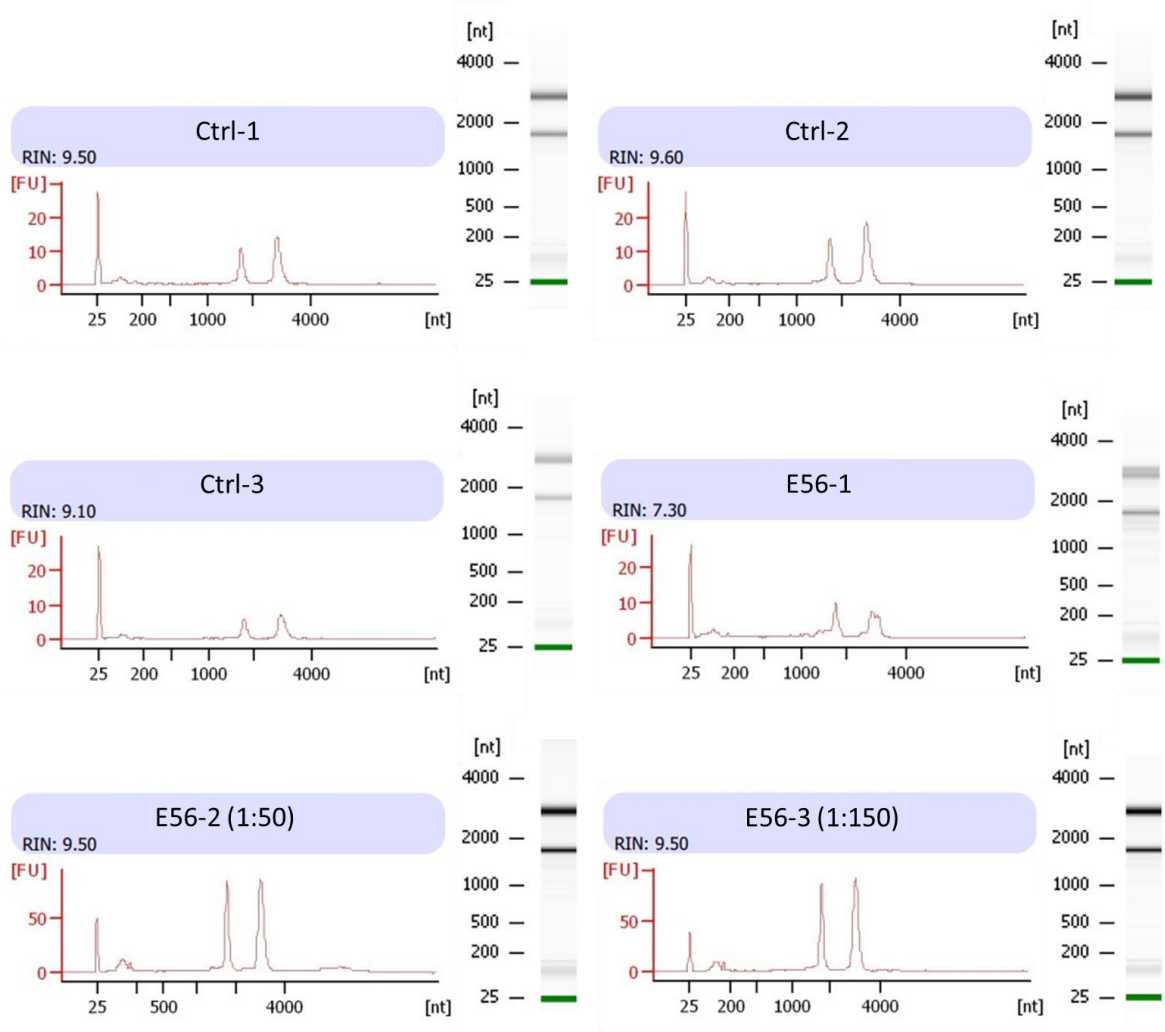

Figure 5.1 Results generated by the Agilent Bioanalyzer for six total RNA samples (extracted with TRIzol® method) of females of *A. clausi* exposed for 4 days to control conditions (Ctrl) and to elutriates of polluted sediments (E56) (each in three replicates). For each sample the electropherogram, a column with the agarose gel-like visualisation and the calculated RIN are shown. Replicates 2 and 3 of E56 were diluted (1:50 and 1:150 ratios, respectively) and run again on a Pico LabChip.

5.3.2 De novo *transcriptome sequencing and assembly*

After trimming and cleaning, the quality-filtered sequence libraries ranged from 56 to 76 million reads with an average of 65 million. The main parameters are summarised in **Table 5.2**.

The *A. clausi de novo* assembly of these reads generated 106,414 total Trinity transcripts, corresponding to 41,055 Trinity predicted genes. This represented our reference transcriptome and contained either singletons (transcripts with a single isoform), as well as multiple isoforms of the same transcript. **Figure 5.2** shows length distribution (%) of the 106,414 total transcripts. Minimum and maximum length of sequences were 301 and 14,264 bp, respectively, while average length was 825 bp and N_{50} was 1,048 bp. This parameter is defined as the sequence length of the shortest contig at 50% of the total assembly length, *i.e.*, it indicates that half of the assembly is fragmented in contigs with size ≥ N_{50} contig size. Approximately half of the transcripts (46.4%) had length < 500 bp, while in the remaining half of transcripts > 500 bp, 7.5% had a length > 2000 bp.

Table 5.2 Summary of *A. clausi de novo* assembly and mapping stats. * indicates an average of 6 samples.

Total Trinity genes	41,055
Total Trinity transcripts	106,414
GC content (%)	38.49
Minimum length (bp)	301
N_{50} (bp)	1,048
N_{75} (bp)	543
N_{25} (bp)	2,142
Longest transcript (bp)	14,264
Overall mapping rate (%)*	86.21
Mapped >1 (%)*	55.69
BUSCO complete (%) Arthrpoda database (n = 2675)	59
Fragmented (%)	13
Missing (%)	26

5.3.3 Differential expression analysis

As for the differential expression analysis, a total of 37,483 transcripts resulted after the CPM > 1 filtering (**Figure 5.3**). The BCV (which indicates the variability of the data) of this dataset was 0.5272 and its dispersion was 0.2779. Overall, 1000 DEGs were

significantly expressed in *A. clausi* exposed to E56 versus females in control; most of them were up-regulated (743), while the remaining ones (257) were down-regulated.

5.3.4 Functional annotation of the de novo *transcriptome*

BLASTx similarity search of 106,414 *A. clausi* transcripts against non-redundant (nr) protein database resulted in 59,099 matched transcripts (55.5% of the total); of these, 35,162 (33.0% of total transcripts) received complete GO Annotation. Overall, 47,315 transcripts (44.5%) did not have a BLASTx hit (**Figure 5.4**).

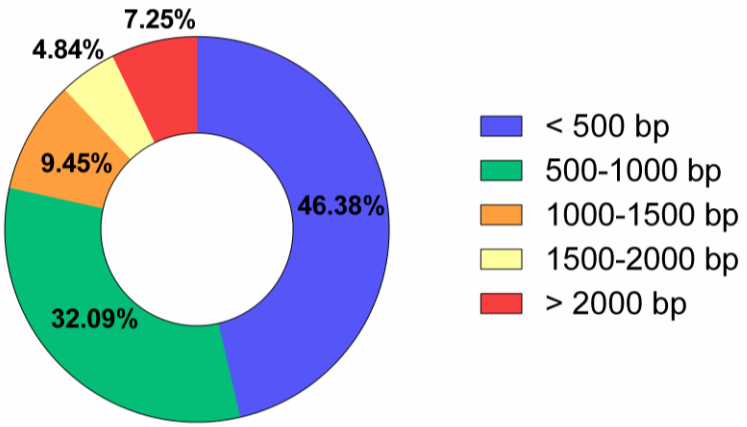

Figure 5.2 Sequence length distribution (%) of the 106,414 total transcripts of the *de novo* transcriptome of *Acartia. clausi*. Sequences are grouped into categories based on their length (bp).

E-value (expectation value) is the number of expected BLAST hits of similar quality (score) that could be found by chance; *i.e.*, a low E-value indicates a greater probability of homology between query sequence and the aligned sequences in the database. The E-value distribution showed that 16.0% and 13.8% of the transcripts (making up for almost 30% of the total) had strong homology in the nr database, with E-values less than 1×10^{-100} and from 1×10^{-100} to 1×10^{-60}, respectively (**Figure 5.5A**).

Percentages of similarity values, which express the similarity between the *de novo* assembled sequences and proteins in the nr, were in general high, with almost two thirds of the sequences (65.3%) having similarity percentages > 60% (**Figure 5.5B**). In particular, 2.8% of the sequences showed a very high similarity percentage (> 95%).

The top 20 species distribution of the top BLASTx hits for the transcriptome of *A. clausi* against the nr database resulted in a great majority of hits (41,834 out of 60,179, 69.5%) registered for copepod species, 5 out of the top 20 species: most notably *Eurytemora affinis* (37,944 hits), but also *Tigriopus californicus*, *Acartia pacifica*, *Lepeophtheirus*

salmonis, *Pseudodiaptomus poplesia* (**Figure 5.6**). Other species with top-hits belonged to other taxa in the subphylum Crustacea, to the Hexapoda class or to the subphylum Chelicerata. This reflected both phylogenetic relationship and abundant genomic information for those species.

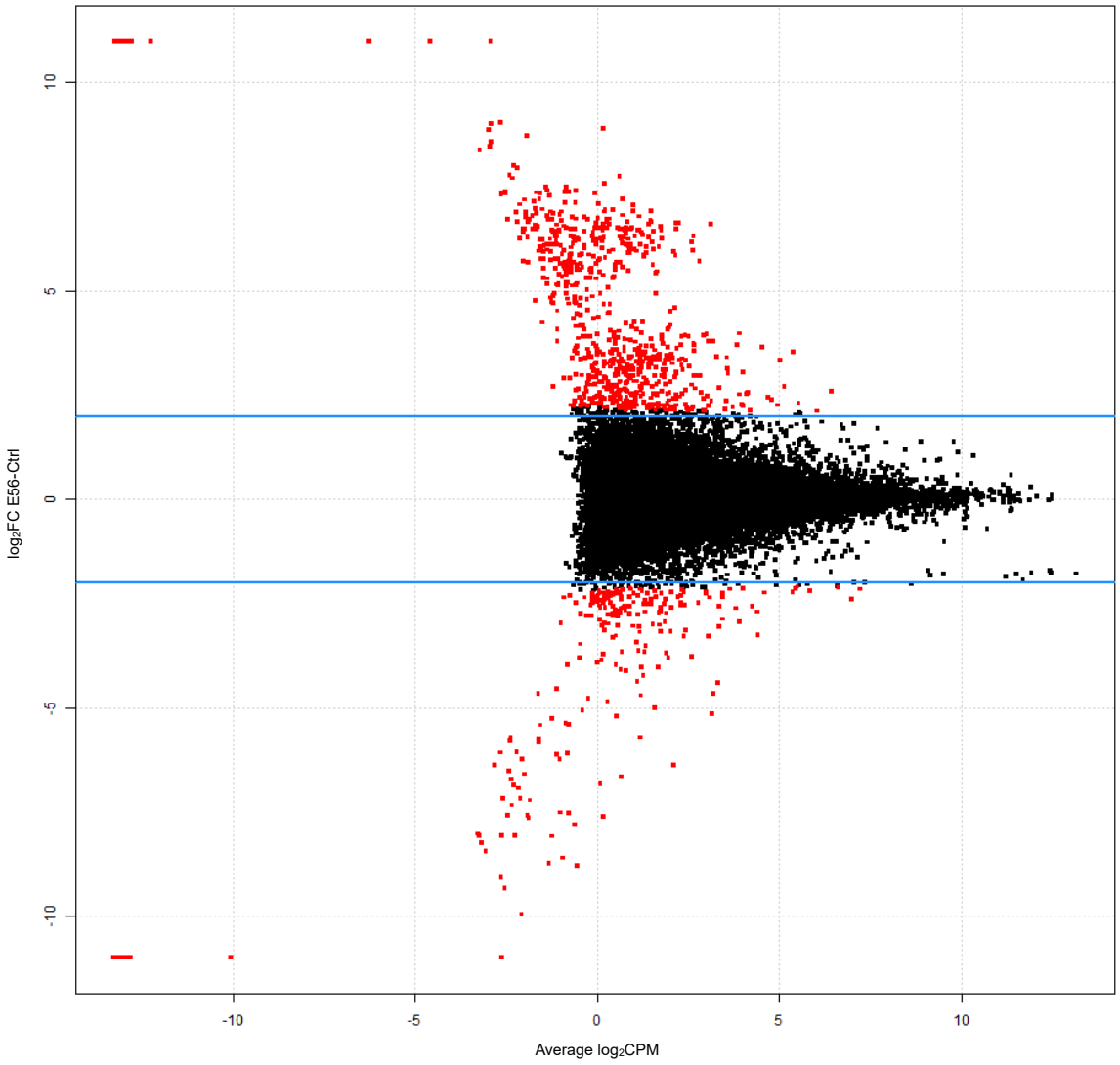

Figure 5.3 Visualisation of differential expression analysis of the *A. clausi* transcriptome (E56 versus control) performed with R/Bioconductor and the edgeR package. Each dot represents a transcript; red dots represent differentially expressed genes (DEGs), *i.e.*, transcripts with FDR ≤ 0.05 and $|\log_2 FC|$ (fold change) ≥ 2. Light blue lines correspond to $\log_2 FC \pm 2$.

Results of the functional annotation with OmicsBox are reported in **Figure 5.7**. The 35,162 GO-annotated sequences received a total of 113,721 annotations, distributed among the three GO terms – biological process (BP; 32.4% of the total annotations), molecular function (MF; 43.6%) and cellular component (CC; 24.0%). As for the number of annotated sequences, we found that in GO level 2, in the BP category, among the top 20 most

represented subcategories there were cellular process (33.9% of the total sequences), metabolic process (26.2%), biological regulation (8.4%), localisation (7.2%) and response to stimulus (5.5%); at the same GO level, MF category comprised mostly binding activity and catalytic activity (45.7 and 35.4% of the total sequences, respectively) (**Figure 5.7**). For CC, the most represented subcategories of level 3 were intracellular anatomical structure (21.9% of the total), organelle (18.3%), membrane (14.5%) and cytoplasm (12.4%) (we chose GO level 3 as in the 2nd there were only three represented subcategories in total).

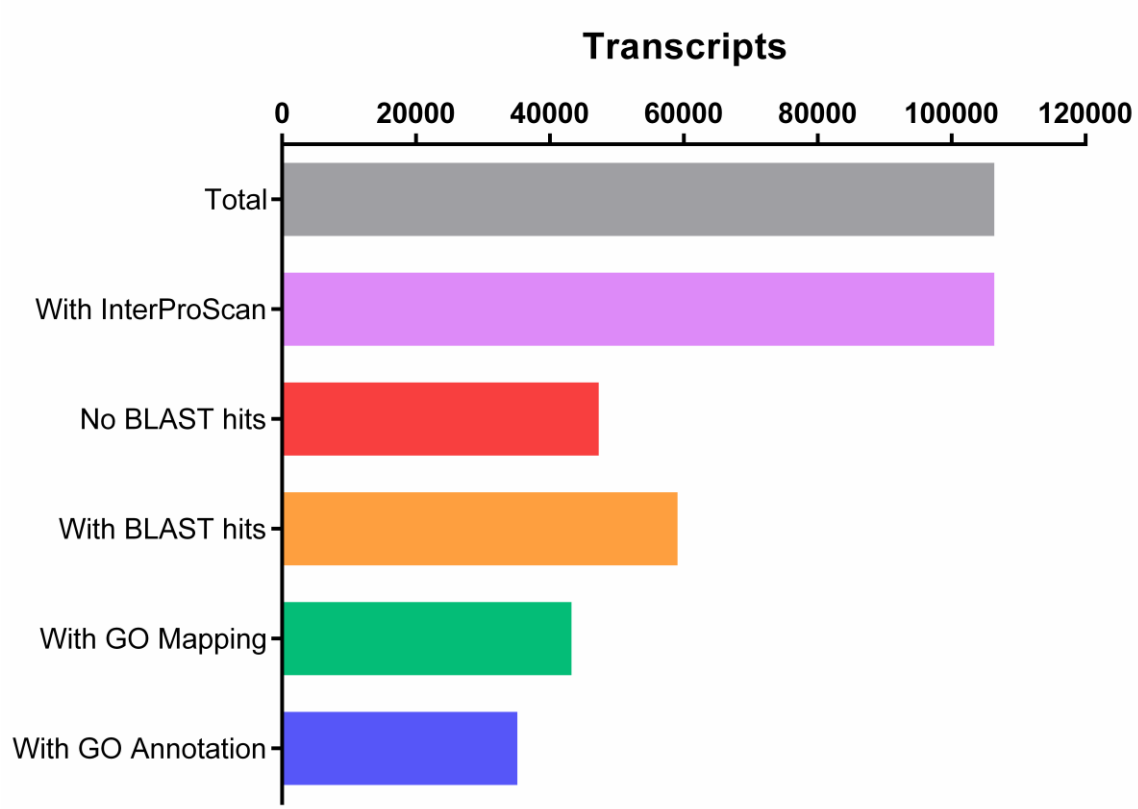

Figure 5.4 OmicsBox statistics output for functional annotation of *A. clausi* transcriptome. The number of total transcripts is indicated, as well as those annotated with InterProScan. Sequences with or without BLAST hits (*i.e.*, which found or not a match by BLASTx) are indicated, as well as sequences which received further GO Mapping or Annotation.

5.3.5 Functional annotation and functional enrichment analysis of DEGs

Results of functional annotation of DEGs are summarised in **Figure 5.8**. The top 20 most represented subcategories, for each GO category, were very similar to those relative to the whole transcriptome and already discussed. The ratio between DEGs in a subcategory was constant in most cases, with roughly a 75% of up- and a 25% of down-regulated genes for each subcategory. Among the few exceptions for which down-regulated genes exceeded up-regulated ones there were, for example, the CC subcategories DNA packaging complex,

protein-DNA complex (100% of genes, out of 4, were down-regulated, for both subcategories) and nuclear protein-containing complex (50% of down-regulated genes). Processes that comprised a greater percentage of up-regulated genes were positive regulation of biological process (BP; 84.6% of genes were up-regulated), ATP-dependent activity (MF; 88.9% up), structural molecule activity (MF; 84.5% up), protein tag (MF; 100% of up-regulated genes out of 6), supramolecular complex (CC; 100% of up-regulated genes out of 17), membrane protein complex (CC; 100% of up-regulated genes out of 12).

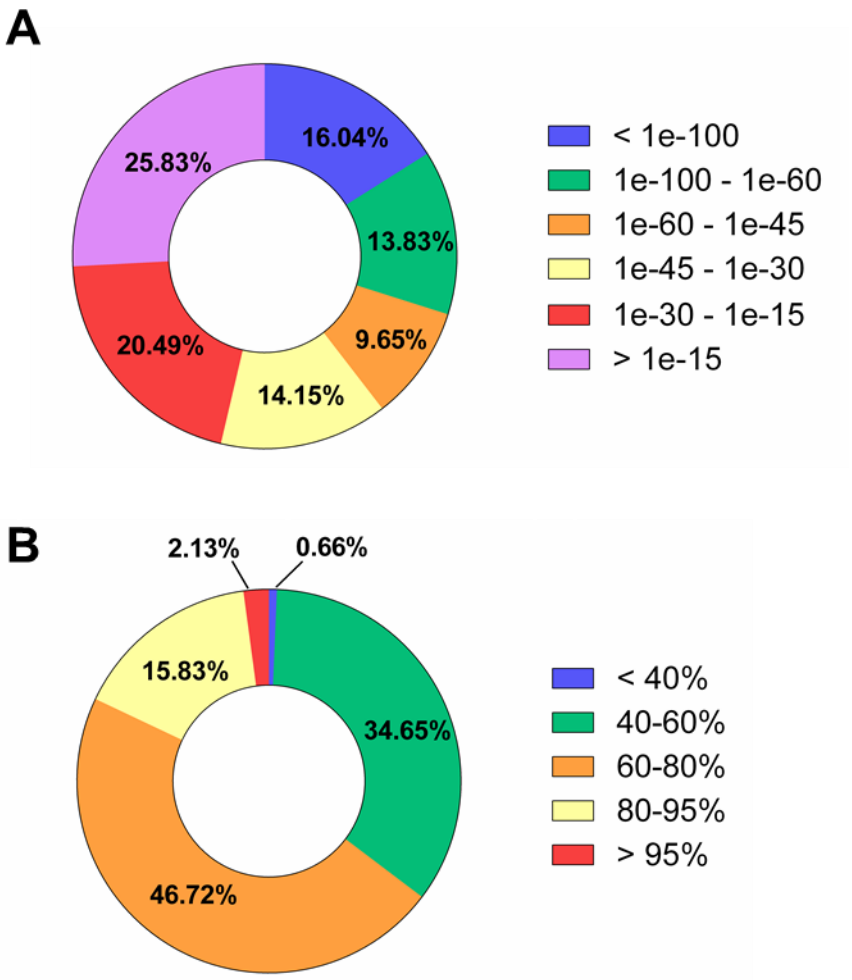

Figure 5.5 Statistics of homology BLASTx search of transcripts of the *A. clausi* transcriptome against the nr protein database. **A** – E-value distribution (%) of BLASTx hits, with E-value cut-off set to 10^{-3}. **B** – Sequence similarity distribution (%) of the top BLAST hits for each transcript.

Among the single sequences which were the most up-regulated, there were genes encoding for proteins involved with generic stress (heat-shock proteins, platelet-activating factor acetylhydrolase), oxidative stress and detoxification (superoxide dismutases, glutathione-S-transferases, cytochrome P450), proteases (lysosomal proteases, peptidases, cathepsins) and cytoskeleton structure (α- and β-tubulin); down-regulated sequences included mostly

genes involved with ribosome structure (ribosomal proteins), cellular transport (ATP-binding cassettes) and DNA binding (histone proteins, transcription factors). The complete lists of DEGs (with sequence length, sequence description, $\log_2$FC, FDR, *etc.*) is shown in the Appendix (**Table A.1** and **A.2**).

The functional enrichment analysis using Fisher's exact test, showed that 97 and 28 BP subcategories were significantly enriched in up- and down-regulated genes (FDR < 0.05), respectively, *i.e.*, these processes were featured among DEGs significantly more than among the whole transcriptome.

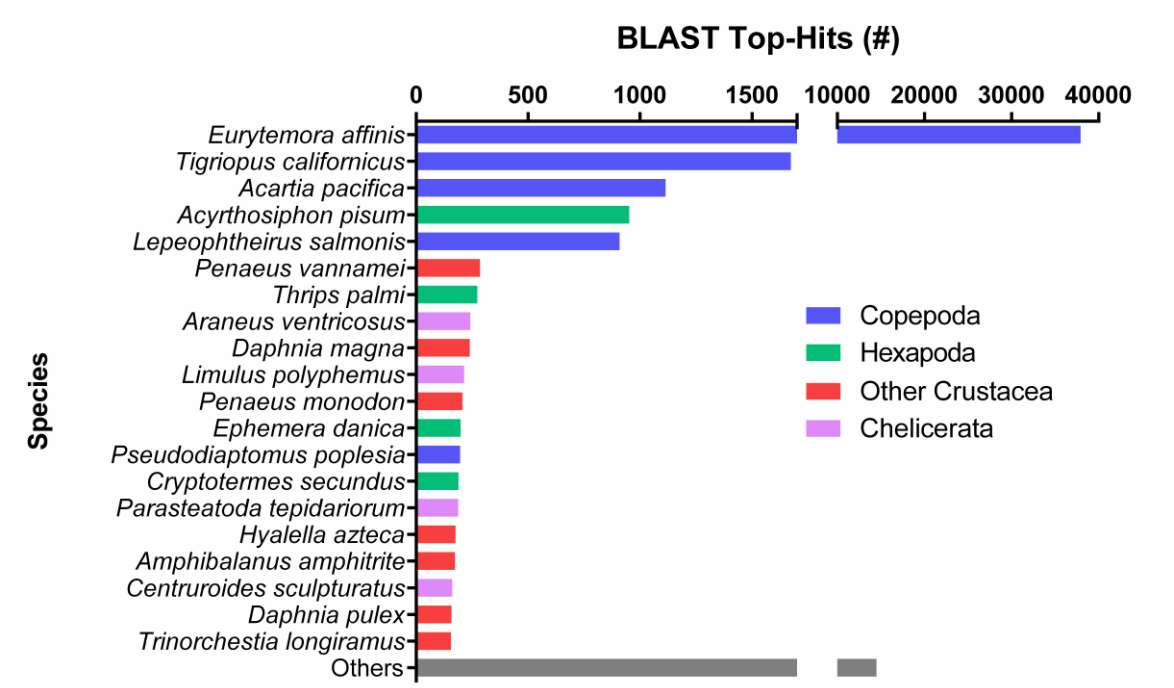

Figure 5.6 Top-Hit species distribution for the first 20 species of BLASTx similarity search for the *A. clausi* transcriptome, against the nr protein database with a taxonomy filter for Arthropods. Species are grouped in colours depending on their taxonomic group. Species after the 20th were grouped into the "Others" column.

Among the enriched processes of up-regulated genes, there were protein metabolism, biosynthesis, lysis and ubiquitination; biosynthesis of nucleic acids; gene expression. These genes were assigned GO subcategories until GO level 9, with most subcategories being represented by few sequences. On the other hand, enriched processes among down-regulated genes were more equally distributed until GO level 6, with fewer subcategories represented by a similar number of sequences each. Enriched processes among down-regulated genes were gene biosynthesis of macromolecules (especially peptides and amides), gene expression and translation. The complete list of enriched processes belonging to the BP category, among up- and down-regulated genes, is available in Appendix (**Table A.3** and **A.4**, respectively).

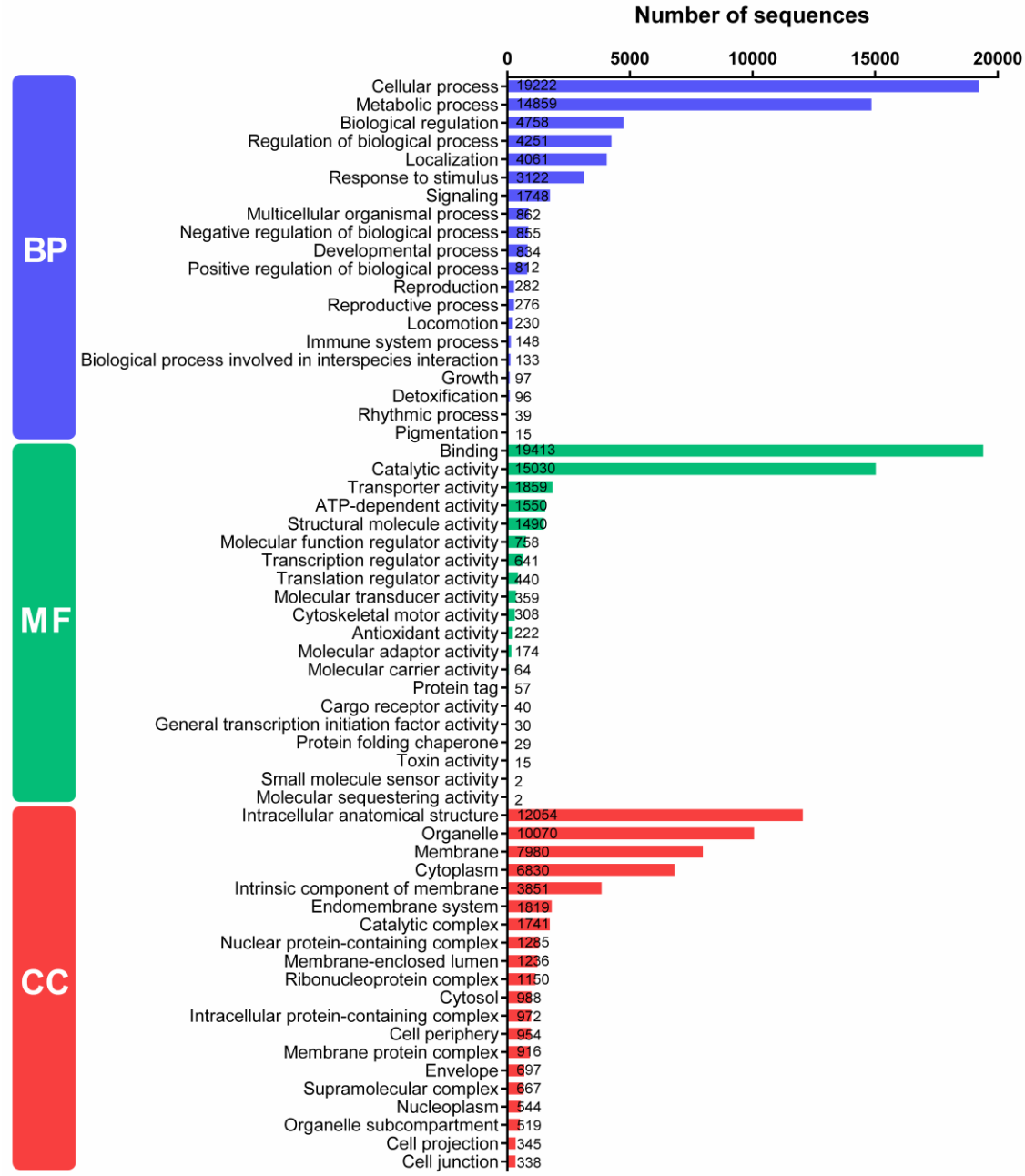

Figure 5.7 *Acartia clausi* annotated transcripts, distributed by gene onthology (GO) categories. The three GO categories are represented by a coloured bar on the left: biological process (BP), molecular function (MF) and cellular component (CC). GO level is 2 for BP and MF, 3 for CC. For each category, the top 20 subcategories are shown; next to each subcategory, the number of sequences to which that subcategory was assigned.

5.4 Discussion

Within this thesis, we provided a whole-body transcriptome for *A. clausi* females exposed to elutriates of polluted sediments. To our knowledge, this is the first available transcriptome for this copepod species and the first transcriptome of a copepod exposed to polluted sediments.

During RNA extraction we did not perform the heat denaturation step, suggested by some protocols, because in preliminary results we did not observe differences in yield or quality of RNA, and because it was reported to alter copepod 28S rRNA (Asai *et al.*, 2015). During purity and integrity assessment of total extracted RNA through NanoDrop and Bioanalyzer, we noticed absence of contamination of genomic DNA and two separate peaks of rRNA (18S and 28S). Interestingly, we did not observe a denaturation of 28S rRNA in two smaller bands migrating along with the 18S, as it was reported for TRIzol® RNA extraction from the calanoid copepod *Calanus helgolandicus* (Asai *et al.*, 2015). Our RIN values were in general very high, indicating good quality of RNA; usually RIN values > 8 are considered suitable for RNA-seq analysis (Pérez-Portela and Riesgo, 2013), but we managed to generate a *de novo* assembly of good quality also with one sample having a slightly lower RIN.

The RNA yield in terms of ng/μL, however, was low, especially compared with other calanoid copepods and despite the TRIzol® method usually results in higher concentrations of extracted RNA when compared to commercial kits (Asai *et al.*, 2015). Because of this, we suggest to increase, if possible, the number of *A. clausi* individuals for RNA extractions to at least 20 specimens per replicate, as the 10 used in each of our samples provided just enough RNA for next generation sequencing and further validation of gene expression analyses.

The transcriptome we generated for *A. clausi* comprised 106,414 new total Trinity transcripts, most of which were BLASTed (55.5%) and annotated (33.0%). These percentages, as well as the E-value distribution and percentage of similarity, were similar to those of other calanoid copepods transcriptomes (Asai *et al.*, 2020; Russo *et al.*, 2020; Semmouri *et al.*, 2019; Zhou *et al.*, 2018). As pointed out by Russo *et al.* (2020), these values are still low compared to other species and more effort is required to improve genomic resources for copepods. Our *A. clausi* transcriptome, however, showed a slight and promising increase with respect to the transcriptome of *Temora stylifera*, in which percentages of BLASTed and annotated genes were 50% and 25%, respectively (Russo *et al.*, 2020). This improvement could be due to the increase of available copepod sequences in the public databases. Sequence length distribution, average transcript length (825 bp) and N_{50} value (1048 bp) were higher with respect to other copepod transcriptomes (Russo *et al.*, 2020; Semmouri *et al.*, 2019; Yu *et al.*, 2018), indicating less fragmentation in our assembly, which was similar, in this regard, to other transcriptomes (Asai *et al.*, 2020; Zhou *et al.*, 2018). In all these cases, the majority of sequences had length comprised between 500 and 1000 bp, as was in our results.

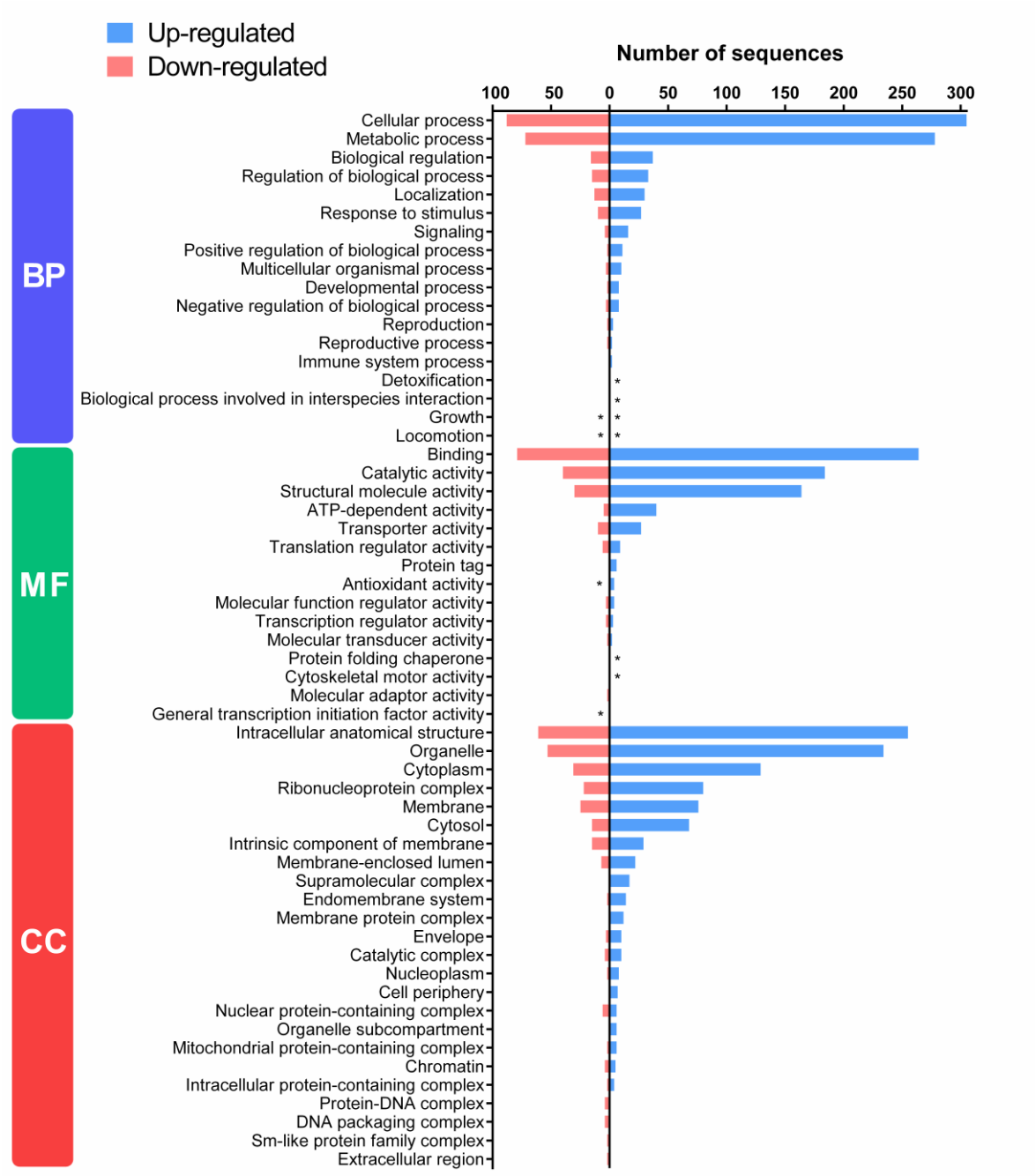

Figure 5.8 *Acartia clausi* up- and down-regulated genes (FDR < 0.05, $|\log_2 FC| \geq 2$), distributed by gene ontology (GO) categories. The three GO categories are represented by a coloured bar on the left: biological process (BP), molecular function (MF) and cellular component (CC). GO level is 2 for BP and MF, 3 for CC. For each category, the top 20 subcategories are shown. Up-regulated genes are represented by light blue bars, while down-regulated genes are represented by light red bars. * indicates only one sequence when bars are not visible.

Twelve out of twenty top BLAST hits belonged to crustaceans, with five being copepod species and most sequences belonging to them, indicating a strong homology of *A. clausi* sequences against the nr database. Similar results on species distribution were reported for

the transcriptome of *T. stylifera* (Russo *et al.*, 2020) and *C. helgolandicus* (Asai *et al.*, 2020), with *Eurytemora affinis* being the most recurring species in all three cases.

Among elutriates of polluted sediments which were previously tested on *A. clausi* females for chronic toxicity (Carotenuto *et al.*, 2020), E56 was chosen to generate our reference transcriptome because it had the most chemical species exceeding environmental quality standards, *i.e.*, threshold values set by the European Commission. Within the substances beyond these values there were Hg (mercury concentration in the elutriate was 0.6 µg/L) and seven different polycyclic aromatic hydrocarbons (PAHs) (total PAH concentration in the elutriate was 8.62 µg/L), including naphthalene, anthracene and B[a]P, whose detrimental effects on marine environment and human health are well-known (Hylland, 2006; International Agency for Research on Cancer, 2020; Wang *et al.*, 2017).

Elutriate E56 was considered highly toxic both for *A. clausi* and *A. tonsa*: it reduced egg production (EP) and egg hatching success (HS) of both copepods and survival of *A. clausi* females after a long-term exposure of 7 days, and induced high immobilisation to nauplii of both species (Carotenuto *et al.*, 2020). The authors suggested that the slight recover in EP and HS occurring after the 3rd day could be explained with up-regulation of genes involved in detoxification, such as the heat shock protein 70 (HSP70), which was up-regulated in *A. tonsa* adults after 3 days of exposure to the emerging contaminant CdSe/ZnS quantum dot nanoparticles (Zhou *et al.*, 2016b). Indeed, we observed a greater percentage of up-regulated genes (74% of all DEGs) in our transcriptome of *A. clausi* females exposed for 4 days to E56 elutriates; this trend was also observed in other copepod transcriptomes (Wang *et al.*, 2017). Overall, the total number of DEGs (1000; FDR < 0.05, $|\log_2 FC| \geq 2$) we identified in *A. clausi* was much greater with respect to DEGs found in transcriptomes of *A. tonsa* (276 DEGs after handling stress and 573 DEGs after salinity shock, FDR < 0.05) (Nilsson *et al.*, 2018) (373 DEGs after exposure to NiNPs, FDR < 0.01, $|\log_2 FC| \geq 2$) (Zhou *et al.*, 2018) or transcriptomes of other copepod (101 DEGs in *T. japonicus* and 18 DEGs in *P. annandalei* exposed to mercury chloride, FDR < 0.05, $|\log_2 FC| \geq 2$) (Wang *et al.*, 2017) or crustacean species (88, 14 and 13 DEGs in *Metapenaeus bennettae* exposed to crude oil at different timepoints, FDR < 0.05, $|\log_2 FC| \geq 2$) (Armstrong *et al.*, 2022). This indicates that the elutriate of sediment triggered a massive transcriptional response in *A. clausi*, which resulted in a high number of differentially regulated genes.

In general, most *A. clausi* transcripts received an annotation in cellular and metabolic process (BP subcategories) and in binding and catalytic activity (MF subcategories), which confirmed similar results in other copepod transcriptomes (Asai *et al.*, 2020; Ning *et al.*, 2013; Russo *et al.*, 2020; Semmouri *et al.*, 2019; Zhou *et al.*, 2018). Our differential

expression analysis allowed us to visualise a list of candidate genes which could be regarded as copepod biomarkers for chronic toxicity to pollutants in sediments. Among DEGs, moreover, we selected a list of genes of interest (GOI) which were then tested in *A. clausi* and *A. tonsa* females exposed to $NiCl_2$ and NiNPs, to determine quantitative gene expression through RT-qPCR (please refer to chapter 6).

Given the high chemical heterogeneity of the elutriates, it is difficult to pinpoint the observed response to a specific compound or class of contaminants. To our knowledge there are no published transcriptomes of copepods exposed to polluted sediments. There are, however, transcriptomes of copepods or other crustaceans exposed to either PAHs or mercury, the two more relevant toxicants in the sediments we used: the copepods *T. japonicus* and *P. annandalei* exposed to mercury chloride (Wang *et al.*, 2017), and *E. affinis* exposed to B[a]P (Lee *et al.*, 2018); the amphipod *Melita plumulosa* (Hook *et al.*, 2014) and the greentail prawn *M. bennettae* (Armstrong *et al.*, 2022), both exposed to crude oil-spiked sediments; the Chinese mitten crab *Eriocheir sinensis* exposed to B[a]P (Yu *et al.*, 2018).

It is known that the activation of xenobiotic metabolism and detoxification systems is a common response to exogenous chemical compounds (Asai *et al.*, 2020). One of the most up-regulated genes in the *A. clausi* transcriptome was the heat-shock protein 90 (HSP90), with a $\log_2FC = 10.8$; tens of other isoforms of the same family were also up-regulated. These proteins are usually up-regulated in response to increased temperature, exposure to xenobiotics and generic stress, acting as molecular chaperons which repair misfolded or damaged proteins (Aufricht, 2005; Rhee *et al.*, 2009); however, they seem to have a sex-specific response, as they were up-regulated in male and down-regulated in female copepods of *P. annandalei* exposed to cadmium (Kadiene *et al.*, 2020). In the transcriptome of the copepods *T. japonicus* and *P. annandalei* exposed to mercury, one of the most recurring up-regulated genes were HSP70 or HSP90, in both species (Wang *et al.*, 2017). This correlation is clear given the known role of mercury in inducing oxidative stress (Benedetti *et al.*, 2009), and that mercury was also abundant in E56 elutriates used for our transcriptome.

In the transcriptome of *T. japonicus* and *P. annandalei*, moreover, the authors also found up-regulation of genes involved in reproduction and growth, like vitellogenin and tubulin (Wang *et al.*, 2017). Vitellogenin, a precursor to several egg yolk proteins, has been proposed as a marker of the reproductive condition in copepods (Tarrant *et al.*, 2019). It is commonly much more expressed in females with respect to males and its up-regulation has been associated with exposure to metals, *e.g.* cadmium (Lee *et al.*, 2008b). The increased expression of *T. japonicus*' vitellogenin after exposure to mercury can be a mechanism to facilitate vitellogenesis in stress conditions (Wang *et al.*, 2017). In the transcriptome of *A.*

clausi, we did observe two up-regulated vitellogenin isoforms, as well as a down-regulated one. Down-regulation of vitellogenin, however, was also reported after exposure to sediments spiked with nickel or crude oil, in the amphipod *M. plumulosa* (Hook *et al.*, 2014) and in the copepod *P. annandalei* exposed to $NiCl_2$ (Jiang *et al.*, 2013). More of this will be discussed in chapter 6, where we will provide results of quantitative gene expression of vitellogenin and other GOI.

We also found that α-tubulin was up-regulated in our *A. clausi* transcriptome, similar to what reported for *T. japonicus* and *P. annandalei* exposed to mercury (Wang *et al.*, 2017). This protein, active component of the cytoskeleton and constituent of microtubules, is also involved in the response to heavy metals, to which exposure is usually up-regulated (Jiang *et al.*, 2013). For *A. clausi*, we noticed tens of α- and β-tubulin isoforms in the transcriptome, all up-regulated. In this view, for *A. clausi* exposed to elutriates, the role of α-tubulin could be to protect or repair microtubules network from oxidative stress, similarly to what was found for the transcriptome of *T. japonicus* and *P. annandalei* exposed to mercury (Wang *et al.*, 2017).

Among our DEGs, one of the most up-regulated protein classes was lysosome-associated proteins, such as aspartic proteases, cathepsins, serine carboxypeptidases. Such proteins play a role in proteolysis (which was included in the enriched processes and in DEGs functional annotation of *A. clausi*) through the hydrolysis of peptide bonds, an enzymatic reaction fundamental for many physiological and pathological processes such as inflammation, immune response, cell proliferation, embryonic development, and other processes of proteins (activation, maturation, catabolism, transport) (Eder *et al.*, 2007; Garcia-Carreño *et al.*, 2014). Proteases can be classified, depending on the characteristics of the active site, in serine, cysteine, aspartate and metallo proteases (Solgaard *et al.*, 2007). Cathepsins were found to be up-regulated in *T. japonicus* after a treatment with bacterial lipopolysaccharide, as well as in the moulting process (Jeong *et al.*, 2015). Cathepsins are also probably involved in the establishment of the parasite on the host, as they were found to be up-regulated in the infective stage of the parasitic copepods *Caligus rogercresseyi* (Maldonado-Aguayo *et al.*, 2015) and *Lepeophtheirus salmonis* (McCarthy *et al.*, 2012). Each class of protease, moreover, has a pH optimum; for example, in the copepod *Calanus finmarchicus*, the aspartic proteases were found to be dominant at acid conditions, while metallo and serine proteases were present in equal amounts at alkaline conditions (Solgaard *et al.*, 2007). Similarly, the lysosomal pathway was also found to be differentially expressed in the transcriptome of the Chinese mitten crab exposed to B[a]P, and immune response was among significantly changed processes (Yu *et al.*, 2018). In the transcriptome of the greentail prawn *M. bennettae* exposed to

crude oil-spiked sediments, serine-type endopeptidase activity and proteolysis were listed among enriched processes (Armstrong *et al.*, 2022). Other classes of proteases (such as trypsin, chymotrypsin and carboxypeptidase) were up-regulated in *M. plumulosa* exposed to crude oil (Hook *et al.*, 2014). This indicates a common response to PAHs which caused an increased catabolism of proteins and possibly inflammation and immune response.

In the partial transcriptome of *M. plumulosa* exposed to crude oil, generated through microarrays, among the up-regulated genes there were different classes of cytochrome P450 (CYP) and of glutathione-S-transferases (GSTs). Several CYP genes were also found both up- and down-regulated in the transcriptome of *E. affinis* exposed to B[a]P (Lee *et al.*, 2018). Cytochromes are involved with phase I metabolic processes (converting xenobiotics to a form which is less toxic more easily excreted) (Kadiene *et al.*, 2020), while GSTs, central in phase II detoxification reactions, catalyse conjugation of reduced glutathione (GSH) to the xenobiotic, facilitating its excretion (Lauritano *et al.*, 2021; Lee *et al.*, 2008a). Several isoforms of GSTs, as well as different enzymes of the cytochrome pathway, were found to be up-regulated also in the transcriptome of *A. clausi* exposed to elutriates of sediments, indicating a common response of detoxification to PAHs (more of this will be discussed in chapter 6, as one GST-σ was chosen as a GOI for transcriptome validation and gene expression analyses). In addition to this, pathways of glutathione metabolism and of cytochrome P450 were listed among the significantly changed processes in the transcriptome of the Chinese mitten crab *E. sinensis* to B[a]P (Yu *et al.*, 2018).

In general, for most of the processes in the transcriptome of *A. clausi*, up-regulated genes exceeded down-regulated genes, with a few exceptions like the CC subcategories DNA packaging complex, protein-DNA complex and nuclear protein-containing complex. Down-regulation we observed for ribosomal proteins was also reported for the transcriptome of *A. tonsa* exposed to NiNPs, indicating a similar response (Zhou *et al.*, 2018). The enrichment analysis too showed more up-regulated genes among enriched processes, which were distributed until GO level 9. A similar result was obtained in the transcriptome of *C. helgolandicus*, where more sequences were distributed among GO subcategories unevenly, with down-regulated genes having less sequences per category (Asai *et al.*, 2020). This could indicate that the organisms responded to elutriate exposure with multiple up-regulated sequences of similar function, as opposite to less down-regulated sequences with specific target functions. Processes involved with transcription and translation, such as ribosome and RNA processing, were enriched in our transcriptome and in the transcriptome of the greentail prawn, *M. bennettae*, exposed to B[a]P (Armstrong *et al.*, 2022). Overall, this indicates that *A. clausi* females, during 4 days of exposure to elutriates, responded mostly by increasing

gene expression of basic processes such as transcription and translation, metabolism of proteins and damaged molecules, detoxification and response to stress, while down-regulating other processes such as ribosome machinery and DNA binding.

In conclusion, the newly-generated *de novo* transcriptome assembly with complete functional annotation of *A. clausi* exposed to elutriates of polluted sediments, was an important step forward for molecular resources of copepods and of the *Acartia* genus, as it was the first reported transcriptome for this species. It helped to gain information on the molecular responses to a variety of classes of contaminants, with most of the responses being in agreement with current scientific literature. It was also useful as a genomic resource, a starting point to mine for genes of interest which could be differentially expressed after exposure to nickel and to design new primer sequences to be tested in RT-qPCR, as it will be discussed in the next chapter.

Chapter 6 Molecular responses of *A. tonsa* and *A. clausi* exposed to $NiCl_2$, NiNPs and other pollutants: transcriptome validation and comparative gene expression

6.1 Introduction

Next generation, high throughput sequencing of the full RNA expression profile is a powerful tool which allows both to identify transcripts and to quantify their gene expression, also from small amounts of genetic material, and it is particularly useful for organisms whose genomic sequence has not been generated yet (Conesa *et al.*, 2016; Wang *et al.*, 2009). However, results of sequencing need to be validated, *i.e.* confirmed, with quantitative gene expression analysis – namely real-time quantitative polymerase chain reaction (RT-qPCR) – to confirm the reliability of RNA-seq data; validation is also required by some journals for scientific publication (Fang and Cui, 2011).

RT-qPCR is a quantitative assay for precise estimation of gene expression, based on the polymerase chain reaction technology. The difference with a regular PCR approach is that in RT-qPCR the instrument measures abundance of complementary DNA (cDNA) molecules, through fluorescent signals, simultaneously, as the cycles of amplification occur. The procedure follows the general principle of PCR: first a denaturation step, obtained through high temperatures, separates the double-stranded cDNA molecules; during the annealing step primers attach to the now single-stranded cDNA template; in the elongation step the enzyme Taq DNA polymerase synthesises a new DNA strand complementary to the cDNA template strand by adding deoxyribose nucleotides triphosphate (dNTPs) in 5'-3' direction, synthesising a new ds-DNA molecule; finally, an elongation step to ensure that any remaining single-stranded DNA is fully extended.

The most common fluorescent detection dye used is SYBR™ Green, a dye which intercalates with double-stranded DNA and that fluoresces at 520 nm once bound to the DNA. The value of emitted fluorescence is hence directly proportional to the amount of target DNA generated. The higher the quantity of cDNA present at the beginning of the reaction, the fewer number of cycles are required to reach a significant increase of fluorescence above a statistical background threshold (Arya *et al.*, 2005). The threshold cycle (C_t) is, therefore, the specific amplification cycle at which, for a specific gene, the threshold level of fluorescence is reached for a specific gene; hence, C_t is a quantification of expression level of the different genes tested.

Amplification in RT-qPCR can vary depending on factors such as starting concentration of RNA, integrity of retrotranscribed RNA, efficiency of reverse transcriptase (used to convert RNA in cDNA), sample-to-sample variations in amplification efficiency, and variation in cDNA sample loading (Arya *et al.*, 2005). However, this technique is considered a gold standard for comparison across different disciplines thanks to its high throughput, reproducibility, specificity and sensitivity (Burns *et al.*, 2005).

In this chapter, we will provide data on quantitative gene expression of *A. tonsa* and *A. clausi* exposed to $NiCl_2$ and to NiNPs. To this purpose, we exposed females of both copepod species to the same conditions of the chronic test (chapter 4), extracted total RNA, retrotranscribed it to cDNA and tested the synthesised cDNA with a panel of genes of interest (GOI) through RT-qPCR. The final aim was to anchor the physiological response recorded in the chronic tests to the molecular response occurring at the same experimental conditions, in terms of comparative gene expression for copepod females. Gene expression was also observed in *A. clausi* females exposed to E56 elutriates of polluted sediments, which were used to generate the *de novo* transcriptome discussed in chapter 5, thus validating RNA-seq results of the transcriptome.

6.2 Selection of GOI

When testing gene expression by means of RT-qPCR, it is important to normalise expression levels to an internal control, which commonly is represented by reference genes (RGs). RGs, or housekeeping genes, encode for proteins whose basal level of expression is usually constant regardless of the experimental condition; they need to be validated with each tested experimental condition, and the use of more than one reference gene is recommended if possible (Vandesompele *et al.*, 2002). Commonly used RGs in copepods include β-actin, elongation factor 1α, 18S rRNA, ribosomal protein S16, ribosomal protein S20, ribosomal protein S7, glyceraldehyde-3-phosphate dehydrogenase, ubiquitin, histone H3, ATP synthase (Tarrant *et al.*, 2019). For *A. clausi* and *A. tonsa*, we selected ten candidate RGs, previously optimized in *Calanus helgolandicus* (Lauritano *et al.*, 2011a) and also tested in *Temora stylifera*.

GOI, on the other hand, were selected based on the available transcriptomes for these two *Acartia* species: the one for *A. tonsa* exposed to NiNPs (Zhou *et al.*, 2018), and the other produced within the work of this PhD, which is the first available transcriptome for *A. clausi* (chapter 5). GOI were selected preferably among the differentially expressed genes (DEGs) of both transcriptomes, paying attention to specific sequences which were among the most up- or down-regulated, and also focusing on genes involved in detoxification processes

(catalase, superoxide dismutase, glutathione-related enzymes), reproduction (vitellogenin), neurological functions (acetylcholinesterase), generic metabolism (chitinase), muscular functions (myosin heavy chain), and others.

The differential expression analysis conducted on *A. clausi* females exposed to elutriates of polluted sediments resulted in 1000 DEGs, of which 743 up- and 257 down-regulated. Within these genes, we selected several GOI which belonged to the oxidative stress and detoxification category. For example, the second most up-regulated gene, with a $\log_2$ fold change ($\log_2$FC) of 11.9, was platelet-activating factor acetylhydrolase (PAF-AH). This gene is a strong phospholipid activator, but it also plays a role in response to oxidative stress, apoptosis and immune response. We selected it in the view that NiNPs caused oxidative stress and lipid peroxidation in the ascidian *Ciona intestinalis* (Gallo *et al.*, 2016), and increased inflammatory and apoptotic responses in the soil oligochaete *Enchytraeus crypticus* (Gomes *et al.*, 2019). PAF-AH, moreover, resulted up-regulated in the transcriptome of *T. stylifera* exposed to phytoplankton-derived oxylipins; the authors hypothesised it could play a role in the lipid pathway alteration and oxidative stress caused by oxylipins (Russo *et al.*, 2020).

Among the other GOI involved in lipid peroxidation, there was the phospholipid-hydroperoxide glutathione peroxidase (PHGPx), which was found up-regulated in the aquatic midge *Chironomus riparius* exposed to Zinc oxide nanoparticles (Gopalakrishnan Nair and Chung, 2015). PHGPx belongs to a class of selenoproteins which can quench the reactive oxygen species (ROS; compounds normally formed in metabolic reactions but more common under exposure to contaminants) phospholipid hydroperoxide, reducing it to a regular phospholipid, by oxidising reduced glutathione (Imai and Nakagawa, 2003). Glutathione is a tripeptide formed by glutamate, cysteine and glycine, with a free thiol group in its reduced form (GSH); when two molecules of GSH react with each other, oxidised glutathione (GSSG) is produced and two electrons are released, which are used to reduce ROS and heavy metals (Lauritano *et al.*, 2021). Glutathione, hence, plays an important role in phase II of detoxification. Among selected GOI, there were other genes encoding for enzymes involved in the glutathione metabolic pathway: similarly to PHGPx, glutathione peroxidase (GPx) converts hydrogen peroxide to H_2O through oxidisation of GSH, while glutathione synthetase (GSS; down-regulated to – 2.6 $\log_2$FC in the transcriptome of *A. clausi*), catalyses the formation of GSH (Imai and Nakagawa, 2003). Glutathione S-transferases, lastly, are responsible for the conjugation of GSH to products of phase I reactions, *i.e.* xenobiotics with polar groups. The transfer of GSH, a polar molecule, converts them in a less lipophilic form, which can more easily be excreted from the cells (Kadiene *et al.*, 2020; Lauritano *et al.*,

2021). Several classes of this enzyme can be identified, depending on factors such as taxa of organisms, cellular localisation (cytosolic, mitochondrial or microsomal), specific substrates, *etc.* (Lauritano *et al.*, 2021). We selected from the transcriptome of *A. clausi* a glutathione S-transferase σ (GSTσ), as it was present among up-regulated DEGs ($log_2FC = 2.3$) and it is the cytosolic class of GST most commonly involved with detoxification of xenobiotics and metals in copepods (Lauritano *et al.*, 2021; Lee *et al.*, 2008a).

Concerning oxidative stress, Mpv17-like protein (M-LP) was one of the most up-regulated gene in the transcriptome of *A. clausi* ($log_2FC = 10.7$). This protein acts as a transcriptional factor of genes involved in oxidative stress: in mouse, M-LP up-regulated expression of superoxide dismutase [Mn] (SOD) (Iida *et al.*, 2003) and down-regulated expression of GPx (Iida *et al.*, 2005). Sestrin (a protein which prevents the accumulation of ROS through alkylhydroperoxide reductase activity), on the other hand, was strongly down-regulated in the transcriptome, with a log_2FC of – 9.6, and was listed among enriched processes, in the category "Reaction to ROS". Other selected GOI involved in the responses to ROS were cytosolic SOD [Cu-Zn] (which was up-regulated to 8.3 log_2FC), and catalase, both encoding for enzymes involved in quenching of ROS in cytosol and peroxisomes (Imai and Nakagawa, 2003).

Other genes involved in the functioning of the nervous system were also selected among DEGs and transcripts included in the reference transcriptomes. Acetylcholine receptor (AChR), an ionic channel for the neurotransmitter acetylcholinesterase (AChE), found especially at the nerve-muscle synapse, was down-regulated to – 3.3. Exposure to ROS caused down-regulation of AChR genes and inactivation of the respective proteins in mouse (Campanucci *et al.*, 2008; Guan *et al.*, 2001; Zhao *et al.*, 2016). Similarly, AChE was also selected, being a well-known biomarker of exposure to several environmental contaminants (Wang and Wang, 2010), also considering that NiNPs interfered with the nervous system of the soil oligochaete *Enchytraeus crypticus* (Gomes *et al.*, 2019).

Other selected GOI included poly [ADP-ribose] polymerase 3-like (PARP), whose function is transferring molecules of ADP-ribose to damaged DNA molecules as a signal for DNA-repairing enzymes. In the transcriptome of *A. clausi* PARP was up-regulated to 7.0 log_2FC, which could imply a DNA damage caused by elutriates of sediments. We chose this GOI also considering that NiNPs caused DNA damage in ascidians and other organisms (Gallo *et al.*, 2016; Wu and Kong, 2020). Vitellogenin 1 (VTG1), the last selected GOI for *A. clausi*, was within down-regulated DEGs, with a – 4.0 log_2FC. This protein, a precursor to egg yolk proteins, is a well-known biomarker of the reproductive condition in copepods (Lee *et al.*, 2008b; Tarrant *et al.*, 2019). Since NiNPs were found to be spermiotoxic for

ascidians (Gallo *et al.*, 2016), possible damages to female copepods' reproduction caused by this toxicant might be confirmed by analysing the expression of this GOI.

In addition to the transcriptome of *A. clausi*, we screened potentially interesting genes also within the *de novo* transcriptome of *A. tonsa* females exposed to NiNPs at 8.5 and 17 mg/L for 4 days (Zhou *et al.*, 2018), among those with highest or lowest fold change. The authors identified 373 differentially expressed genes (179 up- and 194 down-regulated) in treated vs. control copepods; most of those genes were involved in ribosome biogenesis, translation and protein turnover, indicating that NiNPs reduced the expression of ribosomal proteins, hence altering the ribosome biogenesis and functioning in *A. tonsa* (Zhou *et al.*, 2018).

We selected, therefore, different genes encoding for ribosomal proteins, which were all down-regulated: ribosomal protein L3, 60S ribosomal protein L27, 60S ribosomal protein L10, 40S ribosomal protein S27. The copepod *Pseudodiaptomus annandalei* exposed to $NiCl_2$ presented a reduced expression of ribosomal protein L3 (Jiang *et al.*, 2013). Moreover, 60S ribosomal protein L27 was down-regulated in cyprinid fish exposed to Cu (Lewis and Keller, 2009) and protein L10 was found to regulate the expression of proteins related to ROS production, in pancreatic cancer cells (Yang *et al.*, 2018). Similarly, GTP-binding protein Ran was among down-regulated genes, involved in RNA transport through the nucleus.

One of the most down-regulated genes in our *A. clausi* transcriptome (– 7.4 $\log_2$FC) was a SWIB-domain containing DNA topoisomerase (the SWIB domain is involved in chromatin remodelling; Bennett-Lovsey *et al.*, 2002). We chose it as a gene of interest since NiNPs were reported to cause DNA damage and alterations (Gallo *et al.*, 2016; Hou *et al.*, 2018; Wu and Kong, 2020). Metallothioneins are detoxification proteins synthesised especially in the presence of heavy metals, such as Zn, Cu, Cd, Pb; also thioredoxins play a role in response to ROS (Radtke *et al.*, 1993). We found both of these proteins strongly up-regulated among the DEGs of *A. tonsa* (6.7 $\log_2$FC). Similarly, heat-shock proteins 70 and 90 are chaperon involved with the folding of proteins after generic stress in many organisms; they are reported to be both up- (Rhee *et al.*, 2009) and down-regulated (Kadiene *et al.*, 2020) depending on the specific stressor. Hence, we selected them as genes of interest, among down-regulated DEGs.

Genes responsible for metabolism of chitin (chitinase 10 and chitin deacetylase), were found among up-regulated genes. Chitin is the main component of exoskeleton of arthropods and its metabolism is related to fundamental processes like moulting, digestion and disease resistance (Li *et al.*, 2015). Chitin is also known to form strong complexes with metals (Morris *et al.*, 2012). Chitinase is involved in degradation of chitin, while chitin deacetylases

catalyse the deacetylation of chitin forming chitosan, a biomolecule involved in molecular recognition events. Chitinases were up-regulated in *P. annandalei* copepods exposed to cadmium (Kadiene *et al.*, 2020); chitin metabolism was induced in the cladoceran *D. magna* exposed to nickel chloride (Vandenbrouck *et al.*, 2009); chitinases-encoding genes, moreover, were found to have a two- to four-fold increased expression in the amphipod *M. plumulosa* exposed to crude oil (Hook *et al.*, 2014).

Myosin heavy chain, a ubiquitous constituent of muscle cells, was up-regulated in the *A. tonsa* transcriptome; it was also found mildly up-regulated in *P. annandalei* exposed to Cd (Kadiene *et al.*, 2020). Lastly, Fibronectin type II and Neurexin 4, both up-regulated in the transcriptome, were chosen as GOI. The first is a plasma protein which binds various compounds to cellular surface, while the second plays a role in connecting neurons at the synapse and was found down-regulated in the zebrafish *Danio rerio* exposed to Cd, Pb and Mn (Tu *et al.*, 2017).

A list with all the selected GOI and the corresponding forward and reverse designed primers, separately for *A. clausi* and *A. tonsa*, is reported in **Table 6.1**.

Table 6.1 List of all genes of interest (GOI) designed for *Acartia tonsa* and *A. clausi* from the corresponding *de novo* transcriptomes. Name (with the abbreviation in brackets) and biological function are shown; also indicated are primers which successfully amplified (green tick mark) or not (red cross) in PCR and in RT-qPCR. Dashed lines separate genes selected from DEGs with those selected from the whole transcriptome, for each species.

Name	Function	PCR	RT-qPCR
Acartia tonsa			
DNA topoisomerase III (SWIB)	DNA structure	✓	✓
Metallothionein (MT)	Oxidative stress	✗	✗
Thioredoxin (TRX)	Oxidative stress	✗	✗
Heat-shock protein 90 (HSP90)	Generic stress	✓	✗
Heat-shock protein 70 (HSP70)	Generic stress	✗	✗
Chitinase 10 (CHT10)	Chitin metabolism	✓	✓
40S ribosomal protein S27 (RPS27)	Ribosome structure	✗	✗
Ribosomal protein L3 (RPL3)	Ribosome structure	✗	✗
60S ribosomal protein L27 (RPL27)	Ribosome structure	✗	✗
Myosin heavy chain (MHC)	Muscular structure	✓	✓
Chitin deacetylase (CDA)	Chitin metabolism	✓	✓
60S ribosomal protein L10 (RPL10)	Ribosome structure	✗	✗

GTP-binding protein Ran (RAN)	RNA transport	✓	✗
Fibronectin type II (FN2)	Cellular structure	✗	✗
Neurexin 4 (NRXN4)	Nervous system	✓	✗
Mpv17-like protein (M-LP-t)	Transcription	✓	✗
Sestrin (SEST-t)	Oxidative stress	✓	✓
Glutathione synthetase (GSS-t)	Detoxification (phase II)	✓	✓
Glutathione S-transferase σ (GSTσ-t)	Detoxification (phase II)	✓	✓
Vitellogenin 1 (VTG1-t)	Reproduction	✓	✓
Acetylcholine receptor (AChR-t)	Nervous system	✓	✓
Catalase (CAT-t)	Oxidative stress	✓	✗
Superoxide dismutase [Cu-Zn] (SOD-t)	Oxidative stress	✓	✓
Glutathione peroxidase (GPx-t)	Detoxification (phase II)	✓	✗
Phospholipid-hydroperoxide glutathione peroxidase (PHGPx-t)	Detoxification (phase II)	✓	✓
Acetylcholinesterase (AChE-t)	Nervous system	✓	✗
Acartia clausi			
Platelet-activating factor acetylhydrolase (PAF-AH)	Immune response	✓	✗
Mpv17-like protein (M-LP)	Transcription	✓	✓
Superoxide dismutase [Cu-Zn] (SOD)	Oxidative stress	✗	✗
Sestrin (SEST)	Oxidative stress	✓	✓
Glutathione S-transferase σ (GSTσ)	Detoxification (phase II)	✓	✓
Glutathione synthetase (GSS)	Detoxification (phase II)	✓	✓
Vitellogenin 1 (VTG1)	Reproduction	✓	✓
Acetylcholine receptor (AChR)	Nervous system	✓	✓
Poly [ADP-ribose] polymerase 3 (PARP)	Biomolecule metabolism	✗	✗
Catalase (CAT)	Oxidative stress	✓	✓
Superoxide dismutase [Cu-Zn] (SOD-II)	Oxidative stress	✓	✓
Glutathione peroxidase (GPx)	Detoxification (phase II)	✓	✓
Phospholipid-hydroperoxide glutathione peroxidase (PHGPx)	Detoxification (phase II)	✓	✓
Acetylcholinesterase (AChE)	Nervous system	✓	✓
Chitinase 2 (CHT2)	Chitin metabolism	✓	✓
Myosin heavy chain (MHC-c)	Muscular structure	✓	✓

6.3 Materials and methods

6.3.1 Experimental design and specimen collection

In order to compare the physiological response of *A. tonsa* and *A. clausi* adults after 4 days of exposure to $NiCl_2$ and NiNPs with the corresponding molecular response, adults of both species were exposed to the same conditions of the chronic test (salinity, exposure time, toxicant concentrations, algal diet) (please refer to chapter 4.2.5).

Acartia tonsa and *A. clausi* cultures were reared in laboratory conditions and handled according to the methodologies described in detail in chapters 3 and 4. Briefly, cultures were maintained in a thermostatic chamber at 20 ± 2°C, 12:12 h light:dark, with slight aeration provided through a glass pipette. Salinity was 30 and 37 PSU, respectively, for the two species. Before the test, about 200 males and 200 females of *A. tonsa* or *A. clausi* were sorted from the culture and kept in separate beakers. The test was set up in 600 mL beakers with a final volume of 300 mL FSW containing algae and the toxicant; in each beaker, 20 males and 20 females were transferred. For *A. tonsa*, $NiCl_2$ was provided at concentration of 0.2 mg Ni/L and NiNPs at 17 mg/L; for *A. clausi*, in addition to those concentrations, we also exposed females at 0.1 mg Ni/L of $NiCl_2$ and 8.5 mg/L of NiNPs, as these concentrations showed an intermediate effect during the chronic test with *A. clausi*. Algal species were the same of the chronic test, *i.e. Rhodomonas baltica* at 1.2×10^4 cells/mL for *A. tonsa* and *Rhinomonas reticulata* at 2.7×10^4 cells/mL for *A. clausi*. The test was performed in three replicates for each condition.

After preparation, beakers were incubated as reported above on a shaking plate (Labortechnik KS 125 Basic, IKA, Staufen, Germany) with slight agitation (100 RPM), to keep the algae and the nanoparticles suspended. Every 24 hours, adults were collected via filtering onto a 200 µm mesh (one for each treatment), and thoroughly backwashed in a crystallising dish. Dishes were then observed under a stereomicroscope to count and remove dead adults, whereas live adults were transferred into new beakers with fresh solutions and incubated again. On the 4^{th} day of exposure, live females (on average about 17 in each replicate) were transferred into separate 1.5 mL plastic tubes (Eppendorf), for each replicate of each treatment. This procedure was fast enough to avoid any additional stress to the specimens. After removing the water via a thin-mouth Pasteur pipette, tubes were flash-frozen in liquid nitrogen and stored in a refrigerator at – 80°C.

6.3.2 Total RNA extraction and cDNA synthesis

Total RNA of *A. clausi* and *A. tonsa* females was extracted using the TRIzol® reagent (Invitrogen, San Diego, California, USA) following methodologies described in detail in chapter 5.2.1.

After quantity and quality evaluation of extracted RNA, using NanoDrop (ND-1000 UV-Vis spectrophotometer; NanoDrop Technologies Inc., Wilmington, Delaware, USA) as reported in chapter 5.2.1, RNA was retrotranscribed to double-stranded, complementary DNA (cDNA) using the commercial kit iScript™ cDNA Synthesis Kit (Bio-Rad Laboratories, Hercules, California, USA). In total, 500 ng of RNA of *A. clausi* or *A. tonsa* were used in 20 µL of total reaction volume, following the manufacturer's instructions, utilising a thermal cycler (C1000 Touch, Bio-Rad Laboratories, Hercules, California, USA). Briefly, the reverse transcription reaction was carried out with 4 µL 5× iScript reaction mix buffer, 1 µL iScript Reverse Transcriptase enzyme, 500 ng template RNA (corresponding to a variable volume, depending on the concentration) and H_2O to 20 µL final volume. The mix was first incubated 5 min at 25°C, followed by 20 min at 46°C and finally heated at 95°C for 1 min.

6.3.3 Design of oligonucleotide primers

Species-specific forward (F) and reverse (R) oligonucleotide primers were designed on transcripts from *A. tonsa* transcriptome after exposure to NiNPs (Zhou *et al.*, 2018) and from *A. clausi* transcriptome after exposure to elutriates of polluted sediments (chapter 5).

Design of primers was carried out using the online tool Primer3web version 4.1.0 (https://primer3.ut.ee/). Parameters were set as follows: primer size 18-24 bp (optimum 20 bp); primer melting temperature (T_m): 59-61°C (optimum 60°C); primer GC%: 30-70% (optimum 50°C); product size ranges: 110-210 bp. Remaining parameters were left as default.

6.3.4 PCR and agarose gel electrophoresis

Before quantitative gene expression analyses through RT-qPCR, the synthesised cDNA of each species was tested in PCR to test amplification of primers of reference genes (RGs) and of newly-designed genes of interest (GOI). PCRs were performed using 2 µL of 10× PCR reaction buffer (Roche Diagnostics, Indianapolis, Indiana, USA), 2 µL of 10× 2 mM dNTPs (Roche Diagnostics), 0.3 µL of 5 U/µL Taq DNA Polymerase (Roche

Diagnostics), 1 µL of 20 pmol/µL of each primer – forward (F) and reverse (R) –, 1 µL of template cDNA of *A. tonsa* or *A. clausi* and Milli-Q water to 20 µL. For each primer pair one negative control was set up (to infer possible self-annealing of the primers), in which 1 µL of Milli-Q water was used instead of template cDNA.

The PCR program used with the C1000 touch Thermal Cycler (Bio-Rad Laboratories, Hercules, California, USA) consisted of a denaturation step at 95°C for 3 min; 40 cycles at 95°C for 30 s, 60°C for 1 min and 72°C for 30 sec; and a final extension step at 72°C for 7 min, followed by 1 min at 12°C (Lauritano *et al.*, 2011b).

Amplified PCR products were visualized on an agarose gel electrophoresis in 1.5% agarose low EEO gel (AppliChem GmbH, Darmstadt, Germany), with the addition of SYBR™ Safe DNA Gel Stain (Invitrogen, Carlsbad, California, USA), in 0.5× Tris-Borate-EDTA buffer (Sigma-Aldrich Life Science, Milan, Italy), in a Vari-gel electrophoretic chamber (Scie-Plas, Waterbeach, United Kingdom).

6.3.5 RT-qPCR and optimisation of primers

RT-qPCR reactions were performed in MicroAmp Optical 384-well reaction plates (Applied Biosystems, Waltham, Massachusetts, USA) with optical adhesive covers (Applied Biosystems). The final PCR volume for each sample was 10 µL, with 5 µL of SensiFAST SYBR™ Lo-ROX Kit (Bioline Meridian Bioscience, Cincinnati, Ohio, USA), 4 µL of both primer pairs (each at a concentration of 0.7 pmol/µL) and 1 µL of template cDNA (1:5 dilution). All RT-qPCR reactions were carried out in triplicate to capture intra-assay variability. Three negative controls (in which instead of the template cDNA, 1 µL of Milli-Q water was used) were added for each primer pair. Before the reaction, plates were centrifuged (Universal 32R, Hettich Zentrifugen, Tuttlingen, Germany) at 4000 RPM, 4°C, for 2 min.

The reaction was performed using a ViiA 7 Real-Time PCR System (Applied Biosystems). PCR conditions for all samples analysed were set as follows: 95°C for 20 s, then 40 cycles of 95°C for 1 s and 60°C for 20 s. Dissociation protocol with a gradient (0.5°C every 30 s) from 65°C to 95°C was also used to investigate the specificity of the primers and presence of primer dimers. Results were visualised using ViiA 7 Software (Quant-Studio) v. 1.2.4.

For every newly-designed primer the following parameters were analysed in RT-qPCR runs.

- Single peak in the melt curve chart, to confirm amplification of a specific transcript.

- Efficiency calculation with serial dilutions of control cDNA, to quantify the efficiency of amplification and the affinity of primers for the template also at low concentrations.
- Relative expression analyses of treatment vs. control cDNA, among reference and target genes.

In order to analyse expression levels of the selected GOI (**Table 6.1**), a panel of ten candidate RGs, previously optimized in *C. helgolandicus* (Lauritano *et al.*, 2011a), were screened to identify the most stable genes, separately for each species (*A. tonsa*, *A. clausi*) and each experimental condition (E56 vs. control, $NiCl_2$ vs. control, NiNPs vs. control): elongation factor 1-α (EFA), histone 3 (HIS), glyceraldehyde-3-phosphate dehydrogenase (GAPDH), ribosomal units (18S, S7, S20), ubiquitin (UBI), actin (ACT), α-tubulin (α-TUB) and β-tubulin (β-TUB). Gene-specific amplification was confirmed by a single peak in the melting curve analysis. To quantify gene expression of GOI and RGs, primer amplification efficiencies were calculated through six serial dilutions of cDNA (1, 1:5, 1:10, 1:50, 1:100 and 1:500) for all primer pairs. The reference equation for efficiency calculation is $E = 10^{-1/slope}$, where the slope is obtained from a standard curve between threshold cycle (C_t) values and the $\log_{10}$ of each dilution factor.

The stability of candidate reference genes was assessed using RefFinder (https://www.heartcure.com.au/reffinder/), an online tool which integrates results from different major computational programs (BestKeeper, Normfinder, geNorm and the comparative Delta-C_t method) to compare and rank the tested candidate reference genes depending on their specific C_t at each of the dilution mentioned above (Xie *et al.*, 2012).

6.3.6 Transcriptome validation and comparative gene expression with $NiCl_2$ and NiNPs

Relative expression levels of each GOI, normalized by the most stable RGs, were compared to the control condition for each treatment (*i.e.* E56, $NiCl_2$, NiNPs), for both *A. clausi* and *A. tonsa*, through the Pfaffl equation using REST (Relative Expression Software Tool) (Pfaffl *et al.*, 2002, 2004). REST uses a mathematical model based on the PCR efficiencies and the C_t deviation between the sample and the control group to calculate the relative expression ratio ($\log_2$ of fold change). Results were analysed based on the following equation, where the relative expression of a target gene is compared in a treatment versus a control, normalized to a reference gene (Pfaffl *et al.*, 2002).

$$Ratio = \frac{E\ (Target)^{\Delta Ct\ target\ (Control-Sample)}}{E\ (Reference)^{\Delta Ct\ reference\ (Control-Sample)}}$$

Where E (Target) is the RT-qPCR efficiency of amplification of target gene primers; E (Reference) is the RT-qPCR efficiency of the reference gene primers; ΔC_t (Target) is the C_t deviation of control-sample of the target gene transcript; ΔC_t (Reference) is the C_t deviation of control-sample of reference gene transcript.

The validation of the *A. clausi de novo* transcriptome assembly was performed with cDNA of copepod females exposed for 4 days to E56 elutriates of polluted sediments, *i.e.* the same cDNA used for RNA-seq (as reported in chapter 5).

6.4 Results

6.4.1 Total RNA extraction and cDNA synthesis

Twenty-eight total RNA samples were extracted from *A. tonsa* and *A. clausi* females exposed for 4 days to $NiCl_2$ or NiNPs, each with its own control condition. Samples had a mean ± SD concentration of 86.26 ± 43.06 ng/µL, with average A260/A230 and A260/280 ratios of 1.85 and 2.16, respectively. Results of extracted RNA samples of *A. clausi* females exposed to E56 elutriates of sediments, which were used for transcriptome validation, are reported in chapter 5.3.1.

6.4.2 Design of oligonucleotide primers

In total we designed 42 primer pairs for both copepod species. Specifically, we selected and designed 26 primers for *A. tonsa* (15 from DEGs and 11 from the whole transcriptome) and 16 primers for *A. clausi* (9 from DEGs and 7 from the whole transcriptome). Selecting GOI from the whole transcriptome, as opposed to selecting them among DEGs, allowed us to choose from a broader pool of genes, with better parameters (length, percentage of similarity, top BLAST hit, E-value, *etc.*), thus increasing the likelihood of successful amplification.

Primers only amplified cDNA of the species whose transcriptome they were designed from, *i.e.*, they were strongly species-specific. Because of this, we designed more primers for genes with the same function, in order to compare their response between species: genes with a "-t" suffix indicate they were designed for *A. tonsa* after a gene of equivalent function

was selected for *A. clausi*; vice-versa for the "-c" suffix. The "-II" suffix indicates a gene with a precise function for which primers were designed a second time, since the first primer pair did not amplify successfully.

A complete list of all designed oligonucleotide primers of GOI with their function, for the two copepod species separately, is reported in **Table 6.1**. For each primer is also indicated whether it successfully amplified cDNA of the corresponding species in PCR and in RT-qPCR.

6.4.3 PCR and agarose gel electrophoresis

Polymerase chain reactions of primer pairs and sample cDNA of the corresponding species, visualised through 1.5% agarose gel electrophoresis, showed that out of 42 primers, 32 (76.2%) successfully amplified a single PCR product of the appropriate length, with no self-annealing of primers in the negative control. Looking at results for the single copepod species, 14 out of 16 primers (87.5%) were successful for *A. clausi*, and 18 out of 26 (69.2%) primers were successful for *A. tonsa*. This lower value is to be attributed to primers designed from *A. tonsa*'s transcriptome DEGs, of which only 7 out of 15 (46.7%) successfully amplified in PCR.

In **Figure 6.1** are reported only positive PCR results of selected GOI, *i.e.*, those which were also found to be suitable in RT-qPCR. Amplicon length was comprised between 110 and 199 bp, with an average of approximately 148 bp. In **Table 6.2** the list of represented genes and the amplicon length are reported.

6.4.4 RT-qPCR and optimisation of primers

Among the ten total reference genes previously optimized in *C. helgolandicus* (Lauritano *et al.*, 2011a) and tested in *A. clausi* and *A. tonsa*, four were selected as RGs in common for both copepod species: elongation factor 1-α (EFA), histone 3 (HIS), ubiquitin (UBI) and actin (ACT). Those genes, in fact, amplified a single PCR product of the appropriate length, and in RT-qPCR analysis their melting curve showed a single peak and presented no amplification in the negative controls, in both species. In **Table 6.3** are reported the names of the selected RGs, their function, amplification efficiency, full sequences and amplicon length.

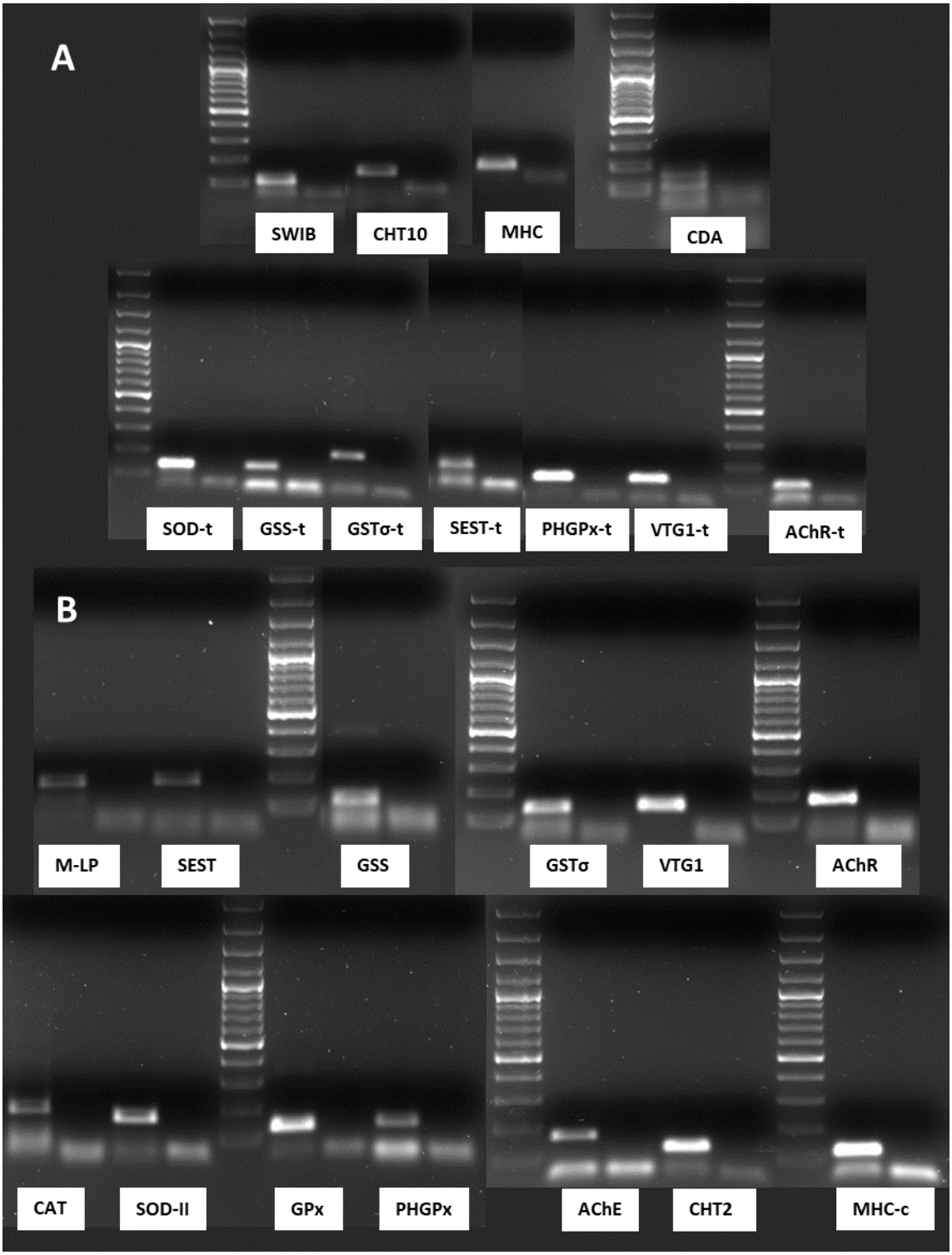

Figure 6.1 All the results of 1.5% agarose gel electrophoresis with PCR products of the selected primer pairs of GOI, with sample cDNA of *A. tonsa* (**A**) and *A. clausi* (**B**) females. The size marker is Ladder-100 (the lowest fragment is 100 bp long; other fragments are progressively 100 bp longer). For each gene, the second well corresponds to the negative control. For the extended name and amplicon length of each GOI, please refer to **Table 6.2**.

Table 6.2 List of genes of interest (GOI) selected for relative gene expression for *Acartia tonsa* and *A. clausi*. Name (with the abbreviation in brackets), function, amplicon length (A_L) in base pairs (bp), sequences of primer forward (F) and reverse (R) in direction 5'-3', and amplification efficiency (E) (%) are shown. For *A. clausi*, the range of efficiencies is reported.

Name	Function	A_L (bp)	Primer sequence	E (%)
Acartia tonsa				
DNA topoisomerase III (SWIB)	DNA structure	110	F AAGATGGCCCCTGTCTTTGG R CTGGGTGGGTACATTCATAAAGGA	106
Sestrin (SEST-t)	Oxidative stress	128	F TGAAGTTTTGTGTTGGCCGC R GCCATGATATCCGCCAGTCA	109
Superoxide dismutase [Cu-Zn] (SOD-t)	Oxidative stress	140	F CTGGTCTCGATGATGGCCTC R ATGACGTTCACCCTTGGCAT	106
Glutathione synthetase (GSS-t)	Detoxification (phase II)	137	F GCCACTCCTCCCTCATTCAC R CCGATGCTGGCTGACTGTAT	99
Glutathione S-transferase σ (GSTσ-t)	Detoxification (phase II)	188	F GATGTGGGAAAGCGTGCAAG R TTCGGACAGCTGCCATTCAT	117
Phospholipid-hydroperoxide glutathione peroxidase (PHGPx-t)	Detoxification (phase II)	142	F TTGGGACCTAACCTTGCGAC R ATGTCAACTTCTCCTCCGCC	101
Vitellogenin 1 (VTG1-t)	Reproduction	139	F GCTCTCTGAAGACCTGGCTG R TCGTGTTGAGCTTGGGAGAC	99
Acetylcholine receptor (AChR-t)	Nervous system	119	F GCTGACGAAGAGTTTGCCAA R ATGTAGAAGTTGCCCTCGCC	102
Chitinase 10 (CHT10)	Chitin metabolism	132	F CACAGCAATCCAGTCCAGGT R GTCAGGGAGTTGAAGGAGGC	119
Chitin deacetylase (CDA)	Chitin metabolism	119	F TCAGTGTTGAGTCTGCCAAGA R CTCTCCAGCCAGCTCCTTG	88
Myosin heavy chain (MHC)	Muscular structure	113	F TGAGGATGAACAGACCCTTGG R CCTTAGCACGGTTGTTGCG	97

Acartia clausi				
Mpv17-like protein (M-LP)	Transcription	183	F ACCGAGCACTACCAGGTCTA R TATTGGACAGGGGAGGAGGC	98-102
Sestrin (SEST)	Oxidative stress	185	F AAAGGCAGCGTAAAGGGAGT R TTCTGGTTCAGCTCGCAACT	98-103
Catalase (CAT)	Oxidative stress	199	F TCCGGGTCCTTTAGATGGGT R CTACTGTGGGTGGTGAGAGC	100-101
Superoxide dismutase [Cu-Zn] SOD-II	Oxidative stress	176	F TCATCTCATCACCCTTGGCG R TACTGCCACCCATCCCCATA	98-103
Glutathione synthetase (GSS)	Detoxification (phase II)	113	F AAGGAAACAGTGCCCAGAGG R CAGCAACCTCATGACCGTCA	102
Glutathione S-transferase σ (GSTσ)	Detoxification (phase II)	144	F ACAGCGGTCAACAGAGCAAT R AACTGAAGTGATGCCAGCCA	104-121
Glutathione peroxidase (GPx)	Detoxification (phase II)	144	F TGTCGCTAGTGATTGTGGCT R TGAAATGCGTTGCCTGGTTC	102-106
Phospholipid-hydroperoxide glutathione peroxidase (PHGPx)	Detoxification (phase II)	154	F TGCATTCACCATTAACCCTCCT R TGAAGAGCCTGGGACTGAGA	100-103
Vitellogenin 1 (VTG1)	Reproduction	153	F TGCTCCCACTTTTGCTTTGG R TGGTGAGAAGGCCAGACTTG	98-100
Acetylcholine receptor (AChR)	Nervous system	190	F GCCAGTCCTCATAAGCCTCA R CCAGCTCAGATGTTGTGGGT	88-100
Acetylcholinesterase (AChE)	Nervous system	178	F TAGACATTCAGCTCGGCCAC R AGCCTTCAACATCACTGCGA	97-100
Chitinase 2 (CHT2)	Chitin metabolism	134	F TGGAGGATGGAACGAGGGAA R ACTCCCAGTCCAGGTCAAGT	97-102
Myosin heavy chain (MHC-c)	Muscular structure	125	F AAGCAACTCTCCAAGGCACA R CCCTCTTGCAGCCTCATCAT	102-104

Table 6.3 List of reference genes (RGs) selected for relative gene expression for *Acartia tonsa* and *A. clausi*. Name (with the abbreviation in brackets), function, amplicon length (A_L) in base pairs (bp), sequences of primer forward (F) and reverse (R) in direction 5'-3', and amplification efficiency (E) (%) (first value is E for *A. tonsa*; second value is the range of E for *A. clausi*) are shown.

Name	Function	A_L (bp)	Primer sequence	E (%)
Actin (ACT)	Cytoskeleton structure	128	F GGCACCACACTTTCTACAACG R GTTGAAGGTCTCGAACATGATC	105, 100
Histone 3 (HIS)	Chromatin structure	137	F GAGGAGTGAAGAAGCCCCAC R TGAAGTCCTGAGCAATCTCCC	98, 102-103
Ubiquitin (UBI)	Protein degradation	113	F GCAAGACCATCACCCTTGAG R CAGCGAAAGATCAACCTCTG	104, 99
Elongation factor 1-α (EFA)	Translation	172	F GACAAGCCCCTCAGACTTCC R GGAGAGACTCGTGGTGCATC	115, 100

Selected RGs were screened with RefFinder after RT-qPCR amplification with cDNA of each copepod species in each treatment, separately (**Figure 6.2**). The most stable RGs were found to be the following: UBI and EFA for *A. clausi* exposed to E56 elutriates (**Figure 6.2A**); HIS for *A. tonsa* exposed to $NiCl_2$ (**Figure 6.2B**); UBI and ACT for *A. tonsa* exposed to NiNPs (**Figure 6.2C**); ACT and HIS for *A. clausi* exposed to $NiCl_2$ (**Figure 6.2D**); HIS for *A. clausi* exposed to NiNPs (**Figure 6.2E**). These specific RGs were used to normalize gene expression of GOI in each treatment. In two cases we chose only one RG because the second most stable RG, according to RefFinder, showed instead a high variability among conditions when tested in RT-qPCR with other GOI.

Among the 32 primers of GOI which amplified in PCR, 24 (75.0%) showed good results in RT-qPCR analysis, as their melting curve presented a single peak and there was no amplification in the negative controls, hence they were selected for relative expression analyses.

The selected and optimised GOI for relative gene expression analyses, 11 for *A. tonsa* and 13 for *A. clausi*, were the following. For *A. tonsa*: DNA topoisomerase III (SWIB-domain containing protein) (SWIB), Sestrin (SEST-t), Superoxide dismutase [Cu-Zn] (SOD-t), Glutathione synthetase (GSS-t), Glutathione S-transferase σ (GSTσ-t), Phospholipid-hydroperoxide glutathione peroxidase (PHGPx-t), Vitellogenin 1 (VTG1-t), Acetylcholine receptor (AChR-t), Chitinase 10 (CHT10), Chitin deacetylase (CDA), Myosin heavy chain (MHC); for *A. clausi*: Mpv17-like protein (M-LP), Sestrin (SEST), Catalase (CAT), Superoxide dismutase [Cu-Zn] SOD-II, Glutathione synthetase (GSS), Glutathione S-transferase σ (GSTσ), Glutathione peroxidase (GPx), Phospholipid-hydroperoxide glutathione

peroxidase (PHGPx), Vitellogenin 1 (VTG1), Acetylcholine receptor (AChR), Acetylcholinesterase (AChE), Chitinase 2 (CHT2), Myosin heavy chain (MHC-c). In **Table 6.2** are summarised name, function, amplicon length, full sequence and amplification efficiency for each selected GOI and for each copepod species. Efficiencies of primer pairs for GOI and RGs in *A. clausi* were calculated with cDNA of laboratory-cultured specimens and with cDNA of each treatment (E56, $NiCl_2$, NiNPs). As differences in efficiencies were negligible, in *A. tonsa* we calculated efficiencies only with cDNA of cultured specimens.

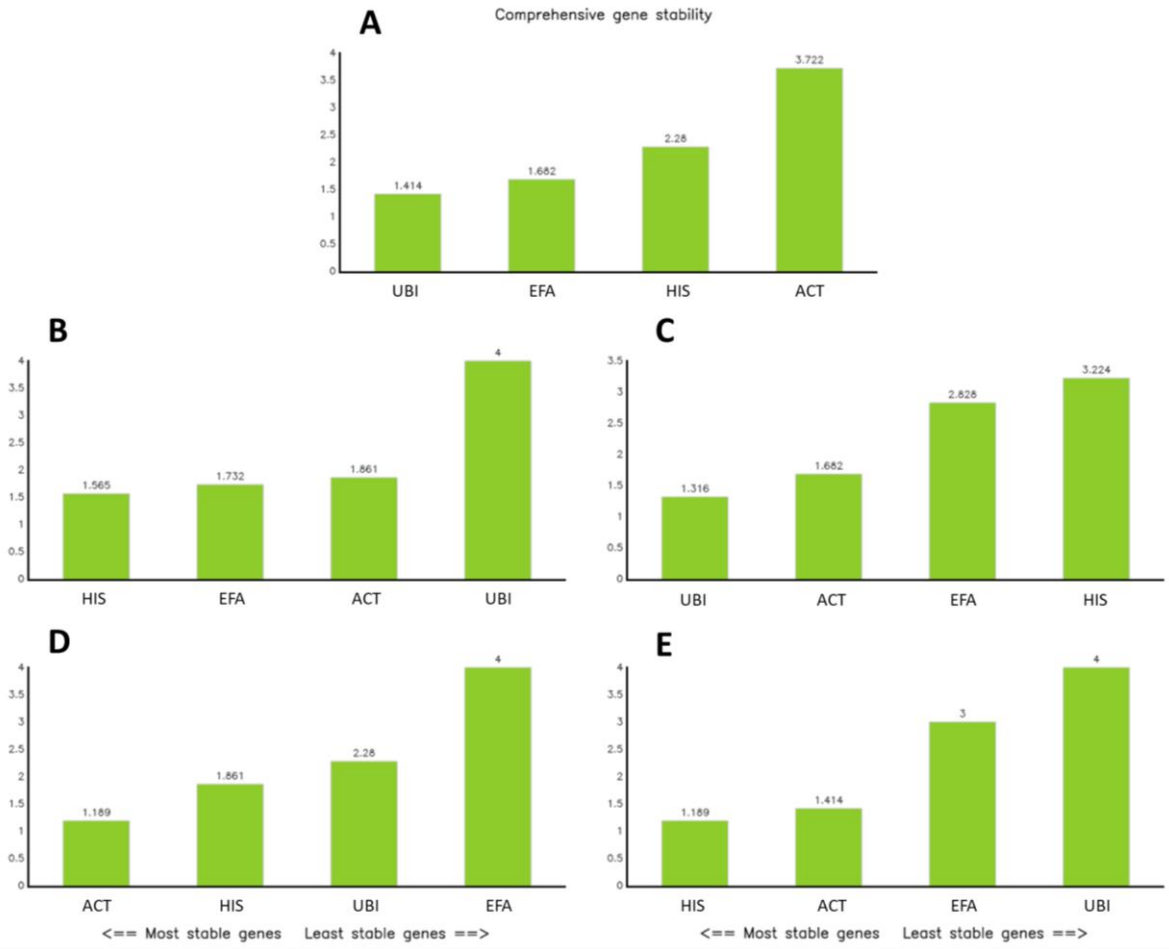

Figure 6.2 RefFinder summary charts of stability of the selected reference genes, separately for each copepod species and each condition. **A** – Results for *A. clausi* exposed to E56 elutriate of polluted sediments; **B** – results for *A. tonsa* exposed to $NiCl_2$; **C** – results for *A. tonsa* exposed to NiNPs; **D** – results for *A. clausi* exposed to $NiCl_2$; **E** – results for *A. clausi* exposed to NiNPs.

6.4.5 Transcriptome validation

Validation of *A. clausi de novo* transcriptome assembly (chapter 5) was carried out by comparing log_2FC of transcripts generated through RNA-seq with log_2FC resulted from RT-qPCR with the same cDNA, *i.e.* cDNA of copepod females exposed for 4 days to E56

elutriates of polluted sediments (**Figure 6.3**). Relative expression ratio of GOI selected from DEGs (left of the dashed line) showed that in some cases fold change calculated from differential expression analysis was higher with respect to results obtained through RT-qPCR. M-LP and SEST, which were among the most up- and down-regulated DEGs (log_2 fold change 10.7 and – 9.6, respectively), presented a fold change close to 0 in RT-qPCR assay. For GSTσ, on the other hand, both results were in agreement, with an up-regulation of 2 log_2FC, approximately; moreover, VTG1 and AChR were down-regulated both in RNA-seq and RT-qPCR, though much more in the former. Results were, instead, quite similar when looking at GOI selected among the whole transcriptome of *A. clausi*. Overall, we observed an up-regulation of genes involved in oxidative stress and detoxification: GSTσ (log_2FC = 2.1), SOD-II (0.9), CAT (0.5), PHGPx (0.6).

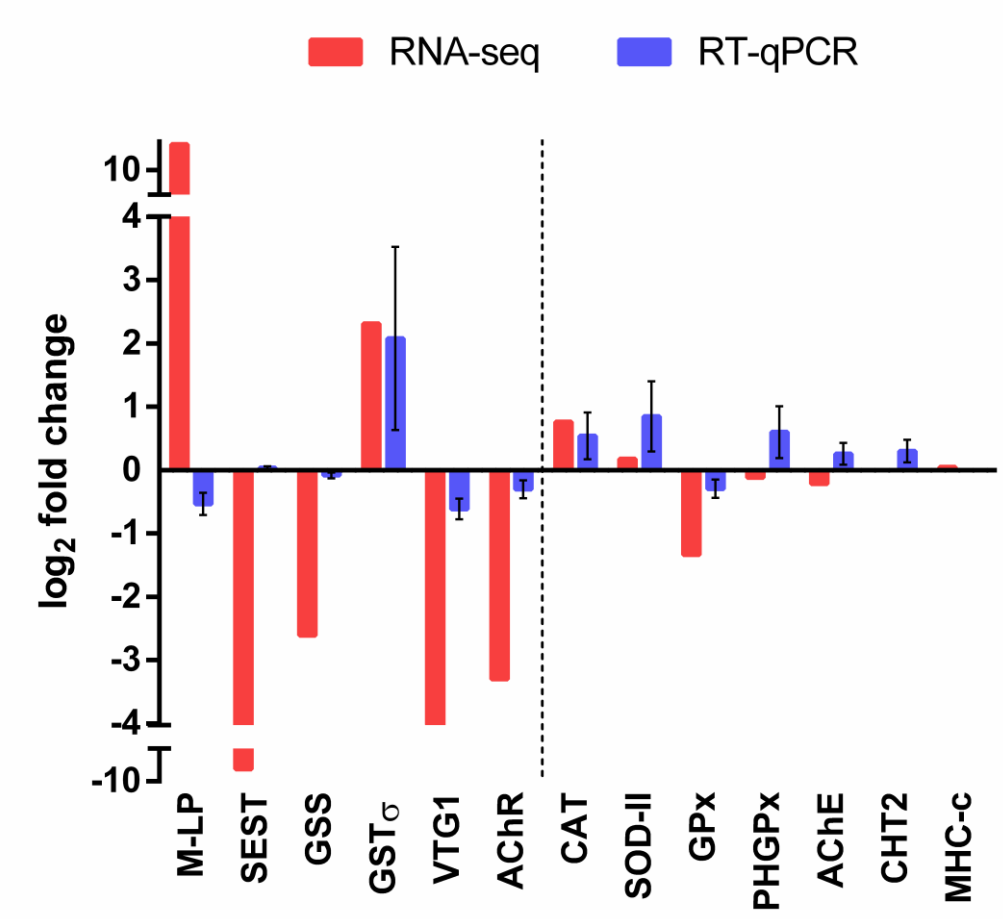

Figure 6.3 Relative expression ratio (log_2 fold change) of GOI selected for transcriptome validation of *Acartia clausi* females exposed to E56 vs. control, normalised on UBI and EFA reference genes. Red bars indicate results of RNA-seq; blue bars indicate results of RT-qPCR (values for the latter are mean ± SD; n = 9). Dashed line separates genes selected among differentially expressed genes of *A. clausi* (left) from genes selected among the whole transcriptome (right). Where no bar is visible, values are < 0.02.

6.4.6 Comparative gene expression with $NiCl_2$ and NiNPs

Results of relative expression ratio of GOI in *A. tonsa* females exposed for 4 days to $NiCl_2$ at 0.2 mg Ni/L are reported in **Figure 6.4**. The most notable registered responses in terms of log_2FC were SWIB (1.0), GSTσ (– 1.2) and VTG1 (– 1.3). The two genes involved in chitin metabolism, CHT10 and CDA, were both mildly up-regulated (0.6 and 0.4 log_2FC, respectively).

In **Figure 6.5** are shown the values of relative expression ratio of GOI in *A. tonsa* females exposed for 4 days to NiNPs 17 mg/L. In this case the responses were less evident, when compared to $NiCl_2$ exposure, and most genes had a fold change of opposite sign: for example, SWIB (log_2FC = – 0.8), AChR-t (– 0.8), GSS-t (– 0.6) and VTG1-t (0.5).

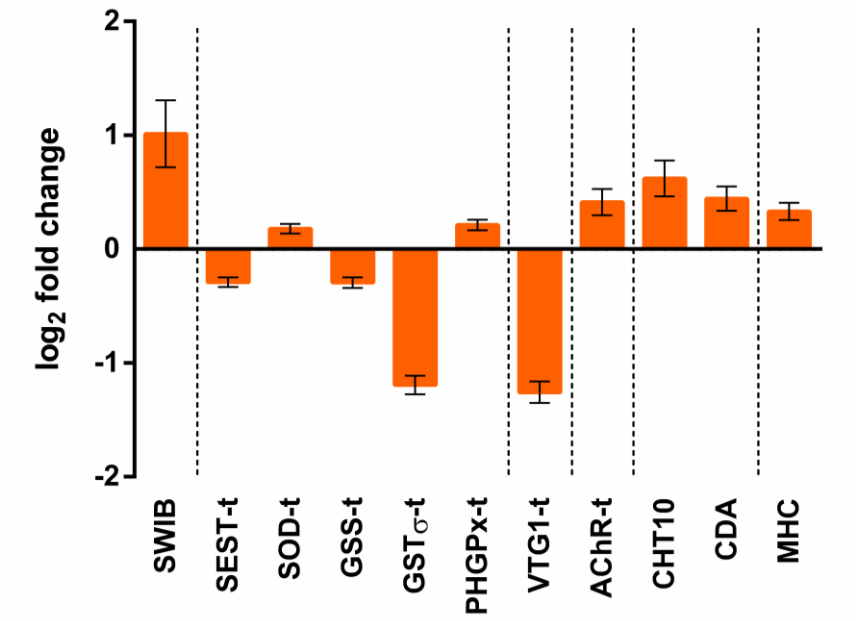

Figure 6.4 Relative expression ratio (log_2 fold change) of selected GOI of *Acartia tonsa* in females exposed to $NiCl_2$ 0.2 mg Ni/L vs. control, normalised on HIS reference gene. Dashed lines separate genes based on their function: from left to right, DNA structure, detoxification and oxidative stress, reproduction, nervous system, chitin metabolism, muscular structure. Values are mean ± SD; n = 9.

Relative expression ratio of GOI in *A. clausi* females, showed, on the other hand, a greater response, also at lower concentrations of the toxicants. Females exposed for 4 days to $NiCl_2$ at 0.2 and 0.1 mg Ni/L showed a trend of general down-regulation, especially for genes involved in detoxification and oxidative stress: SOD-II, GSS, GSTσ, GPx and PHGPx were all down-regulated, with an average fold change of roughly – 1.5 and minimum fold change of – 2.1 (GSTσ, 0.1 mg Ni/L) (**Figure 6.6**). SEST and CAT, which belong to a similar category of proteins, presented instead a slight up-regulation, around 0.5 log_2FC. Both

GOI involved with nervous systems, AChR and AChE, were also down-regulated to less than – 1 log_2FC; a similar value of down-regulation occurred also for MHC. In general, fold change for *A. clausi* was similar among the two concentrations of $NiCl_2$.

Figure 6.7 shows relative expression ratio of GOI in *A. clausi* females after 4 days of exposure to NiNPs at 8.5 and 17 mg/L. For this treatment, genes of oxidative stress and detoxification had a mixed response, with SOD-II, GSTσ, GPx down-regulated to a minimum of – 1.2 log_2FC (SOD-II at 8.5 mg/L) and SEST, CAT, GSS, PHGPx mildly up-regulated, although with a high standard deviation. VTG1 and MHC-c were similarly down-regulated in the 17 mg/L concentration (around – 0.7 log_2FC).

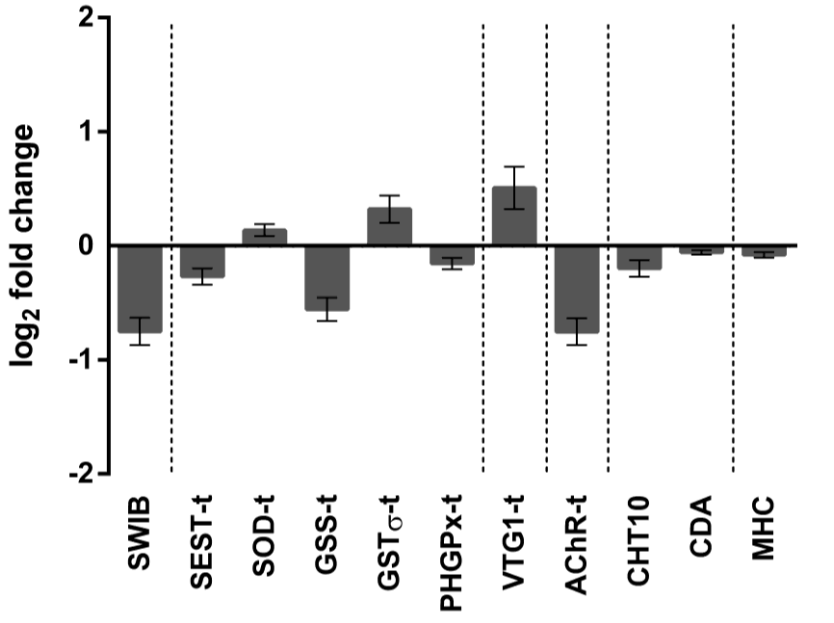

Figure 6.5 Relative expression ratio (log_2 fold change) of selected GOI of *Acartia tonsa* in females exposed to NiNPs 17 mg/L vs. control, normalised on UBI and ACT reference genes. Dashed lines separate genes based on their function: from left to right, DNA structure, detoxification and oxidative stress, reproduction, nervous system, chitin metabolism, muscular structure. Values are mean ± SD; n = 9.

6.5 Discussion

Comparing physiological and molecular responses of organisms in ecological or toxicological studies is encouraged in recent literature, as it allows to have a complete set of biological information which constitutes the so called "ecotoxicogenomic approach" (Tarrant *et al.*, 2019; Tennant, 2002). In this view, it is important to identify biomarkers of effect or exposure, *i.e.*, biological processes triggered in response to a specific class of substances, which might be used to predict a toxic effect or to elucidate molecular mechanisms of toxicity (Waters and Fostel, 2004).

Here, we present results of RT-qPCR gene expression of *A. tonsa* and *A. clausi* females exposed for 4 days to E56 elutriates of polluted sediments, which were used as a validation of the *de novo* transcriptome generated from the same organisms (chapter 5). Gene expression was also tested in females of both species exposed for 4 days to $NiCl_2$ and NiNPs. Length of the exposure and concentrations of toxicants were chosen to allow comparisons with physiological results of the chronic test (chapter 4) and of other studies in scientific literature, but also to obtain an intermediate effect in exposed organisms which could both trigger a relevant molecular response and, at the same time, guarantee an adequate number of surviving specimens at the end of the 4 days of exposure, so to have enough genetic material available.

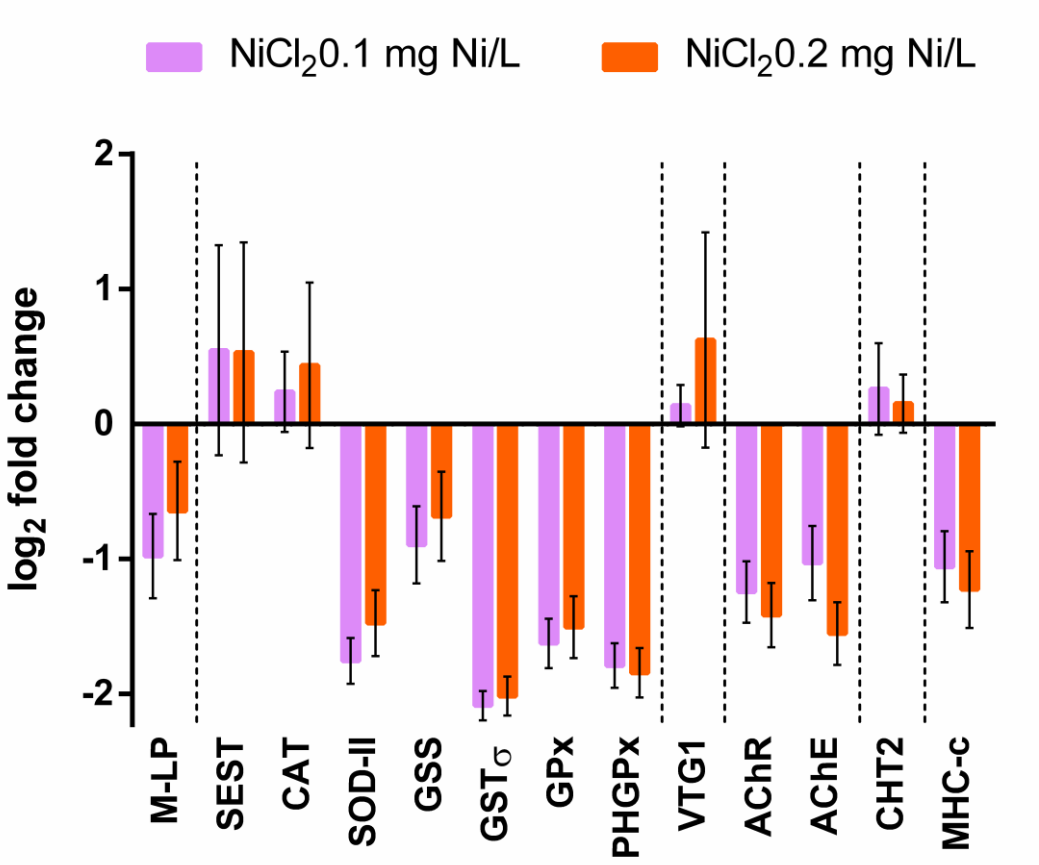

Figure 6.6 Relative expression ratio (log_2 fold change) of selected GOI of *Acartia clausi* in females exposed to $NiCl_2$ 0.1 and 0.2 mg Ni/L vs. control, normalised on ACT and HIS reference genes. Dashed lines separate genes based on their function: from left to right, transcription, detoxification and oxidative stress, reproduction, nervous system, chitin metabolism, muscular structure. Values are mean ± SD; n = 9.

Overall, we designed 26 *A. tonsa*-specific primer pairs and 16 *A. clausi*-specific primer pairs from the corresponding *de novo* assembled transcriptomes. We observed, however, a lower amplification success for primers designed on *A. tonsa* with respect to those designed on *A. clausi*. Interestingly, in the transcriptome generated from *A. clausi* exposed to E56

elutriates we observed a great homology of our assembled transcripts to crustaceans in general and especially to *Eurytemora affinis* copepod species (please refer to chapter 5). On the other hand, for the transcriptome of *A. tonsa*, top species distribution mainly included insects or branchiopods, with copepod occurring at the fourth place (Zhou *et al.*, 2018). This lower homology for the *A. tonsa* transcriptome with copepod sequences, likely due to the paucity of publicly available copepod sequences in nr database at the time of the study (the annotation was performed in 2016), could explain the lower success rate of amplification for the primers designed for *A. tonsa*.

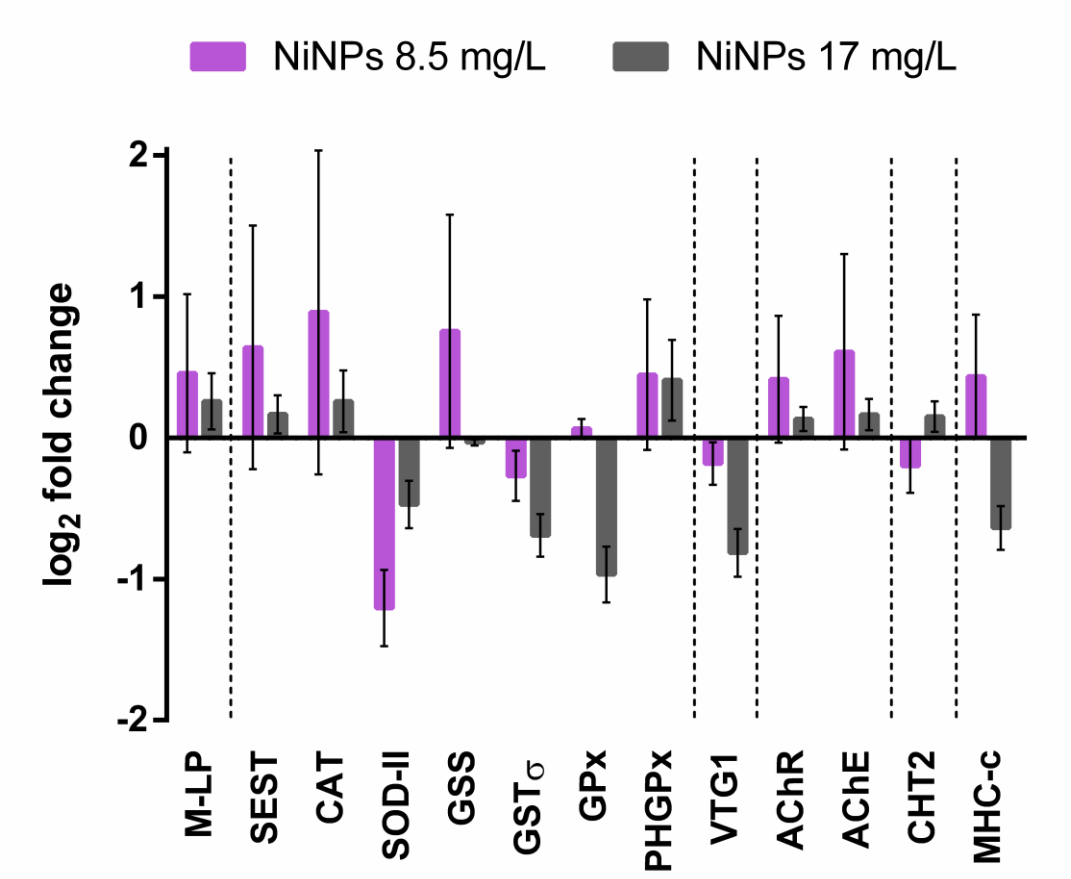

Figure 6.7 Relative expression ratio (log_2 fold change) of selected GOI of *Acartia clausi* in females exposed to NiNPs 8.5 and 17 mg/L vs. control, normalised on HIS reference gene. Dashed lines separate genes based on their function: from left to right, transcription, detoxification and oxidative stress, reproduction, nervous system, chitin metabolism, muscular structure. Values are mean ± SD; n = 9.

Interestingly, none of the primers for GOI designed for *A. tonsa* successfully amplified cDNA of *A. clausi*, and vice-versa. This is quite unexpected, given that the two copepods are co-generic species. It is possible, hence, that the low phylogenetic distance between them is coupled to a higher diversity at gene level. This high specificity has also been observed when primers designed from the transcriptome of *Calanus helgolandicus* did not successfully amplify target genes in *Temora stylifera* (Dr. Ylenia Carotenuto, personal communication). It is

to be noted, however, that four primers of RGs, designed on *C. helgolandicus*' sequences, successfully amplified the same genes in both *A. tonsa* and *A. clausi*, indicating that for these highly conserved sequences there was strong homology. Another possibility is that the Adriatic strain of *A. tonsa*, which has been reared at ISPRA Livorno for more than 14 years, could have undergone genetic drift, and hence genetic mutations, due to the constant inbreeding, which in conclusion increased the genetic diversity between the species. This phenomenon is not rare for laboratory cultures of crustaceans (Ajiboye *et al.*, 2011; Moss *et al.*, 2007; Wang *et al.*, 2020), but further studies are needed to investigate this aspect.

Validation of the transcriptome of *A. clausi* showed that values of log_2FC for genes which were greatly up- or down-regulated in RNA-seq were not always in agreement with values of log_2FC from RT-qPCR. This discrepancy is not rare, as also in other cases gene expression was sometimes more pronounced in RNA-seq with respect to RT-qPCR validation (Russo *et al.*, 2020; Wang *et al.*, 2017). This could be due to the fact that multiple isoforms of the same transcript, having different expression levels, might be amplified by the same primer pairs during the RT-qPCR assay, hence reducing the amplitude of the relative expression values. Genes which were selected from the full transcriptome and not among DEGs, had low values of log_2FC also in RT-qPCR, as expected, confirming the RNA-seq value. In general, RT-qPCR confirmed an up-regulation of genes involved with oxidative stress and detoxification (GSTσ, SOD-II, CAT, PHGPx), as expected after exposure to xenobiotics and heavy metals contained in the polluted sediments (Hook *et al.*, 2014; Kadiene *et al.*, 2020; Lee *et al.*, 2008a). On the other hand, VTG, which in the validation was mildly down-regulated, has a mixed response in literature, as it is documented to be both up- (Lee *et al.*, 2008b; Wang *et al.*, 2017) and down-regulated (Hook *et al.*, 2014; Jiang *et al.*, 2013) in copepods or other crustaceans exposed to xenobiotics. Similarly, in our RT-qPCR results with nickel contaminants in *A. tonsa* and *A. clausi*, VTG1 was either up- or down-regulated.

In general, our RT-qPCR results with *A. clausi* and *A. tonsa* after exposure to $NiCl_2$ and NiNPs showed a greater sensitivity of the former species, which presented stronger responses (in terms of up- or down-regulation) also at lower concentrations of the same toxicants. Regarding gene expression, the GOI which gave the most comparable and consistent results among all four datasets was GSTσ, down-regulated for both copepod species, with both toxicants (with the exception of *A. tonsa* and NiNPs, where it was barely up-regulated). In the scientific literature, GST (and in particular the σ sub-class), are commonly reported to be up-regulated in copepods exposed to metals, including Ni (Lauritano *et al.*, 2021 and references therein; Lee *et al.*, 2008b). Moreover, in our RT-qPCR validation, GSTσ of *A. clausi* was up-regulated. There are, however, studies which reported down-regulation of

GST in copepods: class σ and θ in *T. japonicus* fed the toxic dinoflagellate *Gymnodinium catenatum* (Han *et al.*, 2021); in *T. japonicus* exposed to a polychlorinated biphenyl (organic pollutant) (Lee *et al.*, 2006); in the Chinese mitten crab *Eriocheir sinensis* exposed to cadmium (Silvestre *et al.*, 2006). These results are in agreement with our gene expression levels of GSTσ with nickel contaminants in *A. tonsa* and *A. clausi*, and show that this gene has mixed responses.

Similarly, in *A. clausi* exposed to $NiCl_2$, an overall down-regulation of other genes involved with detoxification and reaction to ROS (SOD-II, GSS, GPx, PHGPx, in addition to GSTσ) was observed, while such genes are usually up-regulated after exposure to heavy metals (Wang and Wang, 2010). As a confirmation, also M-LP was down-regulated, a gene which acts as a transcription factor of oxidative stress genes (Iida *et al.*, 2003). In the same condition, also AChE, AChR and MHC-c were down-regulated. This down-regulation response could indicate that the toxicant inhibited molecular mechanisms of defence in copepod females, which were not able to fully detoxify the heavy metal. A similar down-regulation was observed also in the copepod *P. annandalei* exposed to Cd, and the authors hypothesised that down-regulation might be a strategy to conserve energy, minimising oxidative damage (Kadiene *et al.*, 2020). Another hypothesis is that the copepods could have up-regulated other genes, which were not included among the panel of GOI we selected, that might have positively compensated for the defensive response of the females (high survival). In order to clarify this point, more experiments and a different set of GOI are probably needed.

Comparing these molecular results to the physiological output obtained in the chronic test, we concluded that the copepods appear to be more sensitive to this toxicant in terms of gene expression than in terms of reproductive success. The general down-regulation observed in *A. clausi* exposed to $NiCl_2$ could be, hence, the smoking gun of an inhibition of molecular defences of copepods caused by the toxicants. Despite this, when considering the physiological responses of *A. clausi* females throughout the four days of chronic test, there were little to no differences among control and any concentration of $NiCl_2$: EP, FP production and survival rate were all statistically similar on day 4 (*i.e.*, the day relative to the gene expression results); the only case when there was a statistical difference between control and treatment was day 2, for EP with $NiCl_2$ at 0.1 mg Ni/L. This reinforces the hypothesis we reported above: probably *A. clausi* females were able to maintain overall stable physiological parameters when exposed to $NiCl_2$ precisely because of the down-regulation, which allowed them to conserve energy. Moreover, the fact that there was little to no difference in gene expression at the two concentrations of $NiCl_2$ tested in *A. clausi* (0.1 and 0.2 mg Ni/L)

confirmed the overall similar effects induced by the same two concentrations on the aforementioned physiological parameters.

Conversely, the same species was subject to slightly greater physiological effects when exposed to NiNPs, which caused instead lower changes in gene expression. A similar result was obtained for larvae of the zebrafish *D. rerio* exposed to NiNPs and $NiCl_2$; the authors found that DNA fragmentation and gene expression of target genes, related to stress, were both greater after $NiCl_2$ exposure, and hypothesised that physiological toxicity of NiNPs must be caused by other factors in addition to the release of Ni ions (Boran and Şaffak, 2018). This unknown factor, perhaps, could be represented by the physical ingestion of particles, already documented for *A. tonsa* (Zhou *et al.*, 2016a), which may not efficiently trigger molecular defences. In chapter 4, we hypothesised that the reduction in EP with NiNPs could have been the consequence of a shift in the molecular balance, *i.e.*, a reduction in gene expression for reproduction-related processes to increase transcriptional efforts in other pathways, such as maintenance of physiological homeostasis or integrity of cellular processes. Indeed, for NiNPs we observed a greater inhibition of reproductive ability in *A. clausi* females, when compared to $NiCl_2$ (on day 1 and 2, both NiNPs 8.5 and 17 mg/L caused a statistically significant decrease in EP; and this trend of decreased EP continued for the other two days). As a confirmation, the expression of VTG1 was negative in females exposed to NiNPs, whereas the same gene had a positive log_2FC in females exposed to $NiCl_2$. This appears to confirm a correlation between decreased EP and down-regulation of VTG1, in females of *A. clausi*.

Zhou *et al.* (2016b) exposed *A. tonsa* adults to CdSe/ZnS quantum dot nanoparticles for 4 days. Despite no reductions in EP or egg HS were observed, a gene expression analysis of HSP70 showed a 10-folds increase only on day 3. According to the authors, this meant that, at low quantum dots concentrations, a defensive molecular mechanism was activated before any evident physiological effects could occur, and the decrease of gene expression at day 4 would reflect the success of this defence mechanism (Zhou *et al.*, 2016b). Considering this, another possibility is that we would have observed a greater gene regulation at earlier time-points (*e.g.*, after one day of exposure). It is also to be noted that a recent study of life-history traits over multiple generations, showed how *P. annandalei* males and females exposed to cadmium had a dual gene expression response over several generations, in terms of change of log_2FC sign, for genes such as heat-shock protein 70 and myohemerythrin (Kadiene *et al.*, 2022). Many factors are involved in the dynamics of gene expression, at different scales: parameters such as time of exposure, generation, life stage and sex of tested organisms may all play a role in this complex pathway.

In conclusion, *A. clausi* females proved to be more responsive to $NiCl_2$ with respect to NiNPs, in terms of gene expression of selected GOI (especially down-regulation of genes involved in oxidative stress), and more sensitive with respect to females of *A. tonsa*. The latter species, in fact, showed little variation of log_2FC of GOI. This down-regulation in *A. clausi* could be due to an inhibition of molecular defences of copepods caused by the toxicants. In general, for *A. clausi* physiological data of the chronic test were comparable to results of gene expression at the same conditions. This could indicate that the panel of GOI optimized for this species is to a certain extent representative of physiological conditions of this organism; therefore, these genes might be used as an early-warning biomarker of effect in *A. clausi*, in view of the employment of an ecotoxicogenomic approach (*i.e.*, pairing ecotoxicological results with molecular evidence) with this copepod species, in environmental risk assessment of coastal areas. In particular, a down-regulation of vitellogenin seems linked to a lower production of eggs and can hence be considered a proxy of the reproductive capabilities of *A. clausi*. *A. tonsa*, on the other hand, showed mild molecular responses in comparison to the physiological effects. To explain this, there is also the possibility that genes other than GSTσ and VTG1, not included in our selection of GOI, were differentially regulated in this copepod as a response to the toxicants. Consequently, other target genes should be identified in *A. tonsa* to better define its molecular response to Ni. Our findings confirm once more the importance of an ecotoxicogenomic approach in view of elucidating the mechanisms of toxicity at a molecular level, and also in view of identifying biomarker genes to be used as early-warning signals of toxic impact on copepods.

Conclusions and future perspectives

With the work of this PhD project, new results were produced and presented regarding physiology and molecular biology of the copepod species *Acartia clausi* and *A. tonsa* when exposed to nickel chloride ($NiCl_2$) and nickel nanoparticles (NiNPs).

A study on historical control data of *A. tonsa* maintained in long-term laboratory cultures for ecotoxicological purposes showed that physiological parameters of this copepod species (egg hatching success, naupliar immobilisation both in control conditions and when exposed to the reference toxicant), were stable over a period of eight years. This confirmed the robustness of this species as model organism in ecotoxicology also for long-standing laboratory cultures.

A novel protocol of laboratory culturing of *A. clausi* was also set up. Among different algal diets tested, we identified the cryptophyte *Rhinomonas reticulata* as ideal for this copepod species in terms of production of eggs and faecal pellets, egg hatching success and survival of males and females. Weekly censuses, moreover, revealed that a multi-generational culture of this species is feasible from two to four months, and that approximately 26 days are needed to obtain an F2 generation in laboratory cultures.

Ecotoxicological tests performed with nauplii of both species, exposed to $NiCl_2$ and NiNPs, confirmed that larval stages of *A. clausi* are more sensitive with respect to those of *A. tonsa* approximately 6 (NiNPs) and 95 times ($NiCl_2$) in terms of naupliar immobilisation. Adults of both species, on the other hand, were less affected by these two toxicants at the concentrations tested and showed similar physiological responses, with mild negative effects mostly for egg production. We also confirmed that the effect of both toxicants on eggs, in terms of egg hatching success, is mainly due to the release of Ni ions, which in NiNPs solution occurs continuously over time.

The *de novo* transcriptome assembly of *A. clausi* exposed to elutriates of polluted industrial sediments (containing high concentrations of polycyclic aromatic hydrocarbons and heavy metals), produced during this PhD project, was the first available transcriptomic resource for this copepod species, and an important step forward for molecular resources of this taxon. After functional annotation and differential expression analysis, 1,000 differentially expressed genes were identified, of which 743 up- and 257 down-regulated, indicating a great response. Among up-regulated genes, the most represented functions were generic stress and detoxification (heat-shock proteins; superoxide dismutases; glutathione-S-transferases; cytochrome P450; platelet-activating factor acetylhydrolase), proteolysis (lysosomal proteases, peptidases, cathepsins) and cytoskeleton structure (α- and β-tubulin). Down-

regulated genes were mostly involved with ribosome structure (ribosomal proteins), cellular transport (ATP-binding cassettes) and DNA binding (histone proteins, transcription factors).

Lastly, quantitative gene expression was tested, through RT-qPCR, with a panel of genes of interest selected from the newly-generated transcriptome, in *A. clausi* and *A. tonsa* females exposed to $NiCl_2$ and NiNPs at the same conditions tested for physiological parameters. Responses were greater in *A. clausi*, especially with $NiCl_2$, and consisted mostly in a down-regulation of genes involved in oxidative stress (superoxide dismutase), detoxification (glutathione-S-transferase σ, phospholipid-hydroperoxide glutathione peroxidase), reproduction (vitellogenin), nervous system (acetylcholinesterase), suggesting an inhibition of molecular defences by these toxicants.

To summarise, our physiological and molecular results with adult copepods indicate that, even though at the physiological level (*i.e.*, egg production, production of faecal pellets and adult survival) responses of females of both species to $NiCl_2$ were mild and comparable, *A. clausi* reported greater changes at the molecular level. This could mean that the remarkable inhibition in molecular defences allowed females of *A. clausi* to conserve energy and, thus, maintain a certain stability in physiological parameters. Conversely, NiNPs caused slightly greater physiological effects, but comparatively lower changes in gene expression, in both copepod species. An explanation for this could be that the physical ingestion of particles (which causes documented detrimental physiological effects) may not efficiently trigger molecular defences, at least for the genes we selected and at the time-points we analysed. Interestingly, however, NiNPs in *A. clausi* caused both a reduction in egg production and a mild down-regulation of vitellogenin, whereas for $NiCl_2$ egg production was not reduced and vitellogenin was up-regulated. This evidence points towards a correlation between down-regulation of vitellogenin and a decrease in reproductive capabilities of *A. clausi*. The panel of GOI optimized for *A. clausi*, and particularly vitellogenin, hence, could be used as an early-warning biomarker of effect, and support the employment of an ecotoxicogenomic approach in environmental risk assessment with this copepod species. On the other hand, it appears that other target genes have to be identified in *A. tonsa* to better define its molecular responses to Ni.

Overall, this thesis provided novel and important information on the biology of the copepod *A. clausi*, of great ecological relevance, especially in the Mediterranean Sea, but whose physiological and molecular responses are still poorly studied. This work also contributed to deepen the knowledge on effects and environmental behaviour of NiNPs, a class of broadly employed engineered nanomaterials (ENMs) which could become a threat for the marine environment in the near future.

Looking at future perspectives, there are specific lines of research which remain open after the work of this PhD project.

First, there is much work left to do with the optimisation of multigenerational cultures of *A. clausi*, in order to have available organisms in laboratory conditions throughout the year, not depending on the reproductive or seasonal cycle. A focus should be addressed towards rearing protocols and algal diets of copepods. A broader range of algal diets, also mixed and at different concentrations, should be tested; diets for nauplii and/or copepodids should also be set up, with algal species of smaller dimensions.

In view of proposing *A. clausi* as alternative species in ecological risk assessment, moreover, it should be important to assess viability of eggs after a period of cold-storage, as it has been done with *A. tonsa*. In this way, acute tests could be started more easily, without sorting adults, and most importantly eggs could be transferred for ecotoxicological analyses to other laboratories which are not in conditions to collect wild organisms.

Despite primers for reference genes successfully amplified in PCR and RT-qPCR for both *A. clausi* and *A. tonsa*, the same was not true for primers for genes of interest, as none worked for the other copepod species. Besides the phylogenetic distance between these species, we hypothesised that inbreeding – which occurred for the Adriatic strain of *A. tonsa* in more than ten years of multigenerational culture – caused genetic drift and subsequent mutations in specimens of this species. To confirm this hypothesis, primers designed for *A. clausi* could be tested on wild *A. tonsa* specimens, both of the Adriatic and Baltic strain.

Regarding gene expression analyses, during the 4-days exposure periods male copepods were incubated and collected together with females, for both toxicants and both species. Here, we were able to analyse gene expression only in females, but it will be interesting to verify and compare gene expression of males too, as recommended by recent scientific literature.

Lastly, regarding the study of ENMs, a field in constant progress, there is the need of a standard protocol for the measure of dissolved metal ions (through inductively coupled plasma mass spectrometry), as we noticed great differences in methodologies reported in scientific literature. More studies will be needed to develop and optimise comparable protocols, compatible with the variety in sizes and shapes, which would make easier to compare studies with these complex substances. With this in mind, research works in the future should also focus on the dissolution of ions from metallic ENMs after large periods of time, as this factor could represent a major threat for the marine environment. While protocols for measuring environmental concentrations of ENMs are being developed, studies are needed to

measure ion dissolution from metallic ENMs in laboratory conditions, to deepen the behaviour in the environment of these emerging contaminants.

References

Ajiboye OO, Yakubu AF, Adams TE, Olaji ED and Nwogu NA, 2011, A review of the use of copepods in marine fish larviculture. *Reviews in Fish Biology and Fisheries* 21(2): 225–246, DOI: 10.1007/s11160-010-9169-3.

Alekseev VR and Souissi A, 2011, A new species within the *Eurytemora affinis* complex (Copepoda: Calanoida) from the Atlantic Coast of USA, with observations on eight morphologically different European populations. *Zootaxa* 2767(1): 41, DOI: 10.11646/zootaxa.2767.1.4.

Almeda R, Baca S, Hyatt C and Buskey EJ, 2014, Ingestion and sublethal effects of physically and chemically dispersed crude oil on marine planktonic copepods. *Ecotoxicology* 23(6): 988–1003, DOI: 10.1007/s10646-014-1242-6.

Altschul SF, Gish W, Miller W, Myers EW and Lipman DJ, 1990, Basic Local Alignment Search Tool. *J. Mol. Biol.* 215: 403–410.

Amato A and Carotenuto Y, 2018, Planktonic calanoids embark into the "Omics era." *Trends in Copepod Studies* 12: 287–314.

Anahi BA, Lopez-Abbate MC, Biancalana F and Hoffmeyer MS, 2014, Influence of Experimental Thermal Shifts and Overcrowding on Fecundity in Wild Females of *Acartia Tonsa* of the Bahía Blanca Estuary. *Brazilian Journal of Oceanography* 62(3): 201–207, DOI: 10.1590/S1679-87592014064706203.

APAT-ICRAM, 2007, Corsini, S., Onorati, F., and Pellegrini, D. Manuale per la movimentazione di sedimenti marini. https://www.isprambiente.gov.it/it/pubblicazioni/manuali-e-linee-guida/manuale-per-la-movimentazione-di-sedimenti-marini. .

Araújo CVM, Diz FR, Moreno-Garrido I, Lubián LM and Blasco J, 2008, Effects of cold-dark storage on growth of *Cylindrotheca closterium* and its sensitivity to copper. *Chemosphere* 72(9): 1366–1372, DOI: 10.1016/j.chemosphere.2008.04.022.

Arciszewski TJ, Hazewinkel RR, Munkittrick KR and Kilgour BW, 2018, Developing and applying control charts to detect changes in water chemistry parameters measured in the Athabasca River near the oil sands: A tool for surveillance monitoring: Control charts and water chemistry parameters. *Environmental Toxicology and Chemistry* 37(9): 2296–2311, DOI: 10.1002/etc.4168.

Arciszewski TJ, Munkittrick KR, Kilgour BW, Keith HM, Linehan JE and McMaster ME, 2017, Increased size and relative abundance of migratory fishes observed near the Athabasca oil sands. *FACETS* 2(2): 833–858, DOI: 10.1139/facets-2017-0028.

Armstrong EK, Mondon J, Miller AD, Revill AT, Stephenson SA, Tan MH, Greenfield P, Tromp JJ, Corbett P and Hook SE, 2022, Transcriptomic and Histological Analysis of

the Greentail Prawn (*Metapenaeus bennettae*) Following Light Crude Oil Exposure. *Environmental Toxicology and Chemistry* 41(9): 2162–2180, DOI: 10.1002/etc.5413.

Arya M, Shergill IS, Williamson M, Gommersall L, Arya N and Patel HR, 2005, Basic principles of real-time quantitative PCR. *Expert Review of Molecular Diagnostics* 5(2): 209–219, DOI: 10.1586/14737159.5.2.209.

Asadi Dokht Lish R, Johari SA, Sarkheil M and Yu IJ, 2019, On how environmental and experimental conditions affect the results of aquatic nanotoxicology on brine shrimp (*Artemia salina*): A case of silver nanoparticles toxicity. *Environmental Pollution* 255: 113358, DOI: 10.1016/j.envpol.2019.113358.

Asai S, Ianora A, Lauritano C, Lindeque PK and Carotenuto Y, 2015, High-quality RNA extraction from copepods for Next Generation Sequencing: A comparative study. *Marine Genomics* 24: 115–118, DOI: 10.1016/j.margen.2014.12.004.

Asai S, Sanges R, Lauritano C, Lindeque PK, Esposito F, Ianora A and Carotenuto Y, 2020, De Novo Transcriptome Assembly and Gene Expression Profiling of the Copepod *Calanus helgolandicus* Feeding on the PUA-Producing Diatom *Skeletonema marinoi*. *Marine Drugs* 18(8): 392, DOI: 10.3390/md18080392.

Aufricht C, 2005, Heat-shock protein 70: molecular supertool? *Pediatric Nephrology* 20(6): 707–713, DOI: 10.1007/s00467-004-1812-6.

Baker TJ, Tyler CR and Galloway TS, 2014, Impacts of metal and metal oxide nanoparticles on marine organisms. *Environmental Pollution* 186: 257–271, DOI: 10.1016/j.envpol.2013.11.014.

Barreiro A, Guisande C, Frangópulos M, González-Fernández A, Muñoz S, Pérez D, Magadán S, Maneiro I, Riveiro I and Iglesias P, 2006, Feeding strategies of the copepod Acartia clausi on single and mixed diets of toxic and non-toxic strains of the dinoflagellate *Alexandrium minutum*. *Marine Ecology Progress Series* 316: 115–125, DOI: 10.3354/meps316115.

Barreto FS, Watson ET, Lima TG, Willett CS, Edmands S, Li W and Burton RS, 2018, Genomic signatures of mitonuclear coevolution across populations of *Tigriopus californicus*. *Nature Ecology & Evolution* 2(8): 1250–1257, DOI: 10.1038/s41559-018-0588-1.

Barus BS, Chen K, Cai M, Li R, Chen H, Li C, Wang J and Cheng S-Y, 2021, Heavy Metal Adsorption and Release on Polystyrene Particles at Various Salinities. *Frontiers in Marine Science* 8: 671802, DOI: 10.3389/fmars.2021.671802.

Baudo R, Onorati F, Mugnai C, Pellegrini D, Faimali M, Piazza V, Aragno M, Leoni T and Ziantoni S, 2015, Criticità nel percorso di accreditamento dei saggi ecotossicologici. ISPRA, Manuali e Linee Guida 121/2015. .

Bebianno MJ, Pereira CG, Rey F, Cravo A, Duarte D, D'Errico G and Regoli F, 2015, Integrated approach to assess ecosystem health in harbor areas. *Science of The Total Environment* 514: 92–107, DOI: 10.1016/j.scitotenv.2015.01.050.

Behra R and Krug H, 2008, Nanoparticles at large. *Nature Nanotechnology* 3(5): 253–254, DOI: 10.1038/nnano.2008.113.

Beiras R, Tato T and López-Ibáñez S, 2019, A 2-Tier standard method to test the toxicity of microplastics in marine water using *Paracentrotus lividu* s and *Acartia clausi* larvae. *Environmental Toxicology and Chemistry* 38(3): 630–637, DOI: 10.1002/etc.4326.

Belmonte G and Potenza D, 2001, Biogeography of the family Acartiidae (Calanoida) in the Ponto-Mediterranean Province. In: Lopes RM, Reid JW and Rocha CEF (eds) *Copepoda: Developments in Ecology, Biology and Systematics*. Springer Netherlands: Dordrecht, 171–176, DOI: 10.1007/0-306-47537-5_15.

Benedetti M, Ciaprini F, Piva F, Onorati F, Fattorini D, Notti A, Ausili A and Regoli F, 2012, A multidisciplinary weight of evidence approach for classifying polluted sediments: Integrating sediment chemistry, bioavailability, biomarkers responses and bioassays. *Environment International* 38(1): 17–28, DOI: 10.1016/j.envint.2011.08.003.

Benedetti M, Fattorini D, Martuccio G, Nigro M and Regoli F, 2009, Interactions between trace metals (Cu, Hg, Ni, Pb) and 2,3,7,8-tetrachlorodibenzo-P-dioxin in the Antarctic fish *Trematomus bernacchii*: oxidative effects on biotransformation pathway. *Environmental Toxicology and Chemistry* 28(4): 818, DOI: 10.1897/08-066.1.

Bengston DA, 2007, Status of marine aquaculture in relation to live prey: Past, present and future. *Live feeds in marine aquaculture* 1–16.

Benjamini Y and Hochberg Y, 1995, Controlling the False Discovery Rate: A Practical and Powerful Approach to Multiple Testing. *J. R. Statist. Soc.* 57(1): 289–300.

Bennett-Lovsey R, Hart SE, Shirai H and Mizuguchi K, 2002, The SWIB and the MDM2 domains are homologous and share a common fold. *Bioinformatics* 18(4): 626–630, DOI: 10.1093/bioinformatics/18.4.626.

Bergami E, Pugnalini S, Vannuccini ML, Manfra L, Faleri C, Savorelli F, Dawson KA and Corsi I, 2017, Long-term toxicity of surface-charged polystyrene nanoplastics to marine planktonic species *Dunaliella tertiolecta* and *Artemia franciscana*. *Aquatic Toxicology* 189: 159–169, DOI: 10.1016/j.aquatox.2017.06.008.

Blaise C and Férard J-F, 2006, Microbiotests in aquatic toxicology: the way forward. *Environmental Toxicology*. paper presented at the ENVIRONMENTAL TOXICOLOGY 2006. WIT Press: Mykonos, Greece, 339–348, DOI: 10.2495/ETOX060341.

Blasco J, Corsi I and Matranga V, 2015, Particles in the oceans: Implication for a safe marine environment. *Marine Environmental Research* 111: 1–4, DOI: 10.1016/j.marenvres.2015.10.001.

Bolger AM, Lohse M and Usadel B, 2014, Trimmomatic: a flexible trimmer for Illumina sequence data. *Bioinformatics* 30(15): 2114–2120, DOI: 10.1093/bioinformatics/btu170.

Boran H and Şaffak S, 2018, Comparison of Dissolved Nickel and Nickel Nanoparticles Toxicity in Larval Zebrafish in Terms of Gene Expression and DNA Damage. *Archives of Environmental Contamination and Toxicology* 74(1): 193–202, DOI: 10.1007/s00244-017-0468-8.

Bray NL, Pimentel H, Melsted P and Pachter L, 2016, Near-optimal probabilistic RNA-seq quantification. *Nature Biotechnology* 34(5): 525–527, DOI: 10.1038/nbt.3519.

Brooks AC, Foudoulakis M, Schuster HS and Wheeler JR, 2019, Historical control data for the interpretation of ecotoxicity data: are we missing a trick? *Ecotoxicology* 28(10): 1198–1209, DOI: 10.1007/s10646-019-02128-9.

Burns MJ, Nixon GJ, Foy CA and Harris N, 2005, Standardisation of data from real-time quantitative PCR methods – evaluation of outliers and comparison of calibration curves. *BMC Biotechnology* 5(1): 31, DOI: 10.1186/1472-6750-5-31.

Buttino I, 1994, The effect of low concentrations of phenol and ammonia on egg production rates, faecal pellet production and egg viability of the calanoid copepod *Acartia clausi*. *Marine Biology* 119: 629–634.

Buttino I, Ianora A, Buono S, Vitiello V, Malzone MG, Rico C, Langellotti AL, Sansone G, Gennari L and Miralto A, 2012, Experimental cultivation of the Mediterranean calanoid copepods *Temora stylifera* and *Centropages typicus* in a pilot re-circulating system: Experimental cultivation of the Mediterranean calanoid copepods. *Aquaculture Research* 43(2): 247–259, DOI: 10.1111/j.1365-2109.2011.02822.x.

Buttino I, Pellegrini D, Romano G, Hwang J-S, Liu T-M, Sartori D, Sun C-K, Macchia S and Ianora A, 2011, Study of apoptosis induction using fluorescent and higher harmonic generation microscopy techniques in *Acartia tonsa* nauplii exposed to chronic concentrations of nickel. *Chemistry and Ecology* 27(sup2): 97–104, DOI: 10.1080/02757540.2011.625944.

Buttino I, Vitiello V, Macchia S, Pellegrini D and Gorbi G, 2019, Saggio di sviluppo larvale in presenza di sedimento con il copepode calanoide planctonico *Acartia tonsa* (Dana, 1848). Quaderni di Ecotossicologia. ISPRA, Quaderni – Ricerca Marina n. 13/2019. .

Buttino I, Vitiello V, Macchia S, Scuderi A and Pellegrini D, 2018, Larval development ratio test with the calanoid copepod *Acartia tonsa* as a new bioassay to assess marine sediment quality. *Ecotoxicology and Environmental Safety* 149: 1–9, DOI: 10.1016/j.ecoenv.2017.10.062.

Cairns J and Pratt JR, 1989, The scientific basis of bioassays. *Hydrobiologia* 188: 5–20.

Calliari D, Andersen Borg MC, Thor P, Gorokhova E and Tiselius P, 2008, Instantaneous salinity reductions affect the survival and feeding rates of the co-occurring copepods

Acartia tonsa Dana and *A. clausi* Giesbrecht differently. *Journal of Experimental Marine Biology and Ecology* 362(1): 18–25, DOI: 10.1016/j.jembe.2008.05.005.

Calliari D and Tiselius P, 2005, Feeding and reproduction in a small calanoid copepod: *Acartia clausi* can compensate quality with quantity. *Marine Ecology Progress Series* 298: 241–250, DOI: 10.3354/meps298241.

Camatti E, Pansera M and Bergamasco A, 2019, The Copepod *Acartia tonsa* Dana in a Microtidal Mediterranean Lagoon: History of a Successful Invasion. *Water* 11(6): 1200, DOI: 10.3390/w11061200.

Campanucci VA, Krishnaswamy A and Cooper E, 2008, Mitochondrial Reactive Oxygen Species Inactivate Neuronal Nicotinic Acetylcholine Receptors and Induce Long-Term Depression of Fast Nicotinic Synaptic Transmission. *Journal of Neuroscience* 28(7): 1733–1744, DOI: 10.1523/JNEUROSCI.5130-07.2008.

Carotenuto Y, Esposito F, Pisano F, Lauritano C, Perna M, Miralto A and Ianora A, 2012, Multi-generation cultivation of the copepod *Calanus helgolandicus* in a re-circulating system. *Journal of Experimental Marine Biology and Ecology* 418–419: 46–58, DOI: 10.1016/j.jembe.2012.03.014.

Carotenuto Y, Vitiello V, Gallo A, Libralato G, Trifuoggi M, Toscanesi M, Lofrano G, Esposito F and Buttino I, 2020, Assessment of the relative sensitivity of the copepods *Acartia tonsa* and *Acartia clausi* exposed to sediment-derived elutriates from the Bagnoli-Coroglio industrial area. *Marine Environmental Research* 155: 104878, DOI: 10.1016/j.marenvres.2020.104878.

Carson R, 1962, *Silent Spring*. US: Houghton Mifflin.

Casals E, Barrena R, García A, González E, Delgado L, Busquets-Fité M, Font X, Arbiol J, Glatzel P, Kvashnina K, Sánchez A and Puntes V, 2014, Programmed Iron Oxide Nanoparticles Disintegration in Anaerobic Digesters Boosts Biogas Production. *Small* 10(14): 2801–2808, DOI: 10.1002/smll.201303703.

Castellani C and Lucas IAN, 2003, Seasonal variation in egg morphology and hatching success in the calanoid copepods Temora longicornis, *Acartia clausi* and *Centropages hamatus*. *Journal of Plankton Research* 25(5): 527–537, DOI: 10.1093/plankt/25.5.527.

Castro-Longoria E, 2003, Egg production and hacthing success of four *Acartia* species under different temperature and salinity regimes. *Journal of Crustacean Biology* 23(2): 11.

Cempel M and Nikel G, 2006, Nickel: A Review of Its Sources and Environmental Toxicology. 8.

Chao J, Liu J, Yu S, Feng Y, Tan Z, Liu R and Yin Y, 2011, Speciation Analysis of Silver Nanoparticles and Silver Ions in Antibacterial Products and Environmental Waters via Cloud Point Extraction-Based Separation. *Analytical Chemistry* 83(17): 6875–6882, DOI: 10.1021/ac201086a.

Choi B-S, Kim D-H, Kim M-S, Park JC, Lee YH, Kim H-J, Jeong C-B, Hagiwara A, Souissi S and Lee J-S, 2021, The genome of the European estuarine calanoid copepod *Eurytemora affinis*: Potential use in molecular ecotoxicology. *Marine Pollution Bulletin* 166: 112190, DOI: 10.1016/j.marpolbul.2021.112190.

Committee on Applications of Toxicogenomic Technologies to Predictive Toxicology, 2007, Applications of Toxicogenomic Technologies to Predictive Toxicology and Risk Assessment. .

Conesa A, Madrigal P, Tarazona S, Gomez-Cabrero D, Cervera A, McPherson A, Szcześniak MW, Gaffney DJ, Elo LL, Zhang X and Mortazavi A, 2016, A survey of best practices for RNA-seq data analysis. *Genome Biology* 17(1): 13, DOI: 10.1186/s13059-016-0881-8.

Corsi I, Bellingeri A, Eliso MC, Grassi G, Liberatori G, Murano C, Sturba L, Vannuccini ML and Bergami E, 2021, Eco-Interactions of Engineered Nanomaterials in the Marine Environment: Towards an Eco-Design Framework. *Nanomaterials* 11(8): 1903, DOI: 10.3390/nano11081903.

Corsi I, Cherr GN, Lenihan HS, Labille J, Hassellov M, Canesi L, Dondero F, Frenzilli G, Hristozov D, Puntes V, Della Torre C, Pinsino A, Libralato G, Marcomini A, Sabbioni E and Matranga V, 2014, Common Strategies and Technologies for the Ecosafety Assessment and Design of Nanomaterials Entering the Marine Environment. *ACS Nano* 8(10): 9694–9709, DOI: 10.1021/nn504684k.

Coskun A, 2006, Westgard multirule for calculated laboratory tests. *Clinical Chemistry and Laboratory Medicine (CCLM)* 44(10), DOI: 10.1515/CCLM.2006.233.

D'Agostino A and Finney C, 1974, The effect of copper and cadmium on the development of *Tigriopus japonicus*. *Pollution and Physiology of Marine Organisms* 445–463.

Dahms H-U, Lee SH, Huang D-J, Chen W-Y and Hwang J-S, 2017, The challenging role of life cycle monitoring: evidence from bisphenol A on the copepod *Tigriopus japonicus*. *Hydrobiologia* 784(1): 81–91, DOI: 10.1007/s10750-016-2859-7.

Damasceno ÉP, de Figuerêdo LP, Pimentel MF, Loureiro S and Costa-Lotufo LV, 2017, Prediction of toxicity of zinc and nickel mixtures to *Artemia sp*. at various salinities: From additivity to antagonism. *Ecotoxicology and Environmental Safety* 142: 322–329, DOI: 10.1016/j.ecoenv.2017.04.020.

Das S, Ouddane B, Hwang J-S and Souissi S, 2020, Intergenerational effects of resuspended sediment and trace metal mixtures on life cycle traits of a pelagic copepod. *Environmental Pollution* 267: 115460, DOI: 10.1016/j.envpol.2020.115460.

DeForest DK and Schlekat CE, 2013, Species sensitivity distribution evaluation for chronic nickel toxicity to marine organisms: Nickel Species Sensitivity Distribution Evaluation. *Integrated Environmental Assessment and Management* 9(4): 580–589, DOI: 10.1002/ieam.1419.

deMayo JA, Girod A, Sasaki MC and Dam HG, 2021, Adaptation to simultaneous warming and acidification carries a thermal tolerance cost in a marine copepod. *Biology Letters* 17: 6.

Deville S, Baré B, Piella J, Tirez K, Hoet P, Monopoli MP, Dawson KA, Puntes VF and Nelissen I, 2016, Interaction of gold nanoparticles and nickel(II) sulfate affects dendritic cell maturation. *Nanotoxicology* 10(10): 1395–1403, DOI: 10.1080/17435390.2016.1221476.

Di Capua I, D'Angiolo R, Piredda R, Minucci C, Boero F, Uttieri M and Carotenuto Y, 2022, From Phenotypes to Genotypes and Back: Toward an Integrated Evaluation of Biodiversity in Calanoid Copepods. *Frontiers in Marine Science* 9: 833089, DOI: 10.3389/fmars.2022.833089.

DM 173, 2016, Decreto Ministeriale. Ministero dell'Ambiente e della Tutela del Territorio e del Mare, Supplemento ordinario alla Gazzetta Ufficiale, n. 208 6 settembre 2016. Serie generale. Regolamento recante modalità e criteri tecnici per l'autorizzazione all'immersione in mare dei materiali di escavo di fondali marini, p. 77. .

Doyle JJ, Ward JE and Mason R, 2015, An examination of the ingestion, bioaccumulation, and depuration of titanium dioxide nanoparticles by the blue mussel (*Mytilus edulis*) and the eastern oyster (*Crassostrea virginica*). *Marine Environmental Research* 110: 45–52, DOI: 10.1016/j.marenvres.2015.07.020.

Drexler KE, 1981, Molecular engineering: An approach to the development of general capabilities for molecular manipulation. *Proceedings of the National Academy of Sciences* 78(9): 5275–5278, DOI: 10.1073/pnas.78.9.5275.

Drillet G, Frouël S, Sichlau MH, Jepsen PM, Højgaard JK, Joarder AK and Hansen BW, 2011a, Status and recommendations on marine copepod cultivation for use as live feed. *Aquaculture* 315(3–4): 155–166, DOI: 10.1016/j.aquaculture.2011.02.027.

Drillet G, Goetze E, Jepsen PM, Højgaard JK and Hansen BW, 2008, Strain-specific vital rates in four *Acartia tonsa* cultures, I: Strain origin, genetic differentiation and egg survivorship. *Aquaculture* 280(1–4): 109–116, DOI: 10.1016/j.aquaculture.2008.04.005.

Drillet G, Hansen BW and Kiørboe T, 2011b, Resting egg production induced by food limitation in the calanoid copepod *Acartia tonsa*. *Limnology and Oceanography* 56(6): 2064–2070, DOI: 10.4319/lo.2011.56.6.2064.

Drillet G, Rais M, Novac A, Jepsen PM, Mahjoub M-S and Hansen BW, 2014, Total egg harvest by the calanoid copepod *Acartia tonsa* (Dana) in intensive culture - effects of high stocking densities on daily egg harvest and egg quality. *Aquaculture Research* 46(12): 3028–3039, DOI: 10.1111/are.12459.

Dutz J, 1998, Repression of fecundity in the neritic copepod *Acartia clausi* exposed to the toxic dinoflagellate *Alexandrium lusitanicum*:relationship between feeding and egg

production. *Marine Ecology Progress Series* 175: 97–107, DOI: 10.3354/meps175097.

EC CR, 2008, Directive 2008/105/EC of the European Parliament and of the Council of 16 December 2008 on environmental quality standards in the field of water policy, amending and subsequently repealing Council Directives 82/176/EEC, 83/513/EEC, 84/156/EEC, 84/491/EEC, 86/280/EEC and amending Directive 2000/60. *Off. J. Eur. Communities* 50: 84–97.

Eder J, Hommel U, Cumin F, Martoglio B and Gerhartz B, 2007, Aspartic Proteases in Drug Discovery. *Current Pharmaceutical Design* 13(3): 271–285, DOI: 10.2174/138161207779313560.

Eisler R, 1998, Nickel hazards to fish, wildlife, and invertebrates: a synoptic review. *Contaminant Hazard Reviews Report* 34.

Eissa ME, 2016, Shewhart Control Chart in Microbiological Quality Control of Purified Water and its Use in Quantitative Risk Evaluation. *Pharmaceutical and Biosciences Journal* 45–51, DOI: 10.20510/ukjpb/4/i1/87845.

Environment and Climate Change Canada, 2019, Biological test method: reference method for determining acute lethality using *Acartia tonsa*. Reference Method STB 1/RM/60 June 2019. .

Eyun S, Soh HY, Posavi M, Munro JB, Hughes DST, Murali SC, Qu J, Dugan S, Lee SL, Chao H, Dinh H, Han Y, Doddapaneni H, Worley KC, Muzny DM, Park E-O, Silva JC, Gibbs RA, Richards S and Lee CE, 2017, Evolutionary History of Chemosensory-Related Gene Families across the Arthropoda. *Molecular Biology and Evolution* 34(8): 1838–1862, DOI: 10.1093/molbev/msx147.

Fabricius A-L, Duester L, Meermann B and Ternes TA, 2014, ICP-MS-based characterization of inorganic nanoparticles—sample preparation and off-line fractionation strategies. *Analytical and Bioanalytical Chemistry* 406(2): 467–479, DOI: 10.1007/s00216-013-7480-2.

Fang Z and Cui X, 2011, Design and validation issues in RNA-seq experiments. *Briefings in Bioinformatics* 12(3): 280–287, DOI: 10.1093/bib/bbr004.

Faraponova O, Giacco E, Biandolino F, Prato E, Del Prete F, Valenti A, Sarcina S, Pasteris A, Montecavalli A, Comin S, Cesca C, Francese M, Cigar M, Piazza V, Falleni F and Lacchetti I, 2016, *Tigriopus fulvus*: The interlaboratory comparison of the acute toxicity test. *Ecotoxicology and Environmental Safety* 124: 309–314, DOI: 10.1016/j.ecoenv.2015.10.013.

Férard J-F, 2013, Ecotoxicology: Historical Overview and Perspectives. *Encyclopedia of aquatic ecotoxicology*. Springer: Dordrecht ; New York, 377–386.

Férard J-F and Blaise C (eds), 2013, Preface. *Encyclopedia of aquatic ecotoxicology*. Springer: Dordrecht ; New York, xi–xiii.

Feynman RP, 1959, There's plenty of room at the bottom. *Talk delivered at the annual meeting of the American Physical Society, transcribed online at http://www.zyvex.com/nanotech/feynman.html*.

Gallo A, Boni R, Buttino I and Tosti E, 2016, Spermiotoxicity of nickel nanoparticles in the marine invertebrate *Ciona intestinalis* (ascidians). *Nanotoxicology* 10(8): 1096–1104, DOI: 10.1080/17435390.2016.1177743.

Garcia-Carreño F, Navarrete del Toro M and Muhlia-Almazan A, 2014, The role of lysosomal cysteine proteases in crustacean immune response. *Invertebrate Survival Journal* 11(1).

Garner KL, Suh S and Keller AA, 2017, Assessing the Risk of Engineered Nanomaterials in the Environment: development and application of the nanoFate model. *Environmental Science & Technology*.

Gaudy R, Cervetto G and Pagano M, 2000, Comparison of the metabolism of *Acartia clausi* and *A. tonsa*: influence of temperature and salinity. *Journal of Experimental Marine Biology and Ecology* 247(1): 51–65, DOI: 10.1016/S0022-0981(00)00139-8.

Gaudy R, Moraitou Apostolopoulou M, Pagano M and Saint-Jean L, 1989, Salinity as a decisive factor in the length of cephalothorax of *Acartia clausi* from three different areas (Greece and Ivory Coast). *Rapp. Comm. Int. Mer. Mediterr.* 31: 233.

Gaudy R and Viñas M, 1985, Première signalization en Méditerranée du copépode pélagique *Acartia tonsa*. *Rapp Comm Int Mer Médit* 29(9): 227–229.

Ghobashy MM, Elkodous MA, Shabaka SH, Younis SA, Alshangiti DM, Madani M, Al-Gahtany SA, Elkhatib WF, Noreddin AM, Nady N and El-Sayyad GS, 2021, An overview of methods for production and detection of silver nanoparticles, with emphasis on their fate and toxicological effects on human, soil, and aquatic environment. *Nanotechnology Reviews* 10(1): 954–977, DOI: 10.1515/ntrev-2021-0066.

Giesbrecht VW, 1892, Systematik und Faunistik der pelagischen Copepoden des Golfes von Neapel und der angrenzenden Meeres-Abschnitte. .

Goerke H, Weber K, Bornemann H, Ramdohr S and Plötz J, 2004, Increasing levels and biomagnification of persistent organic pollutants (POPs) in Antarctic biota. *Marine Pollution Bulletin* 48(3–4): 295–302, DOI: 10.1016/j.marpolbul.2003.08.004.

Gomes SIL, Roca CP, Scott-Fordsmand JJ and Amorim MJB, 2019, High-throughput transcriptomics: Insights into the pathways involved in (nano) nickel toxicity in a key invertebrate test species. *Environmental Pollution* 245: 131–140, DOI: 10.1016/j.envpol.2018.10.123.

Gong N, Shao K, Feng W, Lin Z, Liang C and Sun Y, 2011, Biotoxicity of nickel oxide nanoparticles and bio-remediation by microalgae *Chlorella vulgaris*. *Chemosphere* 83(4): 510–516, DOI: 10.1016/j.chemosphere.2010.12.059.

Gonzalez JG, 1974, Critical thermal maxima and upper lethal temperatures for the calanoid copepods *Acartia tonsa* and *A. clausi*. *Mar. Biol.* 27: 219–223.

Gopalakrishnan Nair PM and Chung IM, 2015, Alteration in the expression of antioxidant and detoxification genes in *Chironomus riparius* exposed to zinc oxide nanoparticles. *Comparative Biochemistry and Physiology Part B: Biochemistry and Molecular Biology* 190: 1–7, DOI: 10.1016/j.cbpb.2015.08.004.

Gorbi G, Invidia M, Savorelli F, Faraponova O, Giacco E, Cigar M, Buttino I, Leoni T, Prato E, Lacchetti I and Sei S, 2012, Standardized methods for acute and semichronic toxicity tests with the copepod *Acartia tonsa*. *Environmental Toxicology and Chemistry* 31(9): 2023–2028, DOI: 10.1002/etc.1909.

Gorbi S, Virno Lamberti C, Notti A, Benedetti M, Fattorini D, Moltedo G and Regoli F, 2008, An ecotoxicological protocol with caged mussels, *Mytilus galloprovincialis*, for monitoring the impact of an offshore platform in the Adriatic sea. *Marine Environmental Research* 65(1): 34–49, DOI: 10.1016/j.marenvres.2007.07.006.

Gottschalk F, Sun T and Nowack B, 2013, Environmental concentrations of engineered nanomaterials: Review of modeling and analytical studies. *Environmental Pollution* 181: 287–300, DOI: 10.1016/j.envpol.2013.06.003.

Götz S, García-Gómez JM, Terol J, Williams TD, Nagaraj SH, Nueda MJ, Robles M, Talón M, Dopazo J and Conesa A, 2008, High-throughput functional annotation and data mining with the Blast2GO suite. *Nucleic Acids Research* 36(10): 3420–3435, DOI: 10.1093/nar/gkn176.

Govaerts A, Verhaert V, Covaci A, Jaspers VLB, Berg OK, Addo-Bediako A, Jooste A and Bervoets L, 2018, Distribution and bioaccumulation of POPs and mercury in the Ga-Selati River (South Africa) and the rivers Gudbrandsdalslågen and Rena (Norway). *Environment International* 121: 1319–1330, DOI: 10.1016/j.envint.2018.10.058.

Grabherr MG, Haas BJ, Yassour M, Levin JZ, Thompson DA, Amit I, Adiconis X, Fan L, Raychowdhury R, Zeng Q, Chen Z, Mauceli E, Hacohen N, Gnirke A, Rhind N, di Palma F, Birren BW, Nusbaum C, Lindblad-Toh K, Friedman N and Regev A, 2011, Full-length transcriptome assembly from RNA-Seq data without a reference genome. *Nature Biotechnology* 29(7): 644–652, DOI: 10.1038/nbt.1883.

Graham ML, Renner VE and Blukacz-Richards EA, 2013, Ecological Risk Assessment. *Encyclopedia of aquatic ecotoxicology*. Springer: Dordrecht ; New York, 305–315.

Grassi G, Gabellieri E, Cioni P, Paccagnini E, Faleri C, Lupetti P, Corsi I and Morelli E, 2020, Interplay between extracellular polymeric substances (EPS) from a marine diatom and model nanoplastic through eco-corona formation. *Science of The Total Environment* 725: 138457, DOI: 10.1016/j.scitotenv.2020.138457.

Green AS, Chandler TG and Piegorsch WW, 1996, Life-stage-specific toxicity of sediment-associated chlorpyrifos to a marine, infaunal copepod. *Environmental Toxicology and Chemistry* 15(7): 1182–1188, DOI: 10.1002/etc.5620150725.

Guan Z-Z, Zhang X, Mousavi M, Tian J-Y, Unger C and Nordberg A, 2001, Reduced expression of neuronal nicotinic acetylcholine receptors during the early stages of damage by oxidative stress in PC12 cells. *Journal of Neuroscience Research* 66(4): 551–558, DOI: 10.1002/jnr.1245.

Guillard RRL, 1975, Culture of phytoplankton for feeding marine invertebrates. *Culture of Marine Animals, Plenum Press, New York* 26–60.

Guisande C, Frangópulos M, Carotenuto Y, Maneiro I, Riveiro I and Vergara A, 2002, Fate of paralytic shellfish poisoning toxins ingested by the copepod *Acartia clausi*. *Marine Ecology Progress Series* 240: 105–115, DOI: 10.3354/meps240105.

Hadjidemetriou M and Kostarelos K, 2017, Evolution of the nanoparticle corona. *Nature Nanotechnology* 12(4): 288–290, DOI: 10.1038/nnano.2017.61.

Han J, Park JS, Park Y, Lee J, Shin HH and Lee K-W, 2021, Effects of paralytic shellfish poisoning toxin-producing dinoflagellate *Gymnodinium catenatum* on the marine copepod *Tigriopus japonicus*. *Marine Pollution Bulletin* 163: 111937, DOI: 10.1016/j.marpolbul.2020.111937.

Handy RD, Cornelis G, Fernandes T, Tsyusko O, Decho A, Sabo-Attwood T, Metcalfe C, Steevens JA, Klaine SJ, Koelmans AA and Horne N, 2012, Ecotoxicity test methods for engineered nanomaterials: Practical experiences and recommendations from the bench: Ecotoxicity test methods for engineered nanomaterials. *Environmental Toxicology and Chemistry* 31(1): 15–31, DOI: 10.1002/etc.706.

Hang MN, Hudson-Smith NV, Clement PL, Zhang Y, Wang C, Haynes CL and Hamers RJ, 2018, Influence of Nanoparticle Morphology on Ion Release and Biological Impact of Nickel Manganese Cobalt Oxide (NMC) Complex Oxide Nanomaterials. *ACS Applied Nano Materials* 1(4): 1721–1730, DOI: 10.1021/acsanm.8b00187.

Hansen BW, Buttino I, Cunha ME and Drillet G, 2016, Embryonic cold storage capability from seven strains of *Acartia spp*. isolated in different geographical areas. *Aquaculture* 457: 131–139, DOI: 10.1016/j.aquaculture.2016.02.024.

He X, Fu P, Aker WG and Hwang H-M, 2018, Toxicity of engineered nanomaterials mediated by nano–bio–eco interactions. *Journal of Environmental Science and Health, Part C* 36(1): 21–42, DOI: 10.1080/10590501.2017.1418793.

Heijerick DH and Van Sprang PA, 2008, Determination of Reasonable Worst Case (RWC) Ambient PEC Concentrations for Nickel in the Marine Environment. Final Report. *Nickel Producers Environmental Research* 18.

Holmes LA, Turner A and Thompson RC, 2014, Interactions between trace metals and plastic production pellets under estuarine conditions. *Marine Chemistry* 167: 25–32, DOI: 10.1016/j.marchem.2014.06.001.

Holste L, Peck MA and John MAS, 2004, The influence of temperature, salinity and feeding history on population characteristics of Baltic *Acartia tonsa*: Egg production, hatching success and cohort development. 21.

Hook SE, Osborn HL, Spadaro DA and Simpson SL, 2014, Assessing mechanisms of toxicant response in the amphipod *Melita plumulosa* through transcriptomic profiling. *Aquatic Toxicology* 146: 247–257, DOI: 10.1016/j.aquatox.2013.11.001.

Hou J, Liu H, Wang L, Duan L, Li S and Wang X, 2018, Molecular Toxicity of Metal Oxide Nanoparticles in *Danio rerio*. *Environmental Science & Technology* 52(14): 7996–8004, DOI: 10.1021/acs.est.8b01464.

Huntley M, Sykes P, Rohan S and Marin V, 1986, Chemically-mediated rejection of dinoflagellate prey by the copepods *Calanus pacificus* and *Paracalanus parvus*: mechanism, occurrence and significance. *Marine Ecology Progress Series* 28: 105–120, DOI: 10.3354/meps028105.

Hylland K, 2006, Polycyclic Aromatic Hydrocarbon (PAH) Ecotoxicology in Marine Ecosystems. *Journal of Toxicology and Environmental Health, Part A* 69(1–2): 109–123, DOI: 10.1080/15287390500259327.

Ianora A, Miralto A and Halsband-Lenk C, 2007, Reproduction, hatching success, and early naupliar survival in *Centropages typicus*. *Progress in Oceanography* 72(2–3): 195–213, DOI: 10.1016/j.pocean.2007.01.009.

Ianora A, Miralto A, Poulet SA, Carotenuto Y, Buttino I, Romano G, Casotti R, Pohnert G, Wichard T, Colucci-D'Amato L, Terrazzano G and Smetacek V, 2004, Aldehyde suppression of copepod recruitment in blooms of a ubiquitous planktonic diatom. *Nature* 429(6990): 403–407, DOI: 10.1038/nature02526.

ICRAM, 2006, Istituto Centrale per la Ricerca Scientifica e Tecnologica Applicata al Mare. Avancini, M., Cicero, A. M., Di Girolamo, I., Innamorati, M., Magaletti, E., and Sertorio Zunini, T. Guida al riconoscimento del plancton neritico dei mari italiani. Volume II – Zooplancton neritico – Tavole. https://www.isprambiente.gov.it/it/pubblicazioni/manuali-e-linee-guida/guidaal-riconoscimento-del-plancton-dei-mari. .

Iida R, Yasuda T, Tsubota E, Takatsuka H, Masuyama M, Matsuki T and Kishi K, 2003, M-LP, Mpv17-like Protein, Has a Peroxisomal Membrane Targeting Signal Comprising a Transmembrane Domain and a Positively Charged Loop and Up-regulates Expression of the Manganese Superoxide Dismutase Gene. *Journal of Biological Chemistry* 278(8): 6301–6306, DOI: 10.1074/jbc.M210886200.

Iida R, Yasuda T, Tsubota E, Takatsuka H, Masuyama M, Matsuki T and Kishi K, 2005, A novel alternative spliced Mpv17-like protein isoform localizes in cytosol and is

expressed in a kidney- and adult-specific manner. *Experimental Cell Research* 302(1): 22–30, DOI: 10.1016/j.yexcr.2004.08.027.

Imai H and Nakagawa Y, 2003, Biological significance of phospholipid hydroperoxide glutathione peroxidase (PHGPx, GPx4) in mammalian cells. *Free Radical Biology and Medicine* 34(2): 145–169, DOI: 10.1016/S0891-5849(02)01197-8.

International Agency for Research on Cancer, 2020, *World Cancer Report: Cancer Research for Cancer Prevention*. IARC: Place of publication not identified.

Invidia M, Sei S and Gorbi G, 2004, Survival of the copepod *Acartia tonsa* following egg exposure to near anoxia and to sulfide at different pH values. *Marine Ecology Progress Series* 276: 187–196, DOI: 10.3354/meps276187.

ISO, 1991, International Organization for Standardization. Shewhart control charts. ISO 8258:1991. ISO, Genève, Switzerland. .

ISO, 1999, International Organization for Standardization. Water quality – Determination of acute lethal toxicity to marine copepods (Copepoda, Crustacea). Draft International Standard ISO/DIS 14669. ISO, Genève, Switzerland. .

ISO, 2007, International Organization for Standardization. Control charts — Part 1: General guidelines. ISO 7870-1:2007. ISO, Genève, Switzerland. .

ISO, 2015, International Organization for Standardization. Water Quality – Calanoid Copepod Development Test with *Acartia tonsa*. ISO/FDIS 16778. Calanoid Copepod Early-life Stage Test with Acartia tonsa. ISO, Genève, Switzerland. .

Jarvis TA, Miller RJ, Lenihan HS and Bielmyer GK, 2013, Toxicity of ZnO nanoparticles to the copepod *Acartia tonsa*, exposed through a phytoplankton diet. *Environmental Toxicology and Chemistry* 32(6): 1264–1269, DOI: 10.1002/etc.2180.

Jeong C-B, Kim B-M, Choi H-J, Baek I, Souissi S, Park HG, Lee J-S and Rhee J-S, 2015, Genome-wide identification and transcript profile of the whole cathepsin superfamily in the intertidal copepod *Tigriopus japonicus*. *Developmental & Comparative Immunology* 53(1): 1–12, DOI: 10.1016/j.dci.2015.06.011.

Jeong C-B, Lee B-Y, Choi B-S, Kim M-S, Park JC, Kim D-H, Wang M, Park HG and Lee J-S, 2020, The genome of the harpacticoid copepod *Tigriopus japonicus*: Potential for its use in marine molecular ecotoxicology. *Aquatic Toxicology* 222: 105462, DOI: 10.1016/j.aquatox.2020.105462.

Jiang J-L, Wang G-Z, Mao M-G, Wang K-J, Li S-J and Zeng C-S, 2013, Differential gene expression profile of the calanoid copepod, *Pseudodiaptomus annandalei*, in response to nickel exposure. *Comparative Biochemistry and Physiology Part C: Toxicology & Pharmacology* 157(2): 203–211, DOI: 10.1016/j.cbpc.2012.11.001.

Jørgensen TS, Petersen B, Petersen HCB, Browne PD, Prost S, Stillman JH, Hansen LH and Hansen BW, 2019, The Genome and mRNA Transcriptome of the Cosmopolitan

Calanoid Copepod *Acartia tonsa* Dana Improve the Understanding of Copepod Genome Size Evolution. *Genome Biology and Evolution* 11(5): 1440–1450, DOI: 10.1093/gbe/evz067.

Kadiene EU, Meng P-J, Hwang J-S and Souissi S, 2019, Acute and chronic toxicity of cadmium on the copepod *Pseudodiaptomus annandalei*: A life history traits approach. *Chemosphere* 233: 396–404, DOI: 10.1016/j.chemosphere.2019.05.220.

Kadiene EU, Ouddane B, Gong H-Y, Hwang J-S and Souissi S, 2022, Multigenerational study of life history traits, bioaccumulation, and molecular responses of *Pseudodiaptomus annandalei* to cadmium. *Ecotoxicology and Environmental Safety* 230: 113171, DOI: 10.1016/j.ecoenv.2022.113171.

Kadiene EU, Ouddane B, Gong H-Y, Kim M-S, Lee J-S, Pan Y-J, Hwang J-S and Souissi S, 2020, Differential gene expression profile of male and female copepods in response to cadmium exposure. *Ecotoxicology and Environmental Safety* 204: 111048, DOI: 10.1016/j.ecoenv.2020.111048.

Kanold JM, Wang J, Brümmer F and Šiller L, 2016, Metallic nickel nanoparticles and their effect on the embryonic development of the sea urchin *Paracentrotus lividus*. *Environmental Pollution* 212: 224–229, DOI: 10.1016/j.envpol.2016.01.050.

Klaine SJ, Edgington A and Seda B, 2013, Nanomaterials in the Environment. *Encyclopedia of aquatic ecotoxicology*. Springer: Dordrecht ; New York, 767–779.

Krause KE, Dinh KV and Nielsen TG, 2017, Increased tolerance to oil exposure by the cosmopolitan marine copepod *Acartia tonsa. Science of The Total Environment* 607–608: 87–94, DOI: 10.1016/j.scitotenv.2017.06.139.

Kulkarni D, Gergs A, Hommen U, Ratte HT and Preuss TG, 2013, A plea for the use of copepods in freshwater ecotoxicology. *Environmental Science and Pollution Research* 20(1): 75–85, DOI: 10.1007/s11356-012-1117-4.

Langmead B, Trapnell C, Pop M and Salzberg SL, 2009, Ultrafast and memory-efficient alignment of short DNA sequences to the human genome. *Genome Biology* 10(3): R25, DOI: 10.1186/gb-2009-10-3-r25.

Lauritano C, Borra M, Carotenuto Y, Biffali E, Miralto A, Procaccini G and Ianora A, 2011a, First molecular evidence of diatom effects in the copepod *Calanus helgolandicus*. *Journal of Experimental Marine Biology and Ecology* 404(1–2): 79–86, DOI: 10.1016/j.jembe.2011.05.009.

Lauritano C, Borra M, Carotenuto Y, Biffali E, Miralto A, Procaccini G and Ianora A, 2011b, Molecular Evidence of the Toxic Effects of Diatom Diets on Gene Expression Patterns in Copepods. *PLoS ONE* 6(10): e26850, DOI: 10.1371/journal.pone.0026850.

Lauritano C, Carotenuto Y and Roncalli V, 2021, Glutathione S-Transferases in Marine Copepods. *Journal of Marine Science and Engineering* 9(9): 1025, DOI: 10.3390/jmse9091025.

LeBlanc GA, 2007, Crustacean endocrine toxicology: a review. *Ecotoxicology* 16(1): 61–81, DOI: 10.1007/s10646-006-0115-z.

Lee B-Y, Lee M-C, Jeong C-B, Kim H-J, Hagiwara A, Souissi S, Han J and Lee J-S, 2018, RNA-Seq-based transcriptome profiling and expression of 16 cytochrome P450 genes in the benzo[α]pyrene-exposed estuarine copepod *Eurytemora affinis*. *Comparative Biochemistry and Physiology Part D: Genomics and Proteomics* 28: 142–150, DOI: 10.1016/j.cbd.2018.08.002.

Lee DR, 1980, Reference toxicants in quality control of aquatic bioassays. *Aquatic Invertebrate Bioassays* 715: 188–199.

Lee K-W, Hwang D-S, Rhee J-S, Ki J-S, Park HG, Ryu J-C, Raisuddin S and Lee J-S, 2008a, Expression of glutathione S-transferase (GST) genes in the marine copepod *Tigriopus japonicus* exposed to trace metals. *Aquatic Toxicology* 89(3): 158–166, DOI: 10.1016/j.aquatox.2008.06.011.

Lee K-W, Hwang D-S, Rhee J-S, Ki J-S, Park HG, Ryu J-C, Raisuddin S and Lee J-S, 2008b, Molecular cloning, phylogenetic analysis and developmental expression of a vitellogenin (Vg) gene from the intertidal copepod *Tigriopus japonicus*. *Comparative Biochemistry and Physiology Part B: Biochemistry and Molecular Biology* 150(4): 395–402, DOI: 10.1016/j.cbpb.2008.04.009.

Lee M-C, Choi B-S, Kim M-S, Yoon D-S, Park JC, Kim S and Lee J-S, 2020, An improved genome assembly and annotation of the Antarctic copepod *Tigriopus kingsejongensis* and comparison of fatty acid metabolism between *T. kingsejongensis* and the temperate copepod *T. japonicus*. *Comparative Biochemistry and Physiology Part D: Genomics and Proteomics* 35: 100703, DOI: 10.1016/j.cbd.2020.100703.

Lee WY, 1977, Some laboratory cultured crustaceans for marine pollution studies. *Marine Pollution Bulletin* 8(11): 258–259, DOI: 10.1016/0025-326X(77)90324-1.

Lee WY and McAlice BJ, 1979, Seasonal Succession and Breeding Cycles of Three Species of *Acartia* (Copepoda: Calanoida) in a Maine Estuary. *Estuaries* 2(4): 228, DOI: 10.2307/1351569.

Lee Y-M, Park T-J, Jung S-O, Seo JS, Park HG, Hagiwara A, Yoon Y-D and Lee J-S, 2006, Cloning and characterization of glutathione S-transferase gene in the intertidal copepod *Tigriopus japonicus* and its expression after exposure to endocrine-disrupting chemicals. *Marine Environmental Research* 62: S219–S223, DOI: 10.1016/j.marenvres.2006.04.050.

Leonard EM, Barcarolli I, Silva KR, Wasielesky W, Wood CM and Bianchini A, 2011, The effects of salinity on acute and chronic nickel toxicity and bioaccumulation in two euryhaline crustaceans: *Litopenaeus vannamei* and *Excirolana armata*. *Comparative Biochemistry and Physiology Part C: Toxicology & Pharmacology* 154(4): 409–419, DOI: 10.1016/j.cbpc.2011.07.011.

Lesueur T, Boulangé-Lecomte C, Xuereb B, Budzinski H, Cachot J, Vicquelin L, Giusti-Petrucciani N, Marie S, Petit F and Forget-Leray J, 2013, Development of a larval bioassay using the calanoid copepod, *Eurytemora affinis* to assess the toxicity of sediment-bound pollutants. *Ecotoxicology and Environmental Safety* 94: 60–66, DOI: 10.1016/j.ecoenv.2013.04.025.

Leung KMY, Morritt D, Wheeler JR, Whitehouse P and Sorokin N, 2001, Can Viewpoint Saltwater Toxicity be Predicted from Freshwater Data? *Marine Pollution Bulletin* 42(11): 7.

Levey S and Jennings ER, 1950, The use of control charts in the clinical laboratory. *American Journal of Clinical Pathology* 20: 1059–1066.

Lewis SS and Keller SJ, 2009, Identification of copper-responsive genes in an early life stage of the fathead minnow *Pimephales promelas*. *Ecotoxicology* 18(3): 281–292, DOI: 10.1007/s10646-008-0280-3.

Li X, Xu Z, Zhou G, Lin H, Zhou J, Zeng Q, Mao Z and Gu X, 2015, Molecular characterization and expression analysis of five chitinases associated with molting in the Chinese mitten crab, *Eriocheir sinensis*. *Comparative Biochemistry and Physiology Part B: Biochemistry and Molecular Biology* 187: 110–120, DOI: 10.1016/j.cbpb.2015.05.007.

Lindeque PK, Boyer S and Bonnet D, 2013, A molecular method for the identification of resting eggs of acartiid copepods in the Thau lagoon, France. *Marine Biology* 160(3): 737–742, DOI: 10.1007/s00227-012-2108-1.

Madoui M-A, Poulain J, Sugier K, Wessner M, Noel B, Berline L, Labadie K, Cornils A, Blanco-Bercial L, Stemmann L, Jamet J-L and Wincker P, 2017, New insights into global biogeography, population structure and natural selection from the genome of the epipelagic copepod *Oithona*. *Molecular Ecology*. John Wiley & Sons, Ltd 26(17): 4467–4482, DOI: 10.1111/mec.14214.

Maldonado-Aguayo W, Chávez-Mardones J, Gonçalves AT and Gallardo-Escárate C, 2015, Cathepsin Gene Family Reveals Transcriptome Patterns Related to the Infective Stages of the Salmon Louse *Caligus rogercresseyi*. *PLOS ONE* 10(4): e0123954, DOI: 10.1371/journal.pone.0123954.

Marcus N, Lutz R and Chanton J, 1997, Impact of anoxia and sulfide on the viability of eggs of three planktonic copepods. *Marine Ecology Progress Series* 146: 291–295, DOI: 10.3354/meps146291.

Mazzocchi MG, Dubroca L, García-Comas C, Capua ID and Ribera d'Alcalà M, 2012, Stability and resilience in coastal copepod assemblages: The case of the Mediterranean long-term ecological research at Station MC (LTER-MC). *Progress in Oceanography* 97–100: 135–151, DOI: 10.1016/j.pocean.2011.11.003.

McCarthy E, Cunningham E, Copley L, Jackson D, Johnston D, Dalton JP and Mulcahy G, 2012, Cathepsin L proteases of the parasitic copepod, *Lepeophtheirus salmonis*. *Aquaculture* 356–357: 264–271, DOI: 10.1016/j.aquaculture.2012.05.007.

Medina M, Barata C, Telfer T and Baird DJ, 2002, Age- and Sex-Related Variation in Sensitivity to the Pyrethroid Cypermethrin in the Marine Copepod *Acartia tonsa* Dana. 6.

Miller DD and Marcus NH, 1994, The effects of salinity and temperature on the density and sinking velocity of eggs of the calanoid copepod *Acartia tonsa* Dana. *Journal of Experimental Marine Biology and Ecology* 179(2): 235–252, DOI: 10.1016/0022-0981(94)90117-1.

Miralto A, Barone G, Romano G, Poulet SA, Ianora A, Russo GL, Buttino I, Mazzarella G, Laabir M, Cabrini M and Giacobbe MG, 1999, The insidious effect of diatoms on copepod reproduction. *Nature* 402(6758): 173–176, DOI: 10.1038/46023.

Miri A, Sadat Shakib E, Ebrahimi O and Sharifi-Rad J, 2017, Impacts of Nickel Nanoparticles on Grow Characteristics, Photosynthetic Pigment Content and Antioxidant Activity of *Corianderum sativum* L. *Oriental Journal of Chemistry* 33(3): 1297–1303, DOI: 10.13005/ojc/330329.

Morozova O, Hirst M and Marra MA, 2009, Applications of New Sequencing Technologies for Transcriptome Analysis. 19.

Morris A, Beeram S, Hardaway CJ, Richert JC and Sneddon J, 2012, Use of ground crawfish shells for the removal of chromium in solution. *Microchemical Journal* 105: 2–8, DOI: 10.1016/j.microc.2012.06.009.

Morroni L, Sartori D, Costantini M, Genovesi L, Magliocco T, Ruocco N and Buttino I, 2019, First molecular evidence of the toxicogenetic effects of copper on sea urchin *Paracentrotus lividus* embryo development. *Water Research* 160: 415–423, DOI: 10.1016/j.watres.2019.05.062.

Moss DR, Arce SM, Otoshi CA, Doyle RW and Moss SM, 2007, Effects of inbreeding on survival and growth of Pacific white shrimp *Penaeus (Litopenaeus) vannamei*. *Aquaculture* 272: S30–S37, DOI: 10.1016/j.aquaculture.2007.08.014.

Muñoz A and Costa M, 2012, Elucidating the mechanisms of nickel compound uptake: A review of particulate and nano-nickel endocytosis and toxicity. *Toxicology and Applied Pharmacology* 260(1): 1–16, DOI: 10.1016/j.taap.2011.12.014.

Nasser F and Lynch I, 2016, Secreted protein eco-corona mediates uptake and impacts of polystyrene nanoparticles on *Daphnia magna*. *Journal of Proteomics* 137: 45–51, DOI: 10.1016/j.jprot.2015.09.005.

Naumann E, 1934, Uber die anwendung von *Daphnia magna* Straus als vesuchstier zur experimentellen klarlegung der lenensverhältnisse im wasser. *International Revue der gesamten Hydrobiologie und Hydrographie* 31: 421–431.

Navratilova J, Praetorius A, Gondikas A, Fabienke W, von der Kammer F and Hofmann T, 2015, Detection of Engineered Copper Nanoparticles in Soil Using Single Particle ICP-MS. *International Journal of Environmental Research and Public Health* 12(12): 15756–15768, DOI: 10.3390/ijerph121215020.

Nejstgaard J, Naustvoll L and Sazhin A, 2001, Correcting for underestimation of microzooplankton grazing in bottle incubation experiments with mesozooplankton. *Marine Ecology Progress Series* 221: 59–75, DOI: 10.3354/meps221059.

Newman MC, 2008, Ecotoxicology: The History and Present Directions. *Encyclopedia of Ecology*. Elsevier, 1195–1201, DOI: 10.1016/B978-008045405-4.00431-6.

Nilsson B, Jepsen PM, Bucklin A and Hansen BW, 2018, Environmental Stress Responses and Experimental Handling Artifacts of a Model Organism, the Copepod *Acartia tonsa* (Dana). *Frontiers in Marine Science* 5: 18.

Ning J, Wang M, Li C and Sun S, 2013, Transcriptome Sequencing and De Novo Analysis of the Copepod *Calanus sinicus* Using 454 GS FLX. *PLOS ONE* 8(5): 10.

Nobakht M, Khalesi M, Esmaeili Fereidouni A and Khalili KJ, 2016, Total carotenoids of the copepod *Acartia clausi* Giesbrecht, 1889 from the Caspian Sea at different growth stages fed different microalgal diets. *Crustaceana* 89(3): 291–305, DOI: 10.1163/15685403-00003523.

Oleszczuk P, Jośko I and Skwarek E, 2015, Surfactants decrease the toxicity of ZnO, TiO2 and Ni nanoparticles to *Daphnia magna*. *Ecotoxicology* 24(9): 1923–1932, DOI: 10.1007/s10646-015-1529-2.

Olivotto I, Avella MA, Buttino I, Borroni M, Cutignano A and Carnevali O, 2009, Calanoid copepod administration improves yellow tail clownfish (*Amphiprion clarkii*) larviculture: biochemical and molecular implications. 14.

Olivotto I, Buttino I, Borroni M, Piccinetti CC, Malzone MG and Carnevali O, 2008a, The use of the Mediterranean calanoid copepod *Centropages typicus* in Yellowtail clownfish (*Amphiprion clarkii*) larviculture. *Aquaculture* 284(1–4): 211–216, DOI: 10.1016/j.aquaculture.2008.07.057.

Olivotto I, Capriotti F, Buttino I, Avella AM, Vitiello V, Maradonna F and Carnevali O, 2008b, The use of harpacticoid copepods as live prey for *Amphiprion clarkii* larviculture: Effects on larval survival and growth. *Aquaculture* 274(2–4): 347–352, DOI: 10.1016/j.aquaculture.2007.11.027.

Osachoff H and van Aggelen G, 2013, Ecotoxicogenomics. *Encyclopedia of aquatic ecotoxicology*. Springer: Dordrecht ; New York, 353–362.

Ott FS, Harris RP and O'Hara SCM, 1978, Acute and sublethal toxicity of naphthalene and three methylated derivatives to the estuarine copepod, *Eurytemora affinis*. *Marine Environmental Research* 1(1): 49–58, DOI: 10.1016/0141-1136(78)90013-2.

Padoan E, Romè C and Ajmone-Marsan F, 2017, Bioaccessibility and size distribution of metals in road dust and roadside soils along a peri-urban transect. *Science of The Total Environment* 601–602: 89–98, DOI: 10.1016/j.scitotenv.2017.05.180.

Paffenhöfer GA, 1991, Some characteristics of abundant subtropical copepods in estuarine, shelf and oceanic waters. *Proc. 4th International Conference on Copepoda.* 201–216.

Palza H, Quijada R and Delgado K, 2015, Antimicrobial polymer composites with copper micro- and nanoparticles: Effect of particle size and polymer matrix. *Journal of Bioactive and Compatible Polymers* 30(4): 366–380, DOI: 10.1177/0883911515578870.

Paraskevopoulou V, Triantafyllaki S, Giannikopoulos N and Dassenakis M, 2010, Dissolved and particulate nickel distribution in a coastal marine area affected by geochemical and industrial processes. *Fresenius Environmental Bulletin* 19: 1833–1840.

Payne MF and Rippingale RJ, 2001, Effects of salinity, cold storage and enrichment on the calanoid copepod *Gladioferens imparipes*. *Aquaculture* 201(3–4): 251–262, DOI: 10.1016/S0044-8486(01)00609-3.

Penny C and Adams C, 1863, Fourth report of the royal commission on pollution of rivers in Scotland. *London* 23: 377–391.

Pérez-Portela R and Riesgo A, 2013, Optimizing preservation protocols to extract high-quality RNA from different tissues of echinoderms for next-generation sequencing. *Molecular Ecology Resources* 13(5): 884–889, DOI: 10.1111/1755-0998.12122.

Pfaffl MW, Horgan GW and Dempfle L, 2002, Relative expression software tool (REST©) for group-wise comparison and statistical analysis of relative expression results in real-time PCR. *Nucleic Acids Research* 30(9): 10.

Pfaffl MW, Tichopad A, Prgomet C and Neuvians TP, 2004, Determination of stable housekeeping genes, differentially regulated target genes and sample integrity: BestKeeper – Excel-based tool using pair-wise correlations. *Biotechnology Letters* 26(6): 509–515, DOI: 10.1023/B:BILE.0000019559.84305.47.

Pimentel D, 2012, Silent Spring, the 50th anniversary of Rachel Carson's book. *BMC Ecology* 12(1): 20, DOI: 10.1186/1472-6785-12-20.

Radtke F, Heuchel R, Georgiev O, Hergersberg M, Gariglio M, Dembic Z and Schaffner W, 1993, Cloned transcription factor MTF-1 activates the mouse metallothionein I promoter. *The EMBO Journal* 12(4): 1355–1362, DOI: 10.1002/j.1460-2075.1993.tb05780.x.

Raisuddin S, Kwok KWH, Leung KMY, Schlenk D and Lee J-S, 2007, The copepod *Tigriopus*: A promising marine model organism for ecotoxicology and environmental genomics. *Aquatic Toxicology* 83(3): 161–173, DOI: 10.1016/j.aquatox.2007.04.005.

Rajkumar M and Kumaraguru vasagam KP, 2006, Suitability of the copepod, *Acartia clausi* as a live feed for Seabass larvae (*Lates calcarifer* Bloch): Compared to traditional live-

food organisms with special emphasis on the nutritional value. *Aquaculture* 261(2): 649–658, DOI: 10.1016/j.aquaculture.2006.08.043.

Rand GM, 1995, *Fundamentals of aquatic toxicology: effects, environmental fate and risk assessment*. CRC press.

Rasdi NW and Qin JG, 2016, Improvement of copepod nutritional quality as live food for aquaculture: a review. *Aquaculture Research* 47(1): 1–20, DOI: 10.1111/are.12471.

Regoli F and Giuliani ME, 2014, Oxidative pathways of chemical toxicity and oxidative stress biomarkers in marine organisms. *Marine Environmental Research* 93: 106–117, DOI: 10.1016/j.marenvres.2013.07.006.

Regoli F, Pellegrini D, Cicero AM, Nigro M, Benedetti M, Gorbi S, Fattorini D, D'Errico G, Di Carlo M, Nardi A, Gaion A, Scuderi A, Giuliani S, Romanelli G, Berto D, Trabucco B, Guidi P, Bernardeschi M, Scarcelli V and Frenzilli G, 2014, A multidisciplinary weight of evidence approach for environmental risk assessment at the Costa Concordia wreck: Integrative indices from Mussel Watch. *Marine Environmental Research* 96: 92–104, DOI: 10.1016/j.marenvres.2013.09.016.

Rhee J-S, Raisuddin S, Lee K-W, Seo JS, Ki J-S, Kim I-C, Park HG and Lee J-S, 2009, Heat shock protein (Hsp) gene responses of the intertidal copepod *Tigriopus japonicus* to environmental toxicants. *Comparative Biochemistry and Physiology Part C: Toxicology & Pharmacology* 149(1): 104–112, DOI: 10.1016/j.cbpc.2008.07.009.

Robinson MD, McCarthy DJ and Smyth GK, 2010, edgeR: a Bioconductor package for differential expression analysis of digital gene expression data. *Bioinformatics* 26(1): 139–140.

Robinson MD and Oshlack A, 2010, A scaling normalization method for differential expression analysis of RNA-seq data. *Genome Biology* 11(3): R25, DOI: 10.1186/gb-2010-11-3-r25.

Roncalli V, 2018, Physiological characterization of the emergence from diapause: A transcriptomics approach. *Scientific RePorts* 15.

Rotolo F, Vitiello V, Pellegrini D, Carotenuto Y and Buttino I, 2021, Historical control data in ecotoxicology: Eight years of tests with the copepod *Acartia tonsa*. *Environmental Pollution* 284: 117468, DOI: 10.1016/j.envpol.2021.117468.

Russo E, Lauritano C, d'Ippolito G, Fontana A, Sarno D, von Elert E, Ianora A and Carotenuto Y, 2020, RNA-Seq and differential gene expression analysis in *Temora stylifera* copepod females with contrasting non-feeding nauplii survival rates: an environmental transcriptomics study. *BMC Genomics* 21(1): 693, DOI: 10.1186/s12864-020-07112-w.

Schroeder A, Mueller O, Stocker S, Salowsky R, Leiber M, Gassmann M, Lightfoot S, Menzel W, Granzow M and Ragg T, 2006, The RIN: an RNA integrity number for assigning

integrity values to RNA measurements. *BMC Molecular Biology* 7(1): 3, DOI: 10.1186/1471-2199-7-3.

Sei S, Invidia M and Gorbi G, 2006, Near anoxia and sulfide as possible factors influencing the spatial distribution of *Acartia tonsa* and *Acartia clausi*: Comparative evaluation of egg tolerance. *Journal of Experimental Marine Biology and Ecology* 337(2): 121–130, DOI: 10.1016/j.jembe.2006.05.015.

Sei S, Rossetti G, Villa F and Ferrari I, 1996, Zooplankton variability related to environmental changes in a eutrophic coastal lagoon in the Po Delta. *Hydrobiologia* 329: 45–55.

Semmouri I, Asselman J, Van Nieuwerburgh F, Deforce D, Janssen CR and De Schamphelaere KAC, 2019, The transcriptome of the marine calanoid copepod *Temora longicornis* under heat stress and recovery. *Marine Environmental Research* 143: 10–23, DOI: 10.1016/j.marenvres.2018.10.017.

Semmouri I, De Schamphelaere KAC, Mees J, Janssen CR and Asselman J, 2020, Evaluating the potential of direct RNA nanopore sequencing: Metatranscriptomics highlights possible seasonal differences in a marine pelagic crustacean zooplankton community. *Marine Environmental Research* 153: 104836, DOI: 10.1016/j.marenvres.2019.104836.

Sharma A, Hickman J, Gazit N, Rabkin E and Mishin Y, 2018, Nickel nanoparticles set a new record of strength. *Nature Communications* 9(1): 4102, DOI: 10.1038/s41467-018-06575-6.

Shewhart WA, 1931, Economic Control of Quality of Manufactured Product. Van Nostrand, D. Inc., New York, 1931. Republished by American Society for Quality (1980). .

Silvestre F, Dierick J-F, Dumont V, Dieu M, Raes M and Devos P, 2006, Differential protein expression profiles in anterior gills of *Eriocheir sinensis* during acclimation to cadmium. *Aquatic Toxicology* 76(1): 46–58, DOI: 10.1016/j.aquatox.2005.09.006.

Simão FA, Waterhouse RM, Ioannidis P, Kriventseva EV and Zdobnov EM, 2015, BUSCO: assessing genome assembly and annotation completeness with single-copy orthologs. *Bioinformatics* 31(19): 3210–3212, DOI: 10.1093/bioinformatics/btv351.

Smeti EM, Koronakis DE and Golfinopoulos SK, 2007, Control charts for the toxicity of finished water—Modeling the structure of toxicity. *Water Research* 41(12): 2679–2689, DOI: 10.1016/j.watres.2007.02.036.

Snell TW, Brogdon SE and Morgan MB, 2003, Gene Expression Profiling in Ecotoxicology. *Ecotoxicology* 12(6): 475–483, DOI: 10.1023/B:ECTX.0000003033.09923.a8.

Solgaard G, Standal IB and Draget KI, 2007, Proteolytic activity and protease classes in the zooplankton species *Calanus finmarchicus*. *Comparative Biochemistry and Physiology Part B: Biochemistry and Molecular Biology* 147(3): 475–481, DOI: 10.1016/j.cbpb.2007.02.014.

Steinberg DK and Landry MR, 2017, Zooplankton and the Ocean Carbon Cycle. *Annual Review of Marine Science* 9(1): 413–444, DOI: 10.1146/annurev-marine-010814-015924.

Stohs S and Bagchi D, 1995, Oxidative mechanisms in the toxicity of metal ions. *Free Radical Biology and Medicine* 18(2): 321–336, DOI: 10.1016/0891-5849(94)00159-H.

Støttrup JG, 2006, A Review on the Status and Progress in Rearing Copepods for Marine Larviculture. Advantages and Disadvantages. Among Calanoid, Harpacticoid and Cyclopoid Copepods. *Avances en Nutrición Acuícola VIII* 22.

Sukhikh N, Abramova E, Holl A-C, Souissi S and Alekseev V, 2020, A comparative analysis of genetic differentiation of the E. affinis species complex and some other *Eurytemora* species, using the CO1, nITS and 18SsRNA genes (Copepoda, Calanoida). *Crustaceana* 93(8): 931–955.

Sullivan BK, Buskey E, Miller DC and Ritacco PJ, 1983, Effects of copper and cadmium on growth, swimming and predator avoidance in *Eurytemora affinis* (Copepoda). *Marine Biology* 77(3): 299–306, DOI: 10.1007/BF00395819.

Syberg K, Nielsen A, Khan FR, Banta GT, Palmqvist A and Jepsen PM, 2017, Microplastic potentiates triclosan toxicity to the marine copepod *Acartia tonsa* (Dana). *Journal of Toxicology and Environmental Health, Part A* 80(23–24): 1369–1371, DOI: 10.1080/15287394.2017.1385046.

Tarrant AM, Nilsson B and Hansen BW, 2019, Molecular physiology of copepods - from biomarkers to transcriptomes and back again. *Comparative Biochemistry and Physiology Part D: Genomics and Proteomics* 30: 230–247, DOI: 10.1016/j.cbd.2019.03.005.

Tennant RW, 2002, The National Center for Toxicogenomics: using new technologies to inform mechanistic toxicology. *Environmental Health Perspectives* 110(1), DOI: 10.1289/ehp.110-a8.

Teo WZ and Pumera M, 2014, Fate of silver nanoparticles in natural waters; integrative use of conventional and electrochemical analytical techniques. *RSC Advances* 4(10): 5006, DOI: 10.1039/c3ra43224f.

Teschke R, 2022, Aluminum, Arsenic, Beryllium, Cadmium, Chromium, Cobalt, Copper, Iron, Lead, Mercury, Molybdenum, Nickel, Platinum, Thallium, Titanium, Vanadium, and Zinc: Molecular Aspects in Experimental Liver Injury. *International Journal of Molecular Sciences* 23(20): 12213, DOI: 10.3390/ijms232012213.

Tiselius P, Hansen BW, Jonsson P, Kiørboe T, Nielsen TG, Piontkovski S and Saiz E, 1995, Can we use laboratory-reared copepods for experiments? A comparison of feeding behaviour and reproduction between a field and a laboratory population of *Acartia tonsa*. *ICES Journal of Marine Science* 52(3–4): 369–376, DOI: 10.1016/1054-3139(95)80052-2.

Tolleson WH, 2018, Mechanistic ecotoxicology and environmental toxicology. *Journal of Environmental Science and Health, Part C* 36(3): 164–166, DOI: 10.1080/10590501.2018.1492201.

Tu H, Fan C, Chen X, Liu J, Wang B, Huang Z, Zhang Y, Meng X and Zou F, 2017, Effects of cadmium, manganese, and lead on locomotor activity and neurexin 2a expression in zebrafish: Effects of metals on neurexin 2a expression in zebrafish. *Environmental Toxicology and Chemistry* 36(8): 2147–2154, DOI: 10.1002/etc.3748.

Turner JT, 2004, The Importance of Small Planktonic Copepods and Their Roles in Pelagic Marine Food Webs. *Zoological Studies* 12.

UNICHIM, 2012a, Associazione per l′Unificazione nel Settore dell'Industria Chimica-Ente Federato UNI. Metodo n. 2365. Qualità dell'acqua. Determinazione dell'inibizione della mobilità di nauplii di *Acartia tonsa* Dana (Crustacea:Copepoda) 24h e 48h di esposizione. .

UNICHIM, 2012b, Associazione per l′Unificazione nel Settore dell'Industria Chimica-Ente Federato UNI. Metodo n. 2366. Qualità dell'acqua. Determinazione dell'inibizione della mobilità di nauplii di *Acartia tonsa* Dana (Crustacea: Copepoda) dopo 7 giorni di esposizione. .

UNICHIM, 2014, Associazione per l′Unificazione nel Settore dell'Industria Chimica-Ente Federato UNI. Metodo n. 2396. Qualità dell'acqua – Determinazione della tossicità letale a 24 h, 48 h e 96 h di esposizione con naupli di *Tigriopus fulvus* (Fischer, 1860) (Crustacea: Copepoda). .

US EPA, 1976, U.S. Environmental Protection Agency. Acute toxicity of certain pesticides to *Acartia tonsa* Dana. EPA-600/3-76-033 1976. .

US EPA, 1991, U.S. Environmental Protection Agency. Earl-Standard Operating Procedure Conducting the Sea Urchin *Arbacia punctulata* Fertilization Test. Environmental Research Laboratory, Narraganserr,. , pages 125–131.

US EPA, 2002, U.S. Environmental Protection Agency. Methods for Measuring the Acute Toxicity of Effluents and Receiving Waters to Freshwater and Marine Organisms. EPA-821-R-02-012. .

Valko M, Morris H and Cronin M, 2005, Metals, Toxicity and Oxidative Stress. *Current Medicinal Chemistry* 12(10): 1161–1208, DOI: 10.2174/0929867053764635.

Vandenbrouck T, Soetaert A, van der Ven K, Blust R and De Coen W, 2009, Nickel and binary metal mixture responses in *Daphnia magna*: Molecular fingerprints and (sub)organismal effects. *Aquatic Toxicology* 92(1): 18–29, DOI: 10.1016/j.aquatox.2008.12.012.

Vandesompele J, De Preter K, Pattyn F, Poppe B, Van Roy N, De Paepe A and Speleman F, 2002, Accurate normalization of real-time quantitative RT-PCR data by geometric

averaging of multiple internal control genes. *Genome Biology* 3(7): research0034.1, DOI: 10.1186/gb-2002-3-7-research0034.

Vargas CA, Escribano R and Poulet S, 2006, Phytoplankton food quality determines time windows for successful zooplankton reproductive pulses. *Ecology* 87(12): 2992–2999, DOI: 10.1890/0012-9658(2006)87[2992:PFQDTW]2.0.CO;2.

Veldhoen N, Skirrow RC, Osachoff H, Wigmore H, Clapson DJ, Gunderson MP, Van Aggelen G and Helbing CC, 2006, The bactericidal agent triclosan modulates thyroid hormone-associated gene expression and disrupts postembryonic anuran development. *Aquatic Toxicology* 80(3): 217–227, DOI: 10.1016/j.aquatox.2006.08.010.

Vitiello V, Zhou C, Scuderi A, Pellegrini D and Buttino I, 2016, Cold storage of *Acartia tonsa* eggs: a practical use in ecotoxicological studies. *Ecotoxicology* 25(5): 1033–1039, DOI: 10.1007/s10646-016-1660-8.

Walter TC and Boxshall G, 2022, World of Copepods Database. Accessed at https://www.marinespecies.org/copepoda on 2022-06-06. doi:10.14284/356. .

Wang J, Li J, Ge Q, Chen Z and Li J, 2020, Effects of Inbreeding on Genetic Characteristic, Growth, Survival Rates, and Immune Responses of a New Inbred Line of *Exopalaemon carinicauda*. *International Journal of Genomics* 2020: 1–11, DOI: 10.1155/2020/5735968.

Wang M, Jeong C-B, Li Y and Lee J-S, 2017, Different transcriptomic responses of two marine copepods, *Tigriopus japonicus* and *Pseudodiaptomus annandalei*, to a low dose of mercury chloride (HgCl 2). *Aquatic Toxicology* 187: 124–131, DOI: 10.1016/j.aquatox.2017.03.018.

Wang M and Wang G, 2010, Oxidative damage effects in the copepod *Tigriopus japonicus* Mori experimentally exposed to nickel. *Ecotoxicology* 19(2): 273–284, DOI: 10.1007/s10646-009-0410-6.

Wang Z, Gerstein M and Snyder M, 2009, RNA-Seq: a revolutionary tool for transcriptomics. *Nature Reviews Genetics* 10(1): 57–63, DOI: 10.1038/nrg2484.

Waters MD and Fostel JM, 2004, Toxicogenomics and systems toxicology: aims and prospects. *Nature Reviews Genetics* 5(12): 936–948, DOI: 10.1038/nrg1493.

Wells PG, 1984, Marine ecotoxicological tests with zooplankton. *Ecotoxicological Testing for the Marine Environment* 1: 215–256.

Weng B, Xu Y, Ying J, Yang H, Su L, Yang Y and Chen M, 2020, A novel use for Levey-Jennings charts in prenatal molecular diagnosis. *BMC Medical Genomics* 13(1): 109, DOI: 10.1186/s12920-020-00758-1.

Werbrouck E, Tiselius P, Van Gansbeke D, Cervin G, Vanreusel A and De Troch M, 2016, Temperature impact on the trophic transfer of fatty acids in the congeneric copepods

Acartia tonsa and *Acartia clausi*. *Journal of Sea Research* 112: 41–48, DOI: 10.1016/j.seares.2016.03.001.

Werner I and Hitzfeld B, 2012, 50 Years of Ecotoxicology since *Silent Spring* – A Review. *GAIA - Ecological Perspectives for Science and Society* 21(3): 217–224, DOI: 10.14512/gaia.21.3.13.

World Register of Marine Species, 2022, (WoRMS). Copepoda. Accessed at: https://www.marinespecies.org/aphia.php?p=taxdetails&id=1080 on 2022-06-06. .

Wu Y and Kong L, 2020, Advance on toxicity of metal nickel nanoparticles. *Environmental Geochemistry and Health* 42(7): 2277–2286, DOI: 10.1007/s10653-019-00491-4.

Xie F, Xiao P, Chen D, Xu L and Zhang B, 2012, miRDeepFinder: a miRNA analysis tool for deep sequencing of plant small RNAs. *Plant Molecular Biology* 80(1): 75–84, DOI: 10.1007/s11103-012-9885-2.

Yang J, Chen Z, Liu N and Chen Y, 2018, Ribosomal protein L10 in mitochondria serves as a regulator for ROS level in pancreatic cancer cells. *Redox Biology* 19: 158–165, DOI: 10.1016/j.redox.2018.08.016.

Yeardley RB, Lazorchak JM and Pence MA, 1995, Evaluation of alternative reference toxicants for use in the earthworm toxicity test. *Environmental Toxicology and Chemistry* 14(7): 1189–1194, DOI: 10.1002/etc.5620140710.

Yin Y, Yang X, Zhou X, Wang W, Yu S, Liu J and Jiang G, 2015, Water chemistry controlled aggregation and photo-transformation of silver nanoparticles in environmental waters. *Journal of Environmental Sciences* 34: 116–125, DOI: 10.1016/j.jes.2015.04.005.

Yu N, Ding Q, Li E, Qin JG, Chen L and Wang X, 2018, Growth, energy metabolism and transcriptomic responses in Chinese mitten crab (*Eriocheir sinensis*) to benzo[α]pyrene (BaP) toxicity. *Aquatic Toxicology* 203: 150–158, DOI: 10.1016/j.aquatox.2018.08.014.

Zhang J, Ianora A, Wu C, Pellegrini D, Esposito F and Buttino I, 2015, How to increase productivity of the copepod *Acartia tonsa* (Dana): effects of population density and food concentration. *Aquaculture Research* 46(12): 2982–2990, DOI: 10.1111/are.12456.

Zhang J, Wu C, Pellegrini D, Romano G, Esposito F, Ianora A and Buttino I, 2013, Effects of different monoalgal diets on egg production, hatching success and apoptosis induction in a Mediterranean population of the calanoid copepod *Acartia tonsa* (Dana). *Aquaculture* 400–401: 65–72, DOI: 10.1016/j.aquaculture.2013.02.032.

Zhao J, Zheng Y, Xue F, Chang Y, Yang H and Zhang J, 2016, Molecular basis of reactive oxygen species-induced inactivation of α4β2 nicotinic acetylcholine receptors. *Free Radical Biology and Medicine* 97: 520–530, DOI: 10.1016/j.freeradbiomed.2016.07.012.

Zhou C, Carotenuto Y, Vitiello V, Wu C, Zhang J and Buttino I, 2018, De novo transcriptome assembly and differential gene expression analysis of the calanoid copepod *Acartia tonsa* exposed to nickel nanoparticles. *Chemosphere* 209: 163–172, DOI: 10.1016/j.chemosphere.2018.06.096.

Zhou C, Vitiello V, Casals E, Puntes VF, Iamunno F, Pellegrini D, Changwen W, Benvenuto G and Buttino I, 2016a, Toxicity of nickel in the marine calanoid copepod *Acartia tonsa*: Nickel chloride versus nanoparticles. *Aquatic Toxicology* 170: 1–12, DOI: 10.1016/j.aquatox.2015.11.003.

Zhou C, Vitiello V, Pellegrini D, Wu C, Morelli E and Buttino I, 2016b, Toxicological effects of CdSe/ZnS quantum dots on marine planktonic organisms. *Ecotoxicology and Environmental Safety* 123: 26–31, DOI: 10.1016/j.ecoenv.2015.09.020.

Zingone A, D'Alelio D, Mazzocchi MG, Montresor M, Sarno D and team L-M, 2019, Time series and beyond: multifaceted plankton research at a marine Mediterranean LTER site. *Nature Conservation* 34: 273–310, DOI: 10.3897/natureconservation.34.30789.

Appendix

Table A.1 Complete list of the up-regulated genes (FDR < 0.05, $|\log_2 FC| \geq 2$) of the *Acartia clausi* transcriptome, ordered by decreasing $\log_2 FC$. For each sequence are reported ID, description, length, $\log_2 FC$, FDR, E-value and percentage of similarity.

ID	Sequence description	Sequence length (bp)	$\log_2 FC$	FDR	E-value	Similarity (%)
TRINITY_DN37108_c0_g2_i1	eukaryotic peptide chain release factor GTP-binding subunit ERF3A isoform X1	2357	13,42	2,32E-22	0,00E+00	80,25%
TRINITY_DN32186_c1_g2_i1	Platelet-activating factor acetylhydrolase IB subunit gamma	1939	11,94	1,71E-19	1,40E-117	76,24%
TRINITY_DN33675_c1_g1_i2	ubiquitin-40S ribosomal protein S27a	376	11,04	1,84E-15	4,70E-20	83,53%
TRINITY_DN41340_c2_g2_i5	ubiquitin carboxyl-terminal hydrolase MINDY-1 isoform X1	3439	10,90	4,01E-15	2,00E-07	59,58%
TRINITY_DN31372_c1_g2_i2	heat shock protein 90	1315	10,83	5,92E-15	0,00E+00	74,56%
TRINITY_DN37011_c0_g1_i3	histone-lysine N-methyltransferase, H3 lysine-79 specific-like	1034	10,77	8,26E-15	3,70E-12	79,66%
TRINITY_DN32664_c0_g1_i5	mpv17-like protein [M-LP]	1256	10,73	9,24E-15	3,00E-46	57,79%
TRINITY_DN35786_c2_g3_i4	gag-pol polyprotein-like protein	2142	10,46	5,03E-14	2,20E-104	56,80%
TRINITY_DN32703_c3_g3_i2	Lysosomal aspartic protease	1284	10,30	1,28E-13	1,10E-103	61,10%
TRINITY_DN28633_c0_g1_i1	Cna B-type domain-containing protein	984	10,29	1,30E-13	2,30E-11	53,60%
TRINITY_DN17418_c0_g1_i1	sexually induced protein 3	749	10,10	3,23E-13	9,10E-142	72,53%
TRINITY_DN19742_c0_g1_i1	cytochrome c peroxidase, mitochondrial-like	1391	9,93	8,28E-13	8,80E-84	57,96%
TRINITY_DN36259_c1_g1_i1	Leucine-rich repeat-containing protein 8A	1684	9,74	2,11E-12	4,00E-88	64,90%
TRINITY_DN37511_c2_g1_i9	Surfeit locus protein 1	851	9,54	1,02E-12	4,20E-32	66,70%
TRINITY_DN29548_c2_g1_i6	Actin, cytoplasmic A3a	853	8,77	1,74E-17	9,20E-152	93,60%
TRINITY_DN27900_c0_g1_i1	lysosomal protective protein [serine carboxypeptidase]	1267	8,64	2,43E-13	1,10E-31	45,69%
TRINITY_DN21618_c0_g1_i1	arginine kinase-like	1404	8,44	4,94E-14	6,60E-93	62,45%
TRINITY_DN29290_c1_g1_i1	cell division cycle protein 20 homolog	1937	8,40	9,77E-13	2,70E-141	71,05%
TRINITY_DN5006_c0_g1_i1	superoxide dismutase [Cu-Zn]	623	8,26	1,94E-12	2,40E-58	72,63%
TRINITY_DN5983_c0_g1_i1	migration and invasion enhancer 1	455	8,18	2,82E-12	7,20E-04	56,18%

TRINITY_DN17269_c0_g1_i1	predicted protein	1326	8,07	5,42E-12	8,10E-48	44,38%
TRINITY_DN4382_c0_g1_i1	Ctype lysozyme/alpha-lactalbumin superfamily protein	565	7,78	3,38E-11	7,10E-35	72,07%
TRINITY_DN42165_c0_g1_i1	hypothetical protein FisN_3Lh424	575	7,78	1,35E-12	3,10E-38	67,36%
TRINITY_DN13351_c0_g1_i1	40S ribosomal protein S14	543	7,72	1,90E-15	1,50E-61	90,61%
TRINITY_DN2744_c0_g1_i1	Prostaglandin E synthase 3	742	7,72	2,03E-12	1,50E-13	59,17%
TRINITY_DN12653_c0_g1_i1	60S ribosomal protein L27	483	7,55	9,63E-15	2,90E-47	72,16%
TRINITY_DN33829_c0_g4_i1	endoplasmic reticulum chaperone BiP	823	7,51	5,49E-12	4,80E-90	83,79%
TRINITY_DN25513_c3_g1_i1	dynein beta chain, ciliary	1415	7,50	7,05E-12	5,00E-114	60,02%
TRINITY_DN21604_c0_g1_i1	alpha-aminoadipic semialdehyde dehydrogenase	1404	7,46	1,50E-13	2,00E-176	73,60%
TRINITY_DN9611_c0_g1_i1	40S ribosomal protein S17	435	7,33	1,57E-13	3,90E-60	88,17%
TRINITY_DN29868_c0_g1_i2	unnamed protein product	974	7,30	5,19E-14	2,50E-132	57,01%
TRINITY_DN26418_c0_g1_i1	tyrosine aminotransferase	1580	7,30	2,43E-13	5,20E-22	42,28%
TRINITY_DN39439_c1_g1_i2	sodium- and chloride-dependent GABA transporter 1-like	2744	7,28	5,84E-13	0,00E+00	71,08%
TRINITY_DN24893_c0_g1_i1	probable enoyl-CoA hydratase, mitochondrial	1198	7,23	1,81E-12	5,30E-115	73,27%
TRINITY_DN30875_c0_g1_i18	Ig-like domain-containing protein	420	7,21	2,13E-13	7,80E-10	54,10%
TRINITY_DN34848_c0_g3_i1	unnamed protein product, partial	1468	7,21	6,09E-13	5,50E-102	63,28%
TRINITY_DN30693_c0_g1_i7	Gusb	1861	7,18	4,52E-11	7,80E-04	47,34%
TRINITY_DN19555_c0_g1_i1	predicted protein	1151	7,17	3,07E-12	1,80E-175	62,99%
TRINITY_DN23034_c0_g1_i1	peptidyl-prolyl cis-trans isomerase-like 1	766	7,17	1,30E-12	5,90E-25	49,99%
TRINITY_DN1872_c0_g1_i1	40S ribosomal protein S26	418	7,16	4,36E-14	1,70E-27	81,18%
TRINITY_DN33327_c2_g1_i3	14-3-3-like protein	861	7,16	5,18E-11	8,30E-140	88,06%
TRINITY_DN29109_c0_g1_i1	carboxypeptidase B	1429	7,12	3,07E-12	3,20E-97	60,12%
TRINITY_DN28870_c2_g1_i2	tail fiber domain-containing protein	867	7,08	1,33E-11	2,80E-40	61,22%
TRINITY_DN26431_c0_g1_i1	poly [ADP-ribose] polymerase 3-like [PARP]	1450	7,07	1,01E-10	2,30E-94	54,47%
TRINITY_DN21729_c0_g1_i2	guanine nucleotide-binding protein G(I)/G(S)/G(T) subunit beta-1	1199	7,05	1,16E-10	2,70E-123	68,32%
TRINITY_DN19531_c0_g1_i1	putative cysteine proteinase	1246	7,05	8,78E-13	2,20E-103	61,31%

TRINITY_DN41707_c0_g1_i1	60S ribosomal protein L36-like	409	7,03	1,66E-13	1,40E-20	65,46%
TRINITY_DN42241_c0_g1_i1	40S ribosomal protein S25	399	7,02	5,03E-14	9,40E-22	71,30%
TRINITY_DN16312_c0_g1_i1	predicted protein	1935	7,02	3,70E-13	0,00E+00	48,69%
TRINITY_DN15525_c0_g1_i1	---NA---	414	6,99	7,90E-12		
TRINITY_DN27308_c0_g1_i1	Acetyl-CoA acetyltransferase	1345	6,91	1,07E-11	0,00E+00	78,11%
TRINITY_DN2017_c0_g1_i1	60S ribosomal protein L28	535	6,91	2,00E-13	1,80E-12	51,83%
TRINITY_DN31921_c5_g1_i1	---NA---	832	6,91	4,24E-11		
TRINITY_DN17803_c0_g1_i1	Peptidyl-prolyl cis-trans isomerase D	1581	6,90	1,12E-11	2,30E-60	74,52%
TRINITY_DN29252_c0_g1_i2	reversion-inducing cysteine-rich protein with Kazal motifs-like	475	6,89	1,84E-13	3,90E-05	48,65%
TRINITY_DN41723_c0_g1_i1	60S ribosomal protein L19	661	6,89	8,61E-14	8,60E-63	83,41%
TRINITY_DN29548_c2_g1_i3	Actin, cytoplasmic A3a	860	6,88	1,27E-13	1,00E-151	93,60%
TRINITY_DN41445_c0_g1_i1	60S ribosomal protein L31	441	6,88	3,20E-13	2,00E-37	80,61%
TRINITY_DN31684_c0_g1_i11	---NA---	394	6,86	6,41E-12		
TRINITY_DN23375_c0_g1_i1	cathepsin b	1299	6,84	2,49E-12	2,60E-130	61,49%
TRINITY_DN19467_c0_g1_i1	glutathione S-transferase omega-like 2	1128	6,82	9,88E-12	2,30E-68	56,28%
TRINITY_DN29126_c0_g1_i1	Transitional endoplasmic reticulum ATPase TER94	1380	6,80	4,97E-12	1,80E-179	83,05%
TRINITY_DN41673_c0_g1_i1	60S ribosomal protein L37a	343	6,78	2,17E-13	6,80E-32	85,29%
TRINITY_DN17365_c0_g1_i1	Gamma-interferon-inducible lysosomal thiol reductase	944	6,77	3,92E-12	1,10E-19	45,22%
TRINITY_DN41522_c0_g1_i1	40S ribosomal protein S16	497	6,76	1,80E-13	8,10E-79	89,96%
TRINITY_DN18785_c0_g1_i1	cofilin/actin-depolymerizing factor homolog	507	6,76	1,13E-12	8,70E-25	57,83%
TRINITY_DN21469_c0_g1_i1	notchless protein homolog 1	1232	6,74	1,22E-10	8,40E-07	53,09%
TRINITY_DN711_c0_g1_i1	ribosomal protein L29	469	6,73	2,23E-12	9,20E-43	85,91%
TRINITY_DN23121_c0_g1_i1	glutathione S-transferase Mu 1	684	6,73	3,34E-11	5,50E-14	47,59%
TRINITY_DN28655_c0_g1_i4	unnamed protein product, partial	1813	6,71	6,63E-12	9,40E-176	48,75%
TRINITY_DN28321_c0_g1_i1	Isocitrate dehydrogenase [NADP]	2411	6,71	6,48E-13	0,00E+00	70,95%
TRINITY_DN179_c0_g1_i1	60S ribosomal protein L22-like	431	6,70	5,72E-13	2,60E-28	74,48%

TRINITY_DN2108_c0_g1_i1	ADP-ribosylation factor 1	742	6,70	5,16E-13	3,20E-108	92,67%
TRINITY_DN27628_c0_g1_i1	probable methylmalonate-semialdehyde dehydrogenase [acylating], mitochondrial	1777	6,69	1,26E-12	0,00E+00	76,31%
TRINITY_DN41697_c0_g1_i1	40S ribosomal protein S4	876	6,68	2,20E-13	6,10E-130	82,28%
TRINITY_DN33327_c2_g1_i1	14-3-3-like protein	883	6,68	1,46E-12	1,20E-140	88,38%
TRINITY_DN15481_c0_g1_i1	V-type proton ATPase 16 kDa proteolipid subunit	692	6,68	9,67E-12	3,80E-52	76,39%
TRINITY_DN29900_c0_g2_i2	Roco2, Roco family protein	1748	6,65	2,67E-11	4,40E-120	42,49%
TRINITY_DN25513_c0_g1_i1	dynein beta chain, ciliary-like isoform X2	1391	6,64	1,35E-11	4,00E-116	63,68%
TRINITY_DN23727_c0_g1_i1	60S ribosomal protein L18	669	6,64	2,51E-13	1,70E-76	77,15%
TRINITY_DN17255_c0_g1_i1	40S ribosomal protein S19-like	501	6,63	4,32E-13	1,80E-41	65,98%
TRINITY_DN41981_c0_g1_i1	large subunit ribosomal protein L10e	752	6,63	2,14E-13	3,90E-141	81,68%
TRINITY_DN24808_c0_g1_i1	dihydrolipoyl dehydrogenase, mitochondrial	1616	6,62	9,68E-13	0,00E+00	74,05%
TRINITY_DN37811_c1_g1_i1	60S ribosomal protein L8	837	6,62	2,17E-13	5,80E-177	80,35%
TRINITY_DN16097_c0_g1_i1	unnamed protein product, partial	1573	6,62	7,46E-11	7,40E-05	39,62%
TRINITY_DN27978_c0_g4_i1	uncharacterized protein LOC111711180	800	6,61	1,80E-13	2,30E-30	48,80%
TRINITY_DN29795_c1_g2_i2	ATP synthase F1 subunit alpha	797	6,61	1,40E-12	1,10E-140	84,95%
TRINITY_DN17942_c0_g1_i1	60S ribosomal protein L30	462	6,61	8,73E-13	2,90E-51	85,82%
TRINITY_DN28870_c2_g1_i9	rasGAP-activating-like protein 1-like	437	6,61	1,87E-11	1,10E-19	54,73%
TRINITY_DN27946_c0_g1_i1	ATP-binding cassette sub-family F member 3	2027	6,59	4,55E-12	2,50E-55	48,86%
TRINITY_DN41675_c0_g1_i1	40S ribosomal protein S8	709	6,59	3,72E-13	6,20E-96	79,70%
TRINITY_DN19644_c0_g1_i1	delta-1-pyrroline-5-carboxylate dehydrogenase, mitochondrial	1697	6,58	1,16E-10	0,00E+00	71,86%
TRINITY_DN37617_c1_g1_i1	40S ribosomal protein S9	405	6,56	1,22E-12	2,70E-52	78,93%
TRINITY_DN42264_c0_g1_i1	---NA---	452	6,56	1,09E-12		
TRINITY_DN24889_c0_g2_i1	60S ribosomal protein L21	537	6,55	1,09E-12	6,90E-49	69,46%
TRINITY_DN34656_c0_g1_i3	unnamed protein product	1126	6,55	1,12E-10	7,80E-87	48,49%
TRINITY_DN27954_c1_g1_i5	Peptidyl-prolyl cis-trans isomerase	630	6,55	2,03E-10	3,00E-92	85,31%
TRINITY_DN12241_c0_g1_i1	Cytochrome c oxidase subunit Vb	480	6,54	1,34E-11	1,00E-51	55,05%

TRINITY_DN19249_c0_g1_i1	60S ribosomal protein L4	1230	6,53	4,32E-13	4,40E-134	72,13%
TRINITY_DN27982_c0_g1_i4	---NA---	714	6,53	1,70E-12		
TRINITY_DN33676_c0_g1_i2	arylsulfatase B-like	1588	6,52	1,25E-12	2,30E-117	57,30%
TRINITY_DN8798_c0_g1_i1	60S ribosomal protein L18a	655	6,50	1,84E-12	7,10E-66	73,59%
TRINITY_DN3711_c0_g1_i1	60S ribosomal protein L17	647	6,50	8,01E-13	5,20E-54	69,62%
TRINITY_DN27742_c0_g4_i1	60S acidic ribosomal protein P1-like	422	6,50	1,12E-12	6,00E-08	63,59%
TRINITY_DN573_c0_g1_i1	40S ribosomal protein S24	511	6,49	9,19E-13	1,80E-43	79,97%
TRINITY_DN25352_c1_g1_i3	Cathepsin L-like proteinase	1159	6,49	2,21E-12	1,30E-150	62,83%
TRINITY_DN37461_c0_g1_i9	chromobox protein homolog 1-like	832	6,49	1,20E-12	3,50E-60	71,10%
TRINITY_DN29985_c2_g3_i1	---NA---	1920	6,48	6,35E-12		
TRINITY_DN41511_c0_g1_i1	peptidyl-prolyl cis-trans isomerase	827	6,47	7,31E-11	1,80E-89	83,29%
TRINITY_DN32371_c1_g1_i1	60S ribosomal protein L5	1041	6,47	4,80E-13	3,80E-103	72,08%
TRINITY_DN26904_c0_g1_i1	sphingolipid delta(4)-desaturase DES1	1232	6,47	2,40E-12	9,00E-105	65,75%
TRINITY_DN21887_c0_g1_i1	60S ribosomal protein L13	705	6,46	9,19E-13	5,30E-71	74,43%
TRINITY_DN27742_c0_g1_i1	60S acidic ribosomal protein P2	485	6,45	1,29E-12	1,30E-17	76,08%
TRINITY_DN27444_c0_g5_i1	60s ribosomal protein l23a	490	6,45	9,19E-13	6,40E-70	81,97%
TRINITY_DN16233_c0_g1_i1	extracellular metalloprotease VDBG_01143-like	994	6,45	1,10E-12	8,40E-82	44,57%
TRINITY_DN27303_c0_g1_i1	prohibitin complex subunit 1	1027	6,45	8,71E-12	1,90E-117	79,73%
TRINITY_DN23942_c0_g1_i1	60S ribosomal protein L12	575	6,44	8,55E-13	1,60E-99	85,96%
TRINITY_DN2127_c0_g1_i1	Serine--pyruvate aminotransferase, mitochondrial	1363	6,44	7,25E-12	4,30E-68	46,46%
TRINITY_DN25198_c0_g1_i1	---NA---	1097	6,44	1,08E-10		
TRINITY_DN16172_c0_g1_i1	40S ribosomal protein S18	559	6,44	1,22E-12	2,70E-76	85,19%
TRINITY_DN29900_c0_g1_i2	Leucine-rich repeat serine/threonine-protein kinase 1	892	6,44	1,04E-09	8,60E-38	47,37%
TRINITY_DN29614_c0_g2_i1	translation elongation factor 2	2796	6,44	7,28E-13	0,00E+00	68,50%
TRINITY_DN28101_c0_g2_i1	hemolymph lipopolysaccharide-binding protein-like	1539	6,42	6,41E-12	3,50E-10	45,80%
TRINITY_DN32862_c0_g1_i2	---NA---	1961	6,42	4,97E-12		

TRINITY_DN14810_c0_g1_i1	40S ribosomal protein S10b	552	6,41	1,84E-12	2,70E-33	72,68%
TRINITY_DN2752_c0_g1_i1	60S Ribosomal Protein L9	630	6,41	1,38E-12	1,50E-62	71,46%
TRINITY_DN17960_c1_g1_i1	40S ribosomal protein S3	738	6,41	8,28E-13	4,40E-111	83,50%
TRINITY_DN26914_c0_g2_i1	heat shock 70 kDa protein 4 isoform X2	1711	6,40	2,48E-11	3,10E-36	44,67%
TRINITY_DN41666_c0_g1_i1	ATP synthase subunit gamma, mitochondrial	1106	6,40	1,19E-10	1,10E-56	58,76%
TRINITY_DN26495_c0_g1_i1	---NA---	1457	6,39	4,20E-11		
TRINITY_DN27817_c0_g3_i1	hypothetical protein FQR65_LT15628	1174	6,38	3,25E-10	3,70E-16	41,64%
TRINITY_DN12613_c1_g1_i1	40S ribosomal protein S11	544	6,38	1,18E-12	1,60E-69	80,85%
TRINITY_DN18843_c0_g1_i1	hypothetical protein THRCLA_04878	1428	6,38	4,85E-12	6,60E-06	40,60%
TRINITY_DN25656_c0_g1_i1	rab GDP dissociation inhibitor alpha	1631	6,37	2,86E-11	8,50E-176	73,15%
TRINITY_DN7102_c0_g1_i1	60S ribosomal protein L7	798	6,36	1,22E-12	5,10E-85	70,42%
TRINITY_DN12882_c0_g1_i1	gamma-aminobutyric acid receptor-associated protein	564	6,35	4,49E-10	2,30E-52	75,31%
TRINITY_DN30003_c1_g1_i1	ATP synthase subunit beta, mitochondrial	1683	6,34	1,58E-12	0,00E+00	85,02%
TRINITY_DN14301_c0_g1_i1	ubiquitin-conjugating enzyme E2-17 kDa	537	6,34	1,99E-10	7,50E-87	88,54%
TRINITY_DN34533_c1_g1_i2	60S ribosomal protein L10a	839	6,33	1,40E-12	9,50E-82	76,43%
TRINITY_DN36234_c0_g3_i1	lysosomal protective protein-like	1489	6,31	2,65E-11	1,10E-69	50,57%
TRINITY_DN11544_c0_g1_i1	60S ribosomal protein L13a	665	6,31	1,84E-12	6,20E-115	80,83%
TRINITY_DN28241_c0_g2_i1	ADP,ATP carrier protein 2	1021	6,30	9,68E-13	2,00E-103	68,20%
TRINITY_DN13315_c0_g1_i1	40S ribosomal protein SA	935	6,29	1,62E-12	4,50E-104	80,22%
TRINITY_DN27713_c0_g1_i1	Htp1, partial	1480	6,29	6,11E-10	1,00E-173	83,95%
TRINITY_DN42020_c0_g1_i1	60S ribosomal protein L24	580	6,28	2,76E-12	1,10E-17	64,89%
TRINITY_DN27742_c0_g3_i1	60s acidic ribosomal protein	503	6,28	6,35E-12	1,90E-10	67,83%
TRINITY_DN6985_c0_g1_i1	40S ribosomal protein S7	629	6,26	1,85E-12	2,20E-74	74,44%
TRINITY_DN32512_c2_g2_i1	heat shock protein 90	2250	6,26	3,45E-12	0,00E+00	75,25%
TRINITY_DN4947_c0_g1_i1	60S ribosomal protein L11	560	6,26	3,09E-12	6,40E-89	85,28%
TRINITY_DN34764_c1_g1_i1	60S ribosomal protein L15	681	6,26	1,46E-12	1,90E-79	77,51%

TRINITY_DN30350_c0_g1_i1	aconitate hydratase B	2845	6,26	5,34E-12	0,00E+00	65,24%
TRINITY_DN31317_c0_g1_i1	dynamin-A-like	2278	6,25	4,55E-11	5,40E-04	44,35%
TRINITY_DN42175_c0_g1_i1	40S ribosomal protein S28	356	6,24	2,65E-11	2,10E-29	88,23%
TRINITY_DN29214_c0_g1_i1	thioredoxin reductase 1, mitochondrial isoform X3	1654	6,23	7,28E-11	5,60E-154	67,81%
TRINITY_DN3761_c0_g1_i1	60S ribosomal protein L32	463	6,23	4,24E-12	4,20E-57	82,01%
TRINITY_DN24981_c0_g1_i3	DUF4114 domain-containing protein	1044	6,23	2,01E-11	1,10E-06	60,07%
TRINITY_DN29302_c3_g5_i1	calreticulin	1217	6,22	3,89E-11	1,30E-106	68,58%
TRINITY_DN35216_c0_g1_i7	nudix hydrolase 24, chloroplastic-like	1672	6,22	3,90E-10	3,30E-116	66,33%
TRINITY_DN28612_c0_g1_i1	60S ribosomal protein L7a-2	909	6,21	3,54E-12	8,30E-113	79,90%
TRINITY_DN30293_c1_g1_i1	40S ribosomal protein S9	306	6,20	1,61E-11	2,30E-25	91,79%
TRINITY_DN11407_c0_g1_i1	very long-chain-fatty-acid--CoA ligase bubblegum-like	2054	6,20	2,39E-11	7,30E-176	63,01%
TRINITY_DN5058_c0_g1_i1	40S ribosomal protein S21	322	6,20	6,68E-12	1,00E-28	72,38%
TRINITY_DN9415_c0_g1_i1	electron transfer flavoprotein subunit alpha, mitochondrial	1150	6,20	1,19E-10	1,70E-121	72,59%
TRINITY_DN32095_c1_g1_i1	ubiquitin-60S ribosomal protein L40	441	6,19	9,50E-12	4,40E-74	91,60%
TRINITY_DN19313_c0_g1_i1	unnamed protein product, partial	1261	6,19	2,03E-10	4,30E-17	47,35%
TRINITY_DN41544_c0_g1_i1	40S ribosomal protein S15Aa	479	6,19	9,87E-12	1,00E-68	89,73%
TRINITY_DN9153_c0_g1_i1	apolipoprotein D-like	761	6,18	2,39E-10	7,30E-14	47,55%
TRINITY_DN35272_c0_g2_i1	eukaryotic translation initiation factor 5A	624	6,17	1,14E-11	5,90E-51	69,91%
TRINITY_DN25802_c0_g1_i1	60S ribosomal protein	1365	6,16	1,89E-12	0,00E+00	86,98%
TRINITY_DN17214_c0_g1_i1	60S ribosomal protein L6-like	630	6,16	2,82E-12	1,70E-37	61,43%
TRINITY_DN19013_c0_g1_i1	Drug/Metabolite Transporter (DMT) Superfamily	1236	6,15	1,51E-09	3,70E-106	71,29%
TRINITY_DN25818_c0_g1_i1	unnamed protein product, partial	1607	6,14	3,36E-10	2,50E-34	49,47%
TRINITY_DN30161_c0_g1_i1	hypothetical protein EOO65_04725	1964	6,13	9,87E-11	6,60E-14	46,64%
TRINITY_DN36158_c1_g1_i1	Succinate dehydrogenase [ubiquinone] flavoprotein subunit, mitochondrial	1869	6,13	2,70E-11	0,00E+00	80,69%
TRINITY_DN41825_c0_g1_i1	60S ribosomal protein L14	469	6,13	7,25E-12	4,00E-36	64,02%
TRINITY_DN27492_c1_g2_i1	40S ribosomal protein S15	535	6,12	4,97E-12	8,40E-77	84,15%

TRINITY_DN31879_c0_g1_i3	NADH dehydrogenase subunit 3	942	6,11	6,28E-12	1,90E-23	69,25%
TRINITY_DN1410_c0_g1_i1	60S ribosomal protein L23	497	6,11	5,25E-12	5,70E-72	86,67%
TRINITY_DN25543_c0_g6_i1	40S ribosomal protein S5a	654	6,08	7,02E-12	1,10E-108	88,50%
TRINITY_DN3757_c0_g1_i1	glyoxalase 3-like	882	6,08	1,62E-11	7,30E-36	48,57%
TRINITY_DN16577_c0_g1_i1	40S ribosomal protein S29	353	6,07	1,20E-10	2,80E-16	76,21%
TRINITY_DN41216_c0_g1_i1	LOW QUALITY PROTEIN: uncharacterized protein LOC108624928	6856	6,06	5,23E-12	3,50E-04	42,06%
TRINITY_DN24938_c0_g1_i1	Chaperone protein	2205	6,06	3,10E-10	0,00E+00	68,62%
TRINITY_DN5419_c0_g1_i1	60S acidic ribosomal protein P2	421	6,05	7,56E-12	3,40E-12	73,55%
TRINITY_DN33813_c2_g2_i1	Myelin regulatory factor	1416	6,04	4,44E-11	6,70E-23	63,02%
TRINITY_DN41698_c0_g1_i1	40S ribosomal protein S12	512	6,04	6,13E-12	1,10E-37	72,45%
TRINITY_DN6547_c0_g1_i1	zinc-ribbon domain containing protein	533	6,04	1,24E-10	1,10E-20	78,64%
TRINITY_DN32662_c1_g4_i1	---NA---	819	6,04	3,47E-11		
TRINITY_DN15201_c0_g1_i1	unnamed protein product	790	6,03	1,30E-10	5,70E-110	74,25%
TRINITY_DN32862_c0_g1_i5	---NA---	1961	6,02	1,22E-10		
TRINITY_DN1467_c0_g1_i1	ankyrin repeat domain-containing protein	1757	6,01	6,27E-10	2,30E-37	52,71%
TRINITY_DN28542_c0_g1_i1	teneurin-m-like isoform X2	1843	6,01	2,08E-11	3,40E-10	38,87%
TRINITY_DN29621_c0_g1_i1	40S ribosomal protein S23	514	6,00	1,06E-11	2,40E-70	83,13%
TRINITY_DN18353_c0_g1_i1	60S ribosomal protein L26	527	6,00	9,88E-12	5,20E-51	73,48%
TRINITY_DN28103_c0_g2_i1	Cathepsin Z	934	5,99	2,54E-10	1,80E-51	52,52%
TRINITY_DN15472_c0_g1_i1	40S ribosomal protein S6-like	824	5,99	7,07E-12	2,20E-69	76,77%
TRINITY_DN24445_c0_g1_i1	teneurin-a isoform X2	1294	5,98	4,40E-11	1,20E-15	42,45%
TRINITY_DN28023_c0_g1_i1	ATP-dependent RNA helicase DEAH11, chloroplastic-like	1350	5,97	9,02E-11	3,20E-14	42,69%
TRINITY_DN24044_c0_g1_i1	nucleoredoxin 1	1456	5,96	5,04E-10	7,00E-131	60,24%
TRINITY_DN25352_c1_g1_i1	Cysteine proteinase	1164	5,95	6,27E-12	0,00E+00	65,63%
TRINITY_DN20367_c0_g2_i1	60S ribosomal protein L44	419	5,95	2,10E-11	2,30E-45	83,29%
TRINITY_DN27742_c0_g2_i1	60S acidic ribosomal protein P0	1125	5,94	1,35E-11	1,90E-84	67,89%

TRINITY_DN23019_c0_g1_i1	pyruvate dehydrogenase E1 component subunit beta, mitochondrial	1185	5,94	2,08E-10	1,00E-169	81,71%
TRINITY_DN158_c0_g1_i1	60S ribosomal protein L34	435	5,94	1,48E-11	1,50E-26	63,31%
TRINITY_DN4410_c0_g1_i1	translationally-controlled tumor protein homolog	579	5,93	2,91E-11	2,70E-16	48,38%
TRINITY_DN17431_c0_g1_i1	40S ribosomal protein S3a	913	5,93	8,55E-12	1,00E-174	80,33%
TRINITY_DN16624_c0_g1_i1	Proteasome subunit beta type-5	992	5,92	1,13E-09	6,00E-101	75,54%
TRINITY_DN6353_c0_g1_i1	40S ribosomal protein S20	456	5,90	1,49E-11	4,90E-47	84,65%
TRINITY_DN41580_c0_g1_i1	60S ribosomal protein L35a	412	5,90	1,78E-11	6,50E-28	63,32%
TRINITY_DN28310_c0_g1_i1	unnamed protein product, partial	1917	5,88	1,06E-10	2,60E-81	47,71%
TRINITY_DN19103_c0_g1_i1	hypothetical protein EON65_06110	504	5,88	9,69E-10	1,70E-04	56,06%
TRINITY_DN14260_c0_g1_i1	60S ribosomal protein L27a	513	5,88	1,98E-11	4,00E-56	76,75%
TRINITY_DN2735_c0_g1_i1	DUF2778 domain-containing protein	729	5,88	6,27E-10	3,30E-86	63,02%
TRINITY_DN27975_c0_g1_i1	zingipain-2-like isoform X1	1255	5,87	5,64E-10	3,90E-65	56,39%
TRINITY_DN29252_c0_g1_i3	reversion-inducing cysteine-rich protein with Kazal motifs-like	484	5,86	1,24E-11	3,10E-04	48,65%
TRINITY_DN943_c0_g1_i1	60S ribosomal protein L37	358	5,85	2,49E-10	1,20E-34	84,91%
TRINITY_DN32662_c2_g1_i1	crinkler family protein	2343	5,85	7,40E-11	2,30E-22	41,58%
TRINITY_DN14549_c0_g1_i1	40S ribosomal protein S2	1026	5,83	2,20E-11	5,30E-131	87,23%
TRINITY_DN30587_c1_g3_i1	Calmodulin	533	5,83	1,77E-10	1,30E-100	98,16%
TRINITY_DN29795_c1_g1_i1	ATP synthase subunit alpha, mitochondrial-like	1108	5,83	3,80E-10	0,00E+00	82,43%
TRINITY_DN16677_c0_g1_i1	cathepsin L1-like	1285	5,82	3,12E-10	2,80E-50	50,56%
TRINITY_DN26871_c0_g1_i1	receptor of activated protein C kinase 1	1146	5,81	2,39E-11	2,40E-177	86,11%
TRINITY_DN28318_c1_g1_i1	phosphate carrier protein, mitochondrial	1244	5,81	7,98E-11	3,80E-45	58,72%
TRINITY_DN28817_c0_g1_i1	Tubular mastigoneme-related protein	2247	5,77	7,57E-11	0,00E+00	57,05%
TRINITY_DN12243_c0_g1_i1	Creatine kinase, flagellar	1562	5,77	3,80E-10	1,10E-170	68,68%
TRINITY_DN34848_c0_g1_i2	unnamed protein product, partial	2877	5,75	1,67E-09	0,00E+00	51,94%
TRINITY_DN27102_c0_g1_i1	unnamed protein product	1301	5,72	2,96E-09	1,20E-24	54,95%
TRINITY_DN20405_c0_g1_i2	bacillopeptidase F	1411	5,71	1,15E-10	8,30E-46	51,27%

TRINITY_DN26393_c0_g1_i1	protein kinase	1633	5,71	5,98E-10	2,90E-141	57,70%
TRINITY_DN32054_c5_g2_i2	---NA---	1357	5,71	2,54E-11		
TRINITY_DN13603_c0_g1_i1	nascent polypeptide-associated complex subunit alpha	604	5,69	1,62E-10	9,10E-44	69,16%
TRINITY_DN16497_c0_g1_i1	Mitochondrial-processing peptidase subunit alpha	1429	5,69	6,57E-10	0,00E+00	51,36%
TRINITY_DN14057_c0_g1_i1	dTDP-glucose 4,6-dehydratase-like	1067	5,68	8,25E-10	3,00E-96	56,77%
TRINITY_DN33675_c1_g1_i1	ubiquitin-40S ribosomal protein S27a	345	5,67	9,66E-11	3,20E-20	83,53%
TRINITY_DN30953_c3_g4_i1	actin	331	5,66	9,92E-11	1,20E-69	98,09%
TRINITY_DN29868_c0_g1_i1	unnamed protein product	762	5,65	5,31E-10	1,20E-132	56,82%
TRINITY_DN18011_c0_g1_i1	malate dehydrogenase, mitochondrial	1032	5,65	1,19E-09	5,10E-136	75,83%
TRINITY_DN32361_c0_g1_i1	---NA---	1198	5,63	6,94E-09		
TRINITY_DN21367_c0_g2_i1	cathepsin L-like proteinase	1162	5,63	7,24E-11	8,10E-57	54,23%
TRINITY_DN26180_c1_g2_i1	unnamed protein product, partial	2251	5,62	7,61E-10	8,10E-120	51,60%
TRINITY_DN23493_c0_g1_i1	Phosphoethanolamine N-methyltransferase 3	1343	5,62	3,88E-10	4,40E-12	47,99%
TRINITY_DN23746_c0_g1_i1	---NA---	660	5,62	8,93E-10		
TRINITY_DN35786_c2_g3_i1	Crinkler (CRN)	1552	5,62	2,01E-10	3,40E-28	46,88%
TRINITY_DN32065_c1_g1_i5	heat shock protein 70 kDa	857	5,62	7,11E-10	3,00E-92	85,48%
TRINITY_DN11244_c0_g1_i1	transcription factor BTF3 homolog 4	598	5,61	1,64E-10	1,50E-40	73,97%
TRINITY_DN19382_c0_g1_i1	voltage-dependent anion-selective channel protein 2-like	1027	5,59	5,17E-10	3,30E-04	44,01%
TRINITY_DN29785_c2_g1_i2	polyubiquitin	421	5,57	1,48E-08	5,60E-62	98,95%
TRINITY_DN34848_c0_g1_i1	unnamed protein product, partial	3079	5,56	1,08E-09	0,00E+00	52,95%
TRINITY_DN25165_c0_g2_i1	S-adenosylmethionine synthase-like	1394	5,55	1,75E-10	2,70E-176	79,17%
TRINITY_DN7541_c0_g1_i1	40S Ribosomal Protein S27	348	5,54	6,11E-10	2,40E-44	89,81%
TRINITY_DN29374_c1_g1_i1	Nephrocystin-3 like protein	432	5,53	4,46E-10	4,10E-14	66,88%
TRINITY_DN27583_c0_g2_i1	DUF4114 domain-containing protein	1056	5,53	1,29E-09	2,40E-14	48,54%
TRINITY_DN26770_c0_g2_i1	twitchin isoform X3	2103	5,51	1,07E-09	3,00E-14	45,94%
TRINITY_DN34028_c1_g1_i1	chaperone DnaK	1623	5,50	2,09E-09	0,00E+00	87,01%

TRINITY_DN19517_c0_g1_i1	hypothetical protein EON65_37755	1215	5,50	3,79E-09	1,80E-19	46,97%
TRINITY_DN29785_c2_g1_i6	ubiquitin-related domain-containing protein	601	5,50	1,38E-09	2,50E-102	98,75%
TRINITY_DN38042_c0_g1_i6	Tubulin alpha chain	332	5,49	1,89E-09	5,40E-59	97,78%
TRINITY_DN30208_c0_g1_i1	eukaryotic translation initiation factor 4 gamma 2 isoform X2	2588	5,49	3,29E-10	1,00E-05	56,08%
TRINITY_DN27401_c0_g1_i1	predicted protein	1215	5,48	8,75E-09	3,80E-112	74,15%
TRINITY_DN26329_c0_g1_i1	teneurin-m-like isoform X1	1179	5,48	6,53E-10	2,60E-12	40,07%
TRINITY_DN22906_c0_g1_i1	cytochrome c1, heme protein, mitochondrial-like	918	5,46	1,65E-09	3,90E-89	70,50%
TRINITY_DN6061_c0_g1_i1	40S ribosomal protein S13	541	5,46	2,58E-10	2,00E-90	92,61%
TRINITY_DN25553_c0_g1_i1	polyadenylate-binding protein 4-like	2024	5,46	1,75E-10	1,30E-151	73,67%
TRINITY_DN32448_c1_g2_i1	DNA-directed RNA polymerase II subunit RPB1-like	435	5,45	8,50E-10	1,60E-05	55,43%
TRINITY_DN34762_c1_g1_i1	protein ref(2)P-like isoform X3	2619	5,42	2,26E-10	1,90E-15	54,19%
TRINITY_DN26962_c0_g1_i1	Mitochondrial-processing peptidase subunit beta	1577	5,42	2,58E-09	7,40E-171	68,03%
TRINITY_DN29785_c2_g1_i1	UBIQ1 protein	580	5,42	6,12E-10	5,20E-79	96,37%
TRINITY_DN28081_c0_g1_i1	AMP deaminase 2 isoform X2	2694	5,42	8,93E-10	0,00E+00	83,77%
TRINITY_DN33327_c1_g2_i2	14-3-3-like protein B	820	5,41	2,85E-09	1,10E-106	72,36%
TRINITY_DN30587_c1_g3_i2	Calmodulin	494	5,39	5,34E-09	6,70E-101	98,91%
TRINITY_DN21859_c0_g1_i1	T-complex protein 1 subunit beta	1631	5,37	4,66E-09	0,00E+00	83,65%
TRINITY_DN27733_c0_g1_i1	teneurin-a isoform X1	2132	5,36	9,75E-10	1,80E-07	36,84%
TRINITY_DN17900_c0_g1_i1	unnamed protein product	992	5,34	8,17E-10	3,10E-23	45,74%
TRINITY_DN28237_c0_g2_i1	Dynein heavy chain 8, axonemal	2292	5,32	7,04E-09	1,10E-173	59,11%
TRINITY_DN27603_c0_g10_i1	K(+)-stimulated pyrophosphate-energized sodium pump	2268	5,31	1,10E-09	6,90E-161	59,05%
TRINITY_DN41115_c2_g1_i7	hypothetical protein ALO46_101454	402	5,29	1,89E-09	3,30E-29	74,66%
TRINITY_DN35642_c1_g1_i3	---NA---	379	5,29	2,48E-09		
TRINITY_DN31372_c2_g2_i1	heat shock protein 83	1577	5,28	1,99E-09	3,50E-127	66,25%
TRINITY_DN31263_c0_g2_i1	histone H3	564	5,24	1,62E-08	2,50E-90	98,01%
TRINITY_DN34028_c2_g2_i3	heat shock protein 70	1155	5,21	1,91E-08	0,00E+00	93,24%

TRINITY_DN29302_c3_g2_i1	calreticulin	1288	5,19	1,24E-08	9,40E-100	68,48%
TRINITY_DN23454_c1_g1_i1	unnamed protein product	2260	5,17	9,25E-09	0,00E+00	57,57%
TRINITY_DN31410_c0_g2_i1	alpha tubulin	573	5,16	9,47E-09	2,50E-138	99,66%
TRINITY_DN29252_c0_g1_i1	reversion-inducing cysteine-rich protein with Kazal motifs-like	398	5,15	1,20E-08	8,20E-05	48,65%
TRINITY_DN26757_c0_g1_i1	peptidase S1 and S6, chymotrypsin/Hap	1565	5,13	1,18E-08	8,50E-81	57,74%
TRINITY_DN31557_c1_g1_i1	tubulin alpha chain	471	5,12	5,36E-08	1,70E-64	93,97%
TRINITY_DN13221_c0_g1_i1	propionyl-CoA carboxylase alpha chain, mitochondrial-like	1863	5,11	2,06E-08	2,50E-144	59,04%
TRINITY_DN32065_c1_g1_i1	heat shock protein 70	720	5,10	2,09E-08	1,20E-72	83,21%
TRINITY_DN12889_c0_g1_i1	unnamed protein product	1247	5,09	2,41E-08	0,00E+00	92,31%
TRINITY_DN28213_c0_g1_i1	hypothetical protein B566_EDAN000208	1036	5,09	1,19E-08	2,70E-78	62,62%
TRINITY_DN36535_c0_g1_i7	RNA polymerase II subunit A C-terminal domain phosphatase SSU72	2736	5,08	1,15E-08	3,70E-127	85,64%
TRINITY_DN33813_c2_g1_i2	---NA---	659	5,07	4,73E-09		
TRINITY_DN21367_c0_g3_i1	cathepsin L1-like	1204	5,06	5,58E-09	2,10E-55	52,38%
TRINITY_DN25949_c0_g1_i1	PREDICTED: uncharacterized protein LOC109039891	1929	5,05	3,09E-08	1,20E-52	48,52%
TRINITY_DN34225_c0_g1_i1	---NA---	1817	5,04	1,18E-08		
TRINITY_DN226_c0_g1_i1	GTP-binding nuclear protein Ran	792	4,93	5,53E-08	6,00E-118	87,86%
TRINITY_DN34225_c0_g1_i2	gliding motility-associated C-terminal domain-containing protein	3081	4,93	5,23E-09	1,00E-75	53,96%
TRINITY_DN33710_c0_g1_i2	---NA---	2463	4,92	1,37E-08		
TRINITY_DN29595_c0_g1_i1	---NA---	1271	4,90	1,14E-07		
TRINITY_DN842_c0_g1_i1	ran-specific GTPase-activating protein-like	839	4,85	3,06E-08	6,80E-33	63,56%
TRINITY_DN13761_c0_g1_i1	Ig-like domain-containing protein	954	4,84	6,74E-08	2,20E-24	53,34%
TRINITY_DN16083_c0_g3_i1	---NA---	1089	4,80	1,06E-07		
TRINITY_DN14900_c0_g1_i1	Ras-like GTP-binding protein YPT1	838	4,80	1,59E-07	4,40E-121	88,36%
TRINITY_DN29654_c0_g1_i1	---NA---	2015	4,79	5,84E-08		
TRINITY_DN33829_c0_g4_i2	endoplasmic reticulum chaperone BiP-like	1437	4,78	4,95E-08	0,00E+00	84,04%
TRINITY_DN30089_c0_g2_i4	---NA---	421	4,77	1,80E-07		

TRINITY_DN31412_c1_g1_i4	---NA---	1512	4,73	9,71E-07		
TRINITY_DN38726_c2_g1_i6	C-Myc-binding protein	746	4,73	3,65E-07	6,40E-27	76,92%
TRINITY_DN32924_c2_g1_i2	hypothetical protein FOL47_001262	986	4,71	1,53E-07	9,90E-07	50,33%
TRINITY_DN31317_c0_g1_i2	dynamin-A-like	2232	4,69	1,94E-07	5,20E-04	44,35%
TRINITY_DN15212_c0_g1_i1	putative subtilisin-like proteinase 1	1302	4,68	2,80E-07	6,80E-40	52,96%
TRINITY_DN29598_c3_g1_i17	polyubiquitin	435	4,66	5,64E-08	3,90E-91	94,00%
TRINITY_DN30003_c2_g2_i1	ATP synthase subunit beta, mitochondrial	2218	4,65	6,44E-08	0,00E+00	84,88%
TRINITY_DN38049_c1_g1_i15	Survival of motor neuron-related-splicing factor 30	1342	4,64	1,20E-07	2,20E-59	57,15%
TRINITY_DN16232_c0_g1_i1	unnamed protein product	1542	4,64	1,50E-07	2,50E-25	51,26%
TRINITY_DN29540_c0_g1_i1	transforming growth factor-beta-induced protein ig-h3-like isoform X2	746	4,60	3,90E-08	1,60E-38	65,58%
TRINITY_DN34936_c2_g2_i3	heat shock protein 70	1361	4,54	2,68E-07	1,30E-179	84,81%
TRINITY_DN31622_c0_g3_i14	hypothetical protein B566_EDAN011676	823	4,51	7,32E-08	5,90E-07	69,70%
TRINITY_DN30169_c0_g1_i10	tubulin beta chain	485	4,49	7,07E-07	7,90E-102	99,58%
TRINITY_DN31211_c0_g1_i1	hypothetical protein B566_EDAN011676	471	4,45	2,05E-07	1,70E-24	65,13%
TRINITY_DN28473_c0_g1_i2	Mitogen-activated protein kinase kinase kinase 2	717	4,43	6,02E-07	6,60E-25	53,20%
TRINITY_DN38042_c0_g1_i4	tubulin alpha-1 chain-like	877	4,43	4,73E-07	6,80E-170	95,74%
TRINITY_DN33835_c2_g1_i4	tubulin beta chain	959	4,42	2,31E-07	0,00E+00	93,46%
TRINITY_DN29619_c1_g1_i1	hypothetical protein TCAL_13779, partial	4710	4,34	4,98E-07	1,30E-116	48,31%
TRINITY_DN28224_c1_g1_i1	COG1938 domain-containing protein	1231	4,31	7,25E-07	3,10E-15	46,97%
TRINITY_DN28372_c0_g1_i1	DUF4114 domain-containing protein	1159	4,30	1,39E-06	1,30E-08	43,93%
TRINITY_DN38336_c0_g1_i1	longitudinals lacking protein-like	2137	4,25	5,71E-07	2,80E-53	63,77%
TRINITY_DN32006_c1_g1_i3	Low choriolytic enzyme,Tolloid-like protein 2,Zinc metalloproteinase nas-13,Embry-onic protein UVS.2	420	4,24	5,23E-07	1,40E-04	49,10%
TRINITY_DN31821_c0_g1_i2	TENM1	2821	4,23	8,57E-06	2,20E-15	52,37%
TRINITY_DN30057_c0_g3_i6	UDP-N-acetylglucosamine 1-carboxyvinyltransferase-like	486	4,22	7,87E-07	2,30E-16	62,22%
TRINITY_DN37291_c1_g1_i6	eukaryotic translation initiation factor 4E transporter-like isoform X2	368	4,17	6,11E-07	6,40E-11	74,78%
TRINITY_DN37761_c2_g1_i3	tubulin beta chain	809	4,15	2,41E-06	1,20E-164	93,77%

TRINITY_DN15324_c0_g1_i1	zinc finger protein 2-like	745	4,14	3,19E-06	2,40E-04	69,88%
TRINITY_DN37728_c0_g1_i1	xyloside xylosyltransferase 1-like	1244	4,14	2,60E-06	2,20E-22	50,03%
TRINITY_DN30474_c1_g2_i7	Uncharacterised protein	720	4,13	1,24E-06	1,80E-62	73,51%
TRINITY_DN40162_c2_g1_i2	tetratricopeptide repeat protein 37	4080	4,11	8,99E-07	0,00E+00	51,71%
TRINITY_DN36016_c2_g1_i2	---NA---	912	4,08	1,16E-06		
TRINITY_DN31410_c0_g3_i15	Tubulin alpha chain	614	4,08	3,98E-06	2,80E-118	99,17%
TRINITY_DN36403_c0_g2_i5	keratin-associated protein 10-4-like isoform X2	1479	4,07	1,73E-06	1,30E-09	41,38%
TRINITY_DN32519_c0_g1_i1	60S ribosomal protein L7	779	4,06	1,07E-05	1,10E-102	78,27%
TRINITY_DN29339_c3_g3_i1	heat shock protein 68-like	2412	4,06	2,79E-06	0,00E+00	69,86%
TRINITY_DN17848_c0_g2_i1	40S ribosomal protein S11-like	581	4,03	2,70E-06	1,30E-61	78,22%
TRINITY_DN33829_c0_g3_i2	heat shock 70 kDa protein cognate 4-like	1149	4,03	2,59E-06	0,00E+00	85,07%
TRINITY_DN33829_c0_g5_i2	endoplasmic reticulum chaperone BiP	2030	3,99	2,62E-06	0,00E+00	83,98%
TRINITY_DN32006_c1_g1_i4	Low choriolytic enzyme,Tolloid-like protein 2,Zinc metalloproteinase nas-13,Embry-onic protein UVS.2	443	3,99	3,41E-06	1,40E-05	49,82%
TRINITY_DN32313_c1_g1_i10	10 kDa putative secreted protein	484	3,98	1,79E-06	5,70E-23	69,97%
TRINITY_DN33941_c0_g1_i3	cytochrome c oxidase subunit III	2331	3,96	2,09E-06	3,70E-95	81,33%
TRINITY_DN29649_c3_g1_i1	elongation factor 1-alpha 2	1587	3,95	2,49E-06	4,40E-122	61,64%
TRINITY_DN41314_c0_g1_i1	Regulator of rDNA transcription protein 15	521	3,93	2,58E-06	8,70E-43	90,00%
TRINITY_DN33835_c2_g1_i3	tubulin beta chain	959	3,93	3,18E-06	0,00E+00	93,46%
TRINITY_DN33068_c2_g1_i4	UPF0389 protein CG9231	754	3,91	6,38E-06	5,30E-34	53,12%
TRINITY_DN29059_c3_g3_i3	rRNA 2'-O-methyltransferase fibrillarin	3287	3,91	3,19E-06	8,60E-123	88,18%
TRINITY_DN29614_c0_g1_i2	translation elongation factor 2	2798	3,91	3,13E-06	0,00E+00	72,28%
TRINITY_DN30960_c0_g2_i17	mucin-22-like isoform X1	1140	3,91	9,84E-06	5,00E-36	59,40%
TRINITY_DN31410_c0_g3_i10	Tubulin alpha chain	790	3,91	5,74E-06	3,10E-136	89,89%
TRINITY_DN27003_c0_g1_i1	probable acyl-CoA dehydrogenase 6	1658	3,90	1,06E-05	0,00E+00	52,39%
TRINITY_DN39749_c0_g1_i9	receptor-type guanylate cyclase Gyc76C-like	3355	3,88	7,13E-06	0,00E+00	72,34%
TRINITY_DN21763_c0_g1_i1	RGGB, partial	947	3,87	9,84E-06	7,40E-06	71,01%

TRINITY_DN32607_c2_g1_i4	uncharacterized protein LOC111711309	630	3,85	5,21E-06	1,50E-13	66,20%
TRINITY_DN33567_c0_g1_i7	RidA family protein	436	3,85	1,61E-05	5,20E-42	71,29%
TRINITY_DN23780_c0_g1_i2	---NA---	1103	3,84	7,32E-06		
TRINITY_DN36578_c0_g1_i3	GATOR complex protein WDR24-like	2987	3,83	5,94E-06	0,00E+00	55,50%
TRINITY_DN32068_c0_g1_i2	L-xylulose reductase	1025	3,82	7,71E-06	4,10E-107	54,55%
TRINITY_DN12672_c1_g1_i1	60S ribosomal protein L32	573	3,81	7,71E-06	1,30E-37	72,40%
TRINITY_DN16405_c0_g1_i1	40S ribosomal protein S24, putative	636	3,81	1,16E-05	8,70E-55	70,18%
TRINITY_DN31049_c4_g2_i5	---NA---	3339	3,80	9,92E-06		
TRINITY_DN31464_c0_g1_i1	---NA---	491	3,80	5,87E-06		
TRINITY_DN31052_c1_g1_i3	Hypothetical predicted protein	618	3,79	6,25E-06	1,90E-40	55,07%
TRINITY_DN30827_c1_g1_i9	hypothetical protein Ae201684_019105, partial	536	3,77	1,00E-05	3,20E-19	75,28%
TRINITY_DN32379_c1_g1_i7	putative transcription factor	397	3,74	8,87E-06	5,40E-30	87,59%
TRINITY_DN37225_c0_g1_i3	---NA---	1574	3,74	1,57E-05		
TRINITY_DN37761_c2_g1_i5	tubulin beta chain isoform X2	798	3,73	2,41E-05	3,30E-163	93,45%
TRINITY_DN30373_c1_g2_i3	---NA---	669	3,72	1,10E-05		
TRINITY_DN30292_c0_g1_i2	unc-112-related protein-like	1741	3,71	5,36E-05	0,00E+00	74,36%
TRINITY_DN34065_c2_g2_i1	transcript antisense to ribosomal rna protein	1012	3,71	1,06E-05	4,80E-18	62,59%
TRINITY_DN31737_c1_g1_i1	heat shock 70 kDa protein 1-like	882	3,71	1,11E-05	4,70E-129	85,65%
TRINITY_DN30088_c1_g2_i1	hypothetical protein FQR65_LT18893	711	3,70	1,02E-05	6,90E-17	59,78%
TRINITY_DN18968_c0_g1_i1	60S ribosomal protein L13a	670	3,68	1,63E-05	1,10E-68	75,69%
TRINITY_DN37318_c0_g1_i2	60S ribosomal protein L34	472	3,68	2,72E-05	7,90E-28	70,14%
TRINITY_DN29594_c2_g1_i1	uncharacterized protein LOC111712120 isoform X2	792	3,68	1,55E-05	1,50E-73	87,13%
TRINITY_DN38308_c1_g4_i1	60S ribosomal protein L9	681	3,67	1,68E-05	3,50E-62	70,86%
TRINITY_DN25543_c0_g1_i1	40S ribosomal protein S5	668	3,67	4,37E-05	3,60E-102	84,22%
TRINITY_DN33835_c2_g1_i1	tubulin beta chain	959	3,66	2,37E-05	0,00E+00	93,46%
TRINITY_DN34550_c0_g1_i5	---NA---	957	3,65	1,26E-05		

TRINITY_DN41269_c1_g1_i1	chromatin-remodeling ATPase INO80	5722	3,65	1,83E-05	0,00E+00	65,80%
TRINITY_DN33622_c0_g2_i1	40S ribosomal protein S3a	925	3,64	1,76E-05	1,50E-91	76,62%
TRINITY_DN18874_c0_g1_i1	40S ribosomal protein S4	874	3,63	6,37E-05	1,80E-125	77,65%
TRINITY_DN30766_c1_g1_i8	---NA---	458	3,62	1,89E-05		
TRINITY_DN20613_c0_g1_i1	60S ribosomal protein L31	504	3,61	2,47E-05	9,00E-65	79,07%
TRINITY_DN29532_c0_g1_i14	putative salivary gland protein 14	1185	3,60	3,48E-05	2,80E-19	68,37%
TRINITY_DN18147_c0_g2_i1	40S ribosomal protein S7	693	3,60	2,86E-05	9,70E-53	67,69%
TRINITY_DN28681_c0_g1_i5	OmpA family protein	2379	3,57	4,21E-05	7,80E-106	48,66%
TRINITY_DN32379_c1_g1_i16	RRT15 protein	603	3,57	2,39E-05	8,00E-44	70,42%
TRINITY_DN40711_c1_g2_i6	---NA---	333	3,57	9,07E-05		
TRINITY_DN31755_c0_g1_i6	leucine-rich repeat-containing protein 20 isoform X2	2292	3,56	5,79E-05	2,60E-65	73,05%
TRINITY_DN30875_c0_g1_i5	---NA---	448	3,56	2,84E-05		
TRINITY_DN41720_c0_g1_i1	Eukaryotic translation initiation factor 5A	594	3,56	5,35E-05	9,50E-38	63,35%
TRINITY_DN31393_c1_g1_i1	40S ribosomal protein S17	672	3,55	4,03E-05	4,90E-37	81,40%
TRINITY_DN29189_c0_g4_i1	40S ribosomal protein S9	749	3,53	3,93E-05	1,50E-54	76,95%
TRINITY_DN32519_c1_g1_i2	60S ribosomal protein L7	930	3,53	3,94E-05	3,90E-80	75,72%
TRINITY_DN31994_c1_g1_i4	uncharacterized protein LOC111698109	1314	3,52	2,77E-05	4,50E-63	86,71%
TRINITY_DN32893_c0_g1_i1	myelin P2 protein-like	822	3,52	5,98E-05	3,40E-36	55,81%
TRINITY_DN32607_c2_g1_i1	uncharacterized protein LOC111711309	481	3,52	6,03E-05	3,30E-13	66,93%
TRINITY_DN12404_c0_g1_i1	60S ribosomal protein L19	665	3,50	4,95E-05	5,80E-47	82,30%
TRINITY_DN30169_c0_g1_i12	beta-tubulin	515	3,49	1,18E-04	8,40E-100	99,17%
TRINITY_DN37468_c0_g1_i3	4-aminobutyrate aminotransferase, mitochondrial	1736	3,48	6,74E-05	0,00E+00	73,16%
TRINITY_DN32743_c0_g4_i1	60S acidic ribosomal protein P2	485	3,47	5,61E-05	1,50E-14	77,97%
TRINITY_DN30474_c1_g3_i1	Cell wall-associated hydrolase	536	3,47	4,71E-05	1,80E-65	83,42%
TRINITY_DN25543_c0_g2_i1	40S ribosomal protein S5	747	3,47	4,88E-05	6,30E-94	80,80%
TRINITY_DN35502_c1_g6_i1	---NA---	2123	3,47	8,22E-05		

TRINITY_DN35269_c0_g1_i8	---NA---	336	3,47	6,01E-05		
TRINITY_DN10935_c0_g1_i1	60S ribosomal protein L29	384	3,46	8,97E-05	2,70E-14	75,65%
TRINITY_DN33999_c1_g1_i1	---NA---	659	3,46	9,26E-05		
TRINITY_DN9945_c0_g1_i1	40S ribosomal protein S19a-like	668	3,46	7,39E-05	6,40E-38	61,55%
TRINITY_DN42167_c0_g1_i1	40S ribosomal protein S14a	591	3,46	6,42E-05	9,20E-76	89,37%
TRINITY_DN41929_c0_g1_i1	60S ribosomal protein L27	770	3,45	6,42E-05	6,10E-35	63,56%
TRINITY_DN31821_c0_g1_i1	TENM1	3913	3,45	5,77E-05	3,80E-15	52,37%
TRINITY_DN16343_c0_g1_i1	40S ribosomal protein S3	907	3,44	6,83E-05	1,20E-92	74,25%
TRINITY_DN32307_c0_g2_i1	60S ribosomal protein L8	954	3,44	5,82E-05	5,10E-105	78,52%
TRINITY_DN26756_c0_g4_i1	60S ribosomal protein L23	588	3,43	7,39E-05	2,30E-77	88,53%
TRINITY_DN30066_c3_g2_i9	actin, cytoplasmic A3a	961	3,43	1,39E-04	0,00E+00	93,91%
TRINITY_DN27492_c0_g1_i1	40S ribosomal protein S15-4	635	3,42	7,38E-05	7,50E-91	78,75%
TRINITY_DN17819_c0_g2_i1	60S ribosomal protein L21	649	3,42	7,88E-05	8,40E-51	67,98%
TRINITY_DN35340_c1_g1_i1	presenilins-associated rhomboid-like protein, mitochondrial isoform X1	1371	3,42	6,61E-05	8,60E-143	63,91%
TRINITY_DN10346_c0_g1_i1	60S ribosomal protein L30	577	3,42	8,01E-05	9,20E-47	79,07%
TRINITY_DN29649_c4_g2_i1	elongation factor 1-alpha	1256	3,41	5,92E-05	0,00E+00	78,95%
TRINITY_DN34540_c0_g1_i2	leucine-rich repeat-containing protein 15-like	3546	3,41	1,40E-04	0,00E+00	46,54%
TRINITY_DN40631_c1_g1_i1	ATP-dependent DNA/RNA helicase DHX36 isoform X3	3353	3,41	6,10E-05	0,00E+00	67,99%
TRINITY_DN29043_c0_g1_i1	40S ribosomal protein S6-like	857	3,40	7,85E-05	2,50E-77	75,74%
TRINITY_DN20750_c0_g1_i1	40S ribosomal protein S4	964	3,40	7,39E-05	7,00E-108	76,07%
TRINITY_DN39043_c0_g1_i16	Uncharacterized protein APZ42_005135	658	3,39	7,66E-05	5,00E-05	67,50%
TRINITY_DN29163_c0_g1_i2	---NA---	525	3,39	9,11E-05		
TRINITY_DN37032_c0_g2_i1	guanine nucleotide-binding protein subunit beta-like protein	1050	3,38	8,30E-05	4,00E-143	77,89%
TRINITY_DN26229_c0_g1_i2	60S ribosomal protein L18	904	3,38	8,81E-05	2,20E-59	74,43%
TRINITY_DN31486_c1_g2_i1	40S ribosomal protein S23	566	3,38	9,98E-05	8,70E-88	89,93%
TRINITY_DN34314_c0_g1_i1	predicted protein	3120	3,38	7,88E-05	1,60E-35	47,77%

TRINITY_DN23606_c0_g1_i1	cyclin-dependent kinase 9-like	1847	3,38	1,62E-04	7,80E-67	58,45%
TRINITY_DN33668_c0_g1_i1	heat shock protein 90	2467	3,37	8,57E-05	0,00E+00	65,33%
TRINITY_DN32743_c0_g3_i2	60S acidic ribosomal protein P0-like	1006	3,36	9,39E-05	7,30E-85	67,62%
TRINITY_DN27765_c0_g1_i1	60S ribosomal protein L5-A-like	1220	3,36	9,30E-05	2,00E-66	55,74%
TRINITY_DN28927_c1_g3_i1	40S ribosomal protein S8	737	3,36	9,84E-05	1,30E-73	76,81%
TRINITY_DN29043_c1_g2_i1	60S ribosomal protein L4	1248	3,36	9,53E-05	8,00E-122	72,67%
TRINITY_DN33491_c0_g2_i12	---NA---	1525	3,35	2,00E-04		
TRINITY_DN17689_c0_g1_i2	60S ribosomal protein L24	625	3,35	1,27E-04	5,10E-09	64,00%
TRINITY_DN24479_c0_g2_i1	60S ribosomal protein L10a	980	3,34	9,26E-05	1,80E-71	72,45%
TRINITY_DN38627_c0_g1_i1	RecName: Full=60S acidic ribosomal protein P1; AltName: Full=eL12'/ eL12'-P	495	3,34	1,43E-04	2,80E-04	59,21%
TRINITY_DN32090_c0_g1_i3	---NA---	573	3,34	9,54E-05		
TRINITY_DN31878_c1_g2_i3	ubiquitin-40S ribosomal protein S27a	537	3,34	8,19E-05	6,10E-86	94,30%
TRINITY_DN22803_c1_g1_i1	60S ribosomal protein L12	696	3,33	1,54E-04	6,30E-66	74,76%
TRINITY_DN17220_c0_g1_i1	60S ribosomal protein L28-like protein	476	3,33	1,59E-04	2,60E-06	54,00%
TRINITY_DN27799_c0_g1_i1	protein ILRUN	1468	3,33	2,28E-04	1,70E-17	54,70%
TRINITY_DN5779_c0_g1_i1	40S ribosomal protein S27	546	3,33	1,67E-04	9,60E-32	74,83%
TRINITY_DN41314_c0_g1_i4	Regulator of rDNA transcription protein 15	550	3,33	1,02E-04	1,60E-45	71,48%
TRINITY_DN39277_c1_g1_i8	nuclear transcription factor Y subunit beta isoform X1	1727	3,31	1,17E-04	9,20E-57	83,12%
TRINITY_DN18826_c0_g1_i1	capsid protein	1738	3,31	1,64E-04	2,00E-62	49,33%
TRINITY_DN29235_c0_g1_i4	40S ribosomal protein SA	1128	3,31	1,46E-04	1,20E-92	78,42%
TRINITY_DN28513_c0_g1_i1	Elongation factor 1-gamma	1427	3,31	1,63E-04	1,30E-74	50,70%
TRINITY_DN13345_c0_g1_i1	40S ribosomal protein S10	655	3,30	1,85E-04	3,60E-34	74,42%
TRINITY_DN4328_c0_g1_i1	40S ribosomal protein S15Aa	504	3,30	1,42E-04	1,60E-69	86,66%
TRINITY_DN20500_c0_g1_i1	60S ribosomal protein L13	702	3,30	1,65E-04	8,30E-45	66,99%
TRINITY_DN41925_c0_g1_i1	60S ribosomal protein L44 Q	439	3,29	2,04E-04	5,00E-51	84,14%
TRINITY_DN29370_c1_g2_i2	60S ribosomal protein L11	657	3,28	1,64E-04	1,10E-71	76,94%

TRINITY_DN27444_c0_g1_i1	60S ribosomal protein L23a	608	3,27	1,77E-04	8,40E-75	74,21%
TRINITY_DN24161_c0_g1_i1	40S ribosomal protein S16	575	3,26	2,12E-04	1,40E-70	86,72%
TRINITY_DN41314_c1_g3_i1	Regulator of rDNA transcription protein 15	332	3,26	1,57E-04	5,90E-30	59,81%
TRINITY_DN33327_c1_g1_i1	14-3-3-like protein GF14 iota	893	3,26	2,83E-04	2,90E-105	78,47%
TRINITY_DN20243_c0_g1_i1	hypothetical protein EON62_04840	635	3,25	2,53E-04	2,10E-25	55,00%
TRINITY_DN26487_c0_g1_i3	---NA---	402	3,25	1,91E-04		
TRINITY_DN28906_c2_g2_i1	eukaryotic initiation factor 4A	1292	3,25	1,69E-04	0,00E+00	85,54%
TRINITY_DN24492_c0_g1_i1	60S ribosomal protein L18a	782	3,25	2,54E-04	2,80E-55	63,25%
TRINITY_DN42291_c0_g1_i1	60S ribosomal protein L36	521	3,25	2,58E-04	2,30E-10	59,84%
TRINITY_DN34764_c1_g2_i1	60S ribosomal protein L15	708	3,24	2,04E-04	2,70E-85	80,87%
TRINITY_DN6352_c0_g1_i1	60S ribosomal protein L17	718	3,24	1,97E-04	1,00E-40	60,23%
TRINITY_DN18780_c0_g1_i1	3-hydroxy-3-methylglutaryl-coenzyme A reductase	1653	3,23	3,25E-04	4,00E-144	70,69%
TRINITY_DN26010_c0_g2_i1	60S ribosomal protein L3	1281	3,21	1,93E-04	2,00E-168	75,31%
TRINITY_DN24186_c0_g3_i1	40S ribosomal protein S13	627	3,20	2,74E-04	1,30E-77	84,77%
TRINITY_DN41314_c1_g1_i2	atp synthase subunit beta	479	3,20	2,12E-04	3,00E-37	69,05%
TRINITY_DN31219_c4_g3_i1	60S ribosomal protein L26	606	3,19	2,76E-04	1,30E-43	74,17%
TRINITY_DN25926_c0_g1_i1	polyadenylate-binding protein 4-like	838	3,18	3,96E-04	2,10E-15	46,28%
TRINITY_DN30148_c3_g3_i2	---NA---	1569	3,18	5,01E-04		
TRINITY_DN36016_c1_g1_i1	---NA---	381	3,17	2,99E-04		
TRINITY_DN26023_c0_g1_i1	NHP2-like protein 1	544	3,16	3,67E-04	4,90E-53	85,54%
TRINITY_DN37225_c0_g1_i2	---NA---	1613	3,16	3,60E-04		
TRINITY_DN34404_c1_g1_i3	nuclear receptor	3325	3,16	5,41E-04	2,30E-123	64,37%
TRINITY_DN3155_c0_g1_i1	40S ribosomal protein S20	524	3,16	3,76E-04	2,80E-43	78,92%
TRINITY_DN17780_c0_g1_i1	60S ribosomal protein L7a	885	3,15	3,30E-04	8,10E-124	69,36%
TRINITY_DN37652_c0_g1_i1	isopeptide-forming domain-containing fimbrial protein	4851	3,15	3,05E-04	5,20E-31	46,00%
TRINITY_DN3910_c0_g1_i1	---NA---	329	3,14	3,84E-04		

TRINITY_DN32408_c1_g1_i4	uncharacterized protein LOC106153767	2330	3,13	4,45E-04	1,10E-125	52,92%
TRINITY_DN36403_c0_g1_i1	---NA---	651	3,13	2,91E-04		
TRINITY_DN39207_c4_g1_i3	protein KRI1 homolog	2675	3,12	4,38E-04	1,50E-108	65,16%
TRINITY_DN34314_c0_g1_i2	predicted protein	3120	3,10	3,60E-04	4,00E-31	48,08%
TRINITY_DN29601_c0_g1_i1	60S ribosomal protein L6-like	749	3,10	4,55E-04	5,60E-40	60,52%
TRINITY_DN32006_c1_g1_i2	Low choriolytic enzyme,Tolloid-like protein 2,Zinc metalloproteinase nas-13,Embryonic protein UVS.2	420	3,10	3,98E-04	1,20E-05	49,82%
TRINITY_DN25149_c1_g2_i1	60S ribosomal protein L27a	669	3,09	4,07E-04	4,00E-47	71,73%
TRINITY_DN5940_c0_g1_i1	60S ribosomal protein L14	501	3,09	4,66E-04	2,60E-23	60,53%
TRINITY_DN27621_c1_g1_i1	60S ribosomal protein L35	616	3,09	5,44E-04	2,50E-26	67,02%
TRINITY_DN509_c0_g1_i1	transcription factor BTF3 homolog 4	604	3,09	7,23E-04	1,40E-31	82,30%
TRINITY_DN18857_c0_g1_i1	60S ribosomal protein L37a	432	3,09	5,42E-04	7,90E-40	83,19%
TRINITY_DN13571_c0_g1_i1	40S ribosomal protein S12	592	3,09	5,13E-04	5,60E-31	69,15%
TRINITY_DN33730_c2_g1_i1	ADP,ATP carrier protein	871	3,08	5,03E-04	5,80E-123	83,13%
TRINITY_DN26147_c0_g1_i1	lysine--tRNA ligase isoform X2	2083	3,07	7,60E-04	0,00E+00	74,63%
TRINITY_DN19294_c0_g1_i2	probable 60S ribosomal protein L37-A	470	3,06	6,37E-04	8,20E-37	84,07%
TRINITY_DN30728_c2_g1_i1	nucleolar protein 58-like	1637	3,05	6,36E-04	2,00E-173	76,19%
TRINITY_DN16853_c0_g1_i1	cathepsin Z	1640	3,05	9,04E-04	2,60E-148	47,77%
TRINITY_DN32090_c0_g1_i7	---NA---	522	3,05	5,03E-04		
TRINITY_DN31052_c1_g1_i1	transcript antisense to ribosomal rna protein	1087	3,04	4,76E-04	1,70E-33	65,58%
TRINITY_DN17409_c0_g1_i1	DNA-directed RNA polymerases I and III subunit rpac1-like	1214	3,04	6,36E-04	4,70E-61	64,24%
TRINITY_DN1738_c0_g1_i1	ribosomal protein RPL35A	515	3,04	6,90E-04	1,20E-67	76,41%
TRINITY_DN33669_c0_g2_i1	Putative LOC100868636	2460	3,02	5,79E-04	0,00E+00	55,42%
TRINITY_DN39440_c1_g1_i1	Heat shock protein 83	591	3,01	5,60E-04	2,90E-84	95,05%
TRINITY_DN27508_c0_g1_i1	Fatty acid desaturase 2	1439	3,01	9,49E-04	1,40E-38	43,52%
TRINITY_DN26222_c0_g1_i1	phosphate carrier protein, mitochondrial	1215	3,00	8,30E-04	2,20E-105	67,64%
TRINITY_DN29736_c2_g1_i1	Polyadenylate-binding protein, cytoplasmic and nuclear	2213	3,00	6,56E-04	1,70E-140	63,32%

TRINITY_DN34926_c0_g1_i3	mesoderm induction early response protein 1	2854	3,00	9,63E-04	6,40E-165	71,16%
TRINITY_DN26834_c0_g1_i1	methionine adenosyltransferase	1282	2,99	1,20E-03	0,00E+00	85,78%
TRINITY_DN41410_c0_g1_i1	elongation factor 1-beta'	804	2,99	8,54E-04	1,80E-28	58,62%
TRINITY_DN31624_c0_g1_i10	low-density lipoprotein receptor-related protein 2-like isoform X1	548	2,99	9,51E-04	2,80E-17	49,18%
TRINITY_DN40827_c1_g1_i4	TAR DNA-binding protein 43-like	5770	2,98	9,91E-04	9,50E-100	59,53%
TRINITY_DN37382_c1_g1_i3	EOG090X0CTI	1526	2,98	8,91E-04	1,20E-87	75,50%
TRINITY_DN23234_c0_g2_i1	nucleoside diphosphate kinase	603	2,97	1,68E-03	2,80E-73	78,71%
TRINITY_DN31049_c4_g2_i1	---NA---	3277	2,97	1,60E-03		
TRINITY_DN37516_c1_g1_i7	Cellulose/chitin-binding protein N-terminal	1120	2,97	1,11E-03	4,30E-78	67,07%
TRINITY_DN30478_c2_g2_i1	40S ribosomal protein S2	1270	2,97	8,61E-04	3,10E-144	85,69%
TRINITY_DN39440_c1_g1_i4	heat shock 90 kDa protein	323	2,96	7,59E-04	5,80E-66	94,02%
TRINITY_DN30528_c0_g1_i20	hypothetical protein MYCGRDRAFT_86961	530	2,96	7,84E-04	1,60E-38	80,69%
TRINITY_DN16047_c0_g1_i1	40S ribosomal protein S26	554	2,96	9,64E-04	2,50E-13	77,16%
TRINITY_DN29524_c1_g2_i1	60S ribosomal protein L10	753	2,95	8,75E-04	9,00E-101	80,53%
TRINITY_DN29785_c2_g3_i1	ubiquitin	485	2,95	8,07E-04	1,20E-83	91,39%
TRINITY_DN31351_c1_g3_i1	heat shock 70 kDa protein cognate 4-like	564	2,95	1,02E-03	1,00E-34	80,60%
TRINITY_DN17154_c0_g1_i1	Cathepsin L	1006	2,94	1,67E-03	8,90E-90	63,35%
TRINITY_DN39195_c0_g1_i1	FAD synthase-like isoform X2	2075	2,94	1,67E-03	0,00E+00	64,09%
TRINITY_DN32184_c0_g2_i3	hepatic lectin-like	1398	2,94	9,50E-04	2,40E-05	46,50%
TRINITY_DN31442_c0_g1_i2	oxidative stress-induced growth inhibitor 1	2799	2,94	1,16E-03	5,70E-118	62,05%
TRINITY_DN32303_c1_g1_i4	---NA---	832	2,94	9,45E-04		
TRINITY_DN12918_c0_g1_i1	60S ribosomal protein L38	349	2,92	1,50E-03	5,90E-21	68,84%
TRINITY_DN27959_c0_g1_i1	40S ribosomal protein S18	594	2,91	1,20E-03	2,60E-67	81,28%
TRINITY_DN30587_c0_g1_i2	Myosin-2 essential light chain	870	2,90	1,77E-03	2,10E-70	81,48%
TRINITY_DN29935_c0_g1_i2	trypsin-1-like	901	2,90	1,35E-03	4,50E-44	58,93%
TRINITY_DN36277_c1_g1_i3	---NA---	1846	2,89	3,62E-03		

TRINITY_DN32054_c5_g2_i4	---NA---	1374	2,89	1,72E-03		
TRINITY_DN31013_c0_g1_i3	C-factor-like isoform X2	626	2,88	2,82E-03	5,60E-51	58,46%
TRINITY_DN31176_c0_g1_i3	phosphoethanolamine N-methyltransferase-like	1012	2,88	1,42E-03	9,60E-133	70,59%
TRINITY_DN33804_c1_g1_i9	eukaryotic translation initiation factor 4E transporter-like isoform X2	492	2,86	2,48E-03	3,60E-13	61,17%
TRINITY_DN32789_c0_g3_i2	LOC100176110 isoform X2	607	2,84	1,77E-03	1,50E-25	47,39%
TRINITY_DN29588_c0_g1_i6	---NA---	455	2,83	2,18E-03		
TRINITY_DN29598_c3_g1_i6	polyubiquitin-B isoform X3	901	2,83	1,96E-03	1,90E-110	79,72%
TRINITY_DN37151_c0_g1_i2	Serine-arginine protein 55	852	2,83	2,74E-03	5,90E-13	82,14%
TRINITY_DN38155_c0_g2_i2	ankyrin repeat domain-containing protein 54-like	624	2,82	2,30E-03	3,40E-08	91,96%
TRINITY_DN38458_c0_g1_i9	flotillin-2 isoform X2	1988	2,82	2,13E-03	0,00E+00	93,73%
TRINITY_DN39078_c2_g1_i4	beta-1-syntrophin	1816	2,82	2,03E-03	0,00E+00	55,69%
TRINITY_DN31575_c0_g1_i8	dehydration responsive protein	400	2,82	2,72E-03	1,70E-36	72,37%
TRINITY_DN29598_c3_g2_i1	ubiquitin-40S ribosomal protein S27a	481	2,81	1,95E-03	2,30E-61	87,29%
TRINITY_DN36202_c2_g2_i1	Gamma-crystallin A	872	2,81	1,91E-03	2,30E-68	56,52%
TRINITY_DN28067_c0_g1_i1	sodium/potassium-transporting ATPase subunit alpha-like	2171	2,80	2,92E-03	7,70E-60	48,31%
TRINITY_DN22839_c0_g1_i1	unnamed protein product	1313	2,79	2,35E-03	1,70E-40	63,86%
TRINITY_DN34314_c0_g1_i3	predicted protein	1649	2,78	3,04E-03	1,40E-25	48,80%
TRINITY_DN29985_c2_g3_i2	---NA---	2040	2,78	3,61E-03		
TRINITY_DN32880_c0_g1_i2	SNF-related serine/threonine-protein kinase-like	1313	2,78	2,61E-03	1,70E-20	54,58%
TRINITY_DN30804_c3_g1_i3	---NA---	772	2,77	2,57E-03		
TRINITY_DN35502_c1_g1_i4	---NA---	1998	2,76	2,46E-03		
TRINITY_DN31001_c0_g1_i1	acyl carrier protein, mitochondrial isoform X2	868	2,76	2,61E-03	4,30E-75	69,53%
TRINITY_DN38225_c0_g1_i18	zinc finger protein 558-like	911	2,75	4,64E-03	2,00E-54	56,08%
TRINITY_DN41311_c0_g1_i2	E3 ubiquitin-protein ligase SHPRH-like	6350	2,75	2,53E-03	0,00E+00	65,53%
TRINITY_DN33835_c2_g3_i1	Tubulin beta-4 chain	306	2,74	4,33E-03	3,50E-16	100,00%
TRINITY_DN38834_c0_g3_i6	programmed cell death protein 2-like	689	2,74	3,79E-03	4,10E-48	61,81%

TRINITY_DN38396_c1_g1_i8	glycoprotein-N-acetylgalactosamine 3-beta-galactosyltransferase 1-like	1214	2,74	3,59E-03	5,80E-174	59,05%
TRINITY_DN29168_c7_g2_i2	nucleolar protein 56-like	1721	2,73	3,77E-03	0,00E+00	75,56%
TRINITY_DN40425_c1_g1_i4	guanine nucleotide exchange factor for Rab-3A-like	1908	2,72	3,74E-03	1,40E-67	58,99%
TRINITY_DN40893_c3_g1_i3	unnamed protein product	2620	2,72	3,92E-03	8,30E-04	52,56%
TRINITY_DN38380_c1_g1_i1	Another transcription unit protein	1460	2,71	3,57E-03	9,40E-128	80,00%
TRINITY_DN32476_c2_g7_i1	---NA---	530	2,71	2,76E-03		
TRINITY_DN38727_c0_g1_i4	Protein HIRA	2090	2,70	3,57E-03	1,40E-119	48,49%
TRINITY_DN32976_c0_g2_i2	---NA---	622	2,69	1,04E-02		
TRINITY_DN31959_c0_g2_i7	tubulin alpha-1C chain-like	962	2,69	4,46E-03	0,00E+00	97,36%
TRINITY_DN38339_c1_g1_i4	---NA---	445	2,69	4,17E-03		
TRINITY_DN34312_c0_g1_i3	Hypothetical predicted protein	1286	2,68	5,02E-03	1,70E-179	70,81%
TRINITY_DN31013_c0_g1_i1	C-factor-like isoform X2	766	2,68	4,09E-03	5,70E-64	58,69%
TRINITY_DN37429_c0_g1_i2	endophilin-A isoform X1	1876	2,67	3,58E-03	3,80E-142	82,28%
TRINITY_DN28566_c0_g1_i1	probable medium-chain specific acyl-CoA dehydrogenase, mitochondrial	1336	2,67	5,28E-03	2,50E-169	78,80%
TRINITY_DN25514_c0_g1_i1	4-hydroxyphenylpyruvate dioxygenase	1310	2,66	6,39E-03	5,70E-169	73,31%
TRINITY_DN32512_c2_g3_i1	heat shock protein 83	1181	2,66	3,87E-03	8,00E-178	82,60%
TRINITY_DN31787_c0_g1_i2	PREDICTED: LOW QUALITY PROTEIN: uncharacterized protein LOC108061215	824	2,65	8,28E-03	8,20E-04	51,00%
TRINITY_DN33074_c1_g1_i7	heat shock 70 kDa protein 1-like	876	2,63	4,56E-03	0,00E+00	95,26%
TRINITY_DN38285_c0_g1_i3	CDK5 regulatory subunit-associated protein 2-like	5762	2,63	5,45E-03	7,40E-66	63,93%
TRINITY_DN27299_c1_g2_i1	botryococcus squalene synthase	1866	2,63	6,56E-03	6,00E-63	44,60%
TRINITY_DN40800_c2_g1_i2	importin-11	3634	2,63	4,71E-03	0,00E+00	69,08%
TRINITY_DN29168_c6_g2_i1	H/ACA ribonucleoprotein complex subunit 4	1825	2,62	6,49E-03	0,00E+00	84,43%
TRINITY_DN41314_c2_g2_i3	CHK1 checkpoint-like protein	304	2,62	5,63E-03	3,70E-26	85,51%
TRINITY_DN32902_c3_g2_i5	uncharacterized protein LOC764597 isoform X1	4495	2,62	1,01E-02	1,00E-22	43,33%
TRINITY_DN37265_c0_g1_i10	polycomb group RING finger protein 3	1226	2,62	6,10E-03	3,70E-87	71,08%
TRINITY_DN29396_c0_g1_i2	IQ and ubiquitin-like domain-containing protein	2593	2,61	6,10E-03	9,30E-172	51,85%

TRINITY_DN27603_c0_g5_i2	K(+)-stimulated pyrophosphate-energized sodium pump	2137	2,60	6,63E-03	4,30E-69	59,26%
TRINITY_DN31574_c0_g1_i4	Cell wall-associated hydrolase	531	2,60	7,17E-03	5,90E-68	76,56%
TRINITY_DN33584_c0_g1_i3	2-isopropylmalate synthase	2063	2,60	9,49E-03	1,20E-38	46,38%
TRINITY_DN39996_c1_g1_i1	ruvB-like 1	845	2,59	6,74E-03	1,40E-112	88,83%
TRINITY_DN34783_c2_g1_i5	LOW QUALITY PROTEIN: uncharacterized protein LOC103512334	560	2,59	5,92E-03	1,00E-04	47,57%
TRINITY_DN32607_c1_g2_i2	uncharacterized protein LOC111697637 isoform X2	625	2,58	5,33E-03	9,00E-25	64,97%
TRINITY_DN29935_c0_g1_i3	chymotrypsinogen A-like	894	2,58	6,89E-03	1,60E-43	58,76%
TRINITY_DN31352_c3_g2_i7	control protein HCTL036	477	2,57	8,29E-03	7,60E-43	88,16%
TRINITY_DN39872_c3_g1_i2	lymphocyte-specific helicase-like	2801	2,56	6,54E-03	0,00E+00	67,26%
TRINITY_DN37263_c1_g1_i4	POC1 centriolar protein homolog A-like	888	2,56	6,46E-03	1,30E-75	59,99%
TRINITY_DN33381_c0_g1_i5	uncharacterized protein LOC111698186	1149	2,56	6,12E-03	9,40E-51	44,11%
TRINITY_DN17030_c0_g1_i1	---NA---	789	2,56	9,17E-03		
TRINITY_DN36410_c1_g1_i3	---NA---	791	2,55	8,28E-03		
TRINITY_DN35190_c0_g1_i3	sequestosome-1 isoform X2	886	2,55	7,78E-03	3,90E-36	59,65%
TRINITY_DN31737_c1_g1_i7	heat shock 70 kDa protein 1-like	853	2,55	7,79E-03	6,60E-110	86,28%
TRINITY_DN33714_c1_g1_i6	RRT15 protein	455	2,54	8,46E-03	3,30E-60	68,65%
TRINITY_DN31624_c0_g1_i6	low-density lipoprotein receptor-related protein 2-like isoform X2	1245	2,54	6,65E-03	1,70E-16	43,66%
TRINITY_DN29085_c0_g1_i12	---NA---	383	2,54	8,66E-03		
TRINITY_DN40361_c1_g1_i5	Isocitrate dehydrogenase [NADP]	2838	2,54	8,11E-03	0,00E+00	70,35%
TRINITY_DN34025_c0_g1_i4	phenoloxidase-activating factor 2-like	784	2,53	7,95E-03	1,10E-81	68,64%
TRINITY_DN40550_c0_g1_i7	serine beta-lactamase-like protein LACTB, mitochondrial	2236	2,53	8,72E-03	6,30E-172	63,73%
TRINITY_DN35792_c0_g1_i5	uncharacterized protein LOC111697377	2129	2,53	8,38E-03	1,40E-04	45,02%
TRINITY_DN35425_c0_g1_i5	sericin 1-like isoform X1	1151	2,52	1,02E-02	1,80E-06	56,25%
TRINITY_DN28429_c0_g2_i1	C-type lectin domain family 4 member A	824	2,52	8,22E-03	1,20E-08	49,86%
TRINITY_DN33455_c1_g1_i6	---NA---	555	2,52	8,02E-03		
TRINITY_DN33685_c0_g1_i10	PREDICTED: LOW QUALITY PROTEIN: uncharacterized protein LOC108664000	365	2,52	7,41E-03	7,60E-05	78,26%

TRINITY_DN35999_c0_g1_i1	lysine-specific demethylase 8-like isoform X1	2145	2,52	1,01E-02	2,50E-133	55,90%
TRINITY_DN36145_c0_g2_i1	---NA---	2391	2,51	1,00E-02		
TRINITY_DN33373_c0_g1_i2	arginine and glutamate-rich protein 1-like	1726	2,50	9,15E-03	7,30E-14	57,82%
TRINITY_DN30950_c0_g1_i1	---NA---	1173	2,50	1,20E-02		
TRINITY_DN33217_c1_g1_i8	hypothetical protein	348	2,49	9,25E-03	4,50E-27	71,43%
TRINITY_DN35507_c2_g1_i4	protein FAM135A-like isoform X1	1596	2,49	1,35E-02	0,00E+00	78,05%
TRINITY_DN26808_c0_g3_i1	Very long-chain specific acyl-CoA dehydrogenase, mitochondrial	1908	2,48	1,15E-02	0,00E+00	69,83%
TRINITY_DN34851_c1_g2_i6	cathepsin L1	988	2,48	1,28E-02	2,80E-109	51,30%
TRINITY_DN31890_c1_g2_i3	hypothetical protein B566_EDAN018907	451	2,47	9,58E-03	1,10E-15	72,85%
TRINITY_DN30827_c1_g1_i16	hypothetical protein E3N88_44467	413	2,47	1,17E-02	1,90E-27	76,69%
TRINITY_DN31955_c0_g1_i2	protein D2	1044	2,46	1,65E-02	1,40E-56	51,02%
TRINITY_DN25471_c0_g1_i5	heterogeneous nuclear ribonucleoprotein U-like protein 1	561	2,46	1,34E-02	4,50E-82	62,64%
TRINITY_DN33056_c1_g2_i2	---NA---	1064	2,46	1,09E-02		
TRINITY_DN35167_c0_g2_i9	---NA---	1736	2,46	1,34E-02		
TRINITY_DN37274_c0_g1_i9	Microsomal triglyceride transfer protein large subunit	2472	2,45	1,37E-02	1,50E-107	48,83%
TRINITY_DN31575_c0_g1_i3	Putative membrane protein	350	2,45	1,03E-02	7,30E-28	79,24%
TRINITY_DN34297_c1_g1_i2	probable deoxyhypusine synthase	1636	2,45	1,69E-02	0,00E+00	84,13%
TRINITY_DN35084_c0_g1_i5	selenoprotein H	1339	2,44	1,63E-02	4,70E-14	59,31%
TRINITY_DN29451_c3_g2_i7	U7 snRNA-associated Sm-like protein LSm11	600	2,44	2,02E-02	1,40E-33	57,69%
TRINITY_DN34747_c0_g1_i1	aldose 1-epimerase-like	1175	2,44	1,91E-02	1,40E-136	64,84%
TRINITY_DN36803_c0_g1_i4	innexin inx3	4192	2,44	1,53E-02	2,20E-71	53,64%
TRINITY_DN36025_c0_g1_i4	Na(+)/H(+) antiporter NhaA-like	1183	2,44	1,57E-02	8,50E-126	59,94%
TRINITY_DN33906_c5_g1_i2	Sodium/potassium/calcium exchanger	1993	2,44	1,67E-02	0,00E+00	71,75%
TRINITY_DN40756_c3_g2_i1	Mitotic checkpoint serine/threonine-protein kinase BUB1	1537	2,43	1,23E-02	3,70E-81	54,57%
TRINITY_DN31588_c2_g4_i1	probable cation-transporting ATPase 13A3	2616	2,43	1,30E-02	0,00E+00	63,35%
TRINITY_DN30338_c0_g1_i8	EOG090X07AW	446	2,42	1,49E-02	3,80E-10	78,80%

TRINITY_DN41314_c2_g2_i7	CHK1 checkpoint-like protein	641	2,42	1,30E-02	1,50E-40	80,98%
TRINITY_DN35495_c1_g1_i4	transforming growth factor-beta-induced protein ig-h3-like	2240	2,42	1,23E-02	1,30E-143	53,83%
TRINITY_DN37007_c1_g2_i3	uncharacterized protein LOC111709237	855	2,42	1,33E-02	4,10E-14	43,24%
TRINITY_DN33669_c0_g1_i1	Putative LOC100868636	1874	2,41	2,09E-02	0,00E+00	51,17%
TRINITY_DN39437_c1_g1_i3	E3 ubiquitin-protein ligase UHRF1-like	590	2,41	1,69E-02	2,20E-12	51,69%
TRINITY_DN37011_c0_g1_i6	histone-lysine N-methyltransferase, H3 lysine-79 specific-like	876	2,40	1,82E-02	3,20E-13	79,66%
TRINITY_DN31737_c1_g2_i1	heat shock 70 kDa protein 1-like	331	2,40	1,90E-02	7,50E-64	94,66%
TRINITY_DN35146_c1_g1_i4	Golgi membrane protein 1-like isoform X1	1070	2,40	1,82E-02	6,60E-05	46,54%
TRINITY_DN35579_c0_g1_i2	uncharacterized protein LOC111707954	1433	2,39	1,35E-02	3,40E-163	57,22%
TRINITY_DN29870_c0_g1_i2	collagen alpha-1(I) chain-like isoform X2	1573	2,38	1,95E-02	2,70E-18	85,64%
TRINITY_DN33723_c4_g1_i4	uncharacterized protein LOC111697550	3141	2,38	1,90E-02	4,60E-25	77,17%
TRINITY_DN37262_c2_g1_i1	uncharacterized protein LOC111715129	932	2,37	1,66E-02	8,70E-11	64,52%
TRINITY_DN40400_c3_g1_i7	nucleolar complex protein 2 homolog	2273	2,37	1,59E-02	0,00E+00	57,73%
TRINITY_DN35855_c0_g2_i1	---NA---	611	2,36	2,73E-02		
TRINITY_DN32789_c0_g3_i1	LOC100176110 isoform X2	607	2,36	1,67E-02	2,10E-26	47,35%
TRINITY_DN29753_c0_g1_i6	L-2-aminoadipate reductase large subunit-like	532	2,36	2,05E-02	2,30E-23	76,18%
TRINITY_DN40791_c2_g1_i4	titin-like isoform X1	2842	2,34	2,28E-02	2,60E-50	65,48%
TRINITY_DN36532_c0_g1_i3	transmembrane protein 104-like	2972	2,33	3,24E-02	0,00E+00	65,91%
TRINITY_DN38927_c2_g1_i4	uncharacterized protein LOC111703217	974	2,33	2,25E-02	1,80E-27	51,96%
TRINITY_DN29532_c0_g3_i1	hypothetical protein DAPPUDRAFT_68692, partial	453	2,32	2,25E-02	2,00E-19	63,63%
TRINITY_DN38627_c0_g1_i2	60S acidic ribosomal protein P1	320	2,32	2,79E-02	2,50E-05	59,22%
TRINITY_DN35667_c0_g1_i5	CUB domain	410	2,32	2,31E-02	2,00E-13	69,02%
TRINITY_DN28840_c0_g1_i3	potassium voltage-gated channel protein Shab-like	1990	2,32	2,43E-02	1,70E-149	69,55%
TRINITY_DN28032_c0_g1_i2	glutathione S-transferase	717	2,31	2,51E-02	2,90E-45	54,97%
TRINITY_DN32708_c0_g1_i3	60S ribosomal protein L12	668	2,31	1,96E-02	1,40E-108	92,30%
TRINITY_DN30745_c0_g1_i1	molybdenum cofactor biosynthesis protein 1 isoform X1	1571	2,31	2,80E-02	7,10E-163	65,28%

TRINITY_DN30923_c0_g1_i2	F-box/SPRY domain-containing protein 1	1233	2,31	2,23E-02	3,30E-172	93,93%
TRINITY_DN36767_c0_g3_i5	---NA---	1325	2,31	2,51E-02		
TRINITY_DN39976_c0_g1_i8	mothers against decapentaplegic 4-like isoform X3	2471	2,30	3,23E-02	5,20E-146	88,20%
TRINITY_DN31787_c0_g2_i2	Double-stranded RNA-specific editase Adar	719	2,30	3,02E-02	3,50E-08	59,49%
TRINITY_DN31624_c0_g1_i11	---NA---	1093	2,30	2,38E-02		
TRINITY_DN31684_c0_g1_i8	---NA---	372	2,29	2,94E-02		
TRINITY_DN36662_c0_g1_i3	sequestosome-1	798	2,29	2,60E-02	1,90E-25	56,80%
TRINITY_DN39909_c1_g2_i3	transcriptional adapter 2-beta-like	843	2,29	2,63E-02	1,10E-72	57,25%
TRINITY_DN32081_c0_g1_i2	methyl farnesoate epoxidase-like	1565	2,29	3,12E-02	1,40E-156	57,17%
TRINITY_DN33136_c2_g1_i2	uncharacterized protein LOC111715265	707	2,29	2,60E-02	9,90E-07	49,38%
TRINITY_DN29059_c3_g1_i1	RNA-binding protein 34-like	1314	2,29	2,80E-02	1,80E-20	49,42%
TRINITY_DN31810_c0_g1_i2	calcium-dependent protein kinase 4-like	1231	2,29	3,00E-02	3,20E-99	52,98%
TRINITY_DN33059_c0_g1_i2	uncharacterized protein LOC111714641	1088	2,28	2,84E-02	2,40E-97	59,94%
TRINITY_DN32214_c2_g1_i8	protein spartin-like	1575	2,28	3,84E-02	1,80E-154	53,92%
TRINITY_DN41153_c0_g1_i1	breast cancer type 2 susceptibility protein	8433	2,27	2,43E-02	0,00E+00	47,02%
TRINITY_DN26407_c0_g1_i1	acyl-CoA Delta(11) desaturase-like	1379	2,27	2,80E-02	1,20E-56	55,12%
TRINITY_DN31037_c1_g1_i1	luciferin sulfotransferase-like	1429	2,27	3,02E-02	4,50E-108	61,19%
TRINITY_DN33368_c1_g1_i1	---NA---	1326	2,27	3,01E-02		
TRINITY_DN32789_c0_g3_i3	LOC100176110 isoform X2	607	2,27	2,63E-02	2,10E-25	47,22%
TRINITY_DN32567_c2_g1_i2	serine/threonine-protein kinase pim-3-like	695	2,26	3,10E-02	1,60E-76	76,76%
TRINITY_DN32755_c0_g1_i1	alcohol dehydrogenase-like	1233	2,26	2,84E-02	1,20E-158	62,82%
TRINITY_DN34320_c1_g1_i6	Transposon Ty3-I Gag-Pol polyprotein	5084	2,26	4,87E-02	1,20E-133	43,66%
TRINITY_DN37262_c2_g1_i8	uncharacterized protein LOC111715129	2358	2,26	2,53E-02	8,90E-101	55,49%
TRINITY_DN32056_c0_g2_i5	PC4 and SFRS1-interacting protein isoform X2	1725	2,26	2,81E-02	9,40E-95	64,10%
TRINITY_DN29429_c0_g1_i2	cupin domain-containing protein	831	2,26	3,13E-02	2,50E-11	52,68%
TRINITY_DN38510_c2_g1_i1	Poly(ADP-ribose) glycohydrolase ARH3 [PARG]	1276	2,26	2,82E-02	8,20E-111	61,97%

TRINITY_DN31298_c0_g1_i1	reticulon-1-A isoform X4	939	2,25	2,63E-02	2,00E-45	56,73%
TRINITY_DN39297_c1_g1_i5	Protein cramped-like	3718	2,25	2,87E-02	5,40E-164	63,49%
TRINITY_DN31060_c0_g1_i6	tail fiber protein	927	2,25	4,63E-02	7,30E-13	42,82%
TRINITY_DN29669_c0_g1_i2	Ig gamma-3 chain C region-like	2222	2,24	3,36E-02	1,60E-06	50,54%
TRINITY_DN33782_c0_g1_i4	Beta-1,3-glucan-binding protein	617	2,24	4,33E-02	1,40E-56	67,90%
TRINITY_DN36044_c0_g1_i3	zinc finger protein OZF-like isoform X1	1777	2,24	2,86E-02	1,60E-112	61,24%
TRINITY_DN29782_c5_g2_i1	uncharacterized protein LOC111709853	501	2,24	4,05E-02	5,90E-06	48,05%
TRINITY_DN37652_c0_g1_i3	isopeptide-forming domain-containing fimbrial protein	4851	2,24	3,26E-02	5,20E-31	46,00%
TRINITY_DN28917_c0_g1_i6	vitellogenin 1	809	2,23	3,41E-02	3,20E-64	53,39%
TRINITY_DN36787_c1_g1_i16	Pre-mRNA-splicing factor SPF27	552	2,23	3,60E-02	1,00E-37	76,68%
TRINITY_DN29598_c3_g1_i14	polyubiquitin-B isoform X3	615	2,23	3,30E-02	2,60E-112	78,94%
TRINITY_DN32204_c0_g3_i3	---NA---	680	2,23	3,06E-02		
TRINITY_DN35901_c0_g1_i2	ferritin	479	2,22	3,25E-02	1,70E-76	81,33%
TRINITY_DN31359_c0_g1_i1	beta/gamma crystallin domain-containing protein 1-like	606	2,22	3,07E-02	2,60E-69	58,36%
TRINITY_DN40858_c1_g1_i1	trafficking protein particle complex subunit 11	3714	2,22	3,03E-02	0,00E+00	52,59%
TRINITY_DN38140_c1_g1_i3	R3H domain-containing protein 4-like	1537	2,22	4,32E-02	5,40E-68	54,56%
TRINITY_DN30851_c0_g2_i1	---NA---	659	2,22	3,30E-02		
TRINITY_DN33339_c0_g1_i3	Tyrosine-protein kinase Src42A	3421	2,22	4,74E-02	0,00E+00	90,94%
TRINITY_DN35682_c1_g1_i2	uncharacterized protein LOC111699970	398	2,22	3,38E-02	2,70E-38	57,04%
TRINITY_DN35190_c0_g1_i7	sequestosome-1 isoform X2	838	2,21	3,41E-02	2,80E-36	59,94%
TRINITY_DN35470_c0_g1_i1	---NA---	378	2,21	3,34E-02		
TRINITY_DN31618_c4_g1_i3	bleomycin hydrolase	2735	2,21	3,59E-02	0,00E+00	79,01%
TRINITY_DN31324_c0_g1_i2	probable fatty acid-binding protein	650	2,21	3,79E-02	4,10E-36	57,98%
TRINITY_DN32153_c3_g1_i4	apolipoprotein D-like	668	2,20	3,93E-02	3,90E-93	57,67%
TRINITY_DN34474_c0_g1_i3	spectrin alpha chain, non-erythrocytic 1-like isoform X4	3465	2,20	3,97E-02	3,80E-101	69,24%
TRINITY_DN33074_c1_g1_i2	heat shock 70 kDa protein 1-like	1077	2,19	4,62E-02	0,00E+00	95,61%

TRINITY_DN38915_c1_g1_i3	tRNA wybutosine-synthesizing protein 3 homolog	1473	2,18	4,21E-02	1,30E-85	59,39%
TRINITY_DN33230_c0_g1_i5	uncharacterized protein LOC111715380	957	2,18	4,28E-02	4,10E-48	43,86%
TRINITY_DN38377_c2_g1_i2	---NA---	464	2,18	3,67E-02		
TRINITY_DN39776_c1_g1_i2	uncharacterized protein C1orf112-like	2961	2,17	4,40E-02	1,70E-152	45,48%
TRINITY_DN39852_c3_g1_i2	HEAT repeat-containing protein 6	3099	2,17	4,26E-02	0,00E+00	47,64%
TRINITY_DN30348_c0_g1_i1	uncharacterized protein LOC111707789	4324	2,17	4,66E-02	6,80E-68	48,92%
TRINITY_DN32204_c0_g3_i2	---NA---	487	2,17	4,68E-02		
TRINITY_DN31557_c2_g3_i3	alpha-tubulin	327	2,17	3,88E-02	8,80E-72	95,93%
TRINITY_DN40181_c1_g1_i3	hypoxia-inducible factor 1-alpha isoform X2	2195	2,16	4,55E-02	9,20E-108	54,41%
TRINITY_DN29272_c0_g1_i1	---NA---	334	2,16	3,97E-02		
TRINITY_DN32716_c1_g5_i2	uncharacterized protein LOC111708035	1618	2,15	4,21E-02	3,10E-09	45,80%
TRINITY_DN35829_c0_g1_i2	glutathione S-transferase 1-like	398	2,15	4,28E-02	3,20E-49	67,12%
TRINITY_DN34414_c0_g1_i3	phenoloxidase-activating factor 2-like	1112	2,15	4,41E-02	2,00E-27	59,01%
TRINITY_DN35391_c1_g1_i1	uncharacterized protein CG4449-like	908	2,15	4,88E-02	1,30E-16	54,09%
TRINITY_DN32153_c3_g1_i2	apolipoprotein D-like	665	2,14	4,71E-02	1,50E-84	58,00%
TRINITY_DN35804_c3_g1_i5	transmembrane protein 39A	2527	2,14	4,59E-02	0,00E+00	60,88%
TRINITY_DN30142_c0_g1_i6	vitellogenin 1	978	2,14	4,55E-02	2,10E-88	51,98%
TRINITY_DN29213_c0_g1_i1	uncharacterized protein LOC111715129	753	2,13	4,53E-02	9,70E-69	64,38%
TRINITY_DN36662_c0_g1_i1	sequestosome-1 isoform X2	1646	2,12	4,58E-02	1,20E-53	64,04%
TRINITY_DN3558_c0_g1_i1	odorant-binding protein A10-like protein	469	2,12	4,74E-02	1,20E-10	49,93%
TRINITY_DN34303_c0_g4_i2	elongation factor 1-alpha	1416	2,12	4,66E-02	0,00E+00	82,91%

Table A.2 Complete list of the down-regulated genes (FDR < 0.05, $|\log_2 FC| \geq 2$) of the *Acartia clausi* transcriptome, ordered by decreasing $\log_2 FC$. For each sequence are reported ID, description, length, $\log_2 FC$, FDR, E-value and percentage of similarity.

ID	Sequence description	Sequence length (bp)	log2FC	FDR	E-Value	Similarity (%)
TRINITY_DN31622_c0_g3_i4	Uncharacterized protein APZ42_008836, partial	454	-2,10	4,99E-02	8,80E-10	65,31%
TRINITY_DN33736_c0_g1_i7	glutenin, high molecular weight subunit PW212-like isoform X1	1168	-2,12	4,58E-02	2,70E-46	59,95%
TRINITY_DN41368_c3_g5_i1	AT-rich interactive domain-containing protein 4A-like	2816	-2,14	4,25E-02	1,80E-20	76,84%
TRINITY_DN35400_c2_g1_i8	NAD-dependent protein deacetylase sirtuin-7	4208	-2,14	4,95E-02	0,00E+00	74,12%
TRINITY_DN29914_c0_g1_i6	ice-structuring glycoprotein-like	2555	-2,14	4,12E-02	3,20E-12	50,43%
TRINITY_DN31800_c0_g1_i2	LOC100176110 isoform X2	713	-2,15	4,11E-02	7,60E-24	44,40%
TRINITY_DN29204_c0_g1_i3	---NA---	433	-2,15	4,72E-02		
TRINITY_DN39043_c0_g2_i3	putative salivary protein	578	-2,16	3,89E-02	1,30E-07	59,91%
TRINITY_DN35694_c0_g1_i2	peroxidasin homolog	1471	-2,16	4,74E-02	1,90E-157	60,85%
TRINITY_DN37558_c1_g1_i5	methylosome subunit pICln-like	551	-2,16	4,80E-02	3,90E-39	68,98%
TRINITY_DN38336_c0_g1_i4	longitudinals lacking protein-like	2129	-2,17	4,00E-02	2,70E-53	63,77%
TRINITY_DN36978_c2_g1_i5	---NA---	1896	-2,17	4,87E-02		
TRINITY_DN31576_c1_g1_i9	collagen alpha-1(VII) chain-like	454	-2,19	4,03E-02	2,50E-13	58,35%
TRINITY_DN41115_c2_g1_i2	Uncharacterised protein	326	-2,19	3,41E-02	5,40E-29	85,65%
TRINITY_DN30645_c2_g1_i14	---NA---	680	-2,19	4,26E-02		
TRINITY_DN37448_c1_g1_i4	---NA---	598	-2,20	4,83E-02		
TRINITY_DN37775_c1_g1_i7	dnaJ homolog subfamily C member 22-like	844	-2,20	4,04E-02	3,20E-76	67,83%
TRINITY_DN34457_c0_g1_i1	60S ribosomal protein L17	443	-2,20	3,64E-02	6,20E-34	90,18%
TRINITY_DN39697_c0_g1_i1	WD repeat-containing protein 75	2857	-2,22	3,14E-02	1,70E-172	47,23%
TRINITY_DN31574_c0_g1_i10	hypothetical protein HALTITAN_3299	365	-2,22	2,94E-02	1,90E-39	79,18%
TRINITY_DN40363_c0_g1_i2	rho GTPase-activating protein 10-like isoform X2	3838	-2,22	3,12E-02	0,00E+00	78,93%

TRINITY_DN40224_c2_g1_i4	serine-rich adhesin for platelets	3750	-2,23	3,18E-02	0,00E+00	80,57%
TRINITY_DN37569_c1_g1_i4	EOG090X04JL	581	-2,23	3,87E-02	1,70E-35	67,70%
TRINITY_DN39542_c0_g1_i12	UDP-glucose 6-dehydrogenase	1994	-2,24	3,45E-02	0,00E+00	83,39%
TRINITY_DN41115_c2_g1_i9	hypothetical protein HPS_1373	545	-2,24	2,78E-02	3,20E-45	72,56%
TRINITY_DN33355_c0_g1_i2	TATA-box-binding protein	1791	-2,24	4,09E-02	1,80E-152	70,56%
TRINITY_DN29372_c3_g1_i1	---NA---	311	-2,25	3,01E-02		
TRINITY_DN32534_c0_g1_i3	solute carrier family 13 member 5-like isoform X1	2220	-2,25	3,23E-02	0,00E+00	67,15%
TRINITY_DN4784_c0_g1_i1	hypothetical protein GLIP_2041	334	-2,25	3,38E-02	1,20E-07	85,29%
TRINITY_DN33375_c1_g1_i2	transport and Golgi organization protein 2 homolog isoform X1	1007	-2,25	3,87E-02	1,40E-76	54,34%
TRINITY_DN35950_c0_g5_i2	Hypothetical predicted protein	1069	-2,26	3,00E-02	1,80E-09	45,50%
TRINITY_DN33730_c2_g2_i3	---NA---	519	-2,26	2,61E-02		
TRINITY_DN33507_c3_g1_i9	---NA---	316	-2,26	2,55E-02		
TRINITY_DN33129_c0_g1_i3	---NA---	650	-2,27	3,95E-02		
TRINITY_DN35859_c0_g1_i1	---NA---	593	-2,27	3,36E-02		
TRINITY_DN34441_c0_g1_i2	---NA---	907	-2,27	3,24E-02		
TRINITY_DN35052_c0_g1_i1	histone H3	2525	-2,29	2,61E-02	4,60E-43	67,36%
TRINITY_DN36706_c2_g1_i7	lon protease homolog, mitochondrial-like	583	-2,30	3,01E-02	1,70E-04	47,01%
TRINITY_DN36490_c3_g1_i4	---NA---	537	-2,30	4,43E-02		
TRINITY_DN40035_c2_g1_i5	src substrate cortactin	1762	-2,30	3,13E-02	1,30E-40	77,99%
TRINITY_DN32061_c0_g1_i5	protein IWS1 homolog isoform X3	570	-2,31	2,60E-02	9,40E-05	81,63%
TRINITY_DN40960_c1_g1_i4	E3 SUMO-protein ligase RanBP2	2131	-2,32	2,07E-02	9,00E-136	52,13%
TRINITY_DN33308_c0_g1_i1	---NA---	1489	-2,32	2,70E-02		
TRINITY_DN36813_c0_g1_i1	uncharacterized protein LOC111709235 isoform X1	1525	-2,32	2,64E-02	0,00E+00	77,66%
TRINITY_DN37083_c0_g1_i4	mitochondrial GTPase 1	1475	-2,32	2,81E-02	6,10E-114	65,86%
TRINITY_DN29839_c0_g1_i2	---NA---	395	-2,33	2,38E-02		
TRINITY_DN38210_c0_g1_i12	---NA---	1281	-2,33	2,27E-02		

TRINITY_DN34550_c0_g1_i1	---NA---	569	-2,34	1,85E-02		
TRINITY_DN24277_c0_g1_i1	keratin-associated protein 5-2-like	509	-2,34	1,88E-02	5,40E-11	66,18%
TRINITY_DN34310_c0_g1_i5	---NA---	1347	-2,34	2,86E-02		
TRINITY_DN37481_c1_g1_i6	---NA---	1059	-2,34	3,75E-02		
TRINITY_DN31351_c1_g1_i2	heat shock 70 kDa protein cognate 4-like	673	-2,35	2,42E-02	4,10E-46	81,20%
TRINITY_DN35837_c0_g1_i2	proteasome adapter and scaffold protein ECM29	6286	-2,35	1,93E-02	0,00E+00	64,86%
TRINITY_DN37183_c1_g1_i3	rho GTPase-activating protein 1	1550	-2,36	1,68E-02	0,00E+00	74,66%
TRINITY_DN35726_c1_g1_i7	uncharacterized protein LOC111705570 isoform X1	1283	-2,37	2,42E-02	1,20E-11	61,11%
TRINITY_DN29555_c0_g1_i3	hypothetical protein GWI33_012524	670	-2,38	1,82E-02	1,50E-21	70,72%
TRINITY_DN40238_c2_g1_i2	3-hydroxy-3-methylglutaryl-coenzyme A reductase	3547	-2,39	1,51E-02	0,00E+00	67,47%
TRINITY_DN27820_c0_g12_i1	Elongation factor G	1605	-2,39	1,88E-02	3,80E-129	91,10%
TRINITY_DN30984_c6_g1_i1	tubulin polyglutamylase TTLL5 isoform X1	3507	-2,39	1,55E-02	0,00E+00	67,50%
TRINITY_DN33744_c2_g1_i9	UDP-N-acetylglucosamine 1-carboxyvinyltransferase-like	619	-2,40	1,31E-02	6,80E-21	66,27%
TRINITY_DN38572_c1_g2_i1	28S ribosomal protein S10, mitochondrial	475	-2,40	1,90E-02	1,80E-57	67,21%
TRINITY_DN39675_c1_g2_i2	---NA---	737	-2,41	1,88E-02		
TRINITY_DN33483_c0_g1_i2	translation machinery-associated protein 16 homolog	515	-2,41	1,74E-02	8,20E-34	64,05%
TRINITY_DN32829_c0_g1_i4	Histone H3.3	378	-2,41	1,84E-02	6,40E-82	99,62%
TRINITY_DN25471_c0_g1_i1	heterogeneous nuclear ribonucleoprotein U-like protein 1 isoform X2	644	-2,41	1,49E-02	7,90E-99	62,94%
TRINITY_DN38686_c0_g1_i1	uncharacterized protein LOC111700768	901	-2,43	1,84E-02	5,20E-17	77,33%
TRINITY_DN32326_c2_g1_i1	gastrula zinc finger protein XlCGF8.2DB-like	1781	-2,45	1,67E-02	3,80E-66	64,49%
TRINITY_DN28862_c0_g1_i1	response regulator	417	-2,46	1,82E-02	4,70E-10	49,33%
TRINITY_DN34480_c0_g1_i2	acyl-coenzyme A thioesterase 9, mitochondrial-like isoform X1	1633	-2,46	1,18E-02	0,00E+00	72,11%
TRINITY_DN40410_c1_g1_i2	uncharacterized protein LOC111710934	1383	-2,47	1,56E-02	4,10E-09	57,84%
TRINITY_DN38984_c6_g1_i4	ankyrin repeat-containing domain protein	2076	-2,48	1,30E-02	2,20E-34	49,17%
TRINITY_DN32623_c0_g1_i1	50S ribosomal protein L2	5141	-2,49	8,77E-03	0,00E+00	77,77%
TRINITY_DN35157_c0_g1_i1	---NA---	412	-2,50	9,15E-03		

TRINITY_DN38878_c0_g1_i5	von Willebrand factor A domain-containing protein 8 isoform X1	2932	-2,50	9,58E-03	0,00E+00	64,22%
TRINITY_DN38912_c2_g1_i2	mitochondrial uncoupling protein 2-like	884	-2,51	1,30E-02	8,70E-119	74,69%
TRINITY_DN33702_c0_g1_i6	serine/arginine-rich splicing factor 2 isoform X2	779	-2,52	8,35E-03	3,60E-47	75,26%
TRINITY_DN39598_c2_g1_i9	adhesive plaque matrix protein-like isoform X2	830	-2,52	9,11E-03	1,80E-16	60,13%
TRINITY_DN40912_c2_g1_i8	protein GPR107	2516	-2,52	8,81E-03	5,10E-167	59,61%
TRINITY_DN31624_c0_g1_i7	hypothetical protein TCAL_03762	2001	-2,54	7,17E-03	2,00E-05	39,89%
TRINITY_DN36575_c0_g1_i12	BTB/POZ domain-containing protein KCTD9	1722	-2,54	1,27E-02	1,20E-140	76,45%
TRINITY_DN37412_c0_g1_i8	---NA---	507	-2,55	1,00E-02		
TRINITY_DN31584_c1_g1_i6	---NA---	1774	-2,56	6,79E-03		
TRINITY_DN39541_c0_g1_i1	polycomb group protein Psc-like	5340	-2,56	7,71E-03	8,40E-84	58,28%
TRINITY_DN38003_c0_g1_i1	pre-rRNA processing protein FTSJ3	2802	-2,57	5,73E-03	1,00E-167	61,88%
TRINITY_DN39503_c2_g1_i2	MICOS complex subunit Mic60-like	1290	-2,57	5,92E-03	0,00E+00	64,18%
TRINITY_DN31729_c0_g2_i5	small nuclear ribonucleoprotein F	603	-2,57	8,10E-03	2,20E-43	89,69%
TRINITY_DN34999_c0_g1_i3	Sorting nexin-2	2125	-2,58	7,80E-03	0,00E+00	69,42%
TRINITY_DN36699_c0_g1_i1	zinc finger protein 271-like	2318	-2,59	7,47E-03	5,50E-107	50,75%
TRINITY_DN36346_c0_g1_i1	BAB1 protein	2328	-2,59	8,35E-03	0,00E+00	68,65%
TRINITY_DN39292_c0_g1_i1	protein zyg-11 homolog B	1542	-2,60	5,97E-03	0,00E+00	70,13%
TRINITY_DN33268_c0_g1_i1	rho guanine nucleotide exchange factor 10 isoform X5	3369	-2,60	5,44E-03	0,00E+00	50,45%
TRINITY_DN30559_c0_g1_i4	baculoviral IAP repeat-containing protein 5-like	832	-2,61	8,47E-03	6,30E-29	65,77%
TRINITY_DN37980_c1_g1_i6	glutathione synthetase isoform X1	1881	-2,61	6,79E-03	0,00E+00	76,24%
TRINITY_DN41116_c3_g1_i2	little elongation complex subunit 2-like	2513	-2,61	4,64E-03	2,80E-70	51,42%
TRINITY_DN32925_c2_g1_i1	muskelin isoform X1	3268	-2,62	6,11E-03	0,00E+00	60,18%
TRINITY_DN30706_c1_g1_i5	---NA---	668	-2,65	5,66E-03		
TRINITY_DN30573_c0_g1_i4	elongation factor Tu	1585	-2,66	4,91E-03	0,00E+00	98,98%
TRINITY_DN33928_c0_g2_i3	protein singed	1930	-2,67	4,52E-03	0,00E+00	80,91%
TRINITY_DN37695_c0_g1_i3	---NA---	769	-2,67	4,72E-03		

TRINITY_DN35069_c0_g1_i12	Pyruvate dehydrogenase phosphatase regulatory subunit, mitochondrial	3107	-2,68	3,68E-03	0,00E+00	74,09%
TRINITY_DN31576_c1_g1_i2	NACHT, LRR and PYD domains-containing protein 3-like isoform X1	809	-2,70	2,94E-03	1,40E-16	57,24%
TRINITY_DN31961_c0_g3_i1	Hypothetical predicted protein	461	-2,70	3,46E-03	3,80E-07	44,60%
TRINITY_DN39511_c0_g1_i8	nuclear hormone receptor HR96-like isoform X1	2349	-2,70	3,70E-03	2,30E-137	50,25%
TRINITY_DN32196_c0_g1_i5	---NA---	692	-2,71	4,24E-03		
TRINITY_DN40073_c4_g1_i3	YTH domain-containing protein 1	1337	-2,73	2,97E-03	1,80E-56	83,68%
TRINITY_DN31143_c0_g1_i2	sodium leak channel non-selective protein-like	2384	-2,73	3,43E-03	0,00E+00	76,02%
TRINITY_DN34154_c1_g1_i5	protein Hook homolog 3-like isoform X2	3063	-2,74	5,17E-03	0,00E+00	64,84%
TRINITY_DN39230_c1_g2_i2	---NA---	482	-2,74	3,77E-03		
TRINITY_DN40477_c3_g1_i6	---NA---	447	-2,76	3,73E-03		
TRINITY_DN38340_c0_g1_i3	uncharacterized protein LOC111699147	5997	-2,76	2,92E-03	0,00E+00	72,18%
TRINITY_DN32379_c1_g1_i15	putative transcription factor	563	-2,76	3,84E-03	2,40E-27	85,72%
TRINITY_DN39835_c3_g2_i8	lariat debranching enzyme-like	956	-2,77	4,09E-03	3,20E-20	56,61%
TRINITY_DN34381_c2_g1_i1	SH3KBP1-binding protein 1 isoform X1	801	-2,77	3,22E-03	7,10E-25	56,74%
TRINITY_DN32313_c1_g1_i5	senescence-associated protein	902	-2,80	2,51E-03	5,70E-21	62,80%
TRINITY_DN36456_c1_g1_i8	EOG090X08ST	1291	-2,85	2,14E-03	0,00E+00	75,43%
TRINITY_DN40959_c1_g1_i16	hypothetical protein GWI33_013314, partial	810	-2,87	1,20E-03	1,80E-40	73,60%
TRINITY_DN30861_c1_g6_i1	rhophilin-2-B-like isoform X4	2178	-2,93	9,91E-04	0,00E+00	78,38%
TRINITY_DN34550_c0_g1_i6	---NA---	591	-2,94	8,50E-04		
TRINITY_DN27059_c0_g1_i14	protein timeless homolog	570	-2,96	2,16E-03	1,20E-05	62,50%
TRINITY_DN30088_c1_g2_i24	putative salivary gland protein 13	897	-2,97	1,05E-03	1,00E-12	73,32%
TRINITY_DN40203_c2_g1_i3	Metallophosphoesterase 1	2159	-2,98	1,20E-03	7,40E-156	67,29%
TRINITY_DN37591_c0_g1_i3	dual specificity mitogen-activated protein kinase kinase hemipterous-like	3187	-3,01	7,19E-04	0,00E+00	82,60%
TRINITY_DN28564_c0_g1_i2	zinc finger protein 208 isoform X1	1381	-3,01	6,66E-04	2,60E-79	43,88%
TRINITY_DN39277_c1_g1_i2	nuclear transcription factor Y subunit beta isoform X1	1797	-3,02	8,89E-04	2,10E-56	83,12%
TRINITY_DN31667_c1_g3_i2	---NA---	386	-3,03	7,79E-04		

TRINITY_DN31947_c2_g1_i3	serine-rich adhesin for platelets	979	-3,04	6,40E-04	1,90E-08	61,16%
TRINITY_DN37304_c0_g1_i3	histidine ammonia-lyase-like	2184	-3,05	5,76E-04	0,00E+00	83,89%
TRINITY_DN29671_c1_g1_i9	Uncharacterized protein APZ42_004707, partial	623	-3,06	4,30E-04	2,70E-13	69,80%
TRINITY_DN29982_c0_g1_i2	39S ribosomal protein L52, mitochondrial	458	-3,15	5,20E-04	2,20E-38	60,43%
TRINITY_DN36092_c0_g1_i3	trypsin-1-like	1134	-3,15	2,71E-04	1,70E-92	63,90%
TRINITY_DN34966_c0_g2_i1	THO complex subunit 4-like	1444	-3,16	2,75E-04	8,90E-31	80,95%
TRINITY_DN34065_c2_g2_i2	putative transmembrane protein	741	-3,17	2,68E-04	1,60E-28	57,06%
TRINITY_DN35269_c0_g1_i7	---NA---	373	-3,19	2,79E-04		
TRINITY_DN28539_c0_g2_i2	uncharacterized protein LOC111708460	580	-3,25	1,40E-04	1,50E-06	45,48%
TRINITY_DN36301_c0_g1_i6	N-alpha-acetyltransferase 40	1126	-3,28	1,35E-04	9,10E-124	68,10%
TRINITY_DN36516_c1_g2_i4	heat shock protein 70	708	-3,28	1,27E-04	4,70E-131	98,57%
TRINITY_DN29793_c0_g1_i5	---NA---	488	-3,29	2,17E-04		
TRINITY_DN33463_c0_g2_i3	acetylcholine receptor subunit alpha-type acr-16-like [AchR]	848	-3,30	1,79E-04	2,10E-66	52,23%
TRINITY_DN30529_c1_g4_i1	Regulator of rDNA transcription protein 15	626	-3,43	7,39E-05	4,60E-10	58,44%
TRINITY_DN35315_c0_g2_i2	glycine receptor subunit alpha-4-like	1366	-3,45	1,25E-04	2,40E-130	68,02%
TRINITY_DN32313_c1_g3_i1	10 kDa putative secreted protein	691	-3,51	4,13E-05	3,10E-15	76,22%
TRINITY_DN39016_c0_g1_i4	TAR DNA-binding protein 43 isoform X2	1796	-3,62	2,51E-05	0,00E+00	79,31%
TRINITY_DN34065_c2_g2_i5	Hypothetical predicted protein	1687	-3,64	2,56E-05	7,00E-31	49,63%
TRINITY_DN38756_c0_g2_i2	WW domain-binding protein 11	719	-3,64	1,91E-05	1,30E-22	55,71%
TRINITY_DN30528_c0_g1_i4	hypothetical protein H5410_064037	564	-3,69	2,26E-05	7,60E-34	79,03%
TRINITY_DN40865_c3_g1_i1	F-box/WD repeat-containing protein 7 isoform X1	2623	-3,69	1,31E-05	0,00E+00	89,55%
TRINITY_DN29532_c0_g1_i7	putative salivary gland protein 14	1235	-3,76	2,25E-05	4,70E-18	68,33%
TRINITY_DN35170_c1_g1_i1	BRCA2-interacting transcriptional repressor EMSY	5017	-3,78	6,89E-06	1,30E-60	63,42%
TRINITY_DN37816_c0_g1_i1	putative tRNA pseudouridine synthase Pus10 isoform X1	1708	-3,80	7,04E-06	3,40E-117	59,75%
TRINITY_DN29532_c0_g1_i9	uncharacterized protein LOC113219380, partial	718	-3,85	9,67E-06	1,80E-19	69,37%
TRINITY_DN32313_c1_g1_i4	10 kDa putative secreted protein	484	-3,91	6,99E-06	7,10E-22	74,13%

TRINITY_DN25931_c0_g1_i1	---NA---	618	-3,93	1,03E-05		
TRINITY_DN36733_c0_g1_i6	transcriptional adapter 1 isoform X3	2081	-3,94	4,51E-06	8,40E-87	53,96%
TRINITY_DN40349_c2_g1_i4	vitellogenin 1	1076	-4,02	1,79E-06	3,90E-100	48,47%
TRINITY_DN41314_c0_g2_i2	UNKNOWN	981	-4,02	2,10E-06	2,10E-87	79,13%
TRINITY_DN32664_c0_g1_i4	mpv17-like protein	1255	-4,10	1,87E-06	2,90E-46	57,79%
TRINITY_DN37645_c0_g1_i4	protein obstructor-E	633	-4,10	1,49E-06	2,80E-111	54,62%
TRINITY_DN31871_c1_g1_i6	hypothetical protein GWI33_012444	886	-4,23	5,52E-07	1,80E-30	73,44%
TRINITY_DN35625_c3_g1_i1	Protein aurora borealis	3187	-4,40	2,47E-07	2,70E-98	52,51%
TRINITY_DN33736_c0_g1_i10	---NA---	433	-4,41	1,10E-07		
TRINITY_DN36925_c0_g1_i10	PREDICTED: uncharacterized protein LOC109483342	1957	-4,50	6,88E-07	1,30E-09	51,73%
TRINITY_DN30406_c7_g1_i2	cold and drought-regulated protein CORA-like	653	-4,59	1,46E-06	9,70E-19	62,37%
TRINITY_DN29975_c2_g1_i1	---NA---	1302	-4,67	1,98E-08		
TRINITY_DN38966_c1_g1_i1	deoxyribodipyrimidine photo-lyase	1750	-4,68	2,93E-08	0,00E+00	74,46%
TRINITY_DN36846_c1_g2_i2	uncharacterized protein LOC111709725	2114	-4,71	6,18E-08	8,00E-73	66,83%
TRINITY_DN40280_c4_g1_i3	serrate RNA effector molecule homolog	1677	-4,83	2,38E-08	2,90E-139	61,07%
TRINITY_DN33596_c0_g1_i10	basement membrane-specific heparan sulfate proteoglycan core protein-like isoform X19	1116	-5,00	3,44E-09	3,30E-09	56,82%
TRINITY_DN32313_c1_g6_i1	Putative uncharacterized protein ART2	1794	-5,04	1,14E-08	4,00E-15	69,22%
TRINITY_DN31840_c0_g1_i5	heat shock protein beta-1	797	-5,14	8,93E-10	3,30E-83	58,55%
TRINITY_DN39085_c1_g1_i5	---NA---	836	-5,16	1,59E-08		
TRINITY_DN40596_c0_g1_i4	Glycogen phosphorylase	492	-5,19	1,74E-09	1,00E-94	89,93%
TRINITY_DN30088_c1_g2_i9	putative salivary gland protein 13	894	-5,29	5,86E-09	7,30E-13	74,96%
TRINITY_DN31871_c1_g1_i8	hypothetical protein X975_24482, partial	692	-5,32	2,99E-09	8,60E-23	71,18%
TRINITY_DN30528_c0_g1_i9	Hypothetical predicted protein	474	-5,33	2,09E-08	3,00E-26	69,65%
TRINITY_DN31981_c1_g1_i1	cathepsin L-like	1033	-5,54	5,04E-08	1,80E-70	56,10%
TRINITY_DN29527_c2_g1_i1	Elongation factor 1-alpha	375	-5,56	4,83E-08	2,30E-68	93,42%
TRINITY_DN12556_c0_g1_i1	60S ribosomal protein L7a	955	-5,61	4,39E-09	1,90E-75	70,18%

TRINITY_DN40337_c0_g1_i15	innexin inx2-like	3084	-5,68	5,62E-11	0,00E+00	51,47%
TRINITY_DN29006_c0_g2_i1	teneurin-m isoform X5	807	-5,77	3,95E-09	1,90E-13	38,00%
TRINITY_DN28927_c1_g1_i2	40S ribosomal protein S8	801	-5,82	2,99E-08	1,50E-72	71,27%
TRINITY_DN30581_c0_g5_i1	predicted protein	552	-5,86	5,28E-09	5,00E-26	64,23%
TRINITY_DN35226_c1_g1_i4	---NA---	854	-5,98	7,18E-11		
TRINITY_DN30528_c0_g1_i19	hypothetical protein LOCC1_G008832	385	-6,03	1,14E-09	8,00E-25	64,58%
TRINITY_DN36070_c0_g1_i5	zinc finger protein 271-like isoform X1	1470	-6,06	1,22E-10	8,00E-143	42,72%
TRINITY_DN35170_c1_g1_i4	BRCA2-interacting transcriptional repressor EMSY	5107	-6,15	4,55E-11	1,40E-60	63,42%
TRINITY_DN28639_c1_g3_i1	elongation factor 2	980	-6,27	1,56E-09	2,50E-114	79,18%
TRINITY_DN30529_c1_g6_i1	Regulator of rDNA transcription protein 15	435	-6,28	7,24E-09	4,00E-17	66,27%
TRINITY_DN26756_c0_g2_i2	60S ribosomal protein L23	603	-6,29	1,36E-09	1,10E-77	89,18%
TRINITY_DN33455_c1_g1_i5	---NA---	609	-6,37	7,86E-13		
TRINITY_DN29527_c2_g3_i1	Elongation factor 1-alpha	1113	-6,38	2,26E-10	0,00E+00	82,95%
TRINITY_DN29636_c0_g1_i1	histone H4-like	372	-6,45	4,98E-10	4,80E-27	77,48%
TRINITY_DN32743_c0_g2_i1	60S acidic ribosomal protein P0	1123	-6,59	2,08E-10	9,50E-67	69,83%
TRINITY_DN30944_c0_g1_i11	hypothetical protein CIL05_21475	2068	-6,63	5,11E-13	4,10E-30	60,08%
TRINITY_DN30110_c0_g2_i1	40S ribosomal protein S3-3-like	987	-6,72	8,18E-11	6,70E-92	79,15%
TRINITY_DN33749_c0_g1_i2	---NA---	312	-6,76	5,55E-13		
TRINITY_DN29510_c10_g1_i1	E3 ubiquitin-protein ligase Siah1	1829	-6,93	2,47E-11	5,40E-15	46,22%
TRINITY_DN22159_c0_g1_i1	---NA---	827	-6,94	1,25E-10		
TRINITY_DN35170_c1_g1_i8	BRCA2-interacting transcriptional repressor EMSY	5096	-7,07	4,75E-12	1,40E-60	63,42%
TRINITY_DN28252_c0_g3_i1	NPC intracellular cholesterol transporter 1-like	1379	-7,23	1,78E-11	1,00E-50	53,45%
TRINITY_DN33622_c0_g5_i1	40S ribosomal protein S3a	945	-7,29	1,58E-11	3,20E-104	80,94%
TRINITY_DN29614_c0_g4_i2	elongation factor 2	1612	-7,32	2,33E-12	0,00E+00	74,73%
TRINITY_DN30581_c0_g1_i4	uncharacterized protein TM35_000063130	1926	-7,35	3,20E-13	4,00E-44	66,36%
TRINITY_DN29401_c1_g2_i6	adenosylhomocysteinase	1545	-7,38	1,71E-12	0,00E+00	85,63%

TRINITY_DN34909_c0_g1_i4	serine-rich adhesin for platelets	4109	-7,46	9,02E-14	3,40E-97	66,19%
TRINITY_DN29649_c4_g5_i1	elongation factor 1 alpha	637	-7,48	1,36E-10	3,40E-79	66,37%
TRINITY_DN30944_c0_g1_i3	hypothetical protein TcBrA4_0034560	2122	-7,52	9,30E-15	1,30E-48	70,38%
TRINITY_DN29043_c0_g3_i1	40S ribosomal protein S6	858	-7,53	1,01E-10	3,40E-68	79,51%
TRINITY_DN27423_c0_g3_i1	40S ribosomal protein S15a	585	-7,69	3,59E-11	9,20E-77	91,02%
TRINITY_DN34065_c2_g1_i4	transcript antisense to ribosomal rna protein	839	-7,70	1,10E-11	2,80E-30	64,48%
TRINITY_DN39223_c0_g1_i5	poly(rC)-binding protein 3 isoform X4	3182	-7,72	3,37E-14	3,70E-129	61,14%
TRINITY_DN12439_c0_g1_i1	60S ribosomal protein L8	944	-7,72	1,31E-12	5,70E-125	83,27%
TRINITY_DN29562_c0_g1_i1	teneurin-m isoform X1	2699	-7,87	5,03E-14	9,20E-08	45,61%
TRINITY_DN33698_c0_g2_i1	40S ribosomal protein S2	1061	-7,89	1,06E-11	4,30E-123	87,49%
TRINITY_DN30581_c0_g1_i2	Hypothetical predicted protein	1852	-8,39	1,90E-15	8,70E-35	63,40%
TRINITY_DN30827_c1_g1_i8	hypothetical protein CERSUDRAFT_61118, partial	407	-8,47	4,07E-15	8,90E-18	72,18%
TRINITY_DN27326_c0_g1_i1	mastigoneme putative	1064	-8,63	1,99E-13	4,50E-66	46,42%
TRINITY_DN34065_c2_g1_i7	protein TAR1	1023	-8,68	2,08E-16	4,20E-32	63,45%
TRINITY_DN32379_c1_g2_i1	putative transcription factor	638	-8,79	5,79E-14	3,90E-18	69,34%
TRINITY_DN29524_c1_g1_i1	60S ribosomal protein L10	770	-8,98	1,96E-10	2,30E-95	79,80%
TRINITY_DN19774_c0_g1_i1	Trk system potassium uptake protein TrkA, amine-terminal domain protein	917	-9,14	7,38E-11	4,10E-41	55,17%
TRINITY_DN18147_c0_g1_i1	40S ribosomal protein S7	668	-9,21	4,76E-11	9,40E-65	70,31%
TRINITY_DN18363_c1_g1_i1	60S ribosomal protein L18a	722	-9,24	3,93E-11	2,70E-77	74,07%
TRINITY_DN16172_c0_g2_i1	40S ribosomal protein S18	597	-9,33	2,31E-11	2,20E-71	88,16%
TRINITY_DN29370_c1_g3_i1	60S ribosomal protein L11	632	-9,37	1,78E-11	7,20E-79	79,27%
TRINITY_DN29189_c0_g2_i1	40S ribosomal protein S9	668	-9,43	1,26E-11	4,00E-66	81,58%
TRINITY_DN30088_c1_g2_i4	putative salivary gland protein 13	428	-9,44	1,14E-11	2,90E-16	68,31%
TRINITY_DN2256_c0_g1_i1	60S ribosomal protein L12	661	-9,51	7,77E-12	1,80E-73	81,88%
TRINITY_DN32743_c0_g1_i1	60S acidic ribosomal protein P1-like	490	-9,57	5,49E-12	5,90E-04	55,93%
TRINITY_DN38017_c1_g1_i3	sestrin homolog isoform X3	1627	-9,63	6,05E-16	0,00E+00	60,47%

TRINITY_DN7657_c0_g1_i1	60S ribosomal protein L13a	732	-9,67	3,07E-12	4,00E-72	76,81%
TRINITY_DN25543_c0_g3_i2	40S ribosomal protein S5	757	-9,71	2,45E-12	6,70E-108	86,94%
TRINITY_DN1481_c0_g1_i1	60s ribosomal protein l6	848	-9,71	2,40E-12	8,70E-66	66,77%
TRINITY_DN28765_c0_g1_i1	histone H3	488	-9,74	2,06E-12	9,60E-37	85,80%
TRINITY_DN19063_c0_g1_i1	40S ribosomal protein S4	1020	-9,79	1,56E-12	7,50E-114	79,18%
TRINITY_DN32371_c1_g2_i1	60S ribosomal protein L5	983	-9,81	1,39E-12	1,20E-97	68,68%
TRINITY_DN2413_c0_g1_i1	60S ribosomal protein L13	831	-9,85	1,19E-12	8,90E-37	71,29%
TRINITY_DN26010_c0_g1_i1	60S ribosomal protein L3	1294	-9,85	1,17E-12	1,60E-167	77,17%
TRINITY_DN25165_c0_g1_i1	S-adenosylmethionine synthase-like	1389	-9,94	8,01E-13	6,30E-177	80,27%
TRINITY_DN16453_c0_g1_i1	ribosomal protein S2	1086	-9,95	7,43E-13	1,00E-114	89,82%
TRINITY_DN29106_c6_g1_i3	fha domain protein	2133	-9,98	6,19E-13	1,80E-24	48,18%
TRINITY_DN29043_c1_g1_i1	60S ribosomal protein L4-like	1442	-10,05	4,28E-13	7,80E-131	76,25%
TRINITY_DN10075_c0_g1_i1	60S ribosomal protein L15	784	-10,07	3,82E-13	1,00E-81	82,88%
TRINITY_DN28932_c0_g1_i1	---NA---	1271	-10,09	3,52E-13		
TRINITY_DN28597_c1_g2_i3	protein dispatched	1891	-10,16	2,30E-13	2,00E-24	43,19%
TRINITY_DN21674_c0_g1_i1	ATP-binding cassette sub-family G member 4 isoform X2	1893	-10,24	1,66E-13	1,70E-69	49,46%
TRINITY_DN36591_c0_g1_i4	trichohyalin-like isoform X2	2605	-10,30	5,61E-16	1,10E-83	73,70%
TRINITY_DN30210_c1_g2_i2	ATP-binding cassette sub-family A member 5-like isoform X1	3112	-10,34	9,90E-14	2,60E-63	49,70%
TRINITY_DN37150_c0_g2_i1	---NA---	511	-10,34	9,90E-14		
TRINITY_DN29106_c6_g1_i1	fha domain protein	2167	-10,43	5,79E-14	1,60E-24	48,35%
TRINITY_DN29532_c0_g1_i11	CHK1 checkpoint-like protein	1416	-10,58	2,55E-14	5,80E-09	79,68%
TRINITY_DN28241_c0_g1_i1	ADP,ATP carrier protein	1088	-10,72	1,01E-14	1,00E-131	79,54%
TRINITY_DN29193_c1_g2_i1	uncharacterized protein TM35_000063140	690	-10,79	7,55E-15	2,10E-08	63,60%
TRINITY_DN37011_c0_g1_i1	histone-lysine N-methyltransferase, H3 lysine-79 specific-like	1068	-11,39	2,03E-16	5,80E-13	79,66%
TRINITY_DN34303_c0_g2_i1	elongation factor 1-alpha	1060	-11,71	2,17E-17	1,20E-106	75,11%
TRINITY_DN41198_c2_g1_i4	STE20-like serine/threonine-protein kinase isoform X3	6355	-11,82	1,39E-17	0,00E+00	83,03%

TRINITY_DN30088_c1_g2_i22	putative salivary gland protein 13	727	-11,95	6,40E-18	1,00E-18	60,37%
TRINITY_DN30944_c0_g1_i10	unnamed protein product	2126	-13,53	2,05E-22	2,90E-29	63,15%

Table A.3 Complete list of enriched processes (Fisher's exact test; FDR < 0.05) among up-regulated genes with respect to the whole transcriptome of *Acartia clausi*, ordered by increasing GO level, for the BP category. For each GO subcategory are reported GO level, ID and number of up-regulated genes.

GO level	GO ID	GO subcategory	No. of DEGs
2	GO:0009987	cellular process	309
2	GO:0008152	metabolic process	278
3	GO:0071704	organic substance metabolic process	265
3	GO:0007017	microtubule-based process	19
3	GO:0009058	biosynthetic process	191
3	GO:0044238	primary metabolic process	257
3	GO:0006807	nitrogen compound metabolic process	250
3	GO:0071840	cellular component organization or biogenesis	64
3	GO:0044237	cellular metabolic process	244
3	GO:0046034	ATP metabolic process	10
3	GO:0006457	protein folding	16
4	GO:0043170	macromolecule metabolic process	226
4	GO:0044249	cellular biosynthetic process	184
4	GO:0034220	ion transmembrane transport	18
4	GO:0044248	cellular catabolic process	23
4	GO:1990542	mitochondrial transmembrane transport	6
4	GO:0019538	protein metabolic process	203
4	GO:0031647	regulation of protein stability	3
4	GO:1901576	organic substance biosynthetic process	187
4	GO:0044260	cellular macromolecule metabolic process	182
4	GO:0044085	cellular component biogenesis	35
4	GO:0000278	mitotic cell cycle	10
4	GO:0034641	cellular nitrogen compound metabolic process	197
4	GO:0006754	ATP biosynthetic process	7
4	GO:0016043	cellular component organization	46
4	GO:1901564	organonitrogen compound metabolic process	227
5	GO:0019693	ribose phosphate metabolic process	11
5	GO:0098656	anion transmembrane transport	5
5	GO:0042776	mitochondrial ATP synthesis coupled proton transport	2
5	GO:0006518	peptide metabolic process	158
5	GO:0044271	cellular nitrogen compound biosynthetic process	176
5	GO:0010467	gene expression	175
5	GO:0034645	cellular macromolecule biosynthetic process	154
5	GO:0009059	macromolecule biosynthetic process	164
5	GO:0022613	ribonucleoprotein complex biogenesis	28
5	GO:0098660	inorganic ion transmembrane transport	13
5	GO:0022411	cellular component disassembly	7
5	GO:0072521	purine-containing compound metabolic process	11
5	GO:0006508	proteolysis	39
5	GO:0034250	positive regulation of cellular amide metabolic process	4
5	GO:0043933	protein-containing complex organization	19

5	GO:0044267	cellular protein metabolic process	177
5	GO:0015986	ATP synthesis coupled proton transport	6
5	GO:0006996	organelle organization	39
5	GO:0043603	cellular amide metabolic process	159
5	GO:1901566	organonitrogen compound biosynthetic process	169
5	GO:0006811	ion transport	20
5	GO:0010628	positive regulation of gene expression	5
6	GO:0007010	cytoskeleton organization	20
6	GO:0006414	translational elongation	11
6	GO:0043043	peptide biosynthetic process	154
6	GO:1901293	nucleoside phosphate biosynthetic process	11
6	GO:0006412	translation	153
6	GO:0043604	amide biosynthetic process	155
6	GO:0009141	nucleoside triphosphate metabolic process	8
6	GO:0071826	ribonucleoprotein complex subunit organization	10
6	GO:0070925	organelle assembly	10
6	GO:0009259	ribonucleotide metabolic process	11
6	GO:0045333	cellular respiration	9
6	GO:0051603	proteolysis involved in cellular protein catabolic process	13
6	GO:0006163	purine nucleotide metabolic process	11
6	GO:0043632	modification-dependent macromolecule catabolic process	13
6	GO:0042254	ribosome biogenesis	27
6	GO:0042273	ribosomal large subunit biogenesis	7
6	GO:0022618	ribonucleoprotein complex assembly	10
6	GO:0044257	cellular protein catabolic process	13
6	GO:0042274	ribosomal small subunit biogenesis	10
6	GO:0046390	ribose phosphate biosynthetic process	10
6	GO:0045727	positive regulation of translation	4
6	GO:0032984	protein-containing complex disassembly	6
6	GO:0072522	purine-containing compound biosynthetic process	10
7	GO:0034470	ncRNA processing	14
7	GO:1902600	proton transmembrane transport	10
7	GO:0000028	ribosomal small subunit assembly	9
7	GO:0009142	nucleoside triphosphate biosynthetic process	8
7	GO:0009144	purine nucleoside triphosphate metabolic process	8
7	GO:0006164	purine nucleotide biosynthetic process	10
7	GO:0009165	nucleotide biosynthetic process	11
7	GO:0009150	purine ribonucleotide metabolic process	11
7	GO:0009199	ribonucleoside triphosphate metabolic process	8
7	GO:0140694	non-membrane-bounded organelle assembly	9
7	GO:0042255	ribosome assembly	9
7	GO:0009060	aerobic respiration	9
7	GO:0006364	rRNA processing	14
7	GO:0009260	ribonucleotide biosynthetic process	10
7	GO:0019941	modification-dependent protein catabolic process	13
7	GO:0000470	maturation of LSU-rRNA	6
7	GO:0002181	cytoplasmic translation	16

8	GO:0009152	purine ribonucleotide biosynthetic process	10
8	GO:0009201	ribonucleoside triphosphate biosynthetic process	8
8	GO:0016072	rRNA metabolic process	14
8	GO:0015985	energy coupled proton transport, down electrochemical gradient	6
8	GO:0009205	purine ribonucleoside triphosphate metabolic process	8
8	GO:0009145	purine nucleoside triphosphate biosynthetic process	8
8	GO:0000463	maturation of LSU-rRNA from tricistronic rRNA transcript (SSU-rRNA, 5.8S rRNA, LSU-rRNA)	5
9	GO:0016567	protein ubiquitination	11
9	GO:0009206	purine ribonucleoside triphosphate biosynthetic process	8

Table A.4 Complete list of enriched processes (Fisher's exact test; FDR < 0.05) among down-regulated genes with respect to the whole transcriptome of *Acartia clausi*, ordered by increasing GO level, for the BP category. For each GO subcategory are reported GO level, ID and number of down-regulated genes.

GO level	GO ID	GO subcategory	No. of DEGs
2	GO:0009987	cellular process	91
2	GO:0008152	metabolic process	73
3	GO:0071704	organic substance metabolic process	72
3	GO:0006807	nitrogen compound metabolic process	69
3	GO:0044237	cellular metabolic process	70
3	GO:0009058	biosynthetic process	50
3	GO:0044238	primary metabolic process	70
4	GO:1901564	organonitrogen compound metabolic process	51
4	GO:0019538	protein metabolic process	44
4	GO:0034641	cellular nitrogen compound metabolic process	59
4	GO:0044249	cellular biosynthetic process	50
4	GO:0043170	macromolecule metabolic process	62
4	GO:0044260	cellular macromolecule metabolic process	45
4	GO:0044085	cellular component biogenesis	16
4	GO:1901576	organic substance biosynthetic process	50
5	GO:0034645	cellular macromolecule biosynthetic process	36
5	GO:1901566	organonitrogen compound biosynthetic process	39
5	GO:0022607	cellular component assembly	12
5	GO:0043603	cellular amide metabolic process	38
5	GO:0044267	cellular protein metabolic process	42
5	GO:0044271	cellular nitrogen compound biosynthetic process	47
5	GO:0010467	gene expression	50
5	GO:0006518	peptide metabolic process	36
5	GO:0009059	macromolecule biosynthetic process	44
6	GO:0006414	translational elongation	6
6	GO:0043604	amide biosynthetic process	36
6	GO:0006412	translation	35
6	GO:0043043	peptide biosynthetic process	36